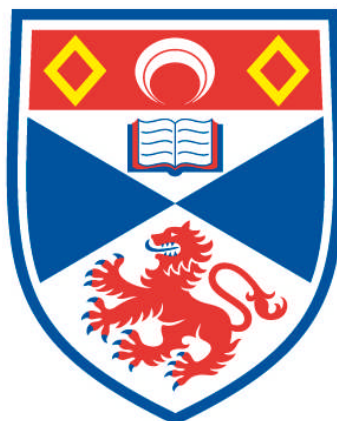


**LIFE AT THE END OF WORLDS
MODELLING THE BIOSIGNATURES OF MICROBIAL LIFE IN
DIVERSE ENVIRONMENTS AT THE END OF THE HABITABLE
LIFETIMES OF EARTH-LIKE PLANETS**

Jack Thomas O'Malley-James

**A Thesis Submitted for the Degree of PhD
at the
University of St Andrews**



2014

**Full metadata for this item is available in
Research@StAndrews:FullText
at:**

<http://research-repository.st-andrews.ac.uk/>

Please use this identifier to cite or link to this item:

<http://hdl.handle.net/10023/5549>

This item is protected by original copyright

Life at the End of Worlds

Modelling the biosignatures of microbial life in diverse environments at
the end of the habitable lifetimes of Earth-like planets

by

Jack Thomas O'Malley-James



University of
St Andrews

600
YEARS

Submitted for the degree of Doctor of Philosophy in Astrophysics

April 2014

Declaration

I, Jack O'Malley-James, hereby certify that this thesis, which is approximately 37,000 words in length, has been written by me, that it is the record of work carried out by me and that it has not been submitted in any previous application for a higher degree.

Date

Signature of candidate

I was admitted as a research student in September 2010 and as a candidate for the degree of PhD in September 2010; the higher study for which this is a record was carried out in the University of St Andrews between 2010 and 2014.

Date

Signature of candidate

I hereby certify that the candidate has fulfilled the conditions of the Resolution and Regulations appropriate for the degree of PhD in the University of St Andrews and that the candidate is qualified to submit this thesis in application for that degree.

Date

Signature of supervisor

Copyright Agreement

In submitting this thesis to the University of St Andrews we understand that we are giving permission for it to be made available for use in accordance with the regulations of the University Library for the time being in force, subject to any copyright vested in the work not being affected thereby. We also understand that the title and the abstract will be published, and that a copy of the work may be made and supplied to any bona fide library or research worker, that my thesis will be electronically accessible for personal or research use unless exempt by award of an embargo as requested below, and that the library has the right to migrate my thesis into new electronic forms as required to ensure continued access to the thesis. We have obtained any third-party copyright permissions that may be required in order to allow such access and migration, or have requested the appropriate embargo below.

The following is an agreed request by candidate and supervisor regarding the electronic publication of this thesis: Access to Printed copy and electronic publication of thesis through the University of St Andrews.

Date

Signature of candidate

Date

Signature of supervisor

Collaboration Statement

This thesis is the result of my own work carried out at the University of St Andrews between September 2010 and March 2014. Parts of the work presented in this thesis have been published in refereed scientific journals or books:

- “From Life to Exolife: The interdependence of astrobiology and evolutionary biology”: **O’Malley-James J.T.**, Lutz S. 2013, In: *Evolutionary Biology: Exobiology and Evolutionary Mechanisms*, ed. Pierre Pontarotti. Springer. pp. 95-108. [**A table from this book chapter was used as a basis for Table 1.1 in Chapter 1. I created the original form of the table.**]
- “Swansong Biospheres: Refuges for life and novel microbial biospheres on terrestrial planets near the end of their habitable lifetimes”: **O’Malley-James J.T.**, Greaves J.S., Raven J.A., Cockell C.S. 2012, *Int. J. Astrobiology*, 12, 99-112 [**Chapter 2 is an extended version of the methods section of this paper. The temperature predictions and discussions of refuges for life on the far-future Earth from this paper form Chapter 4. Discussion of animal and plant extinction sequences from the paper have been incorporated into Chapter 5. Figures 6.1 and 6.2 in Chapter 6 are reproduced from this paper and were originally created by me. All work in this paper was carried out and written by me, with scientific advice from the co-authors.**]
- “Swansong Biospheres II: The final signs of life on terrestrial planets near the end of their habitable lifetimes”: **O’Malley-James J.T.**, Cockell C.S., Greaves J.S., Raven J.A. 2013, *Int. J. Astrobiology* in press, doi:10.1017/S1473550413000426. [**Chapter 3 is an extended version of the methods section from this paper. Plant extinction sequences, discussions on potential biosignatures and**

how they would change over time and the results of modelling microbial biosignatures from this paper are incorporated into Chapter 5. All work in this paper was carried out and written by me, with scientific advice from the co-authors.]

- “Life and Light: Exotic Photosynthesis in Binary and Multiple Star Systems”: O’Malley-James J.T., Raven J.A., Cockell C.S., Greaves J.S. 2012, *Astrobiology*, 12: 115-124 [The core of the work in this paper originally formed a previously examined M.Res. thesis. This work was subsequently expanded during my PhD in order to publish the results. Therefore, the extensions to this work are briefly summarised in Chapter 6, Section 6.2. All work in this paper was carried out and written by me, with scientific advice from the co-authors.]

Each chapter has benefited from collaboration with the authors listed above. However, except where explicitly indicated in the text, the work contained in the chapters is my own. It should be noted that, at the the time of submission of this thesis, the contents of Chapter 6, Section 6.1 have been submitted for publication as a research article.

Jack O’Malley-James

April 2014

Abstract

This thesis investigates how increased global mean temperatures on Earth, induced by the increase in the luminosity of the Sun as it ages, change the types of habitable environments on the planet at local scales over the next 3 Gyr. Rising temperatures enhance silicate weathering rates, reducing atmospheric CO₂ levels to below the threshold for photosynthesis, while simultaneously pushing environments past the temperature tolerances of plant and animal species. This leads to the end of all plant life and animal life (due to reduced food, O₂ and H₂O availability, as well as higher temperatures) within the next 1 Gyr. The reduction in the extent of the remaining microbial biosphere due to increasing temperatures and rapid ocean evaporation is then modelled, incorporating orbital parameter changes until all known types of life become extinct; a maximum of 2.8 Gyr from the present. The biosignatures associated with these changes are determined and the analysis extended to Earth-like extrasolar planets nearing the end of their habitable lifetimes. In particular, the stages in the main sequence evolutions of Sun-like stars within 10 pc are evaluated and used to extrapolate the stage that an Earth-analogue planet would be at in its habitable evolution, to determine the best candidate systems for a far-future Earth-analogue biosphere, highlighting the *Beta Canum Venaticorum* system as a good target. One of the most promising biosignatures for a microbial biosphere on the far-future Earth (and similar planets) may be CH₄, which could reach levels in the atmosphere that make it more readily detectable than it is for a present-day Earth-like atmosphere. Determining these biosignatures will help expand the search for life to the wider range of environments that will be found as the habitable exoplanet inventory grows and planets are found at different stages in their habitable evolution.

Acknowledgements

Firstly I would like to thank my supervisors: Dr Jane Greaves, Prof. Charles Cockell and Prof. John Raven for their support, time, advice and the provision of a wealth of tangents and side-topics that contributed, in big and small ways, to the interdisciplinary beast of a topic that microbes at the end of worlds became. Between all three, any question I could imagine about astrophysics, biology, geophysics and countless other subjects was answerable. Special thanks to Keith Horne and Monica Grady, my thesis examiners, for taking the time to thoroughly read this work and helping to hammer it into its final shape.

Particular thanks goes to the “Cake Class” (Jo B., Sarah, Lizzie, Camille, Rachel, Alex, Ailsa, Danny) for inducting me into the world of astronomy when I first joined the department as a non-astronomer in 2010. Everything from afternoons spent building telescopes in muddy fields to learning about the inner-workings of stars (with compulsory cake breaks) made me into the almost-astronomer that I became.

The bulk of this work took place at one desk, in one office, so a special thanks goes to my office mate for the entirety of my time here, Joe. We both subscribed to a uniquely non-standard working philosophy involving a comfortably furnished office, a good background soundtrack and a number of outlandish (and often unrealised) side-projects. This ultimately led to a 9-5 detachment from reality that, in some small way, was good for thinking about the abstract things that we had to think about. Thanks to Jo B., Louise and Victor who, when this office philosophy was forced upon them, accommodated it so well; there could have been no better office mates to have for this past year in this larger new office. Thanks also to Grant for the lifts, teaching me how to use telescopes and the many good boredom-curing ideas; to Raphie for her boundless enthusiasm that was both infectious and motivating; to Lee for the booming laughter and the Rhubarb Triangle fact, to Craig and Neil for fully getting onboard with the inter-office sunflower growing competition; to John M. for a dour straight-talking commentary on life and to Mehmet, Aaron, John I., Rim, Claire, Colin, Carsten and countless others here who, either professionally, socially, or both, made my time here enjoyable and uniquely unforgettable.

Thank you to the non-astronomers in St Andrews: Jo T., Kate, Laura, Morven and

many others for adding a bit more variety to life, and especially to Kelly, both for the support during my time here and for happily tolerating a life dominated by astronomers.

I would also like to thank those in the UK astrobiology community who have contributed to my academic life through everything from stimulating conversations to full-blown collaborations. In that regard, special thanks goes to Steffi, for helping to write a book chapter with me and for thinking up new ways to kill microbes using balloons, and also to Sean, for bringing me into the world of sub-surface habitable zones and for adding a philosophical side to my view of astrobiology.

Finally, I would like to thank my family and extended family for their constant support and interest. In particular, my mother who, by buying an 8-year-old version of me a book about space that surprised me when it said that nobody knows if aliens exist, may have unwittingly set all of this in motion many years ago.

Contents

Declaration	i
Copyright Agreement	iii
Collaboration Statement	v
Abstract	vii
Acknowledgements	ix
1 Introduction	1
1.1 The meaning of ‘life’	2
1.2 The origins of life on Earth	4
1.3 A brief history of Earth as a habitable planet	11
1.4 Searching for life in the universe	18
1.4.1 Finding other worlds	19
1.4.2 The habitable zone	21
1.4.3 Planetary properties and temperature	22
1.4.4 The extremes of life on Earth	25
1.4.5 The signatures of life	27
1.4.6 Life in the solar system	31
1.4.7 Life beyond the solar system	36
1.5 The future of life	37
1.5.1 Solar evolution and extreme climate change	37
1.5.2 Extinctions	40
1.5.3 Implications for the search for life	41
1.6 Thesis aim	41

2	Methods I - Climate Modelling	43
2.1	Luminosity evolution	43
2.2	Energy balance temperature model	45
2.3	Greenhouse warming and atmospheric absorption	46
2.4	Ocean and land fractions	50
2.5	Insolation variations	51
2.5.1	Varying individual parameters	55
2.5.2	When do the Milankovitch cycles break down?	58
2.6	Latitudinal heat flow	59
2.7	Elevation variations	60
2.8	Water vapour and the runaway greenhouse effect	61
2.9	Testing the model	61
2.9.1	Reproducing present-day surface temperatures	61
2.9.2	Running the model backwards	62
2.10	Summary	64
3	Methods II - Biosignature Modelling	65
3.1	Predicting extinction sequences	65
3.1.1	Predicting the end of plant and animal life	66
3.1.2	Predicting the end of microbial life	68
3.1.3	Initial cell counts	72
3.2	Biosignature predictions	72
3.3	Summary	75
4	Refuges for life near the end of the Earth's habitable lifetime	77
4.1	Far-future temperature evolution	77
4.2	Deep ocean trench remnants	79
4.3	Caves	80
4.4	High altitude refuges	83
4.4.1	Aerial biospheres?	85
4.5	The deep subsurface	85
4.6	Summary	87

5	Biosignatures of Earth-like planets nearing the end of their habitable lifetimes	89
5.1	The end of plant and animal life	89
5.1.1	The end of photosynthetic life	89
5.1.2	The end of animal life	95
5.2	Biogeochemical reactions in a future microbial world	99
5.2.1	High altitude	99
5.2.2	Caves	100
5.2.3	The subsurface	101
5.3	Biosignatures	104
5.3.1	Model results	104
5.3.2	Detectability	107
5.3.3	Other biosignatures: Clouds?	109
5.4	The signatures of extinct biospheres?	110
5.5	Summary	111
6	Applications to other planets within and beyond the solar system	113
6.1	Old stellar systems in the solar neighbourhood	115
6.1.1	Alpha Centauri AB, Beta Canum Venaticorum & HD 197027	118
6.1.2	Tau Ceti	124
6.1.3	Earth analogues at the end of their habitable lifetimes	125
6.1.4	Super-Earths at the end of their habitable lifetimes - Tau Ceti e	126
6.2	Binary and multiple star systems	128
6.3	Martian methane: A cold end to a planet's habitable lifetime?	131
6.3.1	Martian methanogens and methanotrophs?	133
6.4	Chapter summary	135
7	Conclusions	137
7.1	Avoiding total extinction: could life survive an end to habitable conditions (as presently defined on the planet of origin)?	139
7.1.1	Future evolution	140
7.1.2	Passive migration	140
7.1.3	The role of intelligent life	141

7.2 Outlook	142
Glossary	145
Online resources	149
Bibliography	151

List of Figures

1.1	Defining life	2
1.2	The three domains of life on Earth.	5
1.3	The three domains of life including the transfer of genes between domains.	6
1.4	The history Earth	16
1.5	Milankovitch Cycles	24
1.6	Animal extremophiles	26
1.7	Atmospheric transmission spectra	29
1.8	Linda on the surface of Europa.	34
1.9	Hydrocarbon lakes on the surface of Titan.	35
1.10	Expected luminosity evolution for a $1 M_{\odot}$ star	38
1.11	Saturated vapour pressure curve for water	39
2.1	Modelled main sequence luminosity evolution of the Sun.	44
2.2	Variation of intercepted radiation with latitude.	51
2.3	True anomaly	53
2.4	Variation of the hour angle at sunset over latitude	54
2.5	Variation of insolation over latitude	56
2.6	Influence of eccentricity on insolation	57
2.7	Influence of obliquity on insolation	57
2.8	Heat diffusion	59
2.9	Change in lapse rate of moist air with surface temperature	60
2.10	Reproducing the present-day equator-to-pole temperature range	62
2.11	Running the model backwards: Earth's mean surface temperature and solar luminosity	63
3.1	Changes in atmospheric and soil CO_2 (in p.p.m.) with increasing surface temperature	67

3.2	Change in biological productivity with increasing surface temperature . . .	69
3.3	Simplified extinction sequence for a microbial biosphere.	69
3.4	Schematic of the biosphere-atmosphere gas exchange model.	71
4.1	Change in global mean temperatures over time with increasing solar luminosity.	78
4.2	Ice Cave	81
4.3	Seasonal temperature variations between equatorial and polar latitudes for obliquities of 60 and 90 degrees for a solar luminosity of $1.1 L_{\odot}$	82
4.4	Change in lower temperature range over latitude for obliquities of 30, 60 and 90 degrees at 2.0, 2.5, 2.8 and 3.0 Gyr from present.	83
4.5	Mean temperature evolution at the equator and the poles with increasing altitude	84
4.6	Aerosol transport mechanisms from surface to high altitudes within Earth's atmosphere.	86
5.1	Plant extinction sequence	94
5.2	Sequence of events between the present and a far-future microbial world . .	98
5.3	Change in cell abundance per unit surface area over time with increasing temperature.	102
5.4	Points measured during the Earth's future temperature evolution at which biosignature gas levels are measured.	104
5.5	Changes in gas species abundances in the atmosphere between 150 years and 11 Myr.	105
5.6	Points measured during the Earth's future temperature evolution at which biosignature gas levels are measured.	106
5.7	Points measured during the Earth's future temperature evolution at which biosignature gas levels are measured.	106
5.8	Temporal biosignature evolution.	107
6.1	Time windows for complex and microbial life on Earth analogue planets orbiting Sun-like stars.	114
6.2	Main sequence evolution of currently known terrestrial planet ($10M_{\oplus}$ and less) hosting stars.	115
6.3	Time elapsed on the main sequence for G stars within 10 pc.	117
6.4	Mean temperature evolution at the equator (black) and the poles (grey) with increasing altitude on a present-day Earth analogue planet orbiting α Cen A, β CVn and HD 197027.	122

6.5	Mean temperature evolution at the equator (black) and the poles (grey) with increasing altitude on an Earth analogue planet orbiting α Cen A, β CVn and HD 197027 at a stage equivalent to the Sun's current main sequence stage in these star's lifetimes.	123
6.6	Time elapsed on the main sequence for G stars within 10 pc.	124
6.7	Changes in gas species abundances in the atmosphere of τ Ceti e	125
6.8	Proportion of G-M star and G-G star binaries (and multiple-star systems) in the sample of systems with G star primaries from Duquennoy & Mayor (1991)	129
6.9	Peak (photosynthetic) photon flux density results	130

List of Tables

1.1	The limiting factors for life on Earth	18
1.2	Summary of biosignatures of Earth-like life	28
3.1	Microbial organisms that could be supported by environments on the far-future Earth.	72
3.2	Production rates of biosignature gases from model species representing the metabolic pathways that are likely to be favourable on the far-future Earth.	73
3.3	Modelled abiotic gas fluxes.	74
5.1	Microbial organisms that could be supported by the types of habitable environments available on the far-future Earth.	103
5.2	Summary of the biosignature gases in the atmosphere at different habitability stages in the Earth's far future, from 1 Gyr from present to 2.8 Gyr from present.	109
6.1	Summary of the properties of the candidate stellar systems.	118
6.2	Summary of the modelled atmospheric biosignatures in each stage of the biosphere decline on an Earth analogue planet orbiting α Cen A, β CVn and HD 197027	121

“What is not good for the beehive, cannot be good for the bees”

- Marcus Aurelius

“Life finds a way”

- Michael Crichton, *Jurassic Park*, 1990

1

Introduction

THE field of astrobiology is a relatively new discipline, but the questions it aims to answer have been asked throughout much of recorded history. From at least the time of the Ancient Greek Atomist philosophers, the questions of whether there is life beyond Earth, how life originated and what its future might be have been posed and explored. It was not until the latter half of the twentieth century that science had advanced sufficiently to begin to make realistic attempts to answer these questions. Astrobiology is a truly inter-disciplinary field, combining knowledge and methodologies from astronomy, biology, physics, chemistry and the geosciences to find answers to these questions.

These questions can be divided into three main subject matters: (i) the origin of life on Earth, (ii) the search for life elsewhere in the solar system and beyond and (iii) the future of life in the universe. The common theme in each case is “life” and it can be argued that astrobiology is as equally concerned with fully comprehending life, in both a physical and

biological context, as it is with simply finding life elsewhere. Defining what is meant by life is a necessary first-step before many astrobiological questions can be explored.

1.1 The meaning of ‘life’

To use Earth-based biology as a basis for an all-encompassing definition of life may provide too narrow a view when it comes to searching for life elsewhere. Many definitions of life have been suggested, although no single definition has been universally accepted.

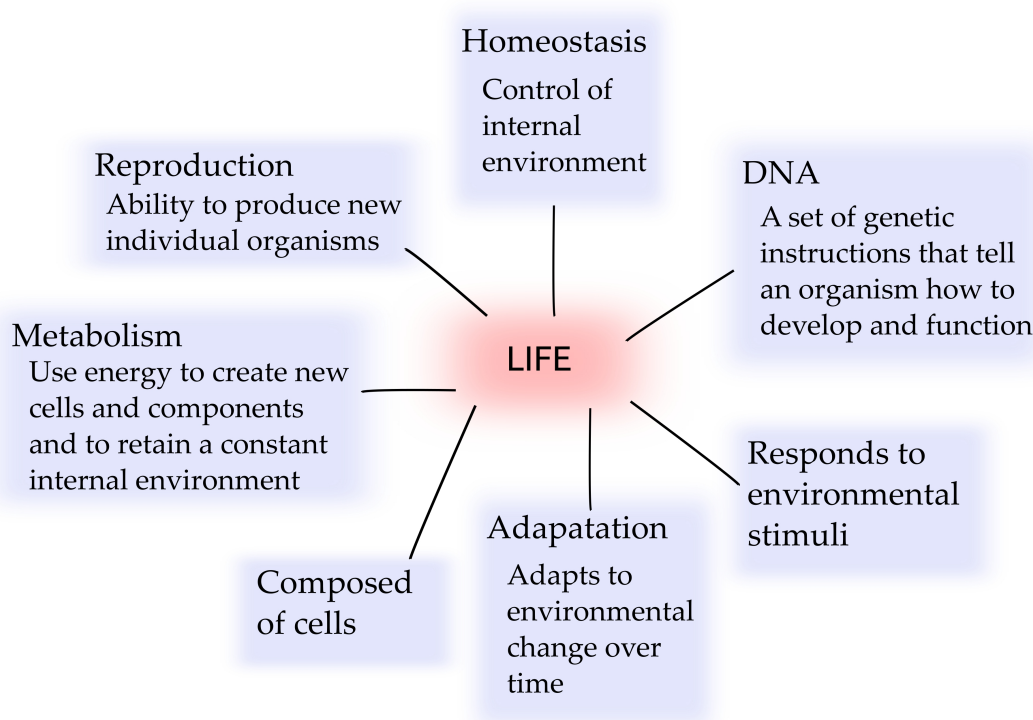


Figure 1.1: Defining life. It is more accurate to say that life can be described, rather than defined. The seven key features of a living organism are outlined here (Koshland, 2002).

The working definition currently used by NASA is: “Life is a self-sustained chemical system capable of undergoing Darwinian evolution” (Kolb, 2007). Originally proposed by Charles Darwin in 1859, Darwinian evolution explains the development of new species through the natural selection of small, inherited variations that increase an individual organism’s ability to compete, survive and reproduce. This original tenet is still at the heart of the theory today, although the theory has altered as science progressed. In its present form, known as “modern evolutionary synthesis” progress in the biological sciences is merged with the original theory of natural selection (Huxley, 1942; Pigliucci, 2009). This includes concepts such as mechanisms for change at the genetic level, the role of

genetic diversity in populations of an organism and the concept of punctuated equilibrium (Eldredge & Gould, 1972), i.e. that a species can split into two species (geologically) rapidly, rather than gradually transforming into another.

The definition of life used by NASA is reasonably broad and would certainly apply to anything resembling life on Earth (although Darwinian evolution is not something that itself is applicable to remote detection). Arguably, given current knowledge and abilities to detect biosignatures (indicators of the presence of life), searching for Earth-like life is the most realistic option at this point in time. Therefore, this definition is an adequate basis for the 'search for life'; however, it is still firmly rooted in terrestrial biology and may be too specific to apply to a truly alien biological system. Indeed, as stated in Kolb (2007), this definition already excludes certain Earth-based life such as mules, which, through being sterile, cannot reproduce and therefore do not undergo Darwinian evolution. This definition also includes viruses. A virus carries genetic information and can undergo evolution by natural selection. However, they cannot carry out their lifecycles without infecting a host cell. Hence, viruses are generally not accepted to be alive (van Regenmortel, 2000; Moreira & Purificación López-García, 2009).

All known life is carbon-based, i.e. living organisms are composed of complex molecules of carbon bonded to other atoms. Carbon atoms have four valence electrons and can readily bond with many other atoms (H, O, N, S, P, Fe, Mg, Zn, etc. - Pace, 2001), resulting in a diverse range of molecules. In particular, by forming bonds with other carbon atoms, large, long-chain molecules can form. The energy required to form or break bonds is such that these are long, stable molecules that are also reactive. It is these complex molecular structures that serve as the information-carrying component of life as well as enabling the variety of different metabolic reactions that power biological organisms to take place (Pace, 2001). These properties are unique to carbon, leading to speculations that any life found beyond Earth would be carbon-based (Irwin & Schulze-Makuch, 2001; Pace 2001; Shapiro & Schulze-Makuch, 2009) - the most similar atom, silicon, has four valence electrons too, but does not interact with as many atoms (Pace, 2001).

Defining life is inherently difficult because life is not a physical substance, but more of a process. In this sense, the various common aspects of the process of being alive can be described (McKay, 2004), as summarised in Figure 1.1. It may be that, as the search

for extraterrestrial life progresses, a more revised, more general definition of life will be agreed upon. At the current level of knowledge, a fuller understanding of life will be needed, before a definitive definition can be made.

1.2 The origins of life on Earth

In order to understand life it is necessary not only to know what life is, but how it came to be. On Earth, it is thought that life emerged relatively soon (approximately 700 Myr based on fossil records) after the planet's formation (Nisbet & Sleep, 2001; Brasier *et al.*, 2006), with reliable fossil evidence dating back 3.47 Gyr (Shen *et al.*, 2001) and possible fossil evidence from 3.8-3.85 Gyr ago (Schidlowski, 1988; Mojzsis *et al.*, 1996; Rosing, 1999; Moorbath, 2005). This timescale neatly coincides with the end of the Late Heavy Bombardment (a period between 4.1 and 3.8 Gyr ago during which there was a high frequency of impact events as a result of the abundance of fragments left over from the formation of the planets). This suggests that life appeared almost as soon as conditions became conducive to its existence, leading to claims that the rapid emergence of life on Earth implies that life is common throughout the universe. Evidence for life that may have existed during this period is difficult to find. Direct fossil evidence of the microbial life from this period would no longer exist today as a result of the intense metamorphosis that rocks of this age would have undergone over geological time. The only evidence life may have left behind would come in the form of geochemical signatures that could only be attributed to biological processes. The claims of evidence of life from 3.8-3.85 Gyr ago rely on such evidence, in this case the abundance of carbon isotopes in carbonaceous inclusions in rocks. There are two stable carbon isotopes ^{12}C and ^{13}C . Breaking bonds with ^{12}C requires less energy than breaking ^{13}C bonds, so ^{12}C is strongly favoured by biological processes. Hence, an over-abundance of ^{12}C compared to ^{13}C in these rock samples suggested biological activity. However, there is some debate about the reliability of this evidence, due to possible abiotic mechanisms for creating these isotope abundances (Fedo & Whitehouse, 2002).

Life on Earth is classified, based on differences between genomes of different organisms, into three categories known as domains: archaea, bacteria and eukaryotes. Archaea (microscopic unicellular organisms that have a separate evolutionary origin to bacteria) are generally considered to be the most ancient domain of life. Single-celled archaea and

However, the tree diagram shown in Figure 1.2, although useful for providing a broad overview of evolutionary relatedness, does not account for processes such as the exchange of genetic information between DNA molecules (recombination), the transfer of genes between organisms via processes other than reproduction (horizontal gene transfer) and hybridisation. Including these processes leads to a more complex tree diagram with links between branches and domains as illustrated in Figure 1.3, suggesting multiple common ancestors that exchanged genetic information (Woese, 1998; Doolittle, 2000).

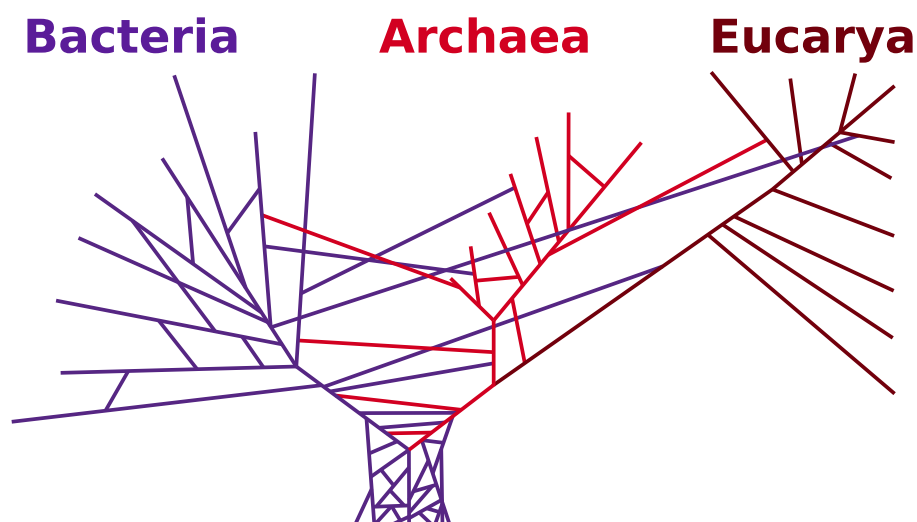


Figure 1.3: The three domains of life including the transfer of genes between domains. *Image: Modified version of commons image by NASA [GFDL (<http://www.gnu.org/copyleft/fdl.html>) or CC-BY-SA-3.0 (<http://creativecommons.org/licenses/by-sa/3.0/>)].*

Since Darwin first postulated the origins of life in a “warm little pond” (Darwin, 1859), there have been many theories about how life first originated. These range from the primordial soup hypothesis (Oparin, 1924; Shapiro, 1987), which has prompted experiments such as the Miller-Urey experiment in which electrical sparks are applied to a gas mixture of CH_4 , NH_3 and H_2 resembling a possible early Earth atmosphere (Miller & Urey, 1959), to the theory that life arose as an extension of geochemical processes, such as serpentinization, in which reactions between seawater and newly exposed ocean crust form precipitate chimneys with mineral membranes across which a pH gradient similar to that in all living cells is produced (Russel *et al.*, 2013). While life has yet to be created in a laboratory, partially synthetic life has been created by transplanting a chemically synthesised genome into the cytoplasm of a natural cell (Gibson *et al.*, 2010). Additionally, organic molecules, including amino acids (the building blocks of proteins) have been successfully created, for example via the Miller-Urey experiment (Parker *et al.*, 2011). However, the Miller-Urey

experiment assumes a very reducing atmosphere (i.e. an atmosphere in which oxidation is prevented), whereas many geologists assume a weakly reducing or neutral early atmosphere, as a result of the expected low abundance of metallic iron (which would have acted as a large oxygen-sink) in the mantle (Kasting & Brown, 1998; Chyba, 2005), which would yield a lesser range of organic compounds (Chyba, 2005).

Another possible source of the ingredients for life could have been impact events. Some comets and meteors have been found to contain amino acids and other biologically important molecules (Hayes, 1967; Sephton, 2002), while interplanetary dust has been found to contain organic carbon (Bradley *et al.*, 2014). Higher impact rates in the past (Panastassiou & Wasserburg, 1968; Tera *et al.*, 1974) and a constant flux of dust particles (Brook *et al.*, 2009) may have delivered some of the building blocks for life to the early Earth. Estimates of impact rates on the early Earth suggest that the flux of pre-biotic organic material from comets and asteroids may have been up to 10^{11} kg yr⁻¹ (Thompson *et al.*, 2006). This is larger than the 10^8 kg yr⁻¹ estimated for the interplanetary dust particle flux (Chyba & Sagan, 1997) and similar to, or greater than, the estimated endogenous production on Earth: 10^8 - 10^{11} kg yr⁻¹, depending on the composition of the early atmosphere (Thompson *et al.*, 2006). However, extreme heating of comets and asteroids upon entry into the atmosphere may have destroyed most organics contained within them (Chyba & Sagan, 1997). Simulations suggest that amino acids could have survived when shielded within the cores of large enough (km-radius) objects (Pierazzo & Chyba, 1999). Simpler carbon molecules would have been more likely to survive impacts and could subsequently have contributed to further endogenous organic chemistry (Thompson *et al.*, 2006).

The origin of life may not have needed pre-formed organic molecules, however. Warm, alkaline hydrothermal vents could have given rise to life without a dependence on pre-formed organic compounds by enabling geochemical reactions to take place that were precursors to early types of biological metabolic processes (Martin & Russell, 2007). Other origin of life theories that do not require pre-formed organic molecules have been proposed. These include the clay hypothesis, which suggests that complex organic molecules arose gradually from non-organic silicon crystal replication (Cairns-Smith, 1987) and the deep hot biosphere hypothesis for an origin of life deep underground (Gold, 1992).

The hypothesis that life is a common consequence of abiotic chemistry could be tested by finding a second sample of life on Earth, a separate shadow biosphere, which had an independent origin to life as we know it (Davies & Lineweaver, 2005). One indicator of an alien biosphere may be the chirality of carbon molecules. Carbon molecules can be found in left- or right-handed configurations; however, life on Earth uses right-handed sugars and left-handed amino acids (Mason, 1984; Bonner, 1991; Davies & Lineweaver, 2005). Chiral molecules induce the circular polarisation of unpolarised light, rotating the plane of incident light to the left or right, depending on a molecule's chirality (Vázquez *et al.*, 2010). It has been suggested that the polarising effect of chiral molecules could be used as a remote indicator for life; however, there are non-biological processes that can induce such polarisation, making this an ambiguous detection method (Vázquez *et al.*, 2010). Recent work hypothesises that an existing preference for a direction of circular polarisation may have led to the selection of a dominant chirality for amino acids (Vázquez *et al.*, 2010). Other suggested mechanisms for selecting a dominant chirality include the stochastic generation of a dominant chirality via small fluctuations in the ratio of left- to right-handed molecules in an initially even (racemic) mix (Blackmond, 2004) and the Vester-Ulbricht hypothesis that a dominant chirality is the result of physical processes such as beta decay that result in slightly different half-lives depending on the chirality of the product (Bonner & Liang, 1984). While chirality is necessary for biochemical reactions to take place effectively, the particular choice of 'handedness' is arbitrary, so life with the chirality reversed could survive equally well in theory (Davies & Lineweaver, 2005). Finding living systems with a reversed chirality would help improve understanding of the commonness of life in the universe.

The rapid emergence of life on Earth also opens up the question of whether terrestrial life actually originated on Earth, or whether it began on one of the other planets in the solar system and was subsequently transferred, via meteorite impact, to the early Earth (Nisbet & Sleep, 2001). This is an idea drawn from the theory of panspermia, an idea discussed by the ancient Greeks and first scientifically proposed in 1834¹ that advances the possibility of an extraterrestrial source for life on Earth (Hansson, 1997). Early Venus and Mars had more suitable environments for life than they presently do (Shaw, A. H., 2006), therefore it has been postulated that life may have originated on one (or both) of

¹In "Analysis of the Alais meteorite and implications about life in other worlds" by Jöns Jacob Berzelius.

these planets. Venus, under a fainter young Sun, may originally have had liquid water oceans similar to the early Earth, as evidenced by the deuterium-to-hydrogen ratio in the planet's atmosphere and the predictions of climate models (Kasting, 1988; Cockell, 1999; Svedhem *et al.*, 2007). Early Mars may have been warmer and wetter than at present, having not yet lost a significant quantity of its original atmosphere (Carr, 1987; Fairén *et al.*, 2010). However, recent work suggests that early Mars may not have been consistently warm enough to maintain liquid surface water, but instead experienced episodic warm periods during which liquid water could flow on the surface (Kite *et al.*, 2014).

Assuming terrestrial life has an extraterrestrial origin, it is more probable that that origin was on Mars rather than Venus, based on the frequency of transfer of material between planets (Mileikowsky *et al.*, 2000; Stöffler *et al.*, 2007). Mars is smaller than Venus, and thus, has a lower escape velocity. Therefore, there would have been a higher frequency of Martian rocks reaching Earth, increasing the likelihood of transference of living cells (Horneck & Brack, 1992; Horneck *et al.*, 2001; Nisbet & Sleep, 2001). However, the existence of permanent bodies of water within the temperature bounds for thermophilic life would have been more likely on early Venus, than early Mars (Cockell, 1999). This suggests that early Venusian environmental conditions would have been more favourable for the origin of life.

If traces of life are found on Venus or Mars (either extant or extinct), which show some similarities to life on Earth, this would be good evidence for the exchange of living materials between the inner planets. It is more likely that fossil evidence of life would be preserved on Mars, rather than Venus, because geological activity on Venus has led to the (possibly global) resurfacing of the planet with the past 700 Myr (Strom *et al.*, 1994). Recent research suggests that the presence of oxidised molybdenum and boron on early Mars and their absence on the wet, anoxic early Earth lend support to a Martian origin for life on Earth. Molybdenum and boron both help to stabilise organic molecules, making them fundamental for making the transition from abiotic to living chemistry (Benner, 2013).

During and after the late heavy bombardment, material was transferred between the terrestrial planets (Gladman *et al.*, 1996). Recent n-body simulations by Worth *et al.* (2013) suggest that the transfer of material between the terrestrial planets was frequent

in the early solar system, with transfers to the moons of Jupiter and Saturn also being possible, but rare. Simulation experiments to examine how these organisms react to the high temperatures, shock and acceleration associated with ejection into space suggest a small fraction of spores could survive re-entry. Horneck *et al.* (2008) found that *Bacillus subtilis* and *Chroococcidiopsis* spores and the fruiting bodies of the lichen *Xanthoria elegans* could survive the pressures associated with ejection from the Mars. Fajardo-Cavazos *et al.* (2009) simulated the stresses of ejection by firing a projectile at a granite target, to which *Bacillus subtilis* spores had been applied. They found a spore survival rate of 10^{-5} .

Experiments have shown that some strains of microbial life can survive exposure to space, either directly, or with some protective membrane or rock layer that prevents damage from ultraviolet (UV) radiation, especially biologically harmful UV-C and UV-B wavelengths, which are largely filtered out by Earth's ozone layer. For example, Horneck *et al.* (2001) exposed *Bacillus subtilis* bacterial spores to space; some protected by mixing with soils of various types and some fully exposed. They found that spores mixed with clay, rock or meteorite powder had a high survival rate after a two-week exposure time. A 100% survival rate was achieved for the case where the spore-to-soil ratio was comparable to that observed in soils on Earth. This lends evidence to the case for the successful transfer of spores between terrestrial planets in rocky ejecta. Olsson-Francis *et al.* (2010) exposed lichens (symbiotic organisms made up of a fungus and a photosynthetic microorganism) and a community of cyanobacteria (photosynthetic bacteria) from limestone cliffs in Beer, UK to conditions in low Earth orbit for ten days, with a single cyanobacterium strain surviving the exposure. Experiments such as this show that certain types of microorganism are able to tolerate the harsh environment of space, perhaps for long enough to survive dormant in a meteor or comet.

The effects of the stresses of re-entry into a planetary atmosphere on bacterial spores suggest that some spores could survive re-entry. Fajardo-Cavazos *et al.* (2005) attached granite samples containing *Bacillus subtilis* spores to the exterior of sounding rockets that were launched to high altitudes to simulate the effects of re-entry. They found a survival rate of approximately 4%. However, actual re-entry experiments, via ESA's STONE experiments, in which samples of microbial organisms are attached to the exterior of re-entry capsules, have not successfully yielded any survivors (de Vera, 2012). For example, in the Olsson-Francis *et al.* (2010) experiment, a sample of one of the lichens (*Rhizocarpon*

geographicum), left on its natural substrate, was attached to the outer surface of the re-entry capsule used in the experiment, but did not survive the re-entry process (de la Torre *et al.*, 2010). However, some bacteria or archaea may survive re-entry in large enough meteorites, with non-photosynthetic microorganisms having the best chance of surviving because the depth to which the rock is heat-sterilised exceeds the light penetration depth (Cockell *et al.*, 2007).

Further to space-exposure experiments, some researchers have claimed to have found signs of fossilised microorganisms in meteorites, which is used as evidence to support the theory of panspermia; most famously the Martian meteorite ALH84001 (McKay & Gibson, 1996) and the Tatahouine meteorite (Barrat *et al.*, 1998). These both contain rod- and ovoid shaped forms that are similar to terrestrial bacterial fossils. It has also been suggested that ALH84001 contains the remains of biofilms based on evidence in the form of carbonates found in the meteorite (McKay, 1997; Steele *et al.*, 1997). However claims that these meteorites contain fossilised extraterrestrial microorganisms remain controversial. For the Tatahouine meteorite it is likely that the observed structures have a terrestrial origin (Barrat *et al.*, 1998; Gillet *et al.*, 2000). The widely publicised case for fossil bacteria in the Martian meteorite ALH84001 was widely rejected as the supposed ‘nanofossils’ were too small to be fossilised bacteria (McKay, 1997). However, some support still remains for the observed structures having a biological origin (Thomas-Keprta *et al.*, 2009).

Studies of geological formations on Earth have given rise to claims that nano-bacteria do exist in nature, but they are not widely accepted as living organisms, being more generally referred to as calcifying nanoparticles that are abiotic crystallisations of minerals and organic molecules (Cisar *et al.*, 2000). The structures in ALH84001 would need to be shown to meet a number of criteria to be classed as fossil bacteria, such as size, shape and arrangement of their crystalline structures, but presently it is claimed that there is still not enough evidence to reject or confirm the claims (Thomas-Keprta *et al.*, 2009).

1.3 A brief history of Earth as a habitable planet

The history of life on Earth is fundamentally linked to the environment in which the Sun originally formed. The composition of a planet’s crust and atmosphere and hence, the possible chemical reactions that could be used to drive biological processes, are initially

determined by the elemental composition of the molecular cloud from which its host star forms.

For the Sun and similar stars, this process began within a giant molecular cloud - an interstellar cloud of gas and dust that is cold enough (10-20 K - Larson, 2003) and dense enough (20-100 $M_{\odot} \text{ pc}^{-2}$ - Elmegreen 1993; Larson, 2003) for simple molecules to form, predominantly H_2 , but also other simple molecules such as CO and H_2O (Lunine, 1999; Larson, 2003). The material in this cloud undergoes internal random motions referred to as turbulence (Lunine, 1999; Larson, 2003). Eventually, gas and dust can become concentrated in regions within the molecular cloud, increasing local density and attracting more material towards it. As the gas and dust move closer together as a result of mutual gravitational attraction, the region becomes denser and the mutual gravitational pull becomes stronger and a dense core is built-up via this process (Lunine, 1999). This nebula of material spins faster as it collapses due to the conservation of momentum, increasing collision rates and thus, increasing temperature. With most mass becoming concentrated at the centre of the nebula, this becomes hotter than the rest of the clump of gas and dust (Lunine, 1999). After a period of approximately 100,000 years, the centre becomes dense enough to collapse into a protostar (Lunine, 1999). The remaining material is flattened into a disc rotating about the rotation axis as a natural consequence of angular momentum conservation, i.e. centrifugal forces generated by rotation prevent the infall of material perpendicular to the rotation axis, but not parallel to the axis. The Orion Nebula is a good example of a nearby giant molecular cloud in which young stars appear to form in this way (Hillenbrand, 1997) and individual protoplanetary discs have now been observed within the nebula (McCaughrean & O'Dell, 1996).

The protostar collapses under gravity and strong stellar winds form along its rotation axis, dissipating part of the surrounding nebula: the T Tauri phase of the star's evolution. This stage lasts approximately 10 Myr before the star reaches the beginning of the main sequence (Larson, 2003). The infall of material onto the star terminates and the remaining parts of the nebula form a circumstellar disc around the star.

This protoplanetary disc is composed of molecules such H_2 , CO, C_2H_2 , HCN, CO_2 , H_2O , silicates and polycyclic aromatic hydrocarbons (Williams & Cieza, 2011). It is initially heated to temperatures that are hot enough (of the order 10^4 K - Guillot &

Hueso, 2006; Williams & Cieza, 2011) to vaporise all of the material within the disc. As the disc cools materials condense. The inner part of the disc is heated by the central star to a higher temperature than the outer parts, with temperatures ranging from approximately 1000 K in the inner disc to <100 K at a radius of 10 au (Boss, 1996), which means that only metals and rocky silicates condense in the inner region of the disc, whereas ices (such as H_2O and CH_4), which are much more abundant in the universe than metals and silicates (these made up only 0.6% of the original solar nebula, for example - Nuth *et al.*, 2005), can also condense in the cooler, outer parts of the disc (Williams & Cieza, 2011).

Initially there are only small gravitational interactions between these condensed, 0.1-1 μm -sized grains of material, but their large surface-to-mass ratio cause them to be swept along with gas in the disc (Williams & Cieza, 2011). During this process, grains collide and stick together, decreasing their surface-to-mass ratio and enabling drag forces to settle them towards the mid-plane of the disc. The increased density of dust in the disc interior then increases the rate of grain growth. Collisions eventually cause them to accrete into 1-100 km sized bodies known as planetesimals (Williams & Cieza, 2011). The initial formation timescale for cm- to decimeter-sized particles is relatively short - approximately 1000 years (Blum & Wurm, 2008). Formation of planetesimals is a longer Myr-timescale process ((Blum & Wurm, 2008)). However, the process of planetesimal formation is still not fully understood. While the collisional growth is efficient for sub-cm sized grains, because inter-particle forces are efficient at sticking dust particles of this size together when they collide, larger particles would also be subject to shattering and compaction (Blum & Wurm, 2008; Williams & Cieza, 2011). Proposed solutions include the formation of larger aggregates in long-lived vortices in the disc, very sticky materials, or re-accretion after fragmentation (Blum & Wurm, 2008; Williams & Cieza, 2011).

For planetesimals, gravitational forces dominate and these accrete material from the disc to form the solid cores of the giant and terrestrial planets (Papaloizou & Terquem, 2006). The abundance of condensed volatile materials (e.g. H_2O , NH_3 , CH_4) beyond the snow-line in the outer part of the disc enables the outer planets to accrete a large amount of material. This led to the formation of cores that were massive enough (typically $> 10 M_{\oplus}$ - Piso & Youdin, 2014) to capture hydrogen and helium atmospheres, leading to the formation of the gas and ice giant planets. The sparsity of material in the inner region of the disc where the only available accretion materials are those that can condense at higher

temperatures, such as iron and silicates, leads to less massive terrestrial planet cores. The time taken to form planets from planetesimals can take up to 10^8 years (Righter & O'Brien, 2011). Via this process of accretion, by approximately 4.54 Gyr ago, Earth reached a significant proportion of its final size (Koeberl, 2006).

The original atmospheres of the planets in the solar system were determined by the composition of the nebula from which the Sun formed, which contained 98% H, He and Li (trace) by mass; the remaining 2% consisted of heavier elements formed via nucleosynthesis in nearby older stars (Zahnle *et al.*, 2010) that subsequently ejected these elements into the interstellar medium through supernovae explosions (Hester *et al.*, 2004). Therefore, the young Earth, like the other planets, initially had a largely hydrogen and helium atmosphere (Zahnle *et al.*, 2010). Unlike the outer gas giant planets, which still have their hydrogen-helium atmospheres due to their large masses, Earth's first atmosphere was mostly lost to space because the low masses of H and He enabled them to escape the atmosphere easily. This was further aided by frequent collisions with other objects (Kasting & Catling 2003; Zahnle *et al.*, 2010; Kasting, 2011).

The most noteworthy of these collisions was the proposed collision between a Mars-sized planetoid that ejected a large amount of material into orbit, leading to the formation of the Moon as this material aggregated and cooled (Benz *et al.*, 1986; Canup & Asphaug, 2001). While this is presently the most widely accepted theory for the origin of the Moon, some doubts have been raised based on the composition of the Moon, which has similar oxygen isotope ratios to the Earth (Wiechert *et al.*, 2001). Oxygen isotope ratios are different for each body in the solar system (Wiechert *et al.*, 2001), therefore, a Moon formed from the mixing of material from the Earth and a second body would be expected to have a different isotope ratio to the Earth. However, recent work has found a higher than terrestrial oxygen isotope ratio in small samples of lunar rocks, supporting the theory (Herwartz *et al.*, 2014).

The secondary atmosphere of the young Earth was built up as result of the outgassing of materials that accumulated during the planet's accretion. Comets, asteroids and clathrate hydrates (icy solids formed from an open arrangement of hydrogen-bonded water molecules, which trap small gas molecules such as CH_4 within, that are expected to have formed within the solar nebula, trapping volatiles - Buffett, 2000) would all have

delivered volatiles to the inner planets in this way. These are heated in the mantle and vaporised, then delivered to the atmosphere as a result of tectonic processes. Initially, Venus, Mars and Earth would all have had similar secondary atmospheres; however, differences in escape velocities, planetary magnetic field strengths, surface temperatures, geology and which geochemical (or bio-geochemical - at least in Earth's case) reactions were possible has led to the different compositions of these atmospheres today (Prinn & Fegley, 1987).

The early Earth was initially a largely molten planet that is thought to have been hostile to life (Kasting & Catling 2003; Kasting, 2011). There is however speculation that life could have appeared as early as 4.4 Gyr ago during this period (Abramov & Mojzsis, 2009). Although there is no direct fossil evidence to support these claims, oxygen isotope ratios measured in zircon crystals that formed 4.4 Gyr ago suggests that they formed from molten rock in contact with a liquid hydrosphere, implying the presence of liquid water on the young Earth at this early stage (Wilde *et al.*, 2001).

The planet is thought to have cooled slowly as a result of extreme volcanism and ongoing collisions (especially during the Late Heavy Bombardment between 4.1 and 3.8 Gyr ago when the flux of impactors increased, late in the formation history of the solar system) - a period known as the Hadean eon. The exact composition of the Hadean atmosphere is unknown; however, the early oxidation of matter on Earth would have led to an atmosphere dominated by CO₂ and N₂ (Kasting, 2011; Trail *et al.*, 2011). Atmospheric CO₂ may have been as abundant as 100-200 bar shortly after the Moon-forming impact, but declined over the course of the Hadean eon to only a few tenths of a bar (Kasting, 2011). The rate at which this happened and the geological constraints on CO₂ are greatly uncertain, depending upon the rate at which CO₂ is removed into the mantle via the subduction of carbonates (Kasting, 2011). On the pre-biotic Earth, atmospheric CH₄ had a low abundance (approximately 10-100 ppmv - Kasting, 2008). The delivery of volatiles to the early Earth can also be used to constrain the composition of the forming atmosphere. The impact flux of dust and larger rocks would determine the rate of volatile delivery. For Earth during the Hadean, this flux could have been between 10³ and 10⁹ times higher than the present-day flux (approximately 10⁷ kg yr⁻¹ - Tajika, 2008).

The end of the Late Heavy Bombardment marked the beginning of the Archean eon 3.8 Gyr ago. By this point, the cooling of the planet had caused atmospheric water vapour

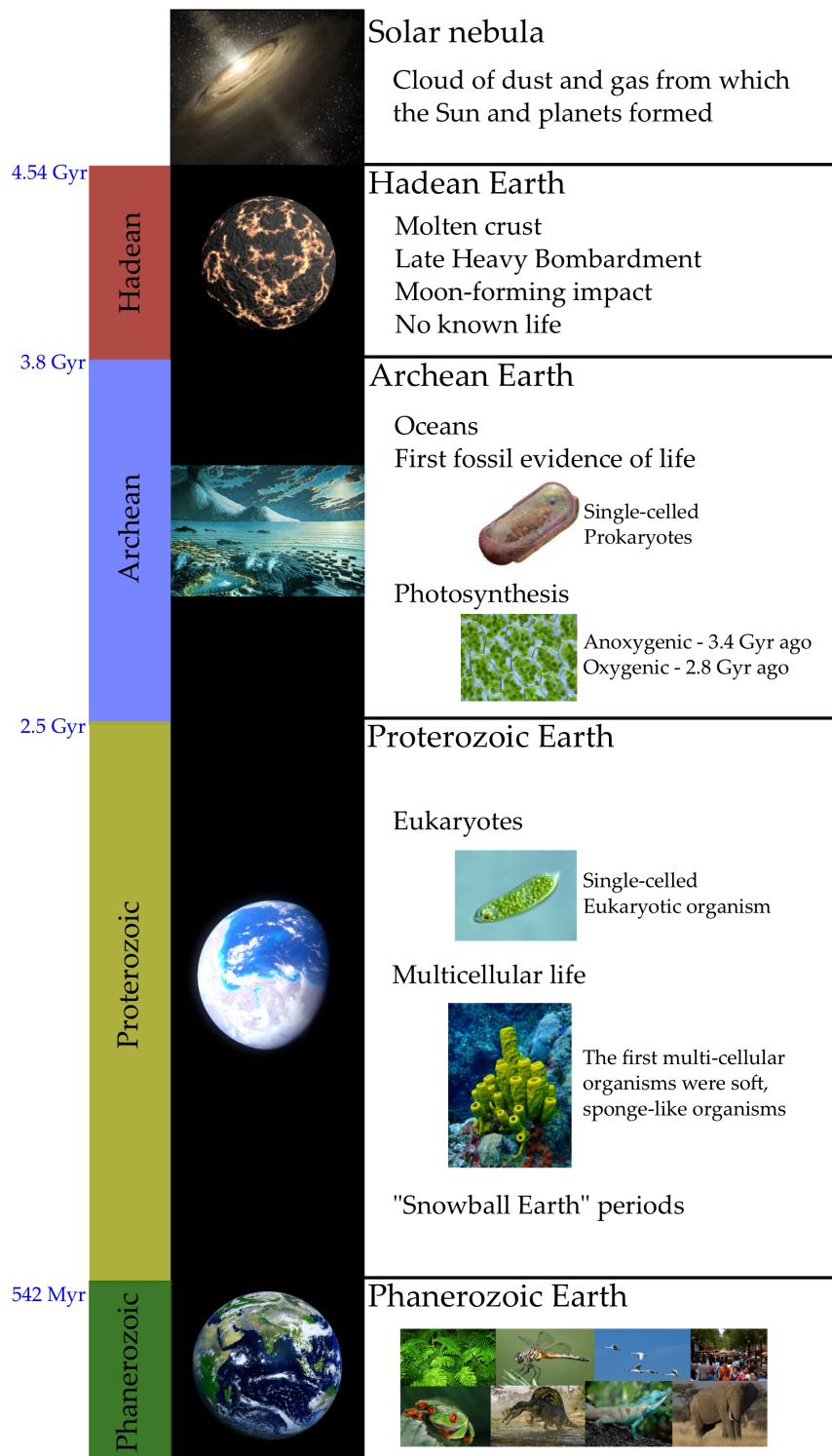


Figure 1.4: The history of Earth. A summary of Earth's geological history and the key steps in the emergence and evolution of life on the planet. Note photosynthesis emergence times are the earliest speculated emergence times (exact times are unknown).

to condense (Tajika, 2008), creating the oceans². At this stage the atmosphere was rich in greenhouse gases, but was still anoxic (Kasting & Catling, 2003; Kasting, 2011). The first (chemical) fossil evidence of life dates back to the beginning of this eon (Schidlowski 1988; Mojzsis et al. 1996; Rosing 1999). The first organisms on Earth were simple, single-celled organisms that lacked cell membranes or nuclei, called prokaryotes (Doolittle, 2000). By as early as 3.4 Gyr ago, life may have adapted to exploit the abundance of solar energy with the first photosynthetic bacteria (cyanobacteria) (Summons *et al.*, 1999; Tice & Lowe, 2004); however, little is known about the origins of photosynthesis because there is no direct evidence of photosynthetic organisms from this time (Summons *et al.*, 1999). There is only suggestive evidence in the form of stromatolite fossils - microbial mats that may have harboured cyanobacteria similar to present-day microbial mats (Blankenship, 2010). Initially photosynthetic organisms are thought to have used anoxygenic (non-oxygen producing) mechanisms to photosynthesise (Nisbet *et al.*, 1995). The exact time at which oxygenic (oxygen producing) photosynthesis evolved is uncertain, with hydrocarbon biomarkers, derived from organisms producing and requiring O₂, found in sedimentary rocks suggesting that it could have arisen 2.7 Gyr ago, or even 3.2 Gyr ago (Buick, 2008). However, by 2.4 Gyr ago it had become the dominant form of photosynthesis (over anoxygenic photosynthetic pathways) on Earth (Nisbet *et al.*, 1995). This led to the next major event in Earth's history: the great oxygenation event.

As a by-product of oxygenic photosynthesis, oxygen started being released into the atmosphere, which, once oxygen sinks such as iron formations were filled, and combined with mechanisms that prevented all the oxygen generated being used in respiration and oxidation, such as organic carbon burial (Blank & Sánchez-Baracaldo, 2010; Tyrrell, 2013) led to an oxygen-rich atmosphere. The oxygenation of the atmosphere was not a steady process, as evidenced by banded iron formations in the geological record. These consist of layers of iron oxides and iron-poor shales and cherts, suggesting oxygen-rich and oxygen-poor environmental conditions respectively (Cloud, 1973). This may have been a result of cyclic changes in nutrient availability or changes in the abundances of prokaryote populations (Cloud, 1973). By the time Earth entered the Proterozoic eon, 2.5 Gyr ago, more complex eukaryotes (initially just single celled organisms, with nuclei and genetically integrated bacterial symbionts) first appeared, paving the way for the rise of multi-cellular

²There is some evidence to suggest that liquid water oceans existed before this time (Wilde *et al.*, 2001), but they were definitely present in the Archean eon

Factor	Value Range	Source
Temperature	Max.: 122°C Min.: -20°C	Takai <i>et al.</i> (2008) Canganella & Wiegel (2011)
Salinity (max.)	< 30% (approx.)	DasSarma & DasSarma (2012)
Pressure (max.)	Observed: 110 MPa Theoretically: 1600 MPa	Yayanos (1995) Sharma <i>et al.</i> (2002)
pH	Max.: 11 Min.: < 1	Horikoshi (1999) Macalady <i>et al.</i> (2004)
Water activity*	Min.: 0.61	Grant (2004)
Radiation	Max.: 30,000 Gray	Jolivet <i>et al.</i> (2003)

Table 1.1: The limiting factors for life on Earth. Adapted from O'Malley-James & Lutz (2013).
*A value between 0-1 describing the amount of water available for the hydration of materials

life approximately 1.2 Gyr ago (Butterfield, 2000; Strother *et al.*, 2011).

Earth entered its current eon, the Phanerozoic, 542 Myr ago. This is the period during which life diversified extensively, from the first simple animals to land plants, insects, amphibians, reptiles, mammals and birds - the complex and diverse forms of life that exist today. Today's familiar biosphere has only existed for a small fraction of Earth's lifetime as an inhabited planet. Knowing how much life on Earth has changed and how that life interacts with the planet at various stages helps to inform the search for life beyond Earth.

1.4 Searching for life in the universe

Finding life beyond Earth would revolutionise our knowledge and understanding of biology. Currently, biology is a science limited to making inferences from a sample set of one. It was once commonly assumed that life would be present on the other planets and rocky bodies in the solar system, from Lowell's vegetation on Mars to the 19th century astronomer Thomas Dick's civilisations of men on the Moon (Crowe, 1997). It was only as our knowledge of conditions in the rest of the solar system increased that we grew to see it increasingly as a place hostile to life (Clancy *et al.*, 2005). However, the situation has reversed to some extent due to the discovery of the physical extremes of factors, such as temperature, pressure and radiation, that some forms of life can tolerate and thrive in. These factors are summarised in Table 1.1. These limits are constantly being revised as new species are discovered, but the current known limits allow for a very wide range of habitable environments beyond Earth.

The search for life can loosely be split into two categories: the search for life within

the solar system and the search for life beyond the solar system. Hunting for life within the solar system has the advantage of proximity, allowing for a more thorough search; however, in order to find life as richly diverse and abundant as on Earth, our sights need to be set beyond the solar system to other stars that perhaps host Earth-like planets.

1.4.1 Finding other worlds

The first step towards searching for life beyond the solar system is to find the right kind of terrestrial (rocky) planets for life to live on. To date, over 1000 extrasolar planets (exoplanets) have been found and 1000s more are awaiting confirmation (Schneider, 2014). A variety of methods are used to detect exoplanets; the methods that have found the most exoplanets to date are the radial velocity method and the transit method. The gravitational microlensing method has also yielded exoplanet detections (Gaudi, 2012) and the method is less dependent on the mass of the planet compared to the transit and radial velocity methods, making it suitable for low-mass planet detection. However, events are rare and the host stars distant (Gaudi, 2012), making the kind of the follow-up observations needed for assessing biological activity difficult.

The radial velocity method involves looking for the gravitational pull of a planet on its host star, which can be detected as slight variations in the velocity with which a star moves towards or away from Earth; its radial velocity. This can be measured by observing the small displacements in the spectral lines of starlight caused by the Doppler effect (the changes in wavelength caused by the motion of the light source) via the standard Doppler formula

$$\frac{\lambda - \lambda_0}{\lambda_0} = \frac{V}{c}, \quad (1.1)$$

where λ_0 is the rest wavelength of the observed feature, and V is the radial velocity. The amplitude of the radial velocity variations, A_{RV} , is related to a planet's mass, allowing a minimum mass to be determined for a planet from

$$A_{RV} = \frac{2\pi a M_p \sin(i)}{(M_p + M_*) P \sqrt{1 - e^2}}, \quad (1.2)$$

where M_p and M_* are the planet and star masses respectively (with the quantity $\frac{M_p}{M_p + M_*}$ representing the effective mass of the system), a is the semi-major axis of the planet, e is the eccentricity of the planet and i is the inclination of the star-planet system with respect

to an observer's reference frame. This method only yields a minimum mass because the inclination of a system is not always known (Wright & Gaudi, 2013); hence, $M_p \sin(i)$ is found, rather than M_p .

The transit method involves observing the small decreases in the light intensity of a star when an orbiting planet moves in front of the star. This change in the flux from a star, ΔF , relates to the radius of the planet, R_p , such that

$$\frac{\Delta F}{F} = \frac{R_p^2}{R_*^2}, \quad (1.3)$$

where R_* is the radius of the star. When these two methods are applied to the same star system, combining radius and mass measurements enables the density of a planet to be constrained, which indicates what material the planet is likely to be made up of. Additionally, for a transit to occur, the condition $a \cos(i) \leq R_* + R_p$ must be satisfied, which places a constraint on the inclination of the system, helping to improve radial velocity mass estimates.

Finding a planet similar in size to Earth is difficult because the variations caused by planets of this size are similar in magnitude to the variations caused by stellar activity, e.g. changes in intensity caused by starspots (Makarov *et al.*, 2009; Wright & Gaudi, 2013). Many larger terrestrial planets in the 1-10 M_\oplus range³ have been found (Mayor *et al.*, 2011; Curto *et al.*, 2013; Kopparapu, 2013), 21 of which have been flagged as potentially habitable⁴, and some Earth-radius and smaller planets have already been confirmed from recent analysis of data from the *Kepler* space telescope, most notably Kepler-186f, a 1.1 R_\oplus planet orbiting at a distance that could allow liquid water to exist on its surface (Bolmont *et al.*, 2014). Other similarly sized planets have also recently been confirmed, e.g. Kepler-107d, Kepler-130b, Kepler-119c, albeit in very close-in orbits to their host stars (Rowe *et al.*, 2014). As techniques are perfected by better constraining the properties of host stars and improving detection of smaller planets, discoveries of more possibly habitable, Earth-sized planets are expected to come in the near future (Silburt *et al.*, 2014).

³1 $M_\oplus = 1$ Earth Mass = 5.972×10^{24} kg

⁴Planetary Habitability Laboratory: <http://phl.upr.edu/projects/habitable-exoplanets-catalog> and references therein.

1.4.2 The habitable zone

Having found candidate planets, the next stage in the search for life involves narrowing the list down to places that are more likely to host life: the concept of habitability. A habitable environment is one in which conditions fall within the phase space of physical limitations for life (see Table 1.1).

The initial assessment of a planet's habitability is constrained by the distance at which it orbits a star. The habitable zone (HZ) of distances around a star is defined as the region in which surface temperatures on a planet would permit liquid surface water to exist (Kasting *et al.*, 1993). Recent calculations define the Sun's HZ as the region from 0.99 - 1.70 au⁵ (Kopparapu *et al.*, 2013). For any given star the HZ boundaries for this simple definition of the HZ depend on the mass of the star, which determines its temperature, the age of the star, which effects its luminosity and the composition and mass of the planet's atmosphere. As a star evolves its luminosity changes, shifting the position of the HZ. Complex life is only likely to evolve if a planet stays within the HZ as the boundaries change over geological time periods, a concept known as the continuously habitable zone (CHZ) (Kasting *et al.*, 1993). Eventually, Earth will leave the HZ, rendering the planet uninhabitable (see Section 1.5).

The outer edge of the HZ is defined by the point at which the greenhouse gas CO₂ condenses out of the atmosphere. A greenhouse gas is any atmospheric gas that absorbs radiation at infrared wavelengths, causing bonds between atoms to vibrate, preventing some of the thermal energy radiated by the planet from escaping to space (Mitchell, 1989). The condensing CO₂ forms clouds, which reduce the atmospheric lapse rate (the rate of temperature decrease with increasing elevation in an atmosphere) as a result of the latent heat released during condensation (Kasting *et al.*, 1993). Increased cloud cover increases the amount of radiation reflected away from the planet, while a reduced lapse rate counteracts the greenhouse effect as warmer air reaches greater heights in the atmosphere, radiating longwave radiation away to space more easily (Kasting, 1993). The inner edge is defined as the distance at which a runaway greenhouse effect is triggered - a feedback effect resulting from the greenhouse warming caused by an increase in atmospheric water vapour, which then increases evaporation of surface water, further increasing the atmospheric water

⁵au = astronomical unit = average distance between the Earth and the Sun = 1.496×10^{11} m

vapour content and further increasing temperatures (see Section 1.5.1.). This is thought to have happened on Venus early in its history (Kasting *et al.*, 1993). For a planet like Earth, rising temperatures increase atmospheric water vapour content to such an extent that the stratosphere becomes moist. As water vapour is a greenhouse gas, this triggers further warming, eventually evaporating the oceans and making water vapour a dominant component of the atmosphere. At present, water vapour on Earth is almost entirely contained within the troposphere. Once water vapour reaches the upper atmosphere, it readily photodissociates and the hydrogen escapes to space. As a result of this process, all water would effectively be lost to space on a rapidly heating planet.

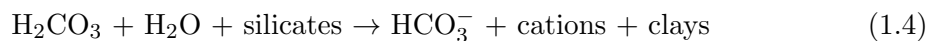
The HZ concept is best regarded as a guideline for evaluating a planet's habitability. Factors like the composition of a planet's atmosphere, cloud cover and the amount of radiation the planet reflects (its bond albedo) can alter surface temperatures, potentially bringing them above or below the liquid water range, even within the HZ. Additionally, there are many environments in the solar system, such as the sub-surface oceans of Europa and the upper-cloud decks of Venus (see Section 1.4.6.), that could be considered habitable that fall outwith the classical liquid water HZ. Some extensions to the classical HZ have been proposed that incorporate planetary mass, atmospheric composition and subsurface temperature profiles (e.g. Spiegel *et al.*, 2010; Abe *et al.*, 2011; McMahon *et al.*, 2013), but these are still based on planet-wide mean temperatures, missing out habitable regions on otherwise uninhabitable planets and moons.

1.4.3 Planetary properties and temperature

Throughout the Earth's history, the luminosity of the Sun steadily increased as a consequence of its main sequence evolution, steadily increasing the magnitude of solar radiation intercepted by Earth. However, this did not lead to a corresponding increase in global temperatures over the planet's lifetime. In fact, the early Earth was much warmer than expected despite a solar luminosity value that stood at 70% of the present value - a phenomenon known as the faint young Sun paradox (Sagan & Mullen, 1972). Many of theories used to explain this involve a stronger greenhouse effect than that of the present day Earth as a result of higher levels of greenhouse gases (Kasting & Catling, 2003; Güdel, 2007). However, other (less subscribed to) explanations include a more massive early Sun, which then lost this extra mass via intense solar winds (Gaidos *et al.*, 2000), or an increase in

protection from cosmic rays as a result of a stronger solar wind - cosmic rays can induce high altitude cloud formation, which could reduce planetary albedo (Shaviv, 2003).

Distance from a star is therefore not the only factor that influences a planet’s habitability. Despite being at a comfortable distance from the Sun and the gradually increasing solar luminosity, the Earth has undergone several ice ages in the past, with some periods where glaciation reached equatorial regions leading to “snowball Earth” states (Tyrrell, 2013). Changes in the greenhouse gas content of the atmosphere and changes in continental configurations may have contributed to lower temperatures. For example, a snowball Earth state 2.2 Gyr ago may have been caused by the rise in atmospheric oxygen, which reacted with CH₄ in the atmosphere, converting it to CO₂, a less potent greenhouse gas (Kasting & Ono, 2006). Similarly, when the super-continent *Rodinia* began to break up, approximately 750 Myr ago, precipitation runoff (the flow of precipitation water over land surfaces) increased, leading to an increase in the rate of silicate weathering (Donnadieu *et al.*, 2004). This occurs because CO₂ in the atmosphere dissolves in raindrops as they fall, forming a weak carbonic acid (H₂CO₃). When this comes into contact with silicate minerals, bicarbonate ions form, removing CO₂ from the atmosphere:



Increased runoff increased the land surface area that precipitation encounters, drawing down more CO₂ from the atmosphere, reducing the greenhouse effect and cooling the planet (Donnadieu *et al.*, 2004).

The extent of a planet’s habitability is also influenced by the planet’s orbital parameter variations. Changes in these parameters can be responsible for extreme climate variations such as ice ages and ice-free periods, which would alter the types, abundance and distribution of life on the surface. Changes in obliquity, eccentricity and precession of equinoxes all influence regional and global climate on Earth over geological time. These variations were predicted by Milankovitch (1941) to follow cycles as a result of gravitational interactions between the Earth and other bodies in the solar system. Evidence of temperature fluctuations from ice core samples (Genthon *et al.*, 1987) and from the growth rates of fossil coral reefs (that were found to vary in response to past warm and cold eras, which varied according to Milankovitch cycle predictions) (Broecker *et al.*, 1968) support this. Collec-

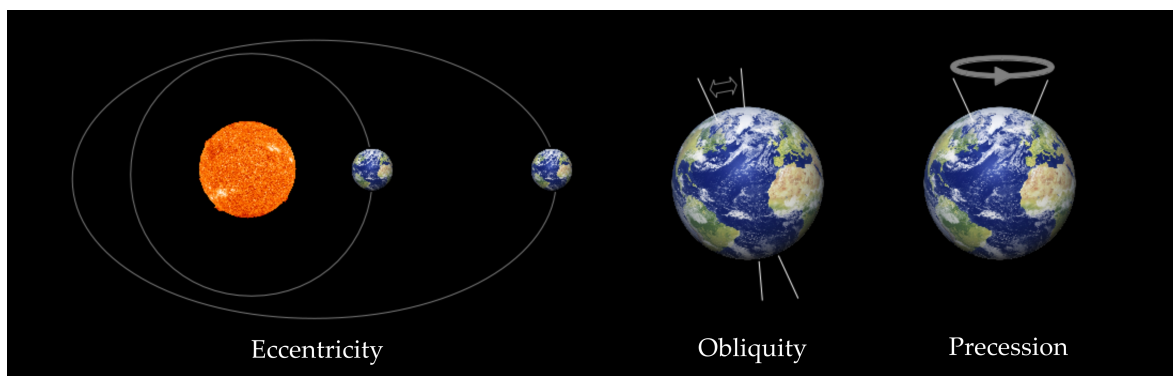


Figure 1.5: Milankovitch Cycles. The eccentricity, tilt (obliquity) and the orientation of the rotation axis (precession) vary cyclically over geological time; collectively known as the Milankovitch Cycles. Increased eccentricity causes the planet to spend part of its orbit further from the Sun (as illustrated by the circular orbit (zero eccentricity) and the elongated orbit (high eccentricity) in the left-hand illustration). Hence, increased eccentricity reduces the radiation flux received over the course of a year. Increased obliquity causes higher latitudes to receive more insolation and lower latitudes less insolation. Axial precession can influence seasonal differences between the northern and southern hemispheres: at present the northern hemisphere summer occurs during aphelion, whereas southern hemisphere summer occurs during perihelion, resulting in hotter summers in the southern hemisphere and warmer winters in the northern hemisphere. This situation reverses over the course of a precession cycle.

tively these are known as the Milankovitch Cycles. On Earth, precession (the orientation of the axial tilt) occurs on a cycle approximately between 19,000-23,000 years, obliquity (the extent of the axial tilt) varies between 22.1° and 24.5° (larger obliquity changes are prevented by the presence of a large moon - Laskar *et al.*, 2004) approximately every 41,000 years and eccentricity cycles between 0 and 0.06 approximately every 100,000 years (Paillard, 2010; Vásquez *et al.*, 2010). Internal properties of a planet also influence its habitability. Plate tectonics, driven by a planet's molten core, affects the recycling of gases like CO_2 to the atmosphere and results in the long-term supercontinent cycles. As the core of a planet cools, tectonic activity decreases, slowing the recycling of gases that may be essential for life. A cooling core also weakens a planet's magnetic field, weakening the protection against the flux of charged particles from the solar wind and cosmic rays that can strip away the upper atmosphere, weakening the ozone layer (Lundin *et al.*, 2007). This allows more DNA-damaging ionising UV radiation to reach the surface.

Other properties of a planet also influence its habitability. A planet's rotation rate alters the duration of the day-night cycle, affecting the efficiency of the transport of heat within an atmosphere. On Earth, heat is presently distributed away from the low latitudes to high latitudes, diffusing out from the tropics (a hot reservoir) to the poles (a cold reservoir) - a process known as latitudinal heat diffusion. Spiegel *et al.* (2008) showed

that the efficiency of this process increases with increasing planetary rotation rate, leading to a more uniform temperature distribution on a planet as rotation rate is increased and vice versa. Heat diffusion is also affected by the density of a planet's atmosphere. As atmospheric density increases, the efficiency of heat distribution increases. Hence, although Venus has a very slow rotation rate (224.65 days), it also has a very dense atmosphere, allowing slow but powerful winds to redistribute heat, leading to a uniform global temperature distribution. The fractions of land-, ocean- and ice-cover also influence climate. These all reflect differing fractions of the incoming radiation (a property called albedo), resulting in different heat capacities (the amount of energy required to raise the temperature by one degree) for the atmosphere above different surfaces. Sea ice and deserts reflect more radiation than oceans and forested land, for example. In particular, oceans absorb a large amount of incoming radiation; hence more energy is required to heat the atmosphere above ocean surfaces than over land surfaces, leading to a heat capacity 40 times greater than the mean heat capacity for the atmosphere above land surfaces (Spiegel *et al.*, 2008).

The variety of different factors that can affect a planet's habitability, can lead to a wide range of potential habitable environments. Even small variations from Earth-like conditions can change the the types and abundances of life that a planet could support, suggesting that identifying an Earth-mass planet, comfortably within the HZ is only a first step towards truly classifying the habitability of a planet.

1.4.4 The extremes of life on Earth

Having assessed an environment's habitability, the next question to answer is what type of life could inhabit that environment. Conditions in the habitable environments within the solar system overlap with those in extreme environments (those in which conditions are similar to the upper or lower boundaries of one or more of the limiting factors for life described in Table 1.1) on Earth. Therefore, studying life that exists within these environments can help constrain the search for life in extreme environments beyond Earth.

Organisms that thrive under extreme conditions are known as extremophiles. In fact, it is thought that life may have arisen in a high temperature environment ($> 90^\circ$ - Miller & Lazcano, 1995) on the early Earth (one that would be considered extreme in comparison to most habitats on Earth today) given the thermal tolerances seen in the most ancient

lineages of microbial life that are still found on Earth today (Harvey, 1924; Stetter, 1994; Miller & Lazcano, 1995). However, this is still a disputed claim and an argument against this suggests that hyperthermophiles may have out-competed other organisms after the emergence of life (Miller & Lazcano, 1995). In either case, this suggests that the ability to survive in extreme temperature environments has existed for much of the history of life, making it more likely that life elsewhere could exhibit a similar tolerance for high temperature conditions (Seckback & Owen, 2000; Schulze-Makuch & Irwin, 2008).

Most organisms that can tolerate or even thrive under extreme conditions are microorganisms and are found in a variety of extreme environments on Earth. For example, there are hyperthermophile organisms (those that thrive at high-temperatures), such as the archaeon *Geogemma barossii* that can grow at temperatures of 121°C (Kashefi & Loveley, 2003) and the methanogen *Methanopyrus kandleri* that can grow at temperatures of 122°C (Takai *et al.*, 2008). Others, like the bacterium *Deinococcus radiodurans*, can survive doses of ionising radiation up to 15,000 Gray (Battista, 1997). Not all extremophiles are unicellular microbes, however. Ice worms, for example, live within ice channels in glaciers (Shain *et al.*, 2001) and tardigrades, water-dwelling micro-animals, can endure multiple extremes, including exposure to space (Jönsson *et al.*, 2008). In many cases, survival

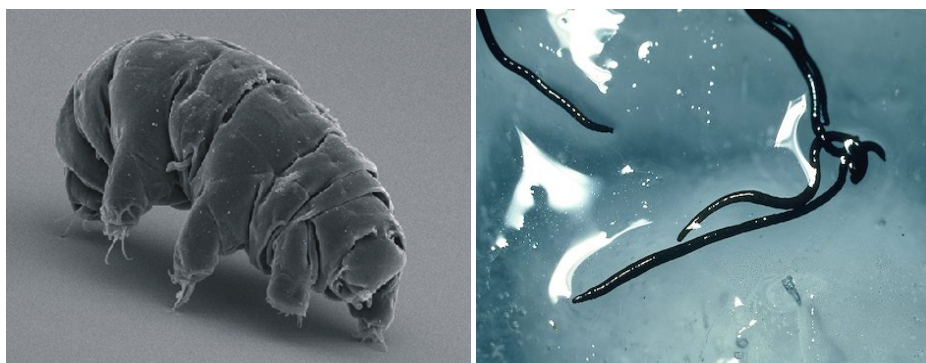


Figure 1.6: Animal extremophiles. Left: *Hypsibius dujardini* (Tardigrade or water bear); Right: *Mesenchytraeus solifugus* (Ice worm). Image source: from Schokraie *et al.* (2010) under the Creative Commons Attribution License.

in extreme environments tends to be achieved by maintaining clement conditions within cells, essentially creating a more moderate inner-environment (Rothschild & Mancinelli, 2001). Examples range from the case of microalgae that survive the arid Atacama Desert by living on dew collected on spider webs in caves (Azua-Bustos *et al.*, 2012) and filamentous cyanobacteria that produce amorphous silica encasings, which appear to act as

protective shields against most UV-B and UV-A radiation, without blocking photosynthetically active radiation (Azua-Bustos *et al.*, 2012), to acidophiles (organisms that tolerate very low pH environments) that consistently maintain a higher internal pH to metabolise (Rothschild & Mancinelli, 2001).

By knowing the types of life able to survive in certain environments, the signatures associated with certain metabolisms can be evaluated, allowing methods for detecting the presence of life to be developed.

1.4.5 The signatures of life

In astrobiology, a biosignature is anything that can be observed or measured that indicates the presence of life. These fall into two broad categories: (i) remotely detectable biosignatures (often spectrally detectable atmospheric gases), which are most applicable to observations of extra solar planets, and (ii) in-situ biosignatures, which are more applicable to the study of solar system bodies, for example, during rover sampling missions to the surface of Mars.

These are all based on what is known about how life on Earth interacts with its environment. This makes identifying a rich, Earth-like biosphere on an Earth-analogue exoplanet theoretically easier than detecting much less diverse and abundant biospheres within the solar system. Table 1.2 summarises the main biosignatures associated with Earth’s biosphere.

Other gases produced by microbial life, such as CO₂, N₂, H₂, H₂S, SO₂, NO and NO₂ are also produced (often in larger quantities) abiotically, via volcanic outgassing or photochemistry, making them “non-unique” biosignature gases (Seager, 2010). They would also, in some cases, not be readily remotely detectable due to the small quantities that would be produced on an Earth-like planet.

Life on less Earth-like exoplanets would not exhibit a suite of biosignatures like those on Earth. For example, arid desert worlds could host plant life, but vegetation would probably be sparse and reflective over a range of wavelengths to prevent moisture loss, leading to a lack of a red-edge spectral feature for such planets. A desert world would also encourage photosynthetic organisms to seek refuges below substrates to a depth that would still permit a sufficient radiation flux for photosynthesis, but would prevent a red-edge

Biosignature	Source
Oxygen/Ozone (O ₂ /O ₃)	O ₂ in Earth’s atmosphere is a result of oxygenic photosynthesis. If present in large concentrations (with other reduced gases) O ₂ and O ₃ could be evidence for photosynthesis (Kiang <i>et al.</i> , 2007a). Large concentrations are generally not thought to be caused by abiotic processes, but recent work suggests photolysis in water-rich atmospheres could produce a similar signature (Wordsworth & Pierrehumbert, 2014). O ₃ produces a strong atmospheric absorption line at infrared wavelengths and, as it depends on continually replenished atmospheric O ₂ , is more readily detectable.
Liquid water (H ₂ O)	While not an indicator of life itself, the presence of liquid water, which is essential for all known life, on a planet, alongside other biosignatures, would help strengthen the case for the presence of life. As well as detecting water in the atmosphere, the glint of star light from exoplanet oceans may also be spectrally detectable (Williams & Gaidos, 2008).
Methane (CH ₄)	CH ₄ has both biological and non-biological sources (e.g. serpentinisation) on Earth. If CH ₄ is present in large quantities, it suggests a biological source. The abiotic CH ₄ flux on Earth today is 5.3×10^{13} g year ⁻¹ (Burton <i>et al.</i> , 2013), while the biological flux is an order of magnitude greater: $5-8 \times 10^{14}$ g year ⁻¹ (Ehhalt, 1974), largely from the decay of organic matter.
Ammonia (NH ₃)	On Earth NH ₃ is released into the biosphere at a similar rate to CH ₄ , but has a shorter lifetime under UV irradiation (Kaltenegger <i>et al.</i> , 2010). Abiotic N ₂ reduction can also act as an NH ₃ source (Brandes <i>et al.</i> , 1998).
Nitrous oxide (N ₂ O)	Produced in abundance by biological processes; only in small quantities by photochemistry. However, if concentrations in an atmosphere were similar to those on Earth, high spectral resolutions would be required to detect this (Kaltenegger <i>et al.</i> , 2010).
Organosulphur compounds	Methanethiol (CH ₃ SH) is a product of the decay of biological material. No other known process could cause its abundant presence (Pilcher, 2003; Seager, 2010). Spectral observation would be possible, but it has a very short atmospheric lifetime. Dissociated methyl groups from CH ₃ SH combine to form ethane (C ₂ H ₆) in the atmosphere. This has a much longer lifetime than CH ₃ SH (Domagal-Goldman <i>et al.</i> , 2011), making it a better biomarker. Dimethyl sulphide, (CH ₃) ₂ S, is the most abundant sulphur compound emitted to Earth’s atmosphere, largely by phytoplankton.
Vegetation “red edge”	Caused by the sharp increase in leaf reflectance at 700 nm exhibited by the majority of land vegetation on Earth. Photosynthesis on Earth is adapted to the peak photon flux from the Sun; hence, on other planets the red edge feature may be observed at different wavelengths depending on the type of star (or stars) an exoplanet orbits (Kiang <i>et al.</i> , 2007a,b; Raven (2007); O’Malley-James <i>et al.</i> , 2012). However, this is not an inevitable biosignature of an Earth-like planet, but depends on the abundance of land vegetation and its reflectivity. Assumes presence of chlorophyll.

Table 1.2: Summary of biosignatures of Earth-like life

being detected (Cockell *et al.*, 2009). However, detecting combinations of biosignatures in the atmospheres of these planets, the presence of which cannot easily be explained by non-biological processes, would still lend support to a case for the presence of life.

Biosignature detection

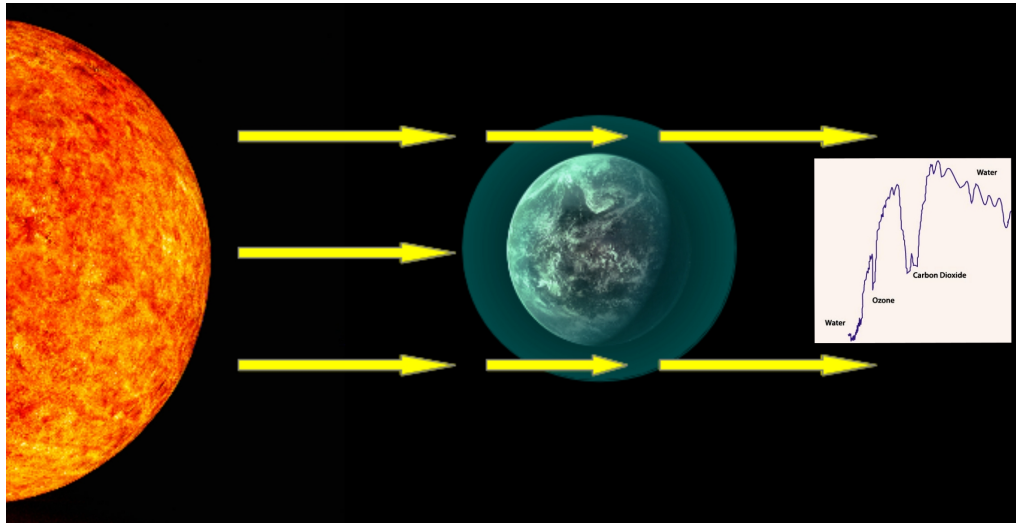


Figure 1.7: Atmospheric transmission spectra. When a planet passes in front of its host star, with respect to an observer, starlight passes through the planet’s atmosphere. Molecules in the atmosphere absorb light at certain wavelengths, producing signatures of the atmospheric composition.

When a planet transits its host star, it provides an opportunity to study the composition of the planet’s atmosphere (Seager, 2010). Any biosignature gases present at detectable levels can be remotely sensed by analysing light from the host star that passes through the planet’s atmosphere (Figure 1.7). By removing the spectral features of the star (when the planet is not transiting) from the combined spectral features of the star and the planet’s atmosphere, a transmission spectrum can be obtained. Additionally, when a planet passes behind its host star (secondary transit), the small contribution the planet makes to the total light observed disappears. Disentangling this light from the light from the host star enables surface reflectance features, such as the vegetation red edge, to be observed. The moons of giant extrasolar planets in the HZ (exomoons) could also potentially be detected using transit timing variations, light curve distortions or planet-moon eclipses (Kaltenegger, 2010). Transmission spectroscopy could also be used to characterise the habitability of Earth-like exomoons (Kaltenegger, 2010).

However, to date, this method has only been able to reveal the atmospheric composi-

tions of some hot Jupiter planets (Jupiter-sized planets orbiting close to their host stars) (Tinetti *et al.*, 2010; Désert *et al.*, 2011; Shporer *et al.*, 2014). The method’s potential has been limited by the available technology. It is an observationally challenging technique, placing the analysis of the atmospheres of Earth-like planets beyond the reach of current ground and space-based telescopes. Most atmospheric composition results have been obtained using the *Hubble* and *Spitzer* space telescopes, removing interference from Earth’s own atmosphere (Tinetti *et al.*, 2010; Désert *et al.*, 2011). Future space missions such as the *James Webb Space Telescope* would push back the limitations on this technique, making it feasible to detect atmospheric spectral features of super-Earth planets (planets in the mass range $1 - 10M_{\oplus}$) (Deming *et al.*, 2009; Miller-Ricci & Fortney, 2010). Some ground-based observations could also be possible. It has been proposed that oxygen in exoplanet atmospheres could be detected using future ground-based telescopes, such as the *European Extremely Large Telescope*, using adaptive optics to filter out interference from Earth’s own oxygen spectral features (Kawahara *et al.*, 2012). Yet, even with more advanced telescopes, there will still be problems to overcome due to interference from clouds in a planet’s atmosphere and the long times between transits for Earth-like planets orbiting within the HZ of Sun-like stars. The magnitude of these problems is reduced for a super-Earth planet, orbiting in the HZ of a cool, low-mass star. The HZ of such a star would be very close-in to the star, resulting in a short orbital period for the planet, while a cooler star would make disentangling the starlight from the light reflected from the planet easier. Given the abundance of low-mass, M-class stars (75% of all stars in the galaxy are M stars - Guinan & Engle, 2009), it is probable that the first terrestrial exoplanet atmosphere to be analysed will belong to a super-Earth orbiting close to a low-mass star. Observations of the atmospheres of Earth-sized planets will come further into the future. For this to be possible, the stronger source of light from the host star would need to be separated from the light coming from the target planet, either using nulling interferometry, where two observations are made and then combined after a signal delay has been induced between the two observations such that the star light is cancelled out (Léger *et al.*, 1996; Mennesson & Mariotti, 1997), or a direct-imaging telescope, which blocks out the stronger source of light from a star in order to view the fainter planet (Seager, 2010).

1.4.6 Life in the solar system

The relative proximity of solar system bodies provides alternative life-detection options to remote spectral characterisation. Spacecraft and landing missions can be (and have been) sent to perform a variety of in-situ tests to determine if life is, or has been, present. The following section discusses the potential for life within the solar system and how its presence could be inferred.

Mars has perhaps the most famous and long-standing connection with the idea of extraterrestrial life, but Mars presents quite a hostile environment for life: freezing temperatures, little available liquid water and, due to the thin atmosphere and weak planetary magnetic field, little protection from biologically damaging radiation. However, this has not always been the case. Evidence suggests that there were three distinct climate stages over Mars' geological history, from a water-rich early phase, to a cold semi-arid phase, to a cold desert phase (Fairén *et al.*, 2010). Hence, the planet had three different habitability stages over the lifetime of the planet, from a habitable early stage to a largely uninhabitable final stage (Fairén *et al.*, 2010). There is plenty of geomorphic evidence for the existence of past and present water on Mars: from ice patches and subsurface ice to features consistent with glaciers and river channels (Baker, 2006) and the discovery of the minerals haematite, jarosite and goethite (Christensen *et al.*, 2000; Madden *et al.*, 2004; Farrand *et al.*, 2009), that only form in the presence of liquid water. Most recently NASA's *Curiosity* rover mission has found strong evidence for flowing surface water in the planet's past (Williams *et al.*, 2013). Early Mars was likely water-rich (Fairén *et al.*, 2010; Squyres & Kasting, 1994), but, after approximately 4 Gyr ago, it was probably also cold with temperatures $< 0^{\circ}\text{C}$ (Shuster & Weiss, 2005), suggesting that if liquid surface water were present later in the planet's lifetime, some other mechanism that allowed liquid water to exist on the surface, such as Martian water having a high salinity, would have been required (Fairén *et al.*, 2009). This does not preclude life originating on early Mars, although it does suggest that the planet was not quite as hospitable as previously thought. The Martian climate progressed to a cold semi-arid epoch during which it is likely that there was a global, thick cryosphere ("Snowball Mars") followed, more recently, by a colder desert-like epoch in which liquid water is absent (or at least extremely rare), making the planet increasingly less hospitable to life as we know it (Fairén *et al.*, 2010).

‘Less hospitable’ does not necessarily imply that present day Mars is uninhabitable. There are many regions (at least in the sub-surface) of the planet deemed habitable (Córdoba-Jabonero *et al.*, 2005; Wang *et al.*, 2010). Soil temperatures can occasionally reach 27°C (as estimated by the Viking Orbiter Thermal Mapper) and, at a depth of 1-2 mm, the top layer of soil would provide adequate protection from biologically harmful UV radiation (Pavlov *et al.*, 2010) - a result of the lack of a protective ozone layer in the oxygen-poor Martian atmosphere (Rettberg *et al.*, 2004), caused by the lack of a strong planetary magnetic field. Observations made by the *Mars Odyssey* spacecraft using a high energy neutron detector suggest there is a large volume of water on Mars, corresponding to a planet-wide subsurface water-ice layer 20 cm thick (Mitrofanov *et al.*, 2002). Sub-surface water ice is known to exist on the planet (Christensen *et al.*, 2000) and this may theoretically become biologically available when diurnal temperature variations (or seasonal temperature variations at the poles) cause the frozen water to sublimate through the surface regolith, leaving condensed films of water attached to soil particles as it does so (Pavlov *et al.*, 2010).

Recent claims of the detection of seasonal methane plumes emanating from three distinct regions on Mars (Mumma *et al.*, 2003) have fuelled speculations that there could be life currently living on the planet. On Earth, methane in the atmosphere is largely biological in origin; hence suggestions that this could be an indicator of biological activity on Mars (although there are abiotic mechanisms that could also be responsible for the atmospheric methane - McMahon *et al.*, 2013). However, there are some problems with the Martian methane detection claims. Methane should have a lifetime of 100s of years in the Martian atmosphere, yet the observed lifetime (weeks to months) is much shorter, which requires a strong methane sink to be present; something that seems physically implausible given current geochemistry knowledge (Zahnle *et al.*, 2011). Zahnle *et al.* (2011) call into question the detection of methane, both from ground based observations on Earth and *Mars Express* orbital observations, due to contamination of results by Earth’s atmosphere and poor model fitting to data, respectively.

Experiments in which organisms have been placed under simulated Mars conditions have shown that some terrestrial organisms could be suitable for life on Mars (Cockell *et al.*, 2005b; Morozova *et al.*, 2007; Schirmack *et al.*, 2013; de Vera *et al.*, 2013). In particular, recent experiments on the lichen *Pleopsidium chlorophanum*, which is found in

high-altitude habitats in Antarctica, have found that these organisms, given some protection from the high biologically damaging radiation flux received at the Martian surface, could survive and continue to photosynthesise (de Vera *et al.*, 2013). Methanogens have also been shown to be able survive under Martian conditions (Schirmack *et al.*, 2013). Even ‘higher organisms’ have been observed under Mars-like conditions, although these relate to making Martian conditions more suitable for habitation. Boston *et al.* (2003) placed mice (dubbed ‘mousetronauts’) in a sealed facility designed to simulate a proposed habitable cave environment for future human astronauts, which uses Argon (an easily extractable gas from the Martian atmosphere that is inert and a good thermal insulator) at normal atmospheric pressure as part of the breathable air-mixture. With present-day technology it would be feasible to alter parts (or even the entirety) of the Martian environment to make it more habitable via converting cave environments (Boston *et al.*, 2003) or terraforming the planet. Terraforming Mars would involve introducing potent greenhouse gases, then oxygen-producing microorganisms and plants - McKay & Marinova, 2001); although fully terraforming the planet would take $> 100,000$ years (McKay & Marinova, 2001). However, given that the existence of native life on the planet has yet to be ruled out, this raises the ethical questions of whether we should introduce terrestrial life that could wipe out an existing Martian biosphere or erase evidence of fossil Martian life (see, for example, McKay & Marinova, (2001), Cockell (2005), Arnould & Debus (2008)).

Earlier in its history, Venus may have had liquid water oceans, with surface conditions favourable for the development of life. However, a runaway greenhouse effect has led to the loss of these oceans and today surface temperatures on Venus are, on average, 460°C (Williams, 1999), which, combined with the rapid recycling of its crust (Shirley & Fairbridge, 1997), makes the surface of Venus uninhabitable for even the most extreme forms of life discovered to date. However, Venus may not be completely inhospitable to life. The possibility of life in the cloud decks of Venus has long been postulated (Sagan & Morowitz, 1967; Sagan & Saltpeter, 1976; Cockell, 1999; Schulze-Makuch & Irwin, 2002; Schulze-Makuch *et al.*, 2004). Any life that may have evolved in the early Venusian oceans could have migrated upwards as the oceans evaporated. Small quantities of water vapour are available in the Venusian cloud layers at altitudes where temperatures fall within the habitable range (Landis, 2003; Schulze-Makuch, 2004). Any airborne biosphere here would have to be able to tolerate the high sulphuric acid content of the clouds and withstand

the intense ultraviolet radiation levels, but it is thought that a form of photosynthetic or chemosynthetic extremophilic sulphur bacteria would be able to exist in these conditions (although this would need to have a greater tolerance to acidic conditions than known sulphur oxidising species on Earth). In fact, some of the trace gases (H_2S , SO_2 , COS) in the clouds could be indicators of sulphur-based microbial life (Cockell, 1999).

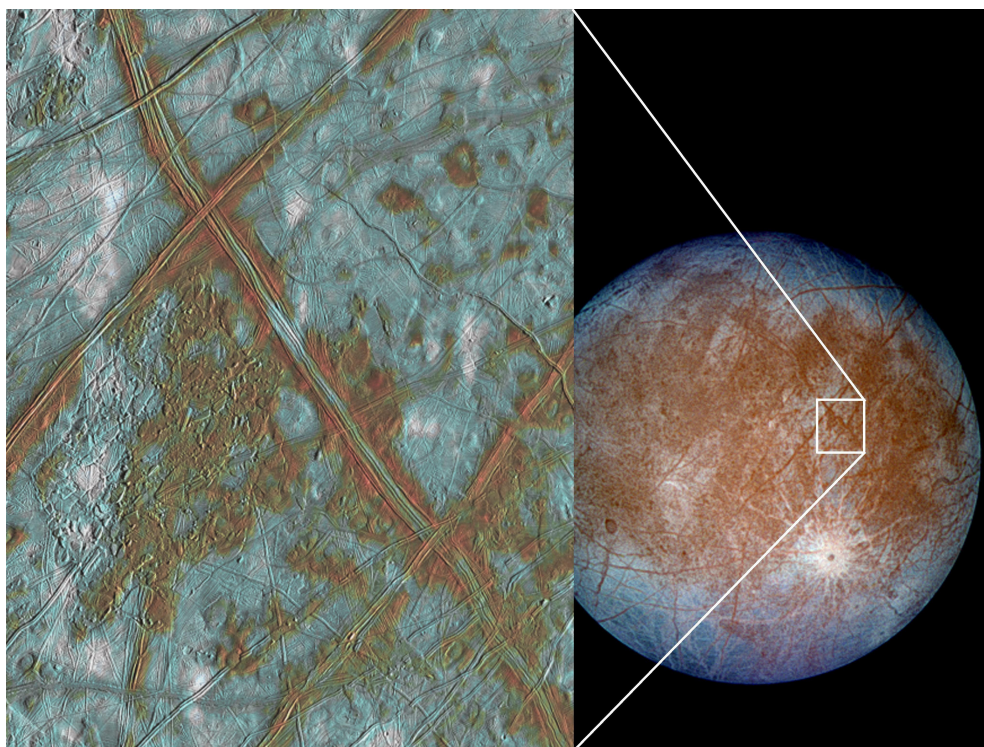


Figure 1.8: Linea on the surface of Europa, suggesting a geologically active young surface. *Image credit: NASA/JPL/University of Arizona.*

Jupiter’s moon Europa and Saturn’s moons Enceladus and Titan are examples of the more astrobiologically interesting outer solar system objects. Europa is one of the major targets in the search for life outside the inner-solar system. There is evidence that the ice-covered moon harbours a briny ocean beneath the outer crust of ice (Marion *et al.*, 2003). There is strong evidence for the existence of this sub-surface ocean, especially after recent *Hubble* observations of plumes of water emanating from the surface (Carr *et al.*, 1998; Roth *et al.*, 2014). Spectroscopy suggests that Europa has an icy crust approximately 150 km thick and a rocky interior (Carr *et al.*, 1998). Voyager and Galileo images show the surface of the moon to be crossed with linea and few crater marks, suggesting a geologically young surface (cf. Figure 1.8). This may be due to a liquid layer beneath the surface layer of ice, which remains unfrozen due to tidal heating effects caused by the gravitational pull

of Jupiter and the other Gallilean moons.

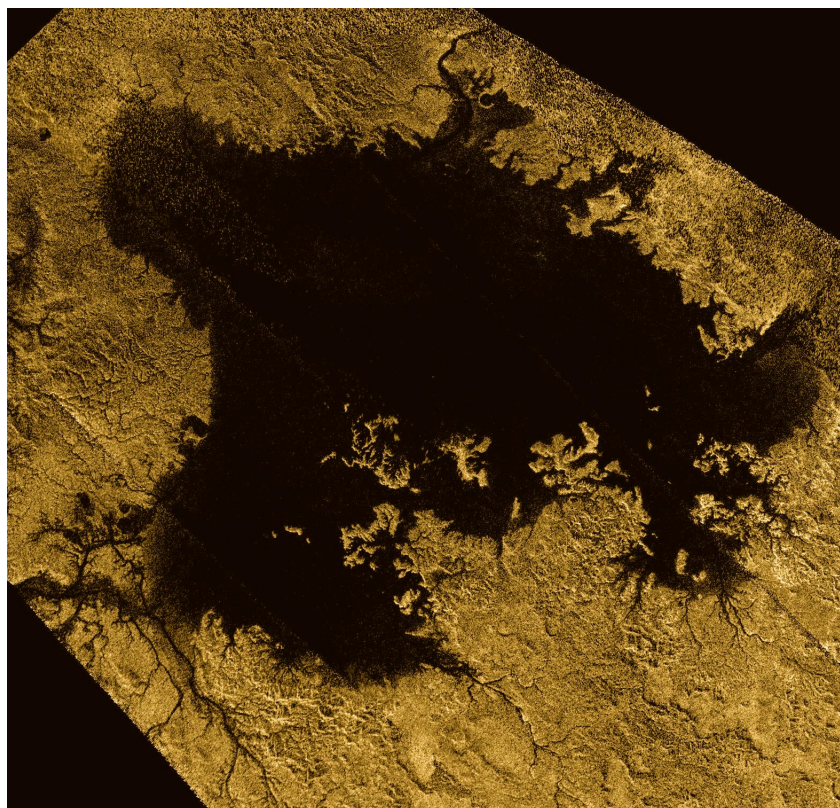


Figure 1.9: Liquid hydrocarbon lake on the surface of Titan taken by the *Cassini* spacecraft. *Image credit: NASA/JPL-Caltech/ASI/Cornell.*

There is also evidence, in the form of observed jets of ice and water emerging from the moon's south pole, for subsurface liquid water on Enceladus (Hansen *et al.*, 2006). When sampled by the Cassini spacecraft these plumes were found to contain simple organic compounds (McKay *et al.*, 2008).

Saturn's moon Titan is known to have a large inventory of organic chemicals (Coustenis *et al.*, 2010). Both methane and complex hydrocarbons have been detected on the moon, which has a methane-cycle analogous to Earth's water cycle with CH₄ lakes, rain and clouds (cf. Figure 1.9 - Stofan *et al.*, 2007). There is also evidence for water ice and carbon dioxide ice on the surface (Coustenis *et al.*, 2010). It is a moon dominated by organic chemistry. A thick haze layer of organics surrounds the moon as a result of photochemistry in a largely CH₄/N₂ atmosphere. A similar haze layer may have been present on the early Earth (Trainer *et al.*, 2006), when the atmosphere may have been dominated by CO₂, CH₄ and H₂ (Kasting & Catling, 2003; Kasting, 2011), resulting in similar photochemistry to that seen on Titan and therefore making Titan a good analogue

for the pre-biotic Earth (Trainer *et al.*, 2006), making it a particularly interesting target for research into the origins of life.

1.4.7 Life beyond the solar system

With (to date; July 2014) 21 potentially habitable exoplanets discovered and 100 HZ exoplanet candidates⁶, the range of possible environments for life beyond the solar system is beginning to grow. While any life elsewhere in our solar system will more closely resemble life found in extreme environments on Earth, the potential for Earth-like environments beyond the solar system increases the diversity of possibilities for life. This means that the best chances for finding rich, diverse biospheres will be on extrasolar Earth-like planets or Earth-analogue planets (planets with some similar habitable environments to Earth and planets that are very similar to Earth in terms of size, climate and range of habitable environments, respectively).

It is on planets such as these that macroscopic plants and animals would be best able to survive. Primary productivity on such planets is likely to be photosynthesis as the most readily available and abundant energy source would be the host star. On Earth, the first photosynthetic life used anoxygenic photosynthesis. By 2.4 Gyr ago oxygenic photosynthesis had become the dominant form of photosynthesis on Earth (Blank & Sáncchez-Baracaldo, 2010). Planet-wide oxygenic photosynthesis lends itself to remote detection in two main ways: it produces an oxygen/ozone-rich atmosphere and abundant surface vegetation produces an infrared reflectance signal in the planet's spectrum. Finding these signatures in the spectrum of an extrasolar planet would provide good evidence for the presence of life.

As the limits of life on Earth are explored, the boundary conditions for habitability are pushed further away from the constraints of the traditional HZ. This allows for planets to be considered habitable, but not necessarily Earth-like. Ocean planets, arid planets, ice planets and even rogue planets that have been ejected from their original systems and are travelling through interstellar space can all potentially be considered habitable. For these cases, it is the extremes of life on Earth that hint at the possible biospheres.

⁶Planetary Habitability Laboratory: <http://phl.upr.edu/projects/habitable-exoplanets-catalog> and references therein.

1.5 The future of life

Since life first began on Earth it has changed and evolved considerably and it will continue to do so into the geological future. The lifetime for which any planet remains habitable is limited.

1.5.1 Solar evolution and extreme climate change

One of the main influences on the long-term future of life on Earth will be the evolution of the Sun over the next 3 Gyr. The Sun is classified as a G2 V star - *G2* describes its effective temperature (approximately 5778 K) and the *V* describes it as a dwarf star, i.e. a star that is currently at the main sequence stage of its evolution, the stage during which a star produces energy by converting hydrogen to helium in its core. With an age of 4.57 Gyr, it is approximately half-way through its main sequence evolution.

As main sequence stars age, their luminosity (or intrinsic brightness) increases; a direct result of fusion reactions that occur in their stellar cores. In the core of a star fusion reactions convert four H atoms into one He nucleus, decreasing the H abundance in the core over time and increasing the mean molecular weight of the core. Stellar material is an almost perfect gas, which means its behaviour can be approximated by the ideal gas law $PV = nR_gT$ for a pressure P , a volume of gas V and a number of particles n at a temperature T . R_g is the universal gas constant. Assuming the core of a star consists of n particles of mass m_g , the ideal gas law can be used to show that

$$P \propto \frac{\rho T}{m_g} \quad (1.5)$$

Therefore, an increase in mean molecular weight in the core over time requires an increase in ρT to maintain hydrostatic equilibrium. The increase in the core's mean molecular weight leads to a corresponding decrease in core pressure, resulting in the contraction of the core as it can no longer support the surrounding outer envelope of gas. This increases the core density, resulting in a release of gravitational potential energy, which increases the fusion rate and increases the temperature of the core via the virial theorem, which links the gravitational potential energy and thermal energy such that

$$T \propto \frac{GMm_g}{Rk_B} \quad (1.6)$$

where, in this case, M is the mass of the core and R is its radius, G is the gravitational constant and k_B is the Boltzmann constant. By substituting in the density ρ , this implies that $T \propto m_g M^{\frac{2}{3}} \rho^{\frac{1}{3}}$. Thus, increasing m_g and ρ increases temperature. This increase in temperature results in a gradual increase in luminosity ($L \propto T^4$), which continues until hydrogen is exhausted in the core (approximately 10 Gyr after entering the main sequence for a solar mass star). Thermal equilibrium is then destroyed in the star and the core contracts, heating the outer shell to hydrogen fusion temperatures, causing the star's outer envelope to expand and marking the beginning of the red giant stage in the star's evolution (see Figure 1.10).

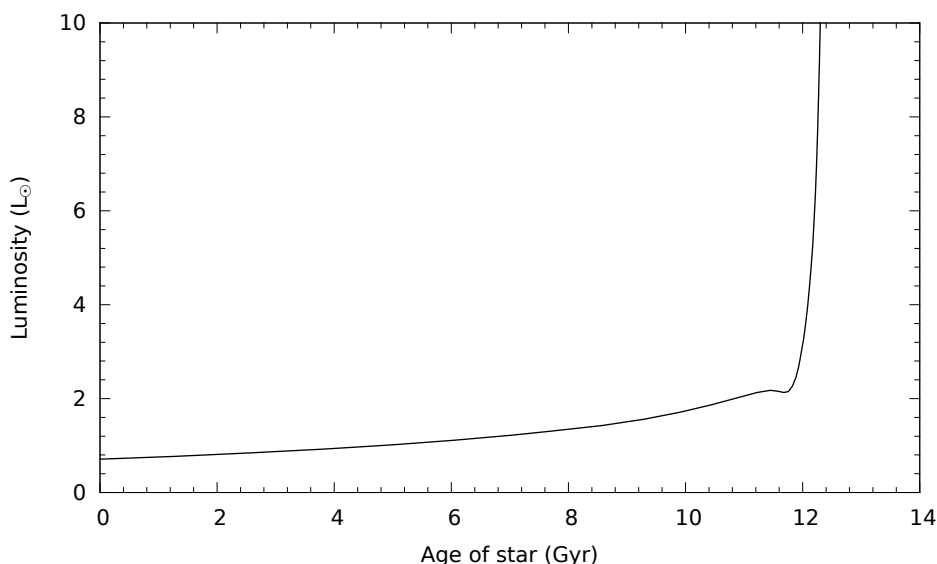


Figure 1.10: Expected luminosity evolution for a $1 M_{\odot}$ star from the beginning of its main sequence lifetime. Luminosity increases steadily until hydrogen in the core is exhausted (after approximately 10 Gyr), which destroys thermal equilibrium in the star. The core of the star contracts, heating an outer shell to hydrogen burning temperatures and causing the star's outer envelope to expand (red giant phase). Within 2 Gyr of leaving the main sequence, core contraction increases the core temperature sufficiently for helium fusion to ignite (helium flash). The helium flash initially causes a drop in luminosity as the ignition of helium breaks down electron degeneracy in the core, allowing it to behave as an ideal gas and expand rapidly and cool, decreasing the temperature of the hydrogen burning shell surrounding it. The outer envelope then contracts, increasing temperature and, thus, luminosity again. Data from: <http://stev.oapd.inaf.it/YZVAR/>

The significance of this increase in luminosity for life on Earth is that it drives climate change by increasing surface temperatures. This in turn causes more evaporation of surface water, raising the levels of water vapour (a potent greenhouse gas) in the atmosphere, setting in motion a feedback loop that can cause further increases in surface temperatures. This can also slow tectonic plate movements as water helps to lubricate plate movements

(Meadows, 2007).

These temperature increases can be counteracted by other negative feedback processes, such as reflection of solar radiation by cloud cover and changes in greenhouse gas levels in the atmosphere, but eventually, with ever increasing solar luminosity, the long-term trend pushes the climate past a temperature threshold at mean surface temperatures of approximately 330 K that allows water vapour, that is normally trapped in the troposphere (the lower portion of the atmosphere), by the temperature inversion at the boundary between the troposphere and stratosphere, to enter the upper atmosphere. When water vapour becomes a dominant component of the atmosphere, the lapse rate tends towards the saturation vapour pressure curve for water (i.e. the pressure at which water vapour becomes saturated for a given temperature), c.f. Figure 1.11.

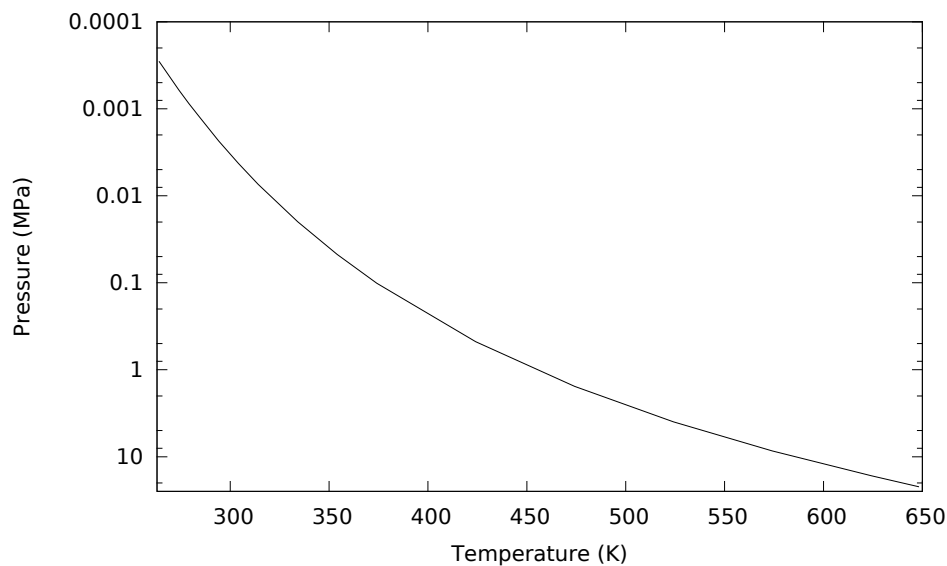


Figure 1.11: Saturated vapour pressure curve for water, i.e. the pressure at which water vapour becomes saturated for a given temperature.

This results in a fixed temperature-pressure structure for the atmosphere (Barnes *et al.*, 2013; Goldblatt & Watson, 2012), which fixes the amount of energy radiated back into space. Hence, when incoming radiation increases beyond this level, there is a net gain of energy, causing runaway heating (provided that water vapour is not lost from the atmosphere). At this point, rapid ocean evaporation begins. When water vapour enters the upper atmosphere it is rapidly photo-dissociated by UV radiation. The dissociated H is then lost to space. While at present, hydrogen escapes at a slow rate, via diffusion through the homopause (the point below which an atmosphere is well mixed), when

photodissociation of water in the upper parts of the atmosphere causes them to become hydrogen-rich, escape is limited only by the solar extreme UV heating rate (which, for an ageing star, should remain at a similar intensity to that of the present-day Sun as solar activity is not expected to decline or increase significantly over the next few Gyr - Ribas *et al.*, 2005), resulting in an escape-rate of 3.06×10^{30} H atoms s^{-1} (Caldeira & Kasting, 1992), leading to the loss of all of the planet's ocean water to space within 1 Gyr from the onset of ocean evaporation. For Earth, rapid ocean evaporation is expected to begin within 1 Gyr from present (see Chapter 4).

During this process life on Earth will have to change and adapt to increasingly extreme conditions, resulting in a series of extinctions that drastically reduce the extent of the biosphere.

1.5.2 Extinctions

Initially, increasing temperatures increase the weathering rate of silicate rocks (Equation 1.4). Increased temperatures and increased precipitation will accelerate this process, causing atmospheric CO_2 levels to fall. This leads to a series of extinctions of plants, which all depend on CO_2 as an essential substrate for photosynthesis.

Oxygenic photosynthesis is responsible for replenishing atmospheric O_2 . Therefore, atmospheric O_2 levels will fall alongside falling CO_2 levels and, since animal life depends on O_2 for respiration, simultaneous animal extinctions will occur alongside plant extinctions. Within 1 Gyr from now the majority of life on Earth will be microbial. As temperatures continue to rise and the planet becomes increasingly arid, microbial species will begin to succumb to extinction, with the hardier extremophiles being the final survivors. Even extremophile species will eventually die out when temperatures cross the threshold beyond which molecular repair and resynthesis becomes unsustainable - in the temperature range $130 - 150^\circ\text{C}$ (Gold, 1992; Cowan, 2004; Holden & Daniel, 2004; Daniel *et al.*, 2004). When temperatures in a habitat cross this boundary, these regions can be considered to be sterile and no longer habitable. Lower temperature refuges may exist for a time beneath the surface or even free-floating within the atmosphere, but these would be small populations that are unlikely to be readily detectable, making the Earth an essentially uninhabitable planet by this point in time.

1.5.3 Implications for the search for life

For assessing the habitability of a planet, the age of its host star is an important factor. For Earth-like planets orbiting late main sequence stars, surface life may be in the process of becoming less complex and abundant. This would make detecting the presence of life more challenging as the recognised associated biosignatures weaken or disappear altogether. This could result in a sub-set of habitable inhabited planets that do not exhibit any remotely detectable signs of life.

1.6 Thesis aim

The aim of this thesis is to investigate the biosignatures associated with microbial life living in a diverse range of environments, with a focus on environments that are likely to be found on the far-future Earth and other planets that are nearing the end of their habitable lifetimes. By taking into account regional mean surface temperatures, solar evolution and the range of possible orbital parameter values for the far-future Earth, estimates of the Earth's habitable lifetime, the sequence of events within the biosphere that lead up to this and how this would influence biosignatures will be made. This modelling work is then applied to other Earth-like planets around solar-type stars. Determining these biosignatures of less Earth-like environments will help expand the search for life to the wider range of environments that will be found as the habitable exoplanet inventory grows.

2

Methods I - Climate Modelling

THE first stage in the process of developing a model of planetary habitability is to describe the factors that would influence environmental conditions on a planet over geological time-scales. This component of the model is initially tested using conditions on the present-day Earth before being used to predict the long-term general temperature trends in Earth's geological future as the the Sun evolves. After being used to predict the future habitability of Earth, this model will then be extended to encompass less Earth-like planets. The first factor to account for in the temperature model is the luminosity evolution of the Sun, one of the major drivers of long-term climate change.

2.1 Luminosity evolution

The luminosity of a star is the total energy emitted per unit time. Given a known temperature and radius for a star, its luminosity can be described using the Stefan-Boltzmann Law, which states that the power per unit area of a black body radiator is directly pro-

portional to the fourth power of its absolute temperature. Hence, the luminosity can be described by

$$L = \sigma A \epsilon T^4, \quad (2.1)$$

where σ is the Stefan-Boltzmann constant ($\sigma = 5.670373 \times 10^8 \text{ Wm}^{-2}\text{K}^{-4}$), A is the radiation surface area given by $A = 4\pi R^2$ - the surface area of a sphere of radius R - and ϵ is the emissivity of the star (i.e. its ability to emit radiation). By approximating the Sun as a perfect black body radiator, ϵ can be considered to be unity.

The flux density of radiation, S_0 , (known as insolation when referring to the Sun, or instellation, for other stars) is then proportional to the inverse square of distance, d_p , from the star such that

$$S_0 = \frac{L}{4\pi d_p^2}. \quad (2.2)$$

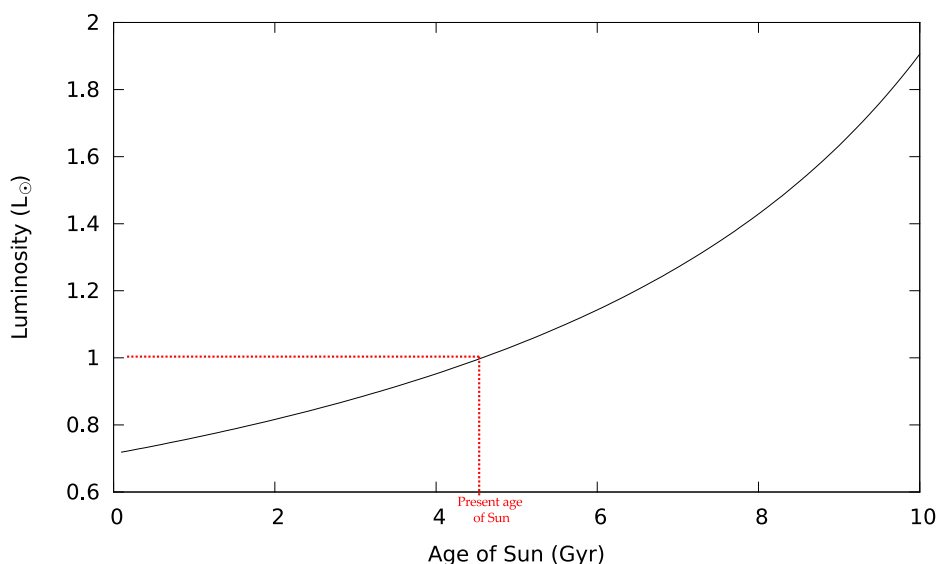


Figure 2.1: Modelled main sequence luminosity evolution of the Sun using Equation 2.3.

The increase in solar luminosity over time can be approximated following the convention of Gough (1981) such that the luminosity at any given time during the Sun's main sequence lifetime is given by

$$L(t) = \left[1 + 0.4 \left(1 - \frac{t}{t_{\odot}} \right) \right]^{-1} L_{\odot}, \quad (2.3)$$

where L_{\odot} is the present day solar luminosity value (3.839×10^{26} W), t_{\odot} is the present age of the Sun (4.57 Gyr) and t is the time elapsed on the main sequence (see **Figure 2.1**).

2.2 Energy balance temperature model

In this section, the surface temperature model is introduced. Beginning with the balance of incoming and outgoing radiation, other factors are introduced such as albedo, the heating effects of greenhouse gases, radiation absorption by the atmosphere, heat capacity (the amount of the energy required to change the global temperature by one degree) and the effects of variation in obliquity and eccentricity. This culminates in a final equation describing surface temperature at a given latitude; Equation 2.28.

In its simplest form, an energy balance model compares the incoming radiation flux from the Sun (F_{in}) with the outgoing radiation flux that escapes to space F_{out} . Any change in surface temperature, T_S , relates to the balance between the two radiation fluxes:

$$\Delta T_S \propto F_{in} - F_{out}. \quad (2.4)$$

The incoming radiation $F_{in} = (1 - a(T_S))S_0/4$, where the $S_0/4$ term accounts for the average of the insolation over the Earth's spherical surface area ($4\pi r^2$) and $a(T_S)$ is the temperature-dependent albedo (the fraction of radiation reflected back into space) determined from

$$a(T_S) = \begin{cases} 0.3 & \text{when } T_S > 280 \text{ K} \\ 0.3 + m(280 - T_S) & \text{when } 250 \text{ K} < T_S < 280 \text{ K} \\ 0.7 & \text{when } T_S < 250 \text{ K} \end{cases}$$

where $m = \frac{0.7-0.3}{280-250}$ (see Warren & Schneider (1979) for sample values). When temperatures are above 280 K in a region, there is no sea ice present, so albedo is lower; whereas, when temperatures are below 250 K, it is assumed that there is a large sea ice coverage (based on estimated temperature of previous large-scale glaciation events in Earth's geological past - Hyde *et al.*, 2000), causing more radiation to be reflected back to space

and hence leading to a higher albedo. Clouds also contribute to the planet's albedo, but the links between climate and cloud-cover are poorly understood, with different climate models producing widely variable cloud feedback effects (Boucher *et al.*, 2013), so the simplifying assumption of no change in cloud cover will be made.

The outgoing radiation F_{out} can be expressed as $F_{out} = \epsilon_p \sigma T_S^4$ by assuming the Earth acts as a black body radiator at a surface temperature T_S . The emissivity, ϵ_p , is the surface emissivity of the planet; for Earth this has a value of approximately 0.96 (Rapp, 2008). For a stable surface temperature, the incoming radiation must balance the outgoing radiation ($F_{in} = F_{out}$), leading to an expression for global mean surface temperature:

$$T_S = \left(\frac{(1 - a(T)) \frac{S_0}{4}}{\epsilon_p \sigma} \right)^{\frac{1}{4}}. \quad (2.5)$$

2.3 Greenhouse warming and atmospheric absorption

The amount of incoming radiation that gets absorbed by a planet is also influenced by the concentrations of greenhouse gases in the atmosphere. The two greenhouse gases that will have the greatest effect on Earth's future habitability over geological time-scales are carbon dioxide and water vapour. Carbon dioxide is released to the atmosphere as a result of geological and biological activity, and is drawn down from the atmosphere as a result of weathering reactions. Water is a potent greenhouse gas that becomes significant when global temperatures reach sufficient levels to induce rapid evaporation of the oceans.

Following the conventions of Lorenz & McKay (2003) and Levenson (2011), by using a grey approximation for the Earth's atmosphere, the effect of greenhouse gases can be modelled. By including the heating effect of greenhouse gases the energy balance between incoming and outgoing radiation can be re-written as

$$F_{out} = F_{in} + F_{CO_2} + F_{H_2O} \quad (2.6)$$

where F_{CO_2} and F_{H_2O} represent the absorption of some of the outgoing radiation flux by CO_2 and H_2O in the atmosphere, respectively. These are found from the optical depths of each gas to the longwave (infrared) radiation emitted from the planet's surface, τ_l , which in this case is assumed to be the sum of the longwave optical depths of CO_2 and H_2O :

τ_{CO_2} and τ_{H_2O} , respectively. Hence,

$$F_{CO_2} = 0.75F_{in}\tau_{CO_2}, \quad (2.7)$$

$$F_{H_2O} = 0.75F_{in}\tau_{H_2O}. \quad (2.8)$$

This is derived by using the Eddington approximation for a grey atmosphere (an atmosphere in which the simplifying assumption of uniform absorption at all infrared wavelengths is made) at the planet's surface level where $F_{out} = F_{in}(1 + 0.75\tau)$, where τ is the total optical depth (Lorenz & McKay (2003)). The CO_2 and H_2O optical depths are derived from the partial pressure P of each gas in the atmosphere such that

$$P_i = \frac{n_i R_g T}{N_A}, \quad (2.9)$$

where $n_i = N_A(\frac{N}{V})$ is the number density of N molecules of gas i in a volume V of the atmosphere. N_A is Avogadro's constant, T is temperature and R_g is the universal gas constant.

The optical depth can be defined using the Beer-Lambert law, which describes the attenuation of light passing through a medium, such that

$$dI = -Ik_{abs}\rho ds, \quad (2.10)$$

where I is the intensity of the radiation, k_{abs} is the absorption coefficient of the medium, ρ is the density of the medium and s is the distance travelled through the medium. Dividing by I and integrating, leads to the expression

$$\ln\left(\frac{I}{I_0}\right) = -k_{abs}\rho s, \quad (2.11)$$

which can be re-written as

$$I = I_0 e^{-k_{abs}\rho s}. \quad (2.12)$$

The term $k_{abs}\rho s$ acts as a measure of the transparency of the medium to radiation; the optical depth, τ . Hence $I = I_0 e^{-\tau}$. As the optical depth $\tau \propto \rho$, it is also related to the partial pressure of the gas, because, in its molar form, the expression for pressure relates to density such that $P = \rho R_g T / M$, where M is the molar mass of the gas.

In Levenson (2011) this pressure dependence was described by fitting the results of radiative-convective climate models (atmospheric climate models that treat the atmosphere as layers in a vertical column rising from the planet's surface level) to a simple power law. This resulted in the empirical approximations for τ_{CO_2} and τ_{H_2O} :

$$\tau_{CO_2} = k_{CO_2} P_{CO_2}^{0.5}, \quad (2.13)$$

$$\tau_{H_2O} = k_{H_2O} P_{H_2O}^{0.3}, \quad (2.14)$$

where k_{CO_2} and k_{H_2O} of $0.029 \text{ (ms}^2\text{kg}^{-1}\text{)}^{-0.5}$ and $0.087 \text{ (ms}^2\text{kg}^{-1}\text{)}^{-0.3}$, respectively.

Thus, the expression for surface temperature can be re-written to account for greenhouse warming such that

$$T_S = \left[\frac{(1 - a(T)) \frac{S_0}{4} [1 + 0.75(\tau_{CO_2} + \tau_{H_2O})]}{\epsilon_p \sigma} \right]^{\frac{1}{4}} \quad (2.15)$$

Some of the solar radiation that enters the atmosphere is absorbed by the atmosphere and does not contribute to heating the surface. When solar radiation first enters Earth's atmosphere, some is absorbed by gases in the atmosphere, reducing the flux that reaches the surface. Absorption is mainly caused by O_2 and N_2 molecules (the most abundant gases in the atmosphere), with the O_2 molecule being the stronger absorber, absorbing over a wider wavelength range (all wavelengths < 350 nm, depending on altitude - Haigh, 2007) than N_2 , which absorbs wavelengths < 100 nm (Haigh, 2007). In the higher parts of the atmosphere (altitudes > 100 km), energy absorbed at EUV and UV wavelengths causes increased vibration of the bonds in these molecules, breaking the bonds and thus splitting them into their component atoms (if enough energy is absorbed), which then travel through the atmosphere at high speeds, heating the upper atmosphere (Haigh, 2007; Trenberth *et al.*, 2009). At altitudes below 80 km, the atmosphere becomes denser, increasing the chances of collisions between liberated O and N atoms and O_2 and N_2 molecules. In particular, collisions between O and O_2 molecules leads to ozone formation (Haigh, 2007; Trenberth *et al.*, 2009). The splitting of O_2 atoms and the absorption of UV radiation by O_3 leads to atmospheric heating, reducing the solar energy that reaches the surface. Other factors such as sensible heat (e.g. the conduction of heat from the surface to the atmosphere) and latent heat (via the evaporation of surface water that

subsequently condenses in the troposphere) also reduce the radiation flux that reaches the surface (Trenberth *et al.*, 2009).

The radiation absorbed by gases in the atmosphere is the incoming shortwave radiation. Revisiting equation 2.11, the optical depth of the atmosphere to shortwave radiation is, $\tau_s = -\ln(\frac{I_s}{I_0})$, where I_s is the shortwave radiation intensity. By looking at the simplifying one-dimensional case, the intensity (a flux per unit area per unit solid angle) can be replaced with a flux density, F (Houghton, 2002; Levenson, 2011):

$$\tau_s = -\ln\left(\frac{F_s}{F}\right). \quad (2.16)$$

Hence, using values for the shortwave flux after absorption, F_s , and total shortwave flux before absorption, F_{in} , for the Earth from Trenberth *et al.* (2009), a value for $\tau_s = 0.385$ is found. For the simple treatment of the absorption by gases in the atmosphere, τ_s can be assumed to be proportional to the optical depth of the outgoing longwave radiation, τ_l (Ozawa & Ohmura, 1997). In Levenson (2011) a linear fit was used to find an approximate relation between these two values: $\tau_s = 0.354 + 0.0157\tau_l$. The incoming flux term can then be altered such that

$$F_{in} = (1 - a(T))\frac{S_0}{4}e^{-\tau_s}. \quad (2.17)$$

The sensible heat and latent heat losses can be accounted for with a convective flux term F_c . Lorenz & McKay (2003) find a simplified relation between the incoming flux and the longwave optical depth, τ_l that can be written in the form $F_c = F_{in}[\tau_l/(A + B\tau_l)]$ where A and B are constants. By using values for Earth's fluxes from Trenberth *et al.* (2009), values for A and B were found by Levenson (2011). However, when these were used to reproduce the surface temperatures on Venus and Mars, these parameterisations did not work. Hence, Levenson (2011) adopted the simplifying assumption of a linear relationship between F_c and $F_{in}\tau_l$, using known values for the convective fluxes for Earth and Mars (Lorenz & McKay, 2003; Levenson, 2011), which yielded the result

$$F_c = 0.4F_{in}\tau_l - Y, \quad (2.18)$$

where $Y = 22.5 \text{ Wm}^{-2}$. This parameterisation produced realistic surface temperature results in surface temperature models for Earth, Mars and Venus (Levenson, 2011).

The energy balance can now be re-written as

$$F_{out} = F_{in} + F_{gh} - F_c \quad (2.19)$$

where $F_{gh} = F_{CO_2} + F_{H_2O}$, allowing the surface temperature to be re-written as

$$T_S = \left[\frac{F_{in} [1 + 0.75(\tau_{CO_2} + \tau_{H_2O}) - 0.4\tau_l] + 22.5}{\epsilon_p \sigma} \right]^{\frac{1}{4}}, \quad (2.20)$$

$$T_S = \left[\frac{(1 - a(T)) \frac{S_0}{4} e^{-\tau_s} [1 + 0.75(\tau_{CO_2} + \tau_{H_2O}) - 0.4\tau_l] + 22.5}{\epsilon_p \sigma} \right]^{\frac{1}{4}}. \quad (2.21)$$

Using the global mean albedo of 0.3 for the Earth today, a CO₂ partial pressure of $\rho_{CO_2} = 33.6 Pa$ and a H₂O partial pressure of $\rho_{H_2O} = 392 Pa$, a mean global temperature $T_S = 289 K$ is obtained, which matches the global mean temperature of the Earth today.

2.4 Ocean and land fractions

Equation 2.4 can be adapted to account for the effects of ocean and land coverage on the planet's surface by including the heat capacity of the Earth C , i.e. the amount of energy required to chance the global temperature by one degree,

$$\frac{dT}{dt} = \frac{F_{in} + F_{gh} - F_c - F_{out}}{C} \quad (2.22)$$

where C is a combination of the heat capacities for the ocean and atmosphere

$$C = (xC_o + yC_a)A_s = (x\rho_o C_{o_p} H_o + y\rho_a C_{a_p} H_a)A_s \quad (2.23)$$

where A_s is the surface area of the Earth, x and y represent the ocean and land fractions such that $x + y = 1$, ρ_o and ρ_a are the densities of the ocean and atmosphere respectively, C_{o_p} and C_{a_p} are the specific heat (at constant pressure) of the ocean and atmosphere respectively and H_o and H_a are the depths of the mixed layer of the ocean (i.e. the depth to which solar radiation is absorbed/transferred) and the scale height of the atmosphere, the height at which pressure decreases by a factor e (McGuffie & Henderson-Sellers, 2005). For Earth, $\rho_o = 1000 \text{ kg m}^{-3}$, $\rho_a = 1.2 \text{ kg m}^{-3}$, $C_{o_p} = 4200 \text{ J kg}^{-1} \text{ K}^{-1}$, $C_{a_p} = 1000 \text{ J}$

$\text{kg}^{-1} \text{K}^{-1}$, $H_a = 8500 \text{ m}$ and $H_o = 70 \text{ m}$, leading to a value of C of approximately $3 \times 10^8 \text{ J m}^{-2} \text{K}^{-1}$. The depth of the mixed layer varies diurnally, regionally and with increased energy input, but the effects of increased heating on this depth are not well constrained as a result of its complicated interaction with the deep ocean, which can act as a heat store and offset changes in the mixed layer depth, and salinity variability (Kara *et al.*, 2003; de Boyer Montegut *et al.*, 2004). For this model the simplifying assumption of the global mean value of $H_0 = 70 \text{ m}$ (McGuffie & Henderson-Sellers, 2005) will be assumed. On Earth today, oceans cover approximately 70% of the surface area; hence, for a surface area of $5.1 \times 10^{14} \text{ m}^2$, $C = 1.07 \times 10^{23} \text{ J K}^{-1}$. This illustrates that the value of the heat capacity is largely determined by the oceans. From Equation 2.23, an ocean-free planet would experience a greater temperature increase with time if extra incoming energy is added to the system. The specific heat capacity for ice can also be incorporated into Equation 2.23; however, in a long-term global warming model, the effect of ice is not expected to be significant (it has a value of approximately $2000 \text{ J kg}^{-1} \text{K}^{-1}$ at 0°C and covers a small surface fraction ($< 10\%$) on the present day Earth - Thomas & Dieckmann, 2009) and is ignored in this case.

2.5 Insolation variations

Depending on location on the planet and the time of day, the amount of intercepted radiation will vary, as illustrated in Figure 2.2.

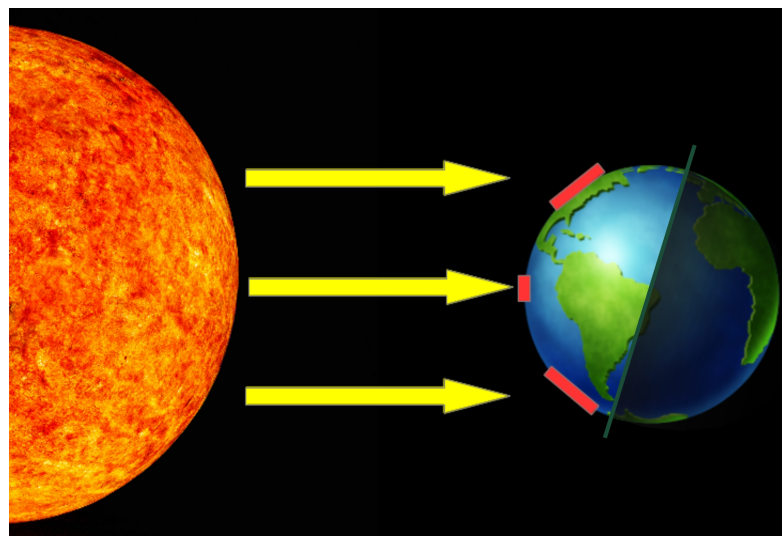


Figure 2.2: Variation of intercepted radiation with latitude. Radiation is spread over a larger surface area at higher latitudes than at lower latitudes.

Additionally, Earth's position and orientation relative to the Sun are not static, but vary sufficiently over time to impact the planet's climate. In particular, eccentricity, precession and obliquity changes (the Milankovitch Cycles) are known to have a major impact on climate over geological timespans (Spiegel *et al.*, 2010). Precession (the rotation of the Earth's axial tilt) occurs on a cycle of between 19,000 - 23,000 years, obliquity varies between 22.1° and 24.5° approximately every 41,000 years and eccentricity cycles between 0 and 0.06 approximately every 100,000 years (Paillard, 2010; Vásquez *et al.*, 2010).

Accounting for these variations in order to model surface temperatures at local scales can be achieved as follows.

From Liou (2002), the solar heating per unit area at the top of the atmosphere is found by integrating the total insolation received between sunrise and sunset, which results in the expression:

$$I = \frac{S_0}{\pi} \frac{d_E^2}{d^2} [h_0 \sin(\lambda) \sin(\delta) + \cos(\lambda) \cos(\delta) \sin(h_0)], \quad (2.24)$$

where S_0 is the solar constant, d_E is the mean Earth-Sun distance, d is the Earth-Sun distance at a given point in the planet's orbit, λ is latitude, h_0 is the solar hour angle (in radians) at sunset (i.e. a measure in degrees of the the offset from solar noon, $h = 0$; the point when the Sun is at its highest point above the horizon) at a particular latitude and δ is the solar declination (the angular distance away from the celestial equator). The factor of $1/\pi$ in Equation 2.24 is a result of the factoring in of the rotation of the Earth (2π rad per day) in the derivation of I - Liou (2002).

The solar declination, δ , at a given point in the planet's orbit depends on the planet's obliquity ϕ , varying from $+\phi$ to $-\phi$ such that

$$\sin(\delta) = \sin(\phi) \sin(\nu + \omega), \quad (2.25)$$

where ν is the true anomaly (i.e. the angle formed by the line joining a planet and star and the central axis of the ellipse formed by the planet's orbit; cf. Figure 2.3) and ω is the longitude of perihelion (i.e. the angle, measured from the point of the vernal equinox, at which the planet would make its closest approach to the Sun if it had an inclination of zero).

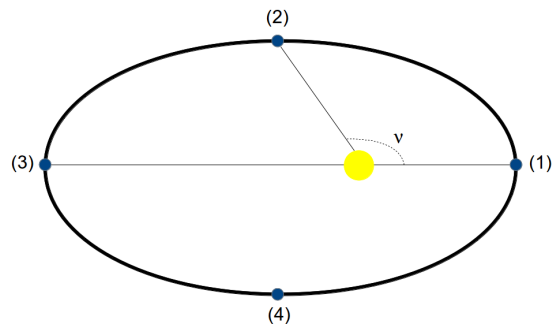


Figure 2.3: The true anomaly, ν , is a measure of the angle between the line joining the planet and star and the central axis of the orbital ellipse. Positions (1) to (4) mark the points at which insolation was measured to show its variation with orbital position (cf. Figure 2.4).

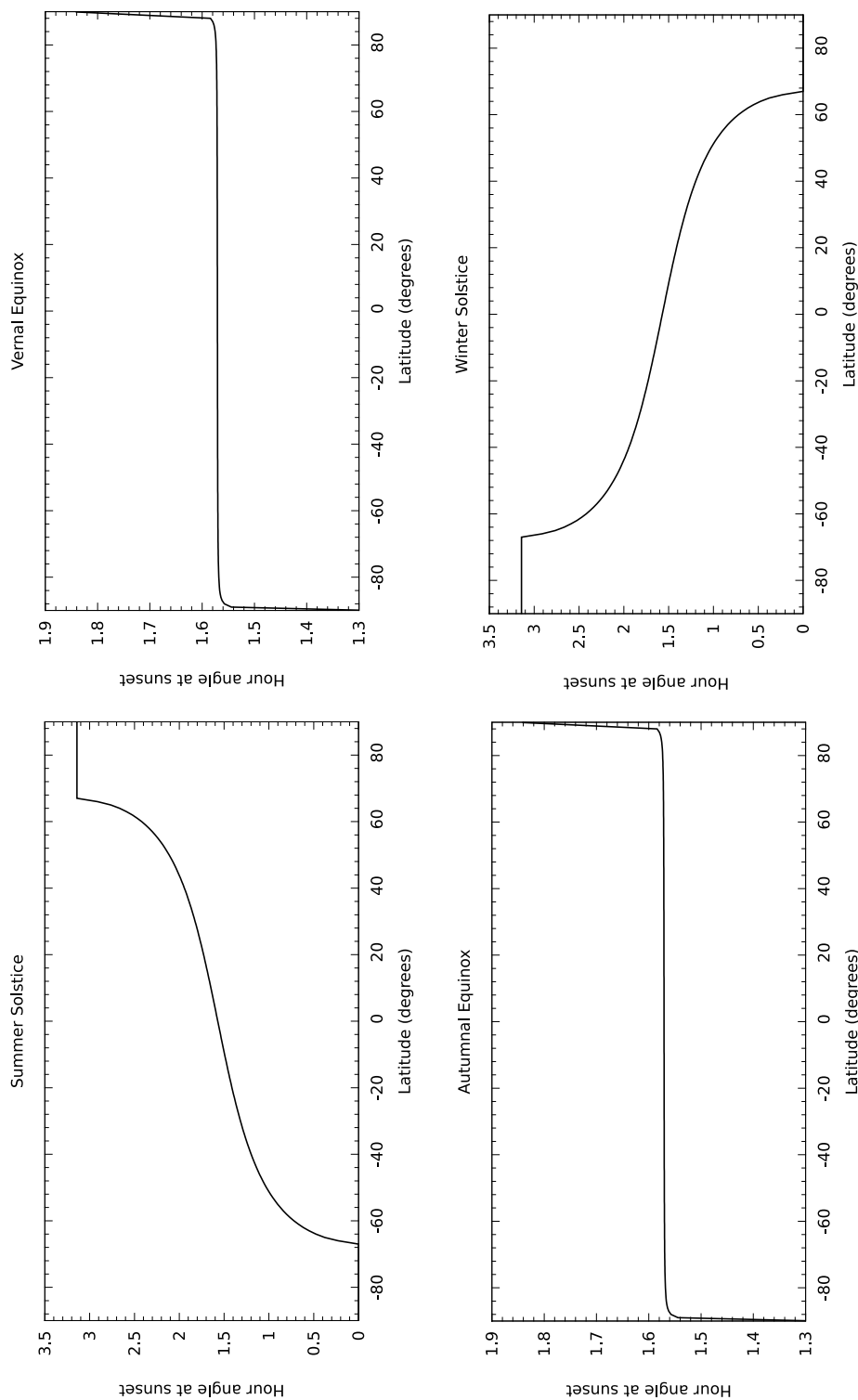


Figure 2.4: Variation of the hour angle at sunset over latitude at the (northern hemisphere) summer solstice (SS), vernal equinox (VE), autumnal equinox and the winter solstice (WS). At SS $\delta = +\phi$, $h_0 = 0$ within the Antarctic Circle and $h_0 = \pi$ within the Arctic Circle corresponding to the Sun not rising and not setting respectively over the course of a day. The reverse is true for the winter solstice ($\delta = -\phi$), as expected. For the equinoxes $\delta = 0$, h_0 remains constant except at high latitudes.

The hour angle (an angular measurement of time before or after solar noon at a given location, varying from -180° to $+180^\circ$) at sunrise (negative), or sunset (positive) can be found from

$$\cos(h_0) = -\tan(\lambda)\tan(\delta), \quad (2.26)$$

with the condition that if $\tan(\lambda)\tan(\delta) > 1$ then $h_0 = \pi$ and if $\tan(\lambda)\tan(\delta) < -1$ then $h_0 = 0$ to account for cases where the Sun does not set ($h_0 = \pi$), or does not rise ($h_0 = 0$) for the duration of a day. The variation of h_0 over latitude at different points in the planet's orbit follows the expected patterns as illustrated in Figure 2.4.

The eccentricity (e) of the planet's orbit influences the planet-star distance (d) at any point in the orbit following the relation

$$d = \frac{d_E(1 - e^2)}{(1 + e\cos(\nu))}. \quad (2.27)$$

An estimate of the expected surface temperature for a particular latitude can then be found by replacing S_0 in F_{in} with I , defining a latitude-dependent surface temperature

$$T_S(\lambda) = \left[\frac{(1 - a(T))\frac{I}{4}e^{-\tau_s} [1 + 0.75(\tau_{CO_2} + \tau_{H_2O}) - 0.4\tau_l] + 22.5}{\epsilon_p\sigma} \right]^{\frac{1}{4}} \quad (2.28)$$

2.5.1 Varying individual parameters

In this section eccentricity, true anomaly and obliquity are all varied individually, while keeping all other factors constant, to check that the modelled insolation behaves as expected. The model responds to each test as expected, as illustrated in Figures, 2.5, 2.6 and 2.7.

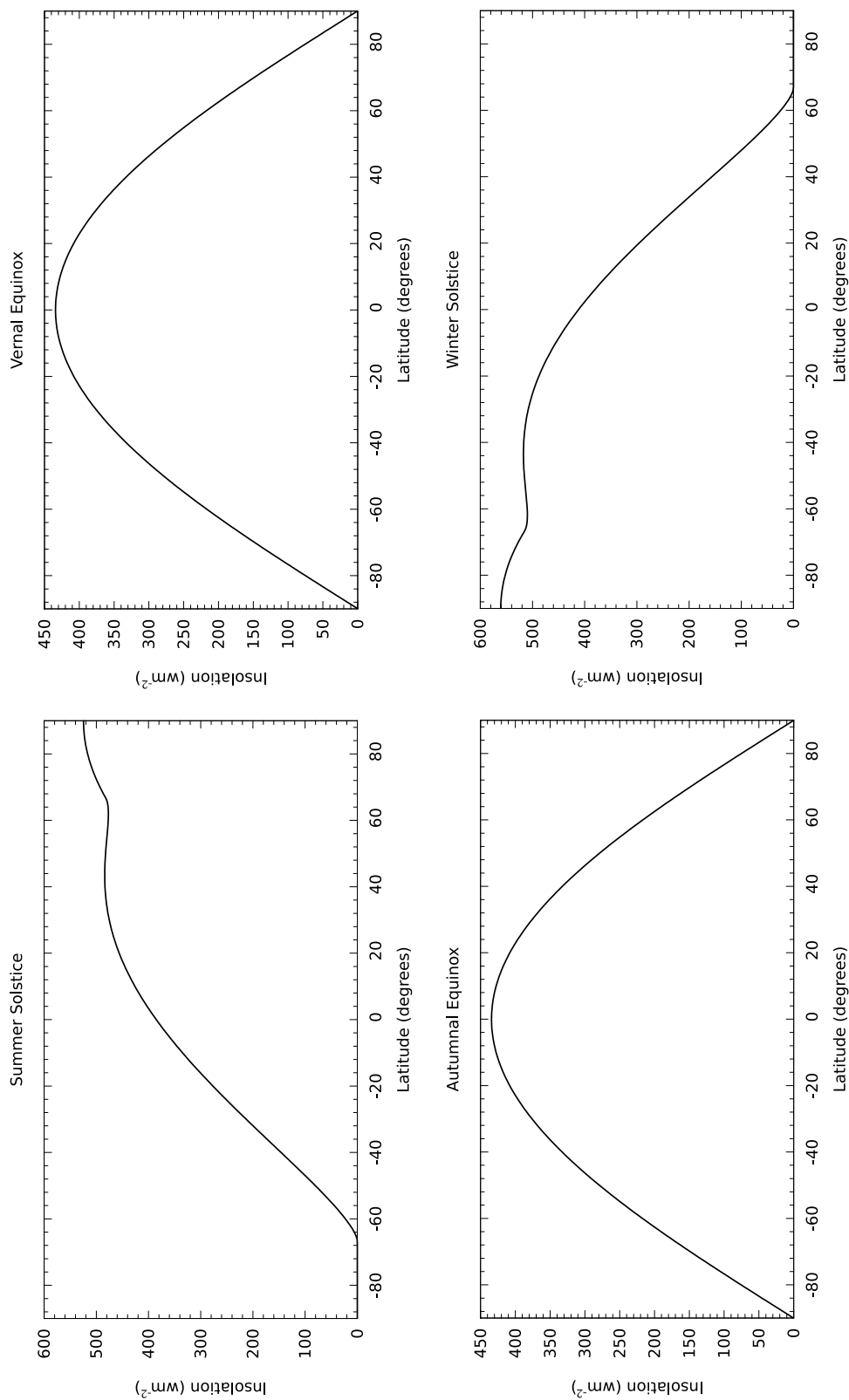


Figure 2.5: Variation of insolation over latitude at different points in the planet's orbit. At (northern hemisphere) summer and winter solstices, the highest insolation is found in the northern and southern polar regions, respectively and insolation is zero in the southern and northern polar regions, respectively. At the equinoxes, maximum insolation is found at the equator and minimum insolation at the poles. Note that the maximum insolation during southern hemisphere summer is greater than the maximum insolation during northern hemisphere summer. This is a result of summer in the southern hemisphere occurring near aphelion and summer in the northern hemisphere occurring near perihelion.

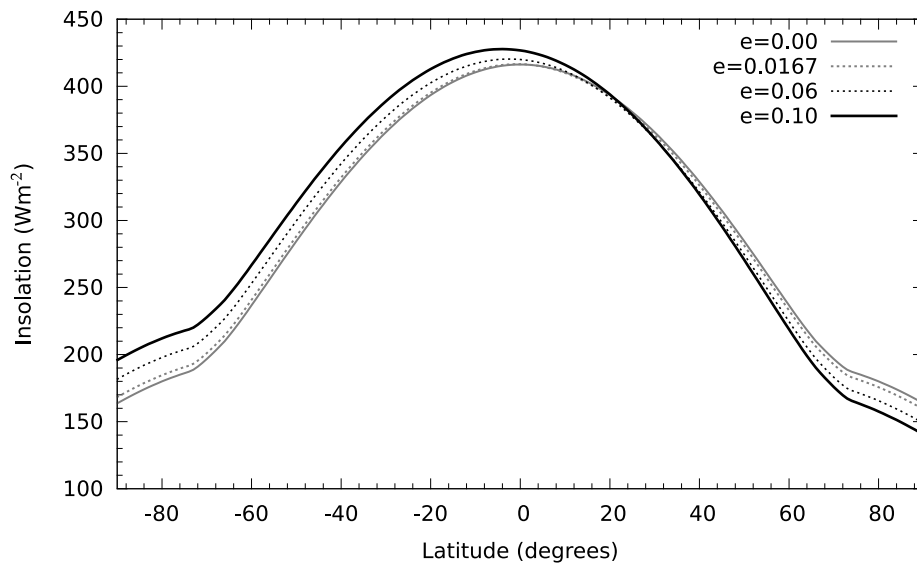


Figure 2.6: Average top of atmosphere insolation values across all latitudes for different eccentricity values. In this case, a larger eccentricity leads to a lower insolation range, as expected. The eccentricity effect will vary depending on the position in the orbit at which insolation is measured, e.g. a higher eccentricity would bring the planet closer to the Sun at perihelion than a lower eccentricity, giving the high eccentricity planet a greater insolation at this point in its orbit. As perihelion occurs during southern hemisphere summer, the southern hemisphere polar insolation increases with increasing eccentricity. This trend is evident at all latitudes below $+23.44^\circ$ - the present obliquity. The reverse is true for the northern hemisphere latitudes above this value.

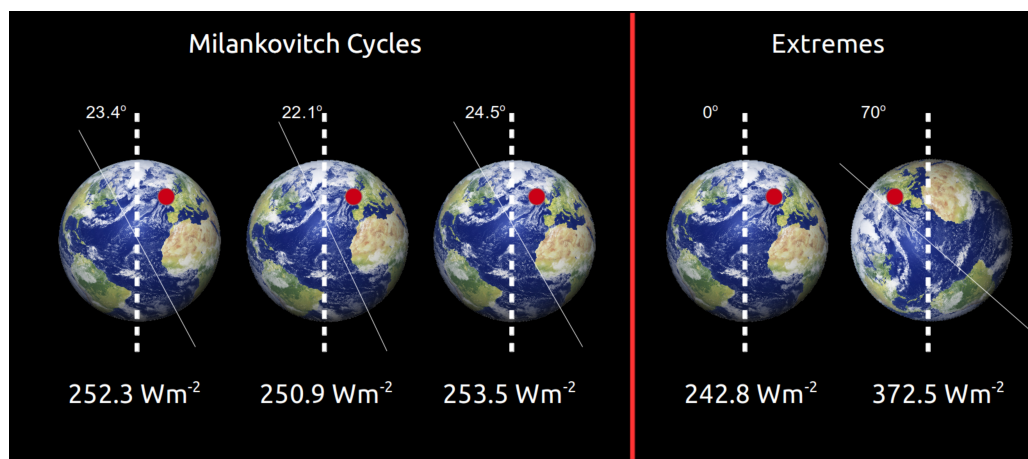


Figure 2.7: St Andrews is situated at a latitude of 56.4° in the northern hemisphere. Varying the obliquity from the present-day value of $\phi = 23.4^\circ$ to the minimum and maximum values that occur during a full obliquity Milankovitch cycle, as well more extreme values, varies the insolation received as expected, i.e. reducing the extent of the planet's tilt, reduces the insolation received, while increasing the tilt places the location more directly into the path of incoming solar radiation, increasing the insolation received.

2.5.2 When do the Milankovitch cycles break down?

While they provide a guide as to the likely behaviour of the planet's orbital characteristics from the present onwards, the Milankovitch cycles are unlikely to remain constant for the entire lifetime of the planet. The presence of a large moon helps to stabilise Earth's obliquity, preventing large obliquity swings like those experienced by Mars for example (Laskar *et al.*, 1993b; Laskar *et al.*, 2004). While the presence of a large moon may not be essential for a stable obliquity range for Earth-like planets (Lissauer *et al.*, 2012), the recession of an already present large moon could potentially induce larger obliquity swings, affecting latitudinal temperature values. Earth's moon currently orbits at a average distance of 384,400 km and is receding due to tidal interactions with Earth at a current rate of approximately 4 cm yr^{-1} (Néron de Surgy & Laskar, 1997). This would place it 40,000 km further away within 1 Gyr, if this recession rate remains constant¹. This would give it an orbital distance of $67 R_{\oplus}$ (R_{\oplus} = Earth radius), exceeding the critical point described by Tomasella *et al.* (1996) for stabilising planetary obliquity. Exceeding this distance places the Earth into a chaotic obliquity regime, permitting large obliquity swings between 30-60° (Tomasella *et al.*, 1996) and possibly allowing even larger obliquities of up to 90° (Laskar *et al.*, 1993b). This would affect the global temperature distribution, causing shifts in the latitude zones that receive maximum and minimum insolation. As the Moon recedes, Earth's rotation rate will slow. At present, the Earth's rotation is slowing by 1.7 ± 0.05 ms/century (del Rio, 1999), which, if this rate were to remain constant, would reduce the day length by up to 20% in 1 Gyr. This reduces the equator-to-pole temperature gradient by reducing the magnitude of the mid-latitude eddies responsible for heat transport (Feulner, 2012), again influencing the global temperature distribution.

Similarly, eccentricity will not remain stable over geological timescales. Laskar & Gastineau (2009) suggest that a resonance between Mercury and Jupiter may eventually increase Mercury's eccentricity, which would destabilise the inner planets in approximately 3 Gyr - a scenario that could lead to Earth's eccentricity reaching a value as high as 0.3. However, this change is likely to come too late to influence Earth's final life.

¹Extrapolating this recession rate backwards results in an underestimate for the age of the Moon (1.5 Gyr instead of 4 Gyr), suggesting this recession rate was slower in the past (Néron de Surgy & Laskar, 1997; Bills & Ray, 1999). This may mean that the Moon's recession will not be constant in the future either.

2.6 Latitudinal heat flow

Heat diffuses across the planet from the equator to the poles due to atmospheric circulation. A simple model for this diffusion is described in Lorenz *et al.* (2001) where the flow of heat, F , in Wm^{-2} , between discrete latitude zones can be described by

$$F = D \frac{\Delta T}{\sin(\delta\lambda)} \quad (2.29)$$

where D is the latitudinal diffusion coefficient, which increases with increased atmospheric density, $\delta\lambda$ is the separation in degrees between the two latitude zones and $\Delta T = T(\lambda_i) - T(\lambda_j)$, i.e. the temperature difference between the two latitude zones. This is summarised in Figure 2.8. For Earth, D has a value of between $0.6-1.1 Wm^{-2}K^{-1}$ (Lorenz *et al.*, 2001)

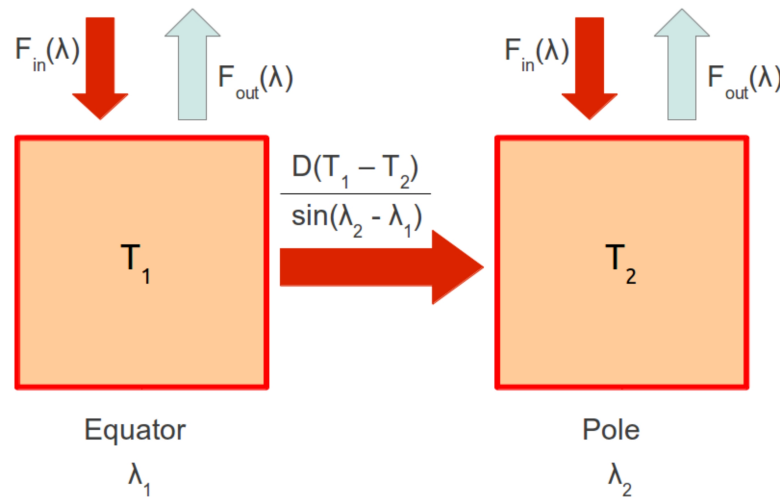


Figure 2.8: Overview of a simplified model of heat flow outwards from the equator.

and is proportional to atmospheric density. Hence, with increasing atmospheric density, the equator-to-pole heat flux increases. By incorporating this heat flow into the incoming radiation received by a particular latitude zone, latitudinal heat flow can be accounted for in the surface temperature model. By scaling the value of D in relation to the increase in atmospheric density expected when temperatures increase enough to cause rapid ocean evaporation, the expected change in latitudinal heat flow rates can also be simulated. For this to be applied to transport processes in exoplanet atmospheres, the density of those atmospheres would need to be known - the simplifying assumption of Earth-like atmospheric density is used in this modelling work.

2.7 Elevation variations

Elevation within the atmosphere of a planet will also influence local temperatures. The lowest component of Earth's atmosphere, the troposphere, is heated from below by the planet's surface, which absorbs incoming radiation and re-radiates it. Hence, with increasing height within the troposphere, temperature decreases. Currently, temperatures in the troposphere follow a mean linear decrease of ~ 6.5 K per km with increasing altitude (an average of the lapse rates (rates of temperature decrease with increasing elevation in an atmosphere) calculated for dry and moist air - approximately 9.8 K and 5.5 K per km, respectively). The point at which this temperature trend ends marks the boundary of

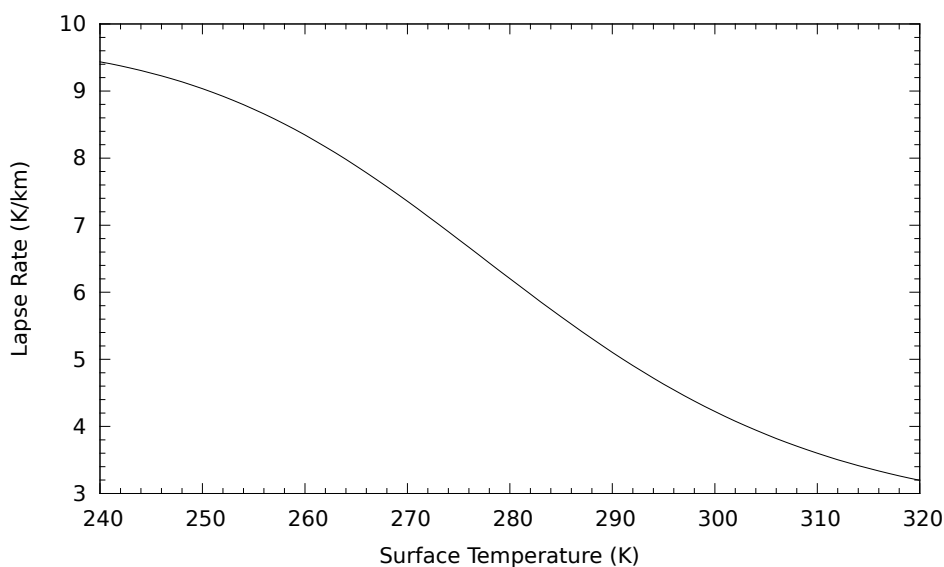


Figure 2.9: Change in lapse rate of moist air with surface temperature. The moist adiabatic lapse rate of a rising parcel of moist air, decreases with increased initial temperature (surface temperature). The global mean lapse rate for moist air on Earth is approximately 5.5 K/km, replicated by equation 2.9 at $T_S \approx 288$ K (the global mean surface temperature of the present-day Earth).

the troposphere, the tropopause, which occurs at average heights of 9 km at the poles to 17 km at the equator; a result of the tropopause height being determined by the mean temperature of the air at surface level. The temperature trend ends when the air becomes completely dry and temperature begins increasing with height due to the presence of ozone, which absorbs sunlight. As the maximum height of Earth's surface, 8.848 km, falls within the troposphere, it is not necessary to calculate stratospheric temperature changes in this case.

When the atmosphere is saturated with water vapour, an estimate of the likely value

of the (adiabatic) lapse rate Γ_w can be obtained from

$$\Gamma_w = g \left[\frac{1 + (H_v r / R_{sd} T_S)}{C_p + (H_v^2 r \epsilon_d / R_{sd} T_S^2)} \right], \quad (2.30)$$

where g is the gravitational acceleration, H_v is the heat of vaporisation for water, R_{sd} is the specific gas constant for dry air, ϵ_d is the ratio of the specific gas constant of dry air to that for water, T_S is the surface temperature and r is the ratio of the mass of water vapour to dry air, which depends on the saturated vapour pressure and atmospheric pressure. The behaviour of this equation is illustrated in Figure 2.9.

2.8 Water vapour and the runaway greenhouse effect

Surface temperatures and incoming radiation can drive positive feedback cycles that eventually send a planet's climate out of radiative equilibrium, potentially causing abrupt environmental changes. In particular, runaway and moist greenhouse effects can end a planet's habitable life.

As the luminosity of a star increases, the radiation intercepted by an orbiting planet increases. This increases evaporation rates of surface water, raising the atmospheric water vapour content. Water vapour being a greenhouse gas, this results in further temperature increase, beginning a positive feedback loop (McGuffie & Henderson-Sellers, 2005; Goldblatt & Watson, 2012). A moist greenhouse state describes the state in which water vapour dominates the troposphere while the water vapour content of the stratosphere starts to increase. A runaway greenhouse scenario occurs when water vapour becomes a dominant component of the atmosphere (see Section 1.5.1.).

2.9 Testing the model

In this section tests on the full temperature model are performed to check that sensible results are obtained.

2.9.1 Reproducing present-day surface temperatures

Temperature predictions under present-day conditions on Earth, with a fixed luminosity and orbital parameters are performed and found to reasonably reproduce the current latitudinal temperature gradient and summer-winter temperature variations (cf. Figure

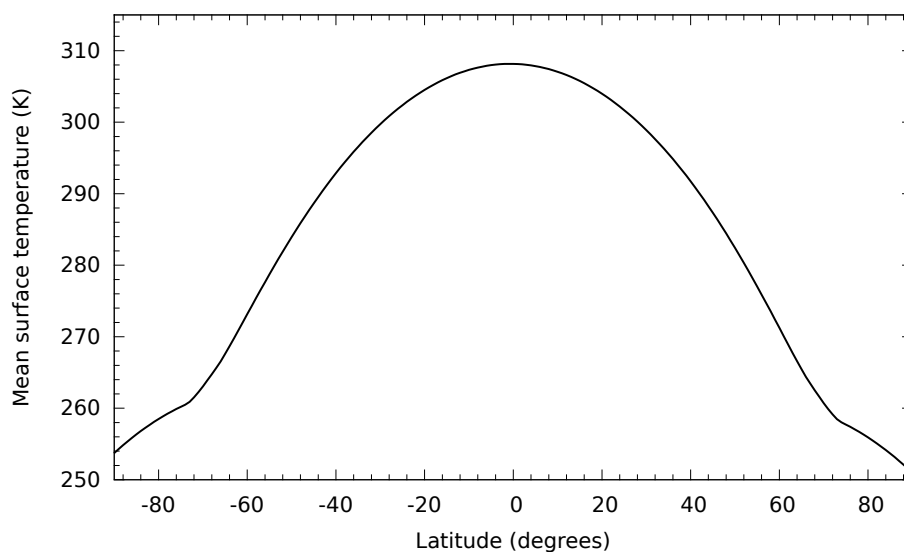


Figure 2.10: Reproducing the present-day equator-to-pole temperature range using the model. The model reasonably reproduces Earth’s present mean global temperature range, from approximately 255 K at the poles to 305 K in equatorial regions. The discontinuities at very high latitudes are a result of restrictions placed on the hour angle calculation because the Sun never sets in summer. In reality, polar temperatures in the south pole should be lower by up to 30 degrees due to the presence of the Antarctic land mass. However, during the billion-year time scales over which this model will be run, plate movements will continually redistribute continental land mass over the surface, so the presence of land in polar regions would not necessarily be constant over geological time.

2.10).

2.9.2 Running the model backwards

Early in the history of the solar system, the Sun’s luminosity was approximately 70% of its present value. For a luminosity of this level and assuming the same albedo and atmospheric composition as at present, the early Earth should have had temperatures below the freezing point of water at times before about 2.6 Gyr ago (Güdel, 2007). Geological evidence in the form of sediment deposition suggest that liquid water was present on the early Earth, implying that the planet was warmer than calculations suggest. For this test, the model is run backwards in time to reproduce these predictions for surface temperatures on the early Earth. Albedo and greenhouse gas levels are kept at present-day values, but obliquity and eccentricity changes follow Milankovitch cycles as before.

Mean surface temperatures are below the freezing point of water before the planet was 2 Gyr old as shown in Figure 2.11, similar to faint young Sun paradox results from other work in which present-day Earth conditions are assumed (Sagan & Mullen, 1972; Kasting

& Catling, 2003; Güdel, 2007). Solutions to the paradox include higher levels of greenhouse gases such as CO_2 or CH_4 on the early Earth than at present, or a brighter young Sun (Güdel, 2007). Recent work with three-dimensional global climate models suggests that the paradox may now be resolved using combinations of atmospheric CH_4 and differences in surface albedos and rotation rate (Wolf & Toon, 2014); however, many combinations of factors effecting climate can solve the problem, suggesting an absolute solution may be difficult to determine.

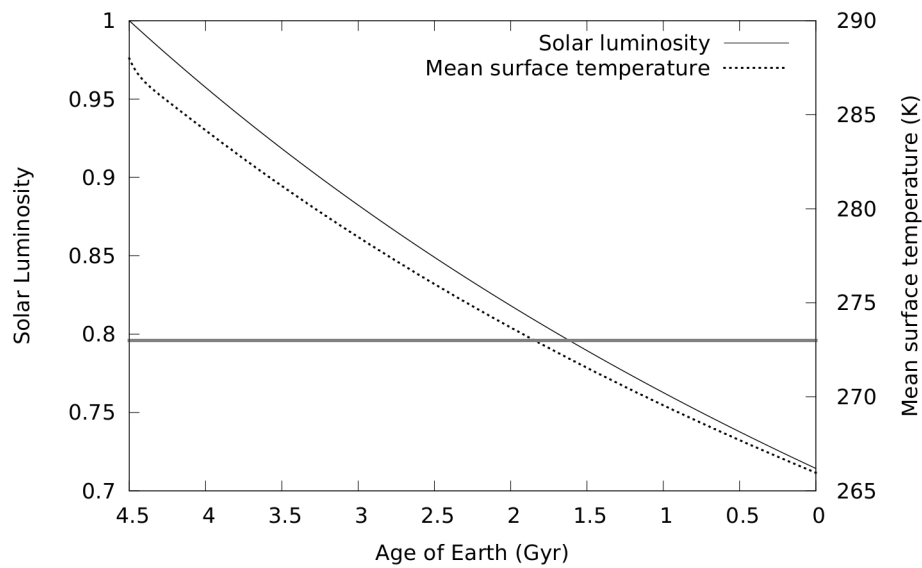
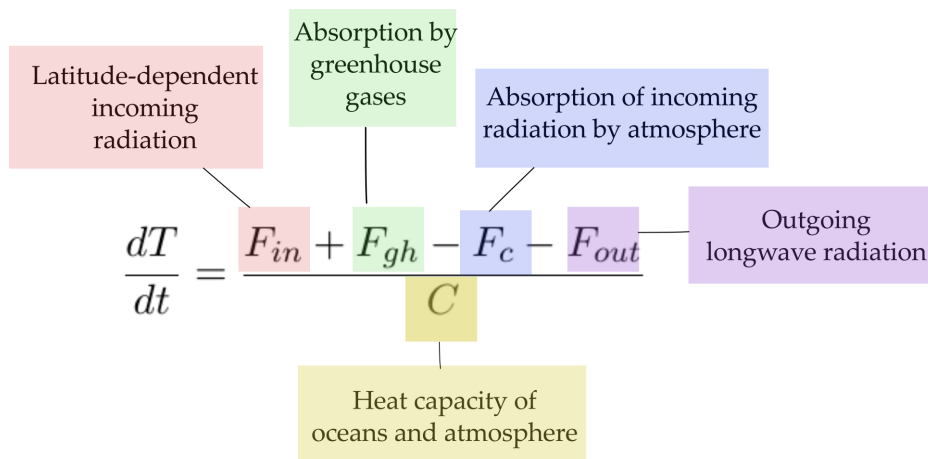


Figure 2.11: Running the model backwards: Earth’s mean surface temperature and solar luminosity. From its present day value, the mean surface temperature falls as time runs backwards and solar luminosity decreases, predicting temperatures below the freezing point of water for times before 2.6 Gyr ago.

2.10 Summary

In this chapter, a procedure was established for modelling the change in the luminosity of the Sun over time in order to establish the solar radiation flux received by a planet. Procedures for varying orbital distance, eccentricity, obliquity and greenhouse gas levels were then outlined, all of which can be combined to estimate a surface temperature for a given latitude, which varies in time according to:



incorporating heat diffusion (from hotter to cooler latitudes) and altitude on the planet.

The resulting model was then tested and found to reproduce the present-day equator-to-pole temperature range on Earth and the subzero temperatures predicted by the “faint young Sun” paradox. Although this modelling procedure will initially be used to estimate future temperature evolution on Earth, orbital parameters, ocean- and land-surface fractions and atmospheric CO₂ and H₂O levels can be changed to model less Earth-like planets.

3

Methods II - Biosignature Modelling

WITH the ultimate aims of (i) predicting the types of life that can live on a planet until it becomes completely uninhabitable and (ii) predicting what the remotely detectable biosignatures associated with that life would be, a process of modelling a biosphere over geological time, coupled to a planet's temperature evolution, is outlined here.

3.1 Predicting extinction sequences

There are three main events that will distinguish distinct eras in the future of a biosphere equivalent to that of the present-day Earth. The first event occurs when atmospheric CO₂ levels fall beyond the level required to sustain photosynthesis, which marks the end of animal life and higher plant life. This is followed by a period during which microbial life continues to exist in a variety of forms. Finally, with the onset of rapid ocean evaporation and increasing temperatures that result from this, only a biosphere of extremophile

organisms can exist until environmental conditions eventually change to such an extent that even these forms of life are precluded.

3.1.1 Predicting the end of plant and animal life

The fate of plant life ultimately depends on atmospheric CO₂. The increase in global mean temperatures caused by the increasing luminosity of the Sun amplifies the silicate weathering cycle, drawing down more CO₂ over time, leading to a decline in atmospheric CO₂. This can be modelled using the method described later in this section. To photosynthesise, embryophytic plant life (liverworts, hornworts, mosses and vascular plants) requires a minimum atmospheric concentration of 10 p.p.m. CO₂ (Caldeira & Kasting, 1992). Once levels cross this threshold, these forms of plant life can be considered to be no longer sustainable.

On Earth, there are three biochemical processes used by plants to fix carbon for photosynthesis: (i) C₃ carbon fixation in which the first product in the carbon fixation process is a 3-carbon molecule, (ii) C₄ carbon fixation in which the first product in the carbon fixation process is a 4-carbon molecule and (iii) Crassulacean acid metabolism (CAM), a process in which carbon is collected overnight and stored as the acid malate, before being used in photosynthesis during the day (this process reduces water loss as stomata can remain closed during the day, making this a useful adaptation to arid climates).

Plants that use the C₃ pathway (the dominant pathway in higher plants) would be the least tolerant to a lower CO₂ atmosphere, surviving until atmospheric CO₂ levels reached 150 p.p.m. (Caldeira & Kasting, 1992). CAM and C₄ plants can cope with lower CO₂ and so survive for longer. Once CO₂ levels fall below 10 p.p.m. these species will also no longer be able to survive. However, as some eukaryotic phytoplankton, benthic macroalgae and cyanobacteria have been shown to be capable of carrying out net photosynthesis at very low CO₂ concentration (Birmingham & Colman, 1979; Maberly, 1996) microbial photosynthesis could continue until the CO₂ concentration falls to 1 p.p.m.

Plants provide both food and oxygen to animal life; hence, as plant abundances decline, animal species will decline alongside them. The temperature and oxygen-level tolerances of animal species will determine their probable extinction sequences.

Carbon dioxide: biological productivity and silicate weathering

Biological productivity is the measure of the productivity of an ecosystem, usually measured by the amount of carbon produced as a result of biological activity; presently approximately 56.4 GT of carbon per year on land. Biological productivity is intricately linked to planetary carbon cycles. Hence, it is necessary to know the silicate weathering rate, which draws down CO_2 from the atmosphere as a result of reactions between precipitation and silicate minerals (cf. Equation 1.2) and the amount of CO_2 present in soils and the atmosphere. Carbon burial via limestone formation and its consequent recycling via volcanic emissions occurs over Myr-timescales and this is unlikely to be significantly altered by temperature changes; hence, this process does not need to be considered in this case (Caldeira & Kasting, 1992).

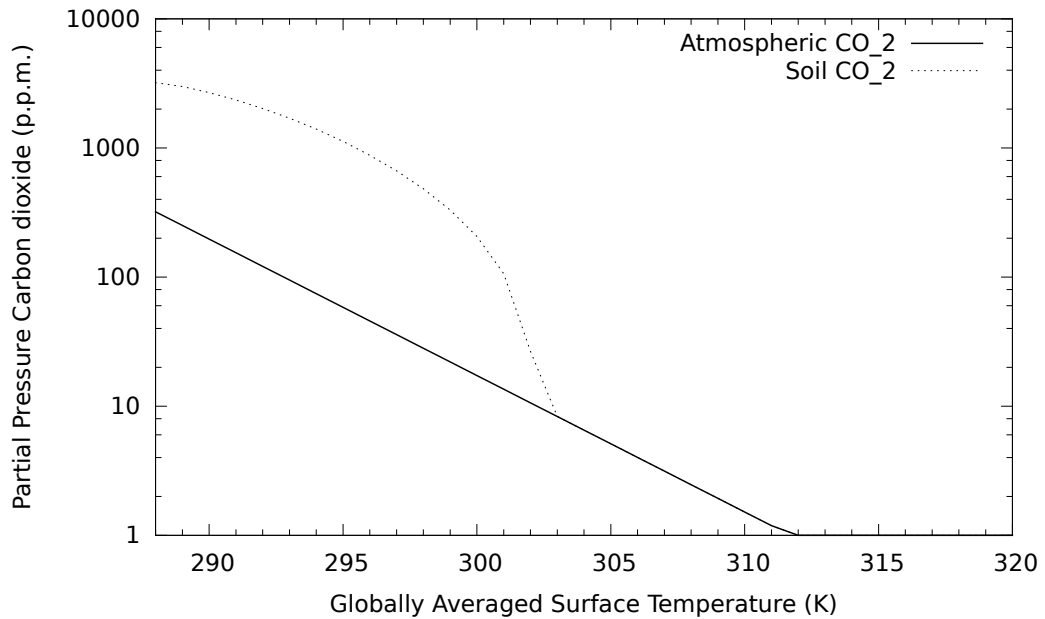


Figure 3.1: Changes in atmospheric and soil CO_2 (in p.p.m.) with increasing surface temperature using the Caldeira & Kasting (1992) model. For the following parameters: $T_0 = 288$ K, $P_{atm,0} = 320$ p.p.m., $P_{soil,0} = 3200$ p.p.m., $\Pi_0 = 56.4$ GT carbon per year, $P_{\frac{1}{2}} = 210.8$ p.p.m.

The change of CO_2 levels in the atmosphere and soil are found using the methods of Caldeira & Kasting (1992). This involved three coupled equations:

(1) The silicate weathering rate, F_{wr}

$$\frac{F_{wr}}{F_{wr,0}} = \left(\frac{a_{H^+}}{a_{H^+,0}} \right)^{\frac{1}{2}} \exp \left(\frac{T - T_0}{13.7} \right), \quad (3.1)$$

where a_{H^+} is the activity of H^+ ions in soil and T is the mean surface temperature. The subscript 0 denotes present day values. When CO_2 dissolves in raindrops it forms a weak carbonic acid, H_2CO_3 , which, when it comes into contact with silicate minerals, forms bicarbonate ions, HCO_3^- , at a rate (determined from experimental evidence) proportional to the square root of the activity of H^+ ions.

(2) Partial pressure of CO_2 in the soil, P_{soil}

$$\frac{P_{soil}}{P_{soil,0}} = \frac{\Pi}{\Pi_0} \left(1 - \frac{P_{atm,0}}{P_{soil,0}} \right) + \frac{P_{atm}}{P_{soil,0}}, \quad (3.2)$$

where Π is the biological productivity (i.e. the amount of biomass produced by photosynthesis per unit time - which presently has a value of 56.4 GT carbon per year on land) and P_{atm} is the partial pressure of CO_2 in the atmosphere, which can be approximated by assuming $F_{wr}=F_{wr,0}$ following the methods of Volk (1987) such that

$$\frac{P_{atm}}{P_{atm,0}} = \left(\frac{1}{\exp[(T - T_0)/13.7]} \right)^{1/0.3}. \quad (3.3)$$

(3) Biological productivity can then be modelled using

$$\frac{\Pi}{\Pi_{max}} = \left(1 - \left(\frac{T - 25^\circ C}{25^\circ C} \right)^2 \right) \left(\frac{P_{atm} - P_{min}}{P_{\frac{1}{2}} + (P_{atm} - P_{min})} \right), \quad (3.4)$$

where Π_{max} is the maximum biological productivity ($\Pi_{max} = 2\Pi_0$), P_{min} is the minimum CO_2 partial pressure ($P_{min} = 10$ p.p.m.) below which photosynthesis is no longer feasible (except perhaps in microbial photosynthesisers) and $P_{\frac{1}{2}}$ is the value at which biological productivity is $0.5\Pi_{max}$. The subscript 0 denotes present day values. The behaviour of the biological productivity with changing surface temperature is shown in Figure 3.2.

3.1.2 Predicting the end of microbial life

With the extinction of all animal and plant species, all remaining life will be microbial. As temperatures increase and water availability lowers, this microbial biosphere will become

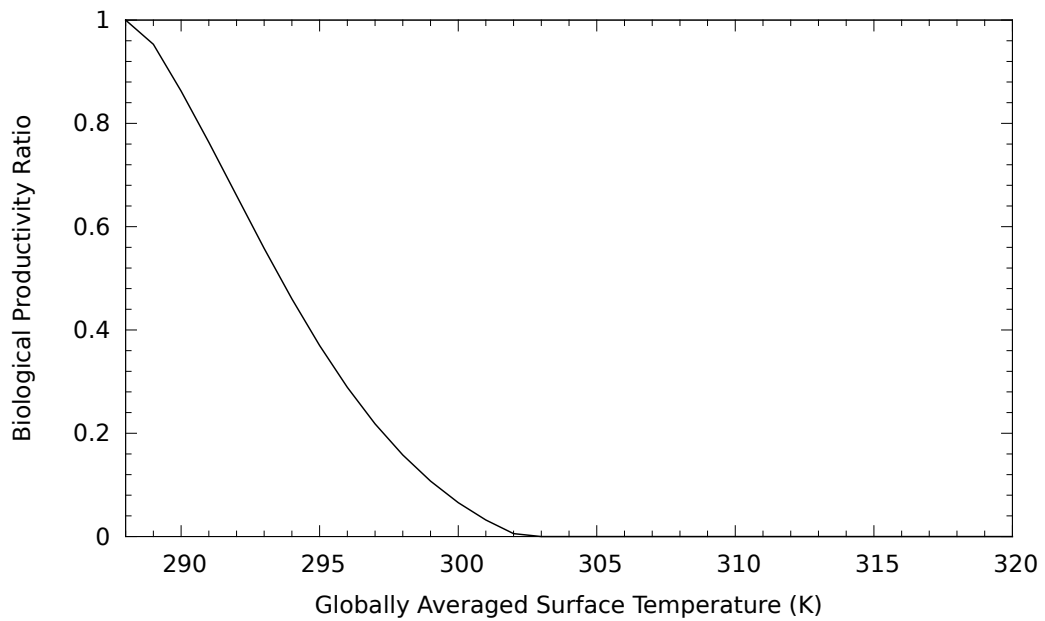


Figure 3.2: Change in biological productivity with increasing surface temperature using the Caldeira & Kasting (1992) model. When temperatures reach approximately 303 K, photosynthesis in all but microbial photosynthesisers ceases.

less diverse until even organisms with the most extreme tolerances to harsh environmental conditions can no longer survive. An overview of this sequence is illustrated in Figure 3.3.

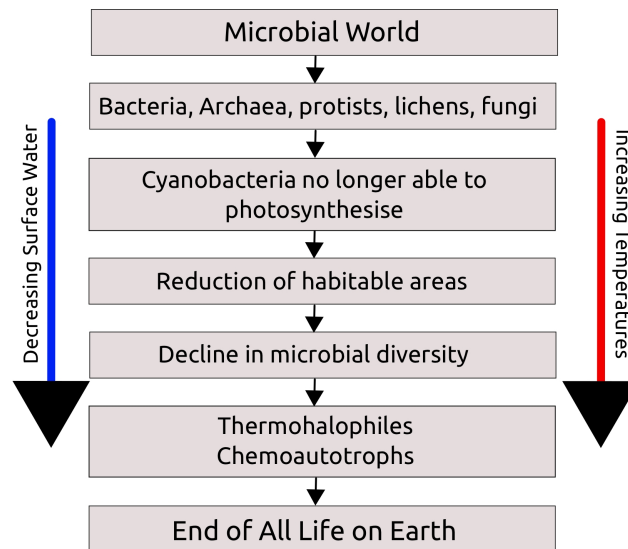


Figure 3.3: Simplified extinction sequence for a microbial biosphere.

To predict in more detail how this process would take place a simple atmosphere-biosphere chemical interaction model will be used. This combines the metabolic reactions that would be possible in a far-future, low-oxygen world (listed in Table 3.1), abiotic gas fluxes and simple atmospheric chemistry all of which are then linked to the surface

temperature evolution derived from the surface temperature model described in Chapter 2.

This model microbial biosphere is assumed to have an initial abundance equal to present estimates for the terrestrial subsurface (2.5×10^{29} cells), soils (2.6×10^{29} cells) and subseafloor sediments (2.9×10^{29} cells) - Whitman *et al.* (1998). This biosphere is initially evenly distributed over the surface area of the Earth, giving an initial cell count of 4.9×10^{15} cells m^{-2} . Splitting the planet into three latitude zones (polar ($\pm 60 - 90^\circ$), mid-latitude ($\pm 30 - 60^\circ$) and equatorial ($0 - \pm 30^\circ$)) and assuming 1% of the surface area is at an elevation > 5 km gives the microbial abundance within the temperature zones assumed in the temperature model. The microbial abundance then evolves in the model as temperatures increase, with the count dropping to zero when temperatures in a particular zone exceed 420 K (a temperature set slightly higher than the upper known temperature limit for life (122°C - Takai *et al.*, 2008) allowing for adaptation to increased temperatures). This falls within the range of temperatures generally believed to be a theoretical maximum for life, beyond which molecular repair and resynthesis would be unsustainable (Gold, 1992; Cowan, 2004; Holden & Daniel, 2004; Daniel *et al.*, 2004).

The chemical reactions occurring in a single cell for each type of microbial metabolism (see Table 3.2) are modelled, drawing reactants from an atmospheric reservoir of gases and adding product gases to that reservoir, assuming the rates described in Table 3.3. The number of reactions taking place is determined by the temperature-dependent cell abundance calculated previously. The number of particular metabolisers is estimated based on their likely abundance in the modelled temperature-atmosphere environment. Abiotic gas fluxes, ocean evaporation and hydrogen escape into space are also accounted for in the model (see Figure 3.4).

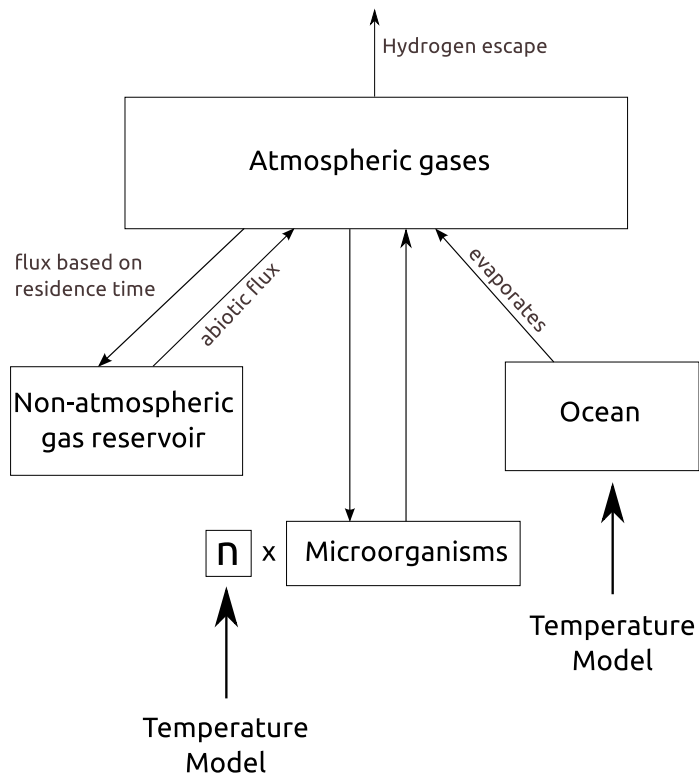


Figure 3.4: Schematic of the biosphere-atmosphere gas exchange model. The temperature model determines the rates of gas fluxes and the abundance of organisms, n . The abundance of specific types of microorganism is weighted based on the favourability of particular metabolisms on the far-future Earth.

Microbe type	Reactions	Source
Methanogens	$\text{CO}_2 + 4\text{H}_2 \rightarrow \text{CH}_4 + 2\text{H}_2\text{O}$ $\text{CH}_3\text{COOH} \rightarrow \text{CH}_4 + \text{CO}_2$ Other C sources, e.g. methanol.	Ferry (2002)
Ammonia oxidisers	$\text{NH}_3 + \text{O}_2 + 2\text{e}^- \rightarrow \text{NO}_2^- + 5\text{H}^+ + 4\text{e}^-$	Bernhard (2012)
Hydrogen oxidisers	$2\text{H}_2 + \text{O}_2 \rightarrow 2\text{H}_2\text{O}$ $2\text{H}_2 + \text{CO}_2 \rightarrow (\text{CH}_2\text{O}) + \text{H}_2\text{O}$	Bongers (1970)
Sulphur oxidisers	$2\text{S} + 3\text{O}_2 + 2\text{H}_2\text{O} \rightarrow 2\text{H}_2\text{SO}_4$ $12\text{FeSO}_4 + 3\text{O}_2 + 6\text{HOH} \rightarrow 4\text{Fe}_2(\text{SO}_4)_3$	Suzuki <i>et al.</i> (1990) Suzuki <i>et al.</i> (1992)
Carboxydotrophs	$\text{CO} + \text{O}_2 + 2\text{e}^- + 2\text{H}^+ \rightarrow \text{CO}_2 + \text{H}_2\text{O}$	Bender & Conrad (1994)
DMS oxidisers	DMS oxidation, producing: SO, dimethylsulphoxide, dimethylsulphone, methanesulfonic-acid, sulphuric acid.	Nicholas Hewitt & Davison (1997)
Iron oxidisers	$2\text{Fe}(\text{OH})_2 + \text{O}_2 \rightarrow \text{H}_2\text{O} + \text{Fe}_2\text{O}_3$ $10\text{FeCO}_3 + 2\text{NO}_3^- + 24\text{H}_2\text{O} \rightarrow 10\text{Fe}(\text{OH})_3 + \text{N}_2 + 10\text{HCO}_3^- + 8\text{H}^+$	Straub <i>et al.</i> (1996)
Aerobic Methanotrophs	$\text{CH}_4 + 2\text{O}_2 \rightarrow \text{CO}_2 + 2\text{H}_2\text{O}$	Mancinelli (1995)

Anaerobic Methanotrophs	$\text{CH}_4 + \text{SO}_4^{2-} + 2\text{H}^+ \rightarrow \text{CO}_2 + 4\text{H}_2 + \text{H}_2\text{S}$	Mancinelli (1995)
Iron reducers	Aquifer soils: $\text{H}_2\text{O} + \text{Fe}_2\text{O}_3 \rightarrow 2\text{Fe}(\text{OH})_2 + \text{O}_2$ Carbohydrate e^- donor: $2\text{Fe}_2\text{O}_3 + 3\text{CH}_2\text{O} \rightarrow 4\text{Fe} + 3\text{CO}_2 + 3\text{H}_2\text{O}$ Hydrogen e^- donor: $2\text{Fe}_2\text{O}_3 + 3\text{H}_2 \rightarrow 2\text{Fe} + 3\text{H}_2\text{O}$	Sawyer & McCarty (1967) Longbottom & Kolbeinsen (2008)
Sulphate reducers	$\text{SO}_4^{2-} + \text{CH}_3\text{COOH} + 2\text{H}^+ \rightarrow \text{HS}^- + 2\text{HCO}_3 + 3\text{H}^+$	Barnes & Goldberg (1976)
Acetogens	CO_2 reduced to CO , converted to acetyl coenzyme.	
Anammox reaction	$\text{NH}_4^+ + \text{NO}_2^- \rightarrow 2\text{CO}_2 + \text{N}_2\text{O} + 3\text{H}_2\text{O}$	Strous <i>et al.</i> (2006)
Denitrification	$5\text{CH}_2\text{O} + 4\text{NO}_3^- + 4\text{H}^+ \rightarrow 5\text{CO}_2 + 2\text{N}_2 + 7\text{H}_2\text{O}$ $2\text{CH}_2\text{O} + 2\text{NO}_3^- + 2\text{H}^+ \rightarrow 2\text{CO}_2 + \text{N}_2\text{O} + 3\text{H}_2\text{O}$	
Ammonia fermentation	$2\text{C}_2\text{H}_5\text{OH} + \text{NO}_3^- + \text{H}_2\text{O} \rightarrow 2\text{CH}_3\text{COOH} + \text{NH}_4^+ + 2\text{OH}^-$	Zhou <i>et al.</i> (2002)

Table 3.1: Microbial organisms that could be supported by environments on the far-future Earth.

3.1.3 Initial cell counts

The number of organisms using a particular metabolism is estimated based on the likely abundance of those metabolisers in the far-future environment. This is calculated from the total initial abundance estimate (8×10^{29} cells), assuming 1% are found at high altitudes (> 5 km) and an order of magnitude fewer aerobic metabolisers than anaerobic metabolisers due to the low oxygen levels on the far future Earth. This difference in abundance is based on the abundance differences between aerobes and anaerobes in low-oxygen environments (Tartakovsky *et al.*, 2005; Ulloa *et al.*, 2012). Hence, this gives an initial cell count of 8×10^{28} aerobes and 7.2×10^{29} anaerobes. These can then be divided into a “per habitat” cell count based on the availability of different types of habitat for particular organism types.

3.2 Biosignature predictions

One of the spectral biosignatures directly associated with vegetation on Earth is the “red edge” reflectance signature (see Table 1.2). This is caused by the infrared reflectance of land vegetation; hence, as vegetation coverage decreases, the strength of this signature

Microbe type	Rate of gas consumption or production		Source
	Rate from source	Rate (g cell ⁻¹ yr ⁻¹)	
Ammonia oxidisers	<i>Nitrosomonas</i> species: 28.1 pmol - 0.2 fmol NH ₃ oxidised cell ⁻¹ d ⁻¹ . Produces: NO	$3 \times 10^{-11} - 4 \times 10^{-6}$	Boyd <i>et al.</i> (2011)
Carboxydotrophs	<i>Roseobacter</i> species: Max. of $1.1-2.3 \times 10^{-10}$ nmol CO oxidised cell ⁻¹ h ⁻¹	$(2.7 - 5.6) \times 10^{-14}$	Tolli <i>et al.</i> (2006)
Methanogens	Wetland study: 273-665 μ g CH ₄ produced per kg soil per day with $1.07-8.29 \times 10^9$ cell per gram soil	$(2.9 - 9.1) \times 10^{-14}$	Liu <i>et al.</i> (2011)
Sulphur oxidisers	<i>Thiooxidans</i> species: $(2.5 - 9.9) \times 10^{-4}$ μ g S oxidised cm ⁻² d ⁻¹	$(0.9 - 3.6) \times 10^{-18}$	Smith <i>et al.</i> (2012)
Anaerobic methanotrophs	Reaction chamber: 8-33 nmol CH ₄ consumed per gram sediment d ⁻¹	$(4.7 - 19.4) \times 10^{-14}$	Girgius <i>et al.</i> (2003)
Aerobic methanotrophs	Landfill sites: 3-6.4 mmol CH ₄ consumed per kg soil d ⁻¹	$(1.8 - 23) \times 10^{-11}$	Kallistova <i>et al.</i> (2005)
Anaerobic iron reducers	Anaerobic sediment sites: 9-130 nmol Fe reduced per g sediment h ⁻¹ Produces: CO ₂ (Other iron reduction products: H ₂ O or O ₂ (aquifer soils; Sawyer <i>et al.</i> , 1967), depending on electron donor; NB: using H ₂ O as an electron donor requires energy input)	$(4.4 - 64) \times 10^{-12}$	Sørensen <i>et al.</i> (1982)
Aerobic iron oxidisers	<i>Leptospirillum ferrooxidans</i> : 10^{-5} μ mol Fe oxidised cell ⁻¹ d ⁻¹ No gases produced	2.1×10^{-7}	Schrenk <i>et al.</i> (1997)
Hydrogen oxidisers	Isolates of soil hydrogen oxidising bacteria: 0.08-0.92 μ mol H ₂ oxidised h ⁻¹ cm ⁻³	$(1.4 - 20) \times 10^{-12}$	Maimaiti <i>et al.</i> (2007)
Anammox	Anoxic water column site: $(1534 - 2228) \times 10^{-9}$ mmol N cell ⁻¹ yr ⁻¹	$(2.0 - 3.0) \times 10^{-11}$	Dalsgaard <i>et al.</i> (2003)

Table 3.2: Production rates of biosignature gases from model species representing the metabolic pathways that are likely to be favourable on the far-future Earth.

Gas	Present-day flux to atmosphere		Source
	Flux g yr^{-1}	Gas source	
CH ₄	5.3×10^{13}	Volcanoes Mud volcanoes Hydrocarbon seepage	Burton <i>et al.</i> (2013)
CO ₂	3×10^{14} 3×10^{14}	Volcanoes Degassing	Burton <i>et al.</i> (2013)
NO ₂	7×10^{12}	Fixation by lightning	Tie <i>et al.</i> (2002)
SO ₂	$(15 - 21) \times 10^{12}$	Volcanoes	Halmer <i>et al.</i> (2002)
H ₂ O	6.5×10^{14}	Volcanoes	Fischer (2008)
CO	CO:CO ₂ flux of 0.03-0.12 $2 - 3 \times 10^{14}$	Volcanoes Photochemical production	Wardell <i>et al.</i> (2004) Zuo & Jones (1996)

Table 3.3: Modelled abiotic gas fluxes. Given reduced tectonic activity on the far-future Earth, volcanic gas fluxes are reduced to 20% of the present-day fluxes to account for the assumption that the only remaining volcanoes are hotspot volcanoes, which make up 20% of present-day active subaerial volcanoes. The photochemical CO flux is linked to the dissolved organic carbon content of atmospheric water droplets and so is assumed to be negligible once plant and animal life becomes extinct. Anthropogenic fluxes of gases such as CH₄ and CO₂ (of the order $1 \times 10^{14} \text{ g yr}^{-1}$ and $1 \times 10^{15} \text{ g yr}^{-1}$, respectively) have a major impact of the present day climate. However, these effects occur over a geologically short period of time and so will not impact the Gyr-scale predictions of this model.

will decrease. The strength of this signature can be linked to the leaf area index (LAI) - a remote sensing term used as an estimate of vegetation coverage, defined as green leaf area/surface area. It has been shown by Filella & Penñuelas (1994) that the area of the red edge peak in spectra changed with LAI, because LAI determines the ratio of near-IR and red reflectance. On Earth, sub-tropical dry zones tend to be sparsely vegetated and therefore would exhibit a much reduced red-edge signature. Warming temperatures would lead to the poleward expansion of Hadley cells - atmospheric circulation cells between 0° and $\pm 30^\circ$ latitude caused by warming air rising from equatorial regions and being deflected polewards by the tropopause temperature inversion. Most of the moisture carried by this warm air is lost as condensation during the upward phase of the circulation, which leads to the descending cooler air being dry (Trenberth & Stepaniak, 2004). This air descends at about $\pm 30^\circ$ latitude, which is why much of the land area around these latitudes is arid or semi-arid (Johanson & Fu, 2009). The expansion of the extent in latitude of equatorial

Hadley cells, ϕ_H , with temperature can be approximated using

$$\phi_H \approx \left(\frac{5gH_t\Delta h}{3\Omega^2 R_p^2 \theta_0} \right)^{\frac{1}{2}}, \quad (3.5)$$

where g is the acceleration due to gravity, H_t is the height of the tropical tropopause, Δh is the equator-to-pole difference in radiative-equilibrium (i.e. under a constant radiation flux) potential temperature¹, Ω is the angular rate of rotation of the Earth, R_p is the radius of the Earth and θ_0 is the global mean temperature (Held & Hou, 1980; Showman *et al.*, 2010).

For animal biosignatures, predictions are made in Chapter 5, via inferences about the rates of extinctions. These can be predicted from factors like the upper temperature tolerances of different species, their tolerances to lower atmospheric oxygen concentrations, their abilities to move to more habitable environments when conditions in their present habitat become more hostile and their tolerances to reduced food supplies due to factors such as changes in vegetation cover (predicted from Hadley cell expansion). The by-products from animal decomposition will also be investigated.

For biosignatures associated with a declining microbial biosphere, the atmospheric gas reservoir from the microbial extinction model can be sampled at any time point. Initially set to the expected levels of biosignature gases after the extinction of all plants and animals, these gases evolve as described in Section 3.1.2. Knowing the mass of a gas in the atmosphere, alongside the general composition of the atmosphere, allows its detectability to be assessed.

3.3 Summary

By combining predictions of regional temperature evolution with methods for predicting the associated atmospheric gas compositions and the types of life able to exist in a given environment, the long-term future of a global biosphere can be outlined. By modelling how life interacts with an atmosphere, the biosignatures a global biosphere would produce and how these change over time can also be predicted, providing a tool-kit for modelling the biosignature changes with time of an Earth-like biosphere from conditions on the

¹For a parcel of air at pressure, the potential temperature is the temperature that parcel would acquire if adiabatically brought to a standard reference pressure.

present-day Earth to the end of an Earth-like planet's habitable lifetime.

4

Refuges for life near the end of the Earth's habitable lifetime

BY using the temperature model described in Chapter 2, the mean temperature evolution of the Earth at local scales, from the present to 3 Gyr into the future, was simulated. This enabled the type, abundance and extent of future habitats to be evaluated and also allowed a timespan for the remainder of Earth's habitable lifetime to be set.

4.1 Far-future temperature evolution

Figure 4.1 shows the general mean surface temperature trends predicted by the model for the next 2.5 Gyr. The steep increase in temperature at around 1 Gyr from the present represents the onset of rapid ocean evaporation. Assuming an upper temperature bound for life of 420 K (allowing some increase over the currently known upper temperature tolerance of thermophiles, cf. Chapter 3) and assuming no changes to obliquity or eccen-

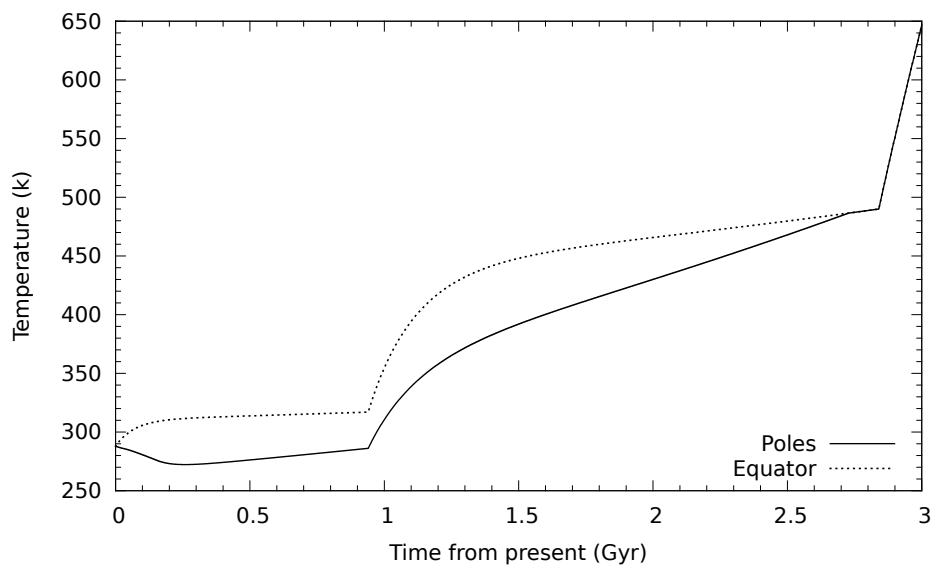


Figure 4.1: Change in global mean temperatures over time with increasing solar luminosity. The dashed line represents equatorial temperature and the solid line represents polar temperature. After about 1 Gyr a moist greenhouse begins when temperatures reach 330 K allowing the water vapour content of the stratosphere to increase rapidly. When temperatures reach approximately 420 K life would likely no longer be able to survive. A runaway greenhouse regime begins after approximately 2.8 Gyr. Initially, the poles warm noticeably less rapidly than the equator; however, as the planet heats up, the equator-to-pole temperature gradient decreases due to an increased latitudinal heat diffusion coefficient, caused by the increase in atmospheric pressure. Note that the initial polar and equatorial temperatures are the same. This is a consequence of the initial temperature of the model being set to the present global mean temperature at all latitudes. The system then evolves away from this initial state.

tricity cycles, life could persist 0.7 Gyr longer at surface levels at polar latitudes than at the equator.

Rapid ocean loss as a result of a moist greenhouse effect would likely represent the end-point of an Earth-like planet's habitable lifetime. Assuming ocean loss was not uniform across the globe due to regional temperature variations, there could potentially be pockets of liquid water that remain for a brief time before total loss of liquid surface water occurs. A source of liquid water is a prerequisite for life as we know it; hence, these last pools of water would represent the final habitable regions on a dying planet. In this section, potential locations for these last habitable regions are discussed. Precession effects (e.g. changes to longitude of perihelion) can be ignored in this case, as this simply changes the hemisphere that receives the most insolation, which will not influence the conclusions made over Gyr time-spans.

4.2 Deep ocean trench remnants

The present mean ocean depth is approximately 4 km; however, deep ocean trenches, depressions in the sea floor caused by the subduction of one tectonic plate under another at divergent plate boundaries can extend the ocean depth to 6 km on average and up to 11 km for the deepest known trench, the Mariana Trench in the Western Pacific Ocean.

One could imagine that as surface water is lost these would provide sheltered regions, cooler than the ambient temperatures outside the trench, much like the shadowing effect of craters on the Moon can reduce the temperatures within them by as much as 295 K compared to surface temperatures (Margot *et al.*, 1999). However, the presence of an atmosphere on Earth complicates the situation. Movement of air into a trench from above would cause that air to be compressed adiabatically the lower it goes (Frederick, 2011). This compression increases the air temperature via the ideal gas law, which could lead to trenches actually being some of the warmest regions on a moist greenhouse planet and thus, making them unlikely candidates for the location of some of the last liquid surface water on the planet.

Additionally, it is possible that deep trench features may be much less common 1 Gyr from now due to the slowing of tectonic plate movements, which would slow their formation and allow weathering processes to erode away exposed features. Plate tectonics is driven by the transfer of heat from the Earth's core to the surface. As described in Meadows (2007), heat is transferred from the core through the mantle via convection (and sometimes conduction). As these plumes of heat reach the crust they give up their heat and are pushed aside by new hot uprisings. This sideways motion in the upper mantle is the driving force for plate movement. However, the Earth is cooling down over time, resulting in a gradually solidifying outer molten core. This slows down convection within the mantle, leaving less power available to move plates. Eventually (approximately 3 Gyr from now), convection will stop altogether, ending plate motions.

Additionally, regardless of whether convection is still occurring in the mantle, once the oceans fully evaporate, tectonic plate movements will stop. The subduction of one plate under another is aided by the presence of liquid surface water, which acts as a lubricant. Without it, plate movements cease due to increased friction (Meadows, 2007).

4.3 Caves

It has previously been speculated that life on Venus earlier in that planet's lifetime may have found refuge in caves and underground as temperatures began to rise (Irwin & Schulze-Makuch, 2011). Similarly, it can be argued that life on the far future Earth would retreat underground and into cave systems (the subsurface biosphere). Many microbial communities are already known to exist independently of solar energy, for example, obtaining the means to metabolise directly from the rocks (*chemolithotrophs*) and in the case of one strain of green sulphur bacteria, even using the light from geothermal radiation around a deep sea vent for photosynthesis (Beatty *et al.*, 2005).

Caves are generally assumed to have constant interior environments, with internal temperatures closely approximating the local mean surface temperature (Tuttle & Stevenson, 1977; Howarth, 1983). This, combined with the general trend of increasing temperatures with depth would not bode well for organisms on a planet with surface temperatures exceeding the boiling point of water. However, some cave systems may be better suited to sheltering life than others. In particular, caves that have their greatest volume below their entrance would act as cold reservoirs (Tuttle & Stevenson, 1977) as colder, denser air would flow downward into the cave, but warmer lighter air would not.

These cold trap caves, (also known as ice caves due to the presence of year-round ice within them) are often formed from collapsed lava tubes (Williams *et al.*, 2010) and generally have a narrow single entrance with a large chamber below, which has a large volume-to-wall surface ratio, because it is conduction through the cave walls that would restore the temperature within the cave to the mean surface temperature (cf. Figure 4.2).

Cold, dense air enters the cave during winter. In-falling snow is compacted into layers of ice, or inflowing water freezes. When temperatures outside increase, the warmer, less dense air cannot enter the cave, leaving the colder air trapped within. This allows ice to remain within the cave throughout the year. However, the ice mass within the cave is not the ice that originally formed there. The ice is continually being melted as a result of heat conduction from the surrounding rocks that are in contact with the ice (which tend to reflect the annual mean temperature of a region) and dripping water inside the cave (Ohata *et al.*, 1994; Leutscher *et al.*, 2005). The melt water is then lost from the cave with the entire ice mass being replaced after between 100-1000 years (Leutscher *et al.*, 2005),

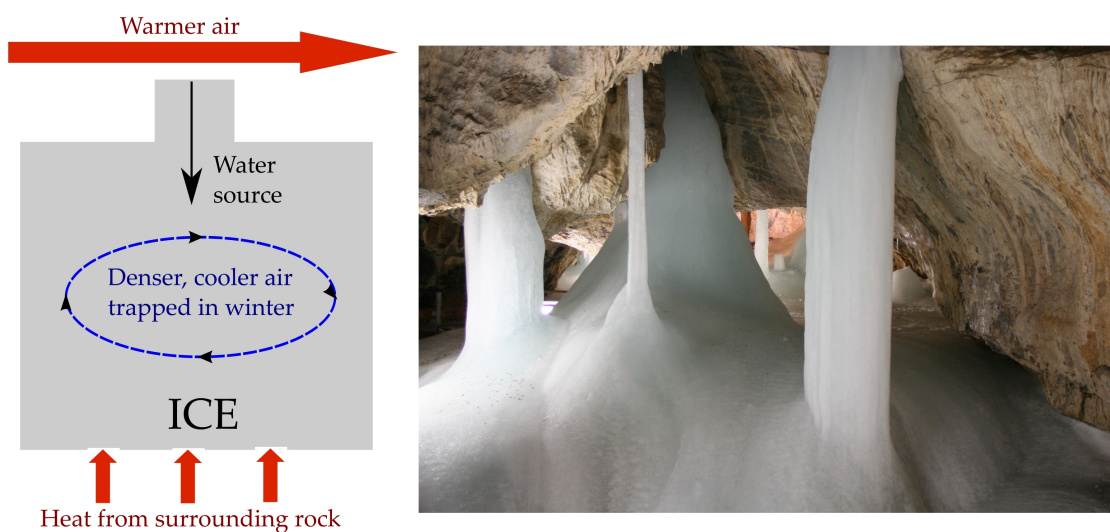


Figure 4.2: Ice caves remain cold enough to retain ice continuously despite above-freezing exterior temperatures. *Image source (right): User:Jojo/WikimediaCommons/CC-BY-SA-3.0.*

depending on the geometry of the particular cave in question. Hence, new water needs to be supplied (Δw) such that

$$\Delta w = \Delta w_{in} - \Delta w_{melted} \quad (4.1)$$

at least remains constant for permanent ice to remain.

Therefore, for this mechanism to provide a useful refuge for life on the far-future Earth, there would need to be some form of water input into the system (perhaps through seepage from the surrounding rock or via water vapour entering from the external atmosphere at times when the outside air density matches, or exceeds that within the cave) for liquid water to remain within such a cave.

Ice caves are found not only in cold regions, but also temperate and tropical latitudes on Earth today. The question of how long such caves would be able to retain water when exposed to rapidly increasing surface temperatures remains open. Leutscher *et al.* (2005) focused on ice caves in the Jura Mountains and found that the temperatures within cold trap caves were dependent on the outside winter temperatures in the region and, more particularly relevant to this work, that the ice mass within the ice caves studied decreased as annual mean winter temperatures increased (most noticeably since the 1980s). This suggests that cold trap cave temperatures on the far-future Earth would only be as (relatively) cool as the coolest temperatures in a region in any given year, which, given the high temperatures expected, may not provide a long stay of execution for life.

However, for Earth, after the Moon recedes beyond the critical distance of $67 R_{\oplus}$

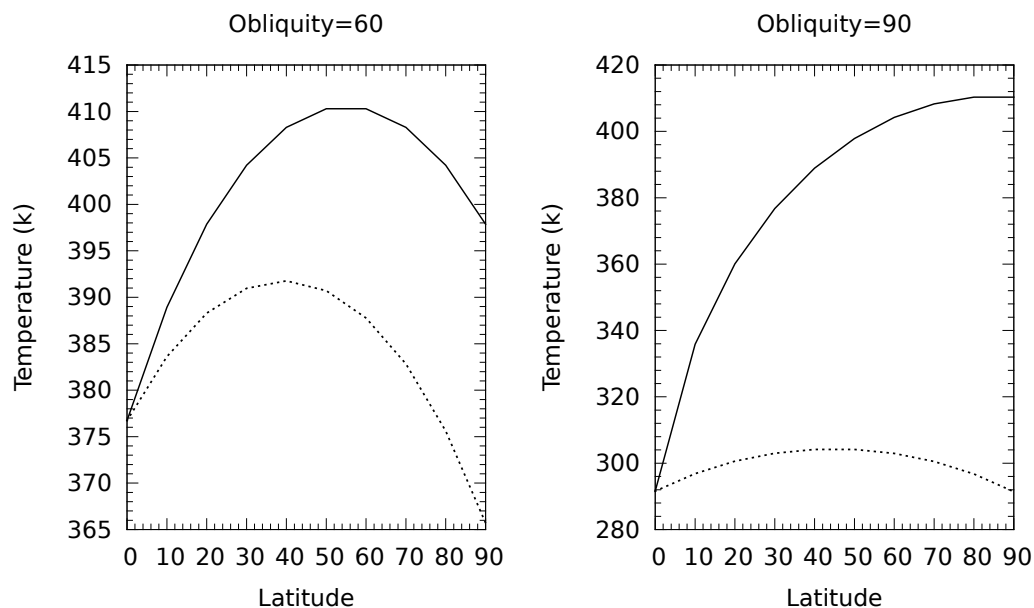


Figure 4.3: Seasonal temperature variations between equatorial and polar latitudes for obliquities of 60 and 90 degrees for a solar luminosity of $1.1 L_{\odot}$. The solid lines represent the upper temperature range and the dashed lines represent the lower temperature range.

described by Tomasella *et al.* (1996) (approximately 1 Gyr from now), Earth's obliquity enters a regime in which it can vary chaotically between much higher values than the present obliquity range. If obliquity cycling in the model is altered to vary between 30-60° (and even up to 90°), the equator-to-pole temperature gradient is effectively reversed by the new, higher obliquity range, which causes the poles to receive more insolation than the equator (in agreement with Tomasella *et al.* (1996)). As such high obliquity planets do not necessarily preclude habitability (Williams & Kasting, 1997) this suggests that equatorial regions may be more accommodating to life than polar regions on the far-future Earth.

These large obliquity swings raise the possibility that the cold trap cave mechanism could extend the lifetime of liquid water habitats further than expected. The more extreme temperature differences between seasons that result from increased obliquity would cause cooler winter temperatures. For example, as illustrated in Figure 4.3, an obliquity of 60° would allow winter temperatures that are up to 40 degrees lower than summer temperatures in some regions, whereas an obliquity of 90° could potentially allow very extreme seasonal temperature variations of more than 100 degrees. This, of course, neglects latitudinal heat transport, which acts to lower the temperature range (especially as atmospheric density increases). By including simple heat transport, an estimate of the magnitude of the lower temperature values over latitude for different obliquity values was

found (Figure 4.4). A high obliquity far-future Earth with a cold-trap cave could extend the stay of execution for life from 1 Gyr to as far as 2.8 Gyr from present.

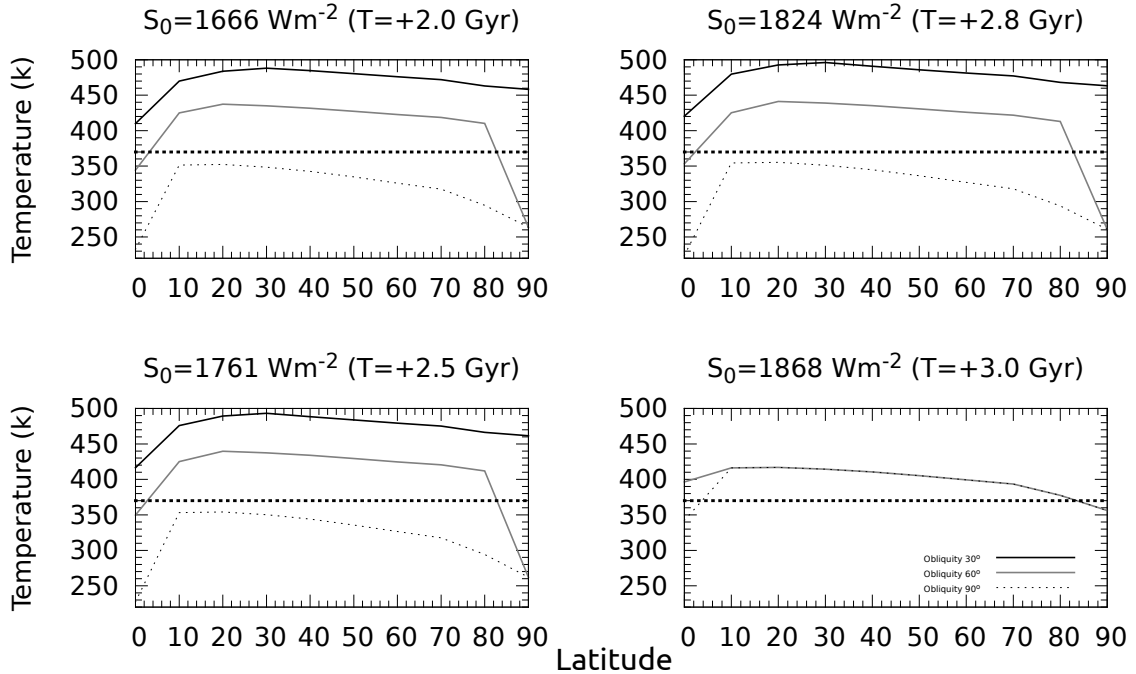


Figure 4.4: Change in lower temperature range over latitude for obliquities of 30, 60 and 90 degrees at 2.0, 2.5, 2.8 and 3.0 Gyr from present. These suggest that, for high obliquities, temperatures may permit liquid water at some, or all latitudes at certain points in the planet’s orbit for at least 2.8 Gyr from present, which would allow for a cold trap cave mechanism to harbour liquid water year-round in these cases. While the +3 Gyr example shows a slight dip below the boiling point of water (bold dashed line) for high/low latitudes for obliquities of 60/90 degrees, the onset of a runaway greenhouse would lead to much less predictable climate dynamics and water availability would be very limited. Note that for the lower right plot, an obliquity of 30° produces temperatures above 500 K at all latitudes.

4.4 High altitude refuges

Another potential refuge could be high altitude lakes. Currently, temperatures in the troposphere follow a mean linear decrease of $\sim 6.5 \text{ K}$ per km with increasing altitude (an average of the lapse rates calculated for dry and moist air) due to the fact that solar radiation is absorbed by the planet’s surface, which re-radiates it, heating the lower atmosphere. Assuming this negative trend still holds on the far future Earth, life could be expected to migrate upwards to more comfortable, liquid water permissible temperatures as surface temperatures rise.

At an altitude of 10 km (with no changes to obliquity or eccentricity cycles) life could persist for approximately 0.7 Gyr longer at polar latitudes than in equatorial regions

(assuming an upper temperature tolerance of 420 K) - see Figure 4.5. Polar surface life could outlast equatorial high-altitude life by approximately 0.2 Gyr. The case for high

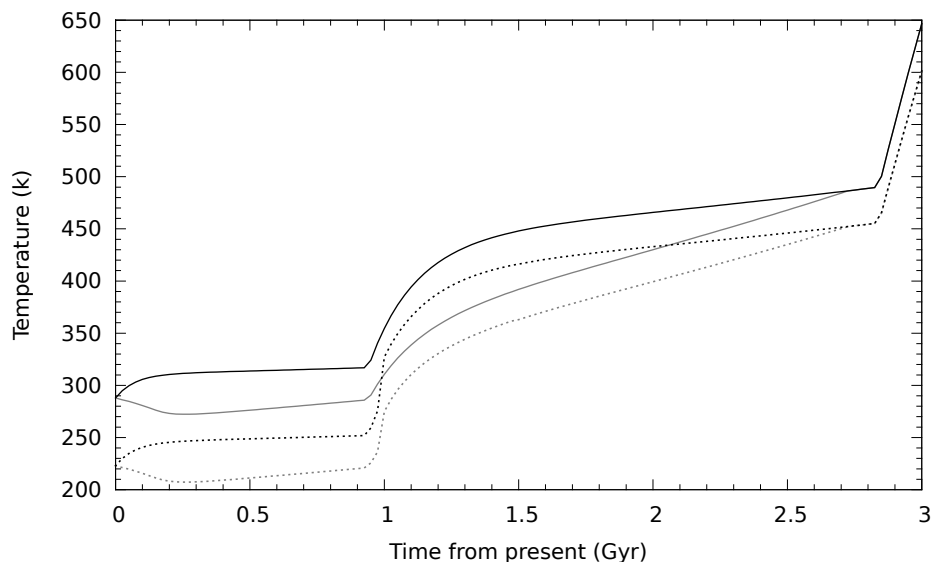


Figure 4.5: Mean temperature evolution at the equator (black) and the poles (grey) with increasing altitude and estimated tropospheric lapse rate from surface level (solid line) to an altitude of 10 km (dashed line).

altitude pools may be complicated by the slowing, or halting of plate tectonics. This would mean that, except in regions where magma plumes continue to rise to the surface, continental uplift could slow down or stop, allowing the weathering rate to exceed the mountain-building rate, potentially resulting in less high altitude land area (Meadows, 2007). However, the lack of plate movements could allow volcanoes surrounding magma plumes (hot spot volcanoes) to grow taller than those on the present Earth as material is able to accumulate in one location for a longer period of time - the driver behind very tall martian volcanoes, such as Olympus Mons, which stands at a height of 21 km (Wood, 1984).

High altitude habitats would be subject to higher biologically damaging radiation fluxes. At higher altitudes UV radiation fluxes are higher because the radiation traverses a shorter pathlength through the atmosphere, so less is absorbed (Blumthaler *et al.*, 1997). DNA strongly absorbs radiation at wavelengths below 320 nm, causing DNA to become damaged (Zenoff *et al.*, 2006). In high altitude environments on Earth today microorganisms use UV screening pigments (such as the red carotenoid pigment used by snow algae, which gives a red-tint to the surfaces of inhabited glacial environments - Lutz *et al.*, 2014)

or DNA-repair mechanisms (Zenoff *et al.*, 2006). Similar radiation defenses would need to be present in far-future high-altitude communities.

4.4.1 Aerial biospheres?

An airborne biosphere of microorganisms could take advantage of the cooler temperatures at higher altitudes. Microorganisms are known to currently be present in the atmosphere (Bowers *et al.*, 2009; Womack *et al.*, 2010), transported there by a variety of mechanisms summarised in Figure 4.6. These organisms are subject to the same DNA-damaging problems as organisms living in high-altitude terrestrial habitats as a result of the high UV radiation fluxes with increasing altitude. Therefore, organisms found in and above the stratosphere tend to be in a dormant spore state to limit DNA damage (Womack *et al.*, 2010). However, some microorganisms found in the troposphere, especially in cloud environments, are in a metabolically active state. (Womack *et al.*, 2010) Some of these organisms have residence times in the atmosphere that are long enough for them to reproduce (Womack *et al.*, 2010; Santl-Temkiv *et al.*, 2013). In particular, clouds could represent a potential refuge for life, much as the upper cloud decks of Venus are believed to be the only potentially habitable environments on Venus (Schulze-Mukuch *et al.*, 2004).

4.5 The deep subsurface

The deep-subsurface environment would likely provide more stable refuges for life. The deep biosphere contains the vast majority of Earth's microbial biomass, with 50-80% of this estimated to occur in the deep marine subsurface (Orcutt *et al.*, 2011). It is officially defined as depths of 50 m or more below the continental surface or the ocean floor (Bell, 2012) although, in practice, deep biosphere research can encompass any depths below 1 m (Bell, 2012; Edwards *et al.*, 2012). The lower depth limit is currently unknown (Kieft *et al.*, 2005; Reith, 2011). The limiting factor is likely to be temperature. It is known that temperature increases with depth, with the mean geothermal temperature gradient for Earth's crust being ~ 30 degrees per km depth (Bohlen, 1987). This would place the lower limit at the depth where temperatures reach the upper-limit for life (122°C) - approximately 3.5 km for the present Earth.

However, the geothermal gradient varies depending on rock type (Pedersen, 2000), increasing or decreasing the maximum habitable depth in a given region. The geothermal

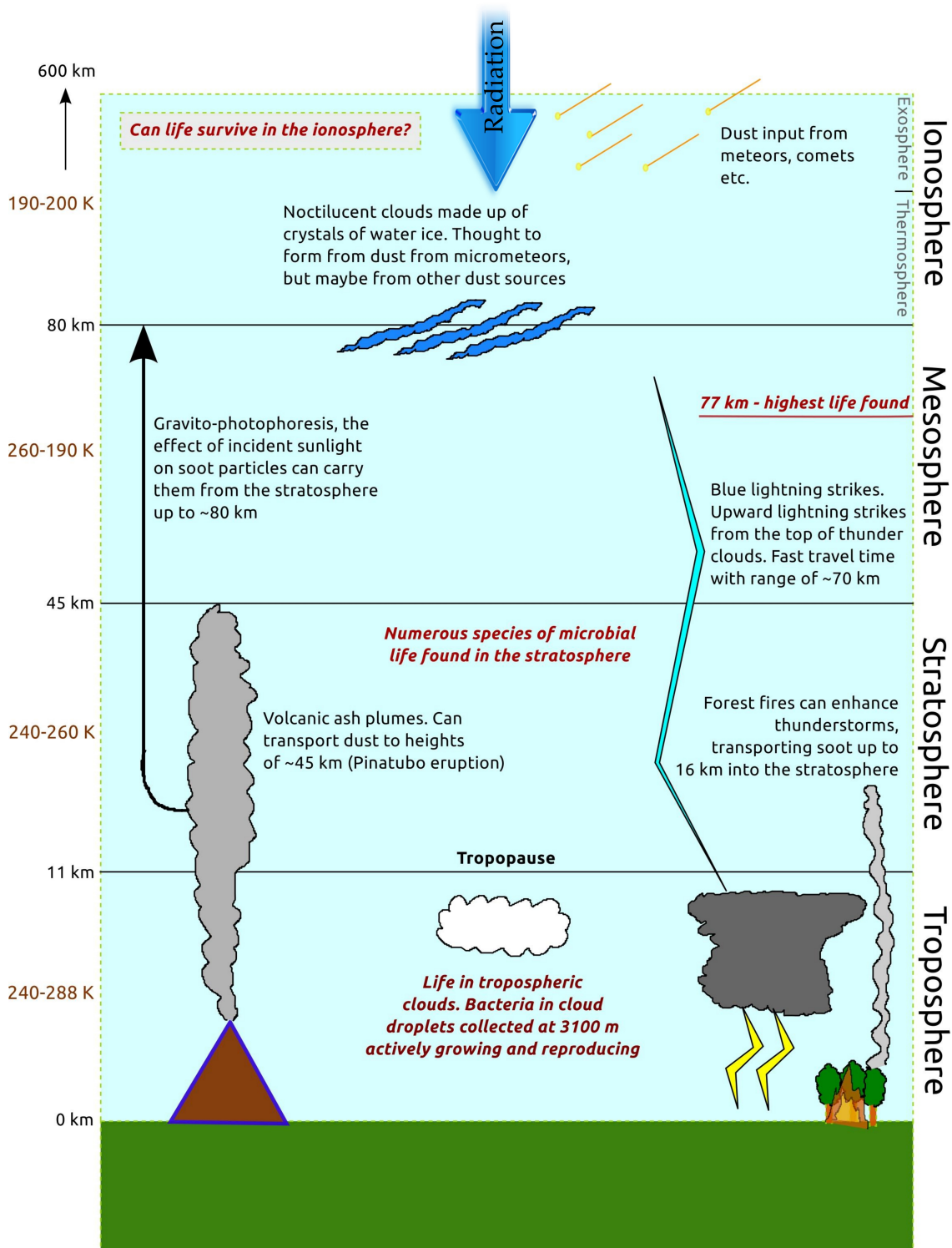


Figure 4.6: Aerosol transport mechanisms from surface to high altitudes within Earth's atmosphere.

gradient of a rock is inversely proportional to its thermal conductivity (Bell, 2004). Therefore, based on differences in thermal conductivity, clays would have a greater geothermal gradient than felsic rocks (igneous rocks such as granite that are rich in elements, such as quartz) - Robertson (1988). The deepest microbial life found to date was found in igneous rock aquifers at depths of 5.3 km. Therefore, although assuming a mean geothermal gradient of 30 degrees would lead to predicted temperatures that preclude habitability once surface temperatures reach the maximum for life, the variable nature of the crustal temperature gradient could allow the deep subsurface biosphere to persist, perhaps for longer than any other refuge.

In the deep subsurface biosphere life has been characterised that operates independently of surface photosynthesis (Kieft *et al.*, 2005; Lin *et al.*, 2005; Lin *et al.*, 2006; Chivian *et al.*, 2008). From a remote detection perspective it may be more challenging to detect the presence of life in these environments; however, life existing independently of photosynthesis might produce methane, which could be detectable (Parnell *et al.*, 2010).

4.6 Summary

By modelling the general temperature trend on Earth for the next 3 Gyr, potential refuges where liquid water would be available and hence, where life could continue to metabolise and reproduce were identified. These far-future refuges could keep a microbial biosphere, albeit at low levels of abundance, present on the planet for up to 2.8 Gyr, with the possibility of a longer stay of execution in subsurface niches and the currently little understood habitable environment that may exist within the planet's atmosphere.

5

Biosignatures of Earth-like planets nearing the end of their habitable lifetimes

HAVING modelled the decline in habitable conditions over geological time into the far future the next step is to model the changes in biosignatures as the biosphere declines. Beginning with the extinction of animals and plants, followed by the decline into an increasingly less diverse microbial world, potential biosignatures for each stage are modelled using the methods discussed in Chapter 3 and their potential for remote detection discussed.

5.1 The end of plant and animal life

5.1.1 The end of photosynthetic life

The end of the higher plants will probably come at the end of a gradual decline in plant diversity as species become less able to survive under changing environmental conditions.

The net primary productivity (essentially the difference between photosynthesis and plant respiration) is $104.9 \text{ Pg C yr}^{-1}$, the terrestrial component of which is $56.4 \text{ Pg C yr}^{-1}$ (Field, 1998). At present 500 Pg of carbon is locked up in terrestrial plant biomass (Mahli 2002); hence, at present rates of primary productivity, this biomass could be produced in < 10 years. However, other loss processes result in the net increase in plant biomass being approximately 1.4 Pg C yr^{-1} (Mahli, 2002), giving an accumulation time of < 500 years at present rates. These loss processes are not presently known, but suggested causes include a bias towards young, growing forests as sampling sites for measuring carbon uptake, carbon loss through dissolution in river water or fluctuating local atmospheric CO_2 levels (Mahli, 2002).

Decaying plant matter initially transfers carbon to the soil carbon pool (1500 Pg C ; Mahli, 2002), microorganisms and, in some cases, to animals. From here it is mostly released to the atmosphere via decomposition or metabolism (CO_2 aerobically and CH_4 anaerobically), with other gases produced as a result of converting some of the energy in plant biomass into a form usable in cell synthesis and maintenance, increasing decomposer biomass (Allison, 2006). Some carbon is transferred to oceans and geological carbon pools. Assuming similar carbon storage in the far-future biosphere, the death of all plants could release up to 500 Pg of carbon into the atmosphere via decomposition or animal metabolism over the time taken for plant species to decline. Higher temperatures are known to increase the rate of decay of dead plant matter into the soil carbon pool, with higher temperatures increasing the rate at which organic matter is broken down (Mahli, 2002).

At present, 80% of the methane flux to the atmosphere comes from the decay of organic matter, estimated as $529-825 \times 10^{12} \text{ g CH}_4 \text{ yr}^{-1}$ (Ehhalt, 1974). The total dead phytomass (not including soil organic carbon) from which this is produced is approximately $184 \times 10^{15} \text{ g}$; approximately 15% of the estimated global total living phytomass, $1243.9 \times 10^{15} \text{ g}$ (Ajtay *et al.*, 1979). In the extreme case, in which the decline in plant life is very rapid, there would be an order of magnitude increase in methane flux until all dead phytomass has decayed. Methane has a relatively short atmospheric lifetime of approximately ten years (Kaltenegger *et al.*, 2007) caused by reactions with hydroxyl radicals and $\text{O}(1\text{D})$ - a highly reactive singlet state of atomic oxygen in which all electrons are paired. Therefore there would be a more intense methane signature in Earth's atmospheric spectrum associated

with this event, but only for a short time period. This period may be shortened by increased production of hydroxyl radicals as a result of the increased atmospheric water vapour content.

However, the plant extinction sequence is likely to be less abrupt, with smaller species being more resistant to temperature increases. The CO₂ uptake (related to the carbon fixation pathway they employ) also varies for different plant types (Mooney 1972), suggesting that those with higher CO₂ uptake rates would be more vulnerable to extinction in a declining CO₂ environment.

Plants using the C₃ pathway to fix carbon (the dominant pathway in higher plants) would be able to survive until atmospheric CO₂ levels drop to 150 p.p.m.; 0.5 Gyr from now (Lovelock & Whitfield, 1982; Caldeira & Kasting, 1992; Raven *et al.*, 2012).

Plant species may be able to continue to exist by becoming able to use lower concentrations of CO₂ for photosynthesis (Raven *et al.*, 2012) and to tolerate arid environments or by implementing other nutritional strategies such as carnivory (Givnish *et al.*, 1984; Rice, 2002; Porembski *et al.*, 2006; Raven *et al.*, 2009; Albert *et al.*, 2010; Flynn *et al.*, 2013; Schmidt *et al.*, 2013) or symbiosis with fungi - mycoheterotrophy (Leake & Cameron 2010; Schmidt *et al.*, 2013). As a survival strategy, carnivory may be useful in certain low-nutrient ecosystems with intense solar radiation where liquid surface water is still abundant (Givnish *et al.*, 1984; Rice, 2002). These conditions would be more common near the beginning of the moist greenhouse stage as the planet begins heating up, e.g. due to the loss of soil nitrogen in wet, high temperature conditions (although carnivory may be generally more related to phosphorus deficiency: Wakefield *et al.*, 2005). However, CO₂ is still fixed from the atmosphere (or freshwater bodies for aquatic species) in carnivorous plants today and almost all carnivorous plant species use the C₃ pathway to fix carbon, which does not permit rapid photosynthesis in very low CO₂ concentration, high-temperature environments (Porembski *et al.*, 2006; Albert *et al.*, 2010). However, terrestrial *Utricularia* species produce more traps (in terms of their overall biomass) than photosynthetic cells, suggesting that the reduced carbon gain from photosynthesis is offset by carbon obtained via carnivory (Porembski *et al.*, 2006; Albert *et al.*, 2010). Some bromeliads (a few of which may be carnivorous: Givnish *et al.*, 1984) use CAM to fix carbon, which helps to acquire and conserve carbon in arid environments. However, ulti-

mately, as a strategy, carnivory would only give a temporary advantage as prey ultimately depend on plants for food. So as plant species decline, so too would prey.

Similar considerations apply to mycoheterotrophs, which are plants obtaining some or all of their organic carbon from symbiotic mycorrhizal fungi, which in turn obtain their organic carbon from soil organic carbon or from fully photosynthetic plants with which the fungi are also symbiotic (Leake & Cameron, 2010). About 10% of vascular plants have a juvenile mycotrophic and subterranean phase growing from (usually) very small spores or seeds which depends on mycoheterotrophy (Leake & Cameron 2010). While almost all of these ultimately become photosynthetic autotrophs, about 450 species never develop photosynthesis and live as mycoheterotrophs through their life cycle (Leake & Cameron 2010). Such plants would only have a short time to live after the last autotrophic plants in a habitat died, using soil organic carbon that is no longer being replenished.

Adaptations that conserve water such as lower surface areas per unit volume (as seen in cacti and other succulents, noting that this adaptation relates mainly to restricting water loss when photosynthesis using external CO₂ is not possible) or increased reflectivity via the use of epicuticular wax, such as in the case of *Dudleya brittonii*, may be more widely adopted as temperatures increase (Jones, 2013; Sage & Zhu, 2011). The drivers for these adaptations are not known, but the cause may have been a prolonged global dry spell, which coincided with a global temperature drop and a fall in atmospheric CO₂ (Arakaki *et al.*, 2011). Present-day C₄ plants are more rapid photosynthesisers in dry, high temperature, CO₂ and nitrogen-limited environments, suggesting adaptations like this may be employed as conditions for plants worsen.

The decrease in atmospheric ozone would lead to less attenuation of DNA damaging UV radiation, particularly UV-C radiation (200-280 nm). The increased UV surface flux would be further enhanced by the decrease in atmospheric CO₂ levels, which, in the present-day atmosphere, scatter shorter wavelengths in the UV-C range. This would lead to surface UV irradiation similar to that of the Archaean Earth, reaching $1 \times 10^{-1} \text{ Wm}^{-2} \text{ nm}^{-1}$ for longer UV-C wavelengths (Cnossen *et al.*, 2007) and a DNA-weighted dose (i.e. a radiation dose that is biologically effective) up to a thousand times higher than on the present-day Earth (Cockell & Raven, 2007). If a similar irradiation environment to the Archaean is assumed, there are likely to still be environments where organisms could survive using

DNA repair mechanisms or in shielded environments (Cockell & Raven, 2007).

Land plants and oceanic phytoplankton produce significant amounts of the volatile compound isoprene, $\text{CH}_2=\text{C}(\text{CH}_3)\text{CH}=\text{CH}_2$ (Seager *et al.*, 2012). Isoprene has a very short atmospheric lifetime, being rapidly oxidised. However, in an increasingly anoxic atmosphere, isoprene may be a plausible atmospheric biosignature. Oceanic phytoplankton would be better able to survive for longer than terrestrial photosynthetic organisms due to their low CO_2 requirements and ability to extract carbon from bicarbonate (Raven *et al.*, 2012). Therefore, if these organisms release isoprene at a rate similar to the present-day rate (0.31-1.09 Tg C yr⁻¹ - Gantt *et al.*, 2009) this could allow a detectable level of isoprene to build up in the atmosphere, although the photodissociation of the increased atmospheric water vapour content could provide enough free oxygen to keep the lifetime of isoprene short (it has a lifetime of < 1 day in an oxygen-rich atmosphere - Palmer *et al.*, 2003).

The end of the vegetation red-edge signature

A decrease in vegetation during the stage in which plant extinction occurs could cause changes in the vegetation red-edge signature. Remote sensing can be used to estimate vegetation coverage from the leaf area index (LAI), defined as green leaf area/surface area. Spectral reflectance in the near infrared and visible wavelength regions is used to determine the normalised difference vegetation index (NDVI) from which an estimate of LAI (locally or globally) can be obtained (see, for example Deng *et al.* (2006), Ganguly *et al.* (2012)). As plant extinction rates increase, the LAI should decrease as leaf area decreases, potentially leading to a less intense red edge spectral feature. Filella & Peñuelas (1994) found that the area of red edge peak changed with LAI as LAI determines the ratio of near-IR and red reflectance. C_4 plants have been shown to exhibit greater leaf area than C_3 plants grown under the same conditions (Anten *et al.*, 1995), suggesting the presence of more rapid photosynthesisers could delay a reduction in the spectral red edge signal. However, as plant species become extinct, vegetation will become increasingly sparse, with LAI values approaching high desert values (<1 - Running *et al.*, 1986) and the LAI - NDVI relation may no longer hold. When vegetation cover becomes too low, the observed spectrum is dominated by soil and rock which have varied red-near-IR slopes, which alter the measured vegetation indices (Huete *et al.*, 1985; Elvidge & Lyon, 1985). Additionally, as

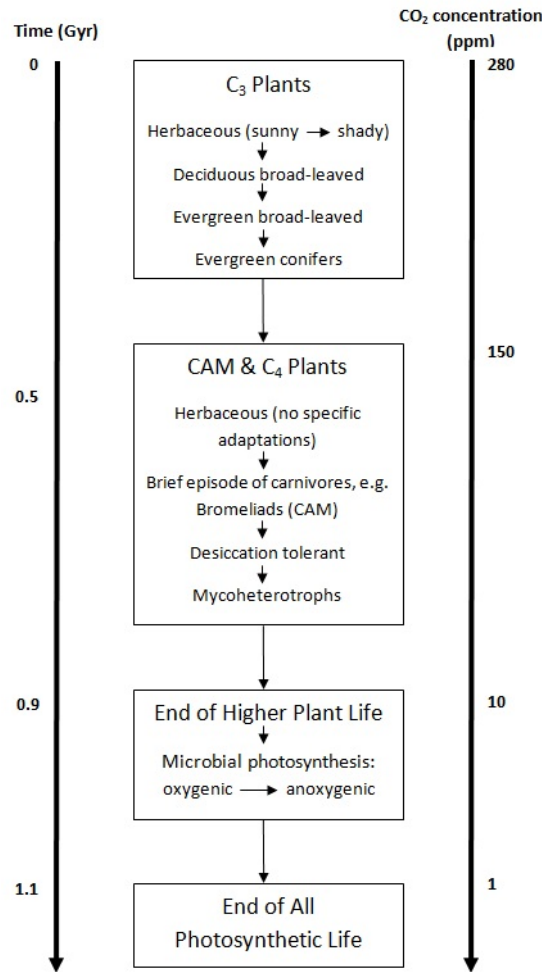


Figure 5.1: Summary of the predicted plant extinction sequence. C₃ plant species disappear before C₄ species. In general, species decline until only those most tolerant to arid, low nutrient and high temperature conditions remain. In each case, larger plants would be more likely to face extinction as these have more mechanical and transport machinery to build and maintain, resulting in a greater loss of photosynthetically gained carbon via respiration. After atmospheric CO₂ falls below 10 ppm, only microbial photosynthesis remains viable until CO₂ levels fall too low for even this to take place.

vegetation becomes more adapted to arid conditions it is likely to incorporate adaptations that decrease the amount of visible light absorbed, making it harder to detect.

Increasingly sparse vegetation will lessen the intensity of the red edge signature, which will eventually disappear completely with the end of all plant life. Warming temperatures lead to a poleward expansion of the boundaries of equatorial Hadley cells (currently at $\pm 30^\circ$ latitude), which has been linked to the simultaneous poleward expansion of subtropical dry zones (Lu *et al.*, 2007). The meridional extent of the equatorial Hadley cells (ϕ_H) can be approximated using Equation 3.5.

Using the model results for temperature evolution and accounting for the slowing of the Earth's rotation due to tidal interactions with the Moon (increasing the day length by 1.70×10^{-5} s yr⁻¹ - Stephenson, 1997), ϕ_H can be used to estimate the expansion of the subtropical dry zones, giving an approximate timescale for the loss of abundant vegetation. Within 0.3 Gyr equatorial Hadley cells would have expanded to approximately 40° north and south of the equator, increasing the arid fraction of the surface by 25%, doubling the current total area of arid land. By assuming plants in arid regions are too sparsely spread to contribute to the red edge signature, this alone would reduce the strength of the signature. However, Earth is currently half-way through a supercontinent cycle, with another supercontinent expected to be formed within the next 250 Myr (Yoshida & Santosh, 2011). The location of this landmass would greatly influence environmental conditions. An equatorial supercontinent would have a more stable climate, but would likely have large dry, arid interiors, whereas polar supercontinents would experience extreme temperature fluctuations, except in coastal regions (Williams & Kasting, 1997). Either case would lead to large areas of land with only sparse vegetation coverage, effectively ending the distinctive vegetation red edge signature. Supercontinent formation and break-up have been linked to past mass extinction events (Santosh, 2010). Increased competition between species due to the merging of continental landmasses and the possibility of increased volcanic emissions from deep mantle superplumes, combined with generally less hospitable conditions on the warming Earth could lead to a mass extinction event for plants and animals from which they may not be able to recover.

5.1.2 The end of animal life

The decline in plant species would lead to a lowering of atmospheric O₂ and O₃, which eventually fall to trace levels in only a few Myr once all plant life has disappeared (Walker, 1991). Decaying plant life would produce methanethiol (CH₃SH). Animal and plant extinction sequences will inevitably overlap. Those animals that are in food chains dependent on live plants will begin declining shortly after the plants at the base of their food chains disappear. Larger animal species could survive for longer in the oceans where phytoplankton would outlast land plants. Animals that are not dependent on live plants could survive for longer. Termites, for example, are able to digest dead wood due to a symbiotic relationship with microorganisms in their guts (Geib *et al.*, 2008), while some isopod

crustaceans are able to digest dead wood without the aid of symbiotic microbes (King *et al.*, 2010). Chemolithotrophically (chemosynthetically) symbiotic vestimentiferan worms (*Riftia*) found near hydrothermal vents may also be well suited to surviving longer than other animals, although these too would face extinction when the oxygen content of deep waters is depleted.

The decline in atmospheric O₂ associated with the decline in plant abundance, the continued oxidation of kerogen (organic carbon in sedimentary rocks) and the continuing consumption of O₂ by organisms that respire aerobically will result in the extinction of multicellular (metazoan) animal life. Large endotherms (mammals and birds) would likely be the first group to become extinct due to their higher oxygen requirements compared with smaller endotherms and exotherms. Hence, with a lower oxygen partial pressure in the atmosphere, the metabolisms and activities of these organisms would be the most affected. As temperatures increase alongside declining atmospheric O₂ levels, eutherians (placental mammals) would be particularly vulnerable. Not only do these have higher oxygen requirements than non-placental mammals, which is said to have delayed the evolution of large placental mammals until atmospheric oxygen reached a certain level (Falkowski *et al.*, 2005), but embryo development is very sensitive to excess heat (McLean 1991). Large herbivorous mammals would suffer from the decrease in food supplies as plant abundance decreases. Smaller mammals would have a slight stay of execution in comparison, due to their lower oxygen requirements and their larger surface-to-volume quotient, which aids in the dissipation of heat (McLean 1991). This scenario is slightly complicated by the fact that eutherians have higher body temperatures than marsupials and monotremes (Clarke & Rothery, 2008), which may, therefore, be more susceptible to increasing temperatures. Birds may be better suited to surviving than larger mammals. Their generally smaller sizes mean they require less oxygen than larger animals, but also, migratory birds especially would be better able than similarly sized mammals to travel long distances to find lower temperature refugia. However, the number of these refugia for such animals would decline as temperatures continue to rise. These refugia would also tend to be at higher elevations where less land surface area is available, restricting population sizes as species migrate upwards (Sekercioglu *et al.*, 2007).

Ectothermic vertebrates (fish, amphibians and reptiles) would be able to survive for longer than endotherms in this scenario due to their better heat tolerances and, in general,

lower oxygen requirements (some ectotherms have been observed to consume oxygen in greater quantities than living endotherms of the same body weight) (Kemp, 2006). Decreasing water availability would make some amphibian species more vulnerable in such a world (Aráujo *et al.*, 2006). Fish species would be similarly vulnerable. It should be noted that rapid ocean evaporation would not yet have begun at this time. Marine species may be able to survive for longer than freshwater species. The orders of magnitude greater volume of ocean water than freshwater would result in freshwater habitats being lost more rapidly than marine habitats. For ectotherms, external temperature influences metabolic rate. An increased environmental temperature results in an increased metabolic rate and therefore, an increased need for food. Hence, surviving species may be vulnerable to starvation (Dillon *et al.*, 2010). Reptile species with temperature-dependent sex determination would be more susceptible to increased temperatures (Aráujo *et al.*, 2006).

Invertebrates could be the final animals present on Earth before all animal species are lost. Some insects, such as the spider beetles *Mezium affine* and *Gibbium aequinoctiale* have been observed to survive (but not necessarily to complete their life cycle) in temperatures of up to 56°C (Yoder *et al.*, 2009). In general, life on land will be more vulnerable than marine life initially as a result of the temperature-buffering effects of water. However, the loss of plant life on land would lead to a reduction in nutrients reaching the ocean once soils have eroded away. Communities isolated from marine food chains, such as volcanic vent communities, would likely survive for the longest (Ward & Brownlee, 2002). Within approximately 0.1 Gyr after the end of higher (embryophytic) plant life, Earth will once more become a microbial world.

Decaying animals (as well as plants) release methanethiol (CH₃SH), a gas that can be spectrally inferred and has no known abiotic source. The extreme case of the extinction of all animals (beginning with vertebrates, then invertebrates) over a few Myr timescale could lead to a large release of CH₃SH into the atmosphere. Assuming a biomass of plants and animals equivalent to present day values (560×10^9 tonnes C - Groombridge & Jenkins, 2002) and cell sulphur contents of 0.3-1% (Pilcher, 2003), this allows for the potential release of 1.12×10^{15} g of CH₃SH (via conversion from methionine). If this were released at the current biological production rate (3×10^{12} g yr⁻¹) it would all be released to the atmosphere within 350 years. CH₃SH itself would not be a useful biosignature as it has a very short atmospheric lifetime, being readily photodissociated. However, the dissociated

methyl groups combine to form Ethane, which would have a much longer atmospheric lifetime under the increasingly anoxic conditions at the end of the age of animals, making it a potential biomarker under these circumstances (Domagal-Goldman *et al.*, 2011). However, as with plant extinctions, the extinction of animal species is likely to occur over a much longer timescale of 10-100s Myr, based on the expected extinction times for plant species. This could lead to a much weaker biosignature associated with the event, e.g. a 100 Myr extinction time would lead to a smaller flux of approximately $10^7 \text{ g CH}_3\text{SH yr}^{-1}$.

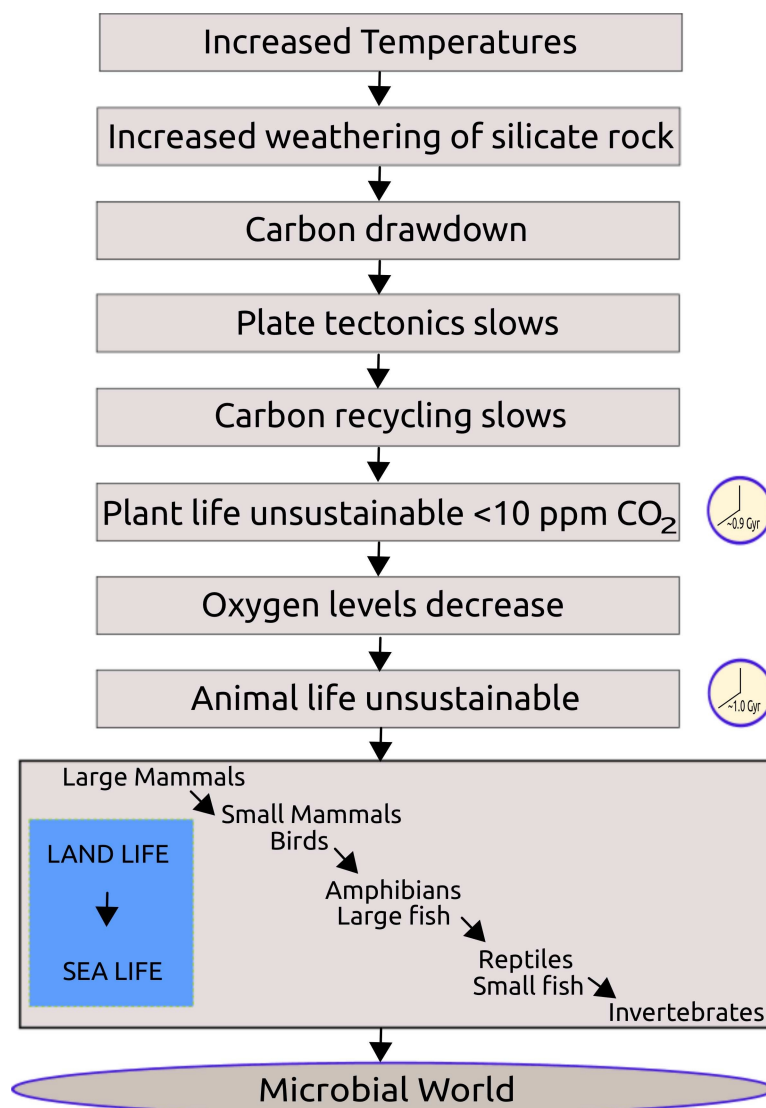


Figure 5.2: A simplified sequence of events between the present and an entirely microbial biosphere approximately 1 Gyr from the present.

5.2 Biogeochemical reactions in a future microbial world

In this section, the probable microbial inhabitants in each of the available habitats are determined based on their likely metabolic reactions (cf. Table 3.1), determined by the nature of high altitude, cave and subsurface refuge habitats. These are summarised in Table 5.1. The microbial abundance in a particular region is then linked to the surface temperature evolution (as described in Chapter 3) such that the modelled cell count drops to zero when the temperature in a particular zone exceeds 420 K; an upper temperature bound for life (set to allow some increase over the currently known upper temperature tolerance of thermophiles) at which biological chemical processes break down. The total modelled cell abundance is shown in Figure 5.3.

5.2.1 High altitude

Temperatures at high altitudes could remain low enough to permit liquid water pools for longer than at surface levels, providing refuges for life as surface temperatures increase. Additionally, any hot spot volcanoes (up-welling plumes from the deep mantle that occur in the middle of plates rather than at plate boundaries) that are present on the far-future Earth would provide refuges for simple microbial communities. Recent findings from a site at high altitude (6000 m) in the Atacama Desert show that life in such environments uses the oxidation of carbon monoxide, ammonia or dimethyl sulphides to obtain energy (Lynch *et al.*, 2012), producing various by-products such as CO₂, N₂, SO₂, CH₄, sulphonate and sulphates (see Table 3.1 for reactions). For oxidation reactions to be feasible, localised O₂ sources would be needed for such communities to exist in far-future refuge environments. A lesser energy gain per mol of substrate oxidised could also be obtained with other oxidants such as ferric iron and nitrate, but the availability of these tends to decrease with oxygen availability. As O₂ levels are reduced, iron will tend to be in a reduced state, making iron oxidation more favourable in a declining biosphere. Life is also known to exist around volcanic steam vents, for example, McMillan and Rushforth (1985) reported the presence of many species of diatom living in condensing steam around a steam vent near Kilauea Crater, Hawaii (as these are photosynthetic species, a sufficient CO₂ flux from the volcanic vent would be needed to support similar communities on the far-future Earth). Water vapour is the most abundant gas released via volcanic activity, which may mean

that high altitude volcanic vents provide oases on the dry future Earth as steam condenses onto lower temperature surfaces.

There are over 1500 subaerial volcanoes that have been recently active, i.e. within the past 10,000 years (Siebert, Simkin & Kimberly, 2010). Only approximately 49 volcanic sites are found at volcanic hotspots (Courtilot *et al.*, 2003). Comparing hypsometric curves for Earth, Venus and Mars (which measure land elevation relative to sea level, or a chosen baseline for dry planets) shows that, while there are clear differences in the surface area-elevation relationships for each planet, in all cases only $< 1\%$ of the surface area is found at elevation above 5 km (Luo & Stoddard, 2002).

5.2.2 Caves

Microbial life in cave environments on Earth today consists of chemolithotrophically based metabolisers and those that make use of organic carbon from external sources (photosynthesis occurring elsewhere) that enters the cave environment, often being found in microbial mat communities. Life in far-future cave refuges is more likely to be chemolithotrophic due to the absence of photosynthetic carbon sources. An example of a cave ecosystem entirely based on chemosynthesis is found in Movile Cave, Romania. Here, life has been separated from the outside world for 5.5 Myr and has similarities to hydrothermal vent communities (Chen *et al.*, 2009). The cave receives a high flow rate of hydrothermal water, which is rich in sulphides and methane; hence, life in the cave is mainly based on sulphide and sulphur oxidation and methane oxidation. This produces by-products such as sulphuric acid, iron III (ferric) sulphate and carbon dioxide (see Table 3.1).

However, sulphur, sulphide and methane oxidation would only be possible to a limited extent on the largely anoxic far-future Earth. Sulphate and anaerobic methanotrophs have been found together in anoxic marine sediment environments (Orphan *et al.*, 2001), suggesting a potential alternative for far-future cave ecosystems although this would not provide as much energy as oxidation reactions. Anammox bacteria, known to be high-temperature tolerant (Byrne *et al.*, 2009), could potentially produce a hydrazine biosignature (assuming gas exchange with the surface) as hydrazine is a free intermediate in the anammox reaction (Strous *et al.*, 2006).

5.2.3 The subsurface

Microbial subsurface life could use anaerobic methane oxidation, ferric iron reduction or sulphate reduction to metabolise (see Table 3.1). Hydrogen driven communities may also be present, although there is some debate as to whether enough abiotic hydrogen (produced by the radiolysis of water (Blair *et al.*, 2007) or reactions between dissolved gases in magma, for example) could be produced to support them (Reith, 2012). Originally it was assumed that subsurface life would be predominantly methanogenic; however, recent work suggests that this may not be the case due to the higher than expected counts of sulphate reducers found, suggesting a syntrophic biosphere of chemolithoautotrophs or organotrophs with fermenting bacteria (Teske, 2005). Life in the deep subsurface would experience higher temperatures than surface dwelling life, as temperature increases with depth due to the geothermal temperature gradient of the Earth's crust. This means it is likely that this would be the first group of microorganisms on the dying Earth to disappear.

Detecting the presence of subsurface life is more challenging than detecting life in other habitats; even on Earth this can be a difficult process. While life in the shallow subsurface could produce waste gases such as methane, which could percolate out into the atmosphere through rock or soil, deeper life would require the presence of deep faults in rocks for biomarker gases to escape into the atmosphere (Stevens 1997). However, in some cases it could be possible to detect subsurface life indirectly by looking at the surface features of the environments that support it (Hegde & Kaltenegger 2013). Temperature below the surface is determined by the surface temperature and increases with depth. The Earth's geothermal temperature gradient varies depending on rock type, but on average it increases by 30° per km depth (Bohlen, 1987). Although this mean temperature gradient would preclude life once surface temperatures exceed the maximum temperature tolerance for life, the variable nature of the crust's temperature gradient could allow life to persist for longer than in any other refuge (O'Malley-James *et al.*, 2013).

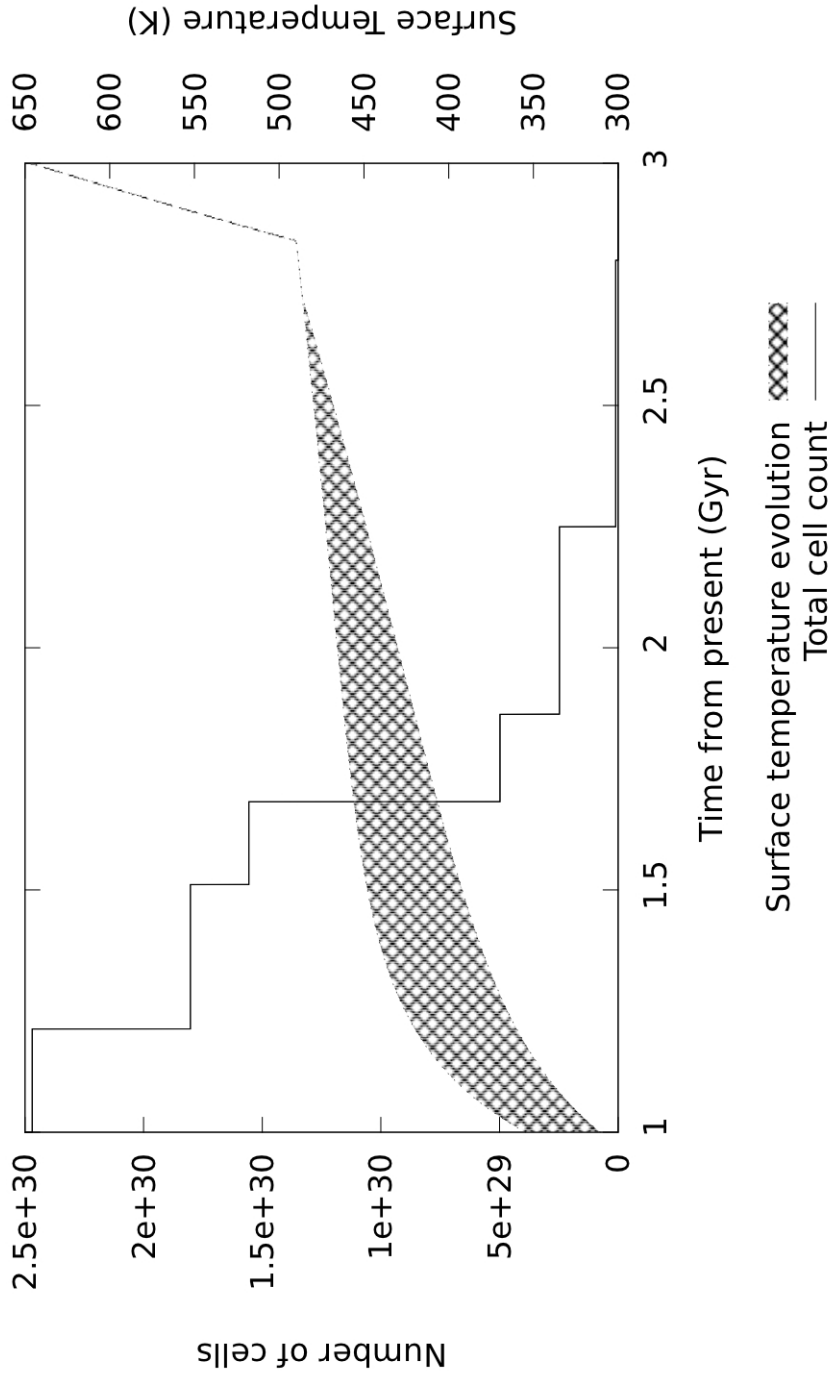


Figure 5.3: Change in cell abundance per unit surface area over time with increasing temperature. The shaded area represents the equator-to-pole temperature range.

Microbe type	Likely Habitat
Methanogens	High elevation, caves. Most abundant before photosynthesising plants die off, but increasingly limited to CO ₂ sites (e.g. volcanic vents) as atmospheric carbon dioxide levels drop.
Ammonia oxidisers	High elevation, caves. Limited to volcanic vents; only until atmospheric oxygen drops to negligible levels.
Hydrogen oxidisers	Subsurface. Anywhere where hydrogen is available. Photolysis of water vapour could provide abundant atmospheric hydrogen.
Sulphur oxidisers	Caves. Limited to volcanic vents and evaporites. Only until atmospheric oxygen drops to negligible levels. May be able to persist near localised O ₂ sources e.g. near anaerobic iron reducers.
Carboxydotrophs	High elevation, caves. Limited to near volcanic vents. Only until atmospheric oxygen drops to negligible levels. May be able to persist near localised O ₂ sources. A reduction in O ₂ levels favours the photodissociation of CO ₂ to CO in the troposphere (Pinto <i>et al.</i> , 1980), perhaps expanding the habitats for CO using microorganisms; however, this is also dependent on CO ₂ availability.
DMS oxidisers	High elevation, caves. Initially very abundant during the end of the age of photosynthesis when photosynthetic microorganisms still exist. Declining as photosynthetic life ends and oxygen levels fall.
Iron oxidisers	Abundant in all areas with liquid water and a source of iron until atmospheric oxygen levels fall to negligible levels.
Aerobic Methanotrophs	Caves, subsurface. Most abundant immediately after photosynthesising plants die off, but increasingly limited to CH ₄ sites (e.g. volcanic vents) as atmospheric CH ₄ levels drop.
Anaerobic Methanotrophs	Subsurface, caves, high elevation. Most abundant immediately after photosynthesising plants die off, but increasingly limited to CH ₄ sites (e.g. volcanic vents) as atmospheric CH ₄ levels drop.
Iron reducers	Subsurface, caves. Abundant in any place with liquid water and a source of iron. Likely to be able to survive until temperatures exceed the maximum temperature tolerance of life.
Sulphate reducers	Subsurface, caves, high elevation. Limited to volcanic vents and evaporites. Likely to be able to survive until temperatures exceed the maximum temperature tolerance of life.
Acetogens	Subsurface, caves. Most abundant before plants die off. Limited to CO ₂ and H ₂ sources thereafter, perhaps associated with other microorganisms (e.g. H ₂ or CO ₂ producers).
Anammox reaction	Subsurface, caves, high elevation.
Denitrification	Subsurface, caves.
Ammonia fermentation	Subsurface, caves.

Table 5.1: Microbial organisms that could be supported by the types of habitable environments available on the far-future Earth.

5.3 Biosignatures

5.3.1 Model results

The gas reservoir of the microbe-atmosphere interaction model is sampled at different points throughout the the temperature evolution predicted in Chapter 4, as illustrated in Figure 5.4.

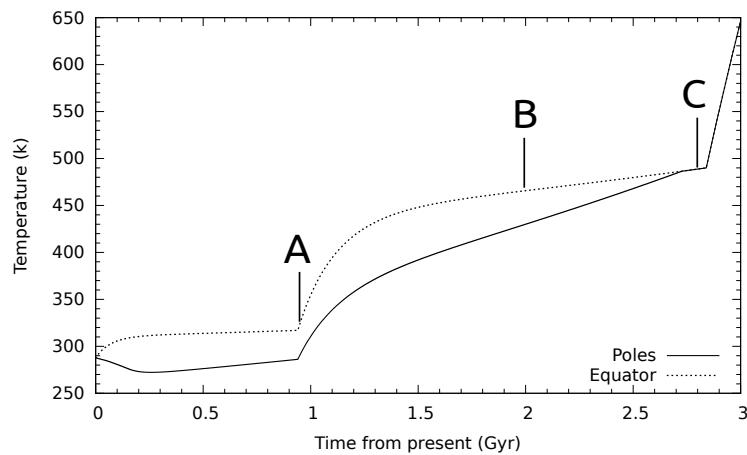


Figure 5.4: Points measured during the Earth’s future temperature evolution at which biosignature gas levels are measured. Point A represents the period during which all plant and animal species become extinct; B represents a low-productivity microbial biosphere and C represents a biosphere of final survivors living in refuge environments before all life on Earth becomes extinct.

At each point, the amount of biosignature gases in the atmosphere is estimated and compared against present levels in Earth’s atmosphere. These results are summarised in Figures 5.5, 5.6 and 5.7.

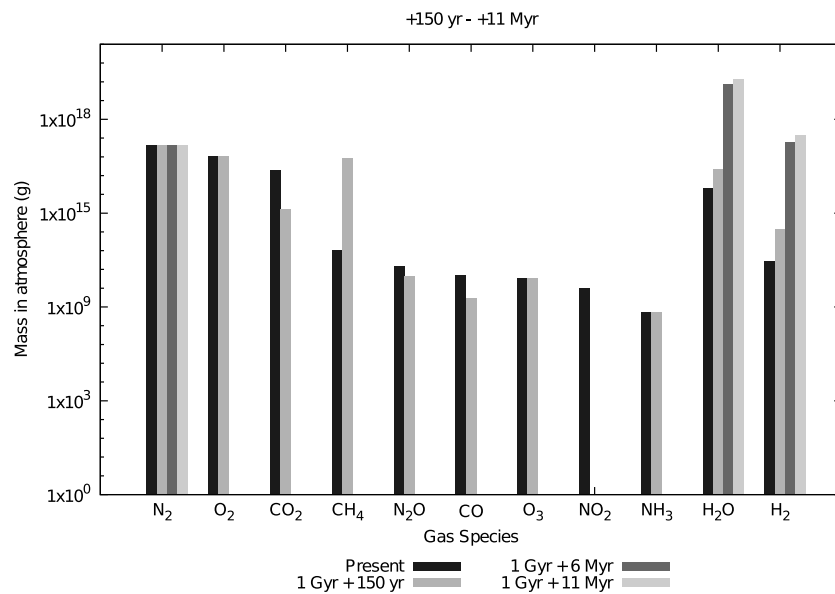


Figure 5.5: (A) Changes in gas species abundances in the atmosphere between 150 years and 11 Myr (+1.011 Gyr from present) after the extinction of higher plant species. The rapid disappearance of CO₂ and O₂ (and CO and O₃) is seen within 6 Myr as is the onset of rapid ocean evaporation and the associated increase in H₂ flux from increased photodissociation is clear. The large increase in CH₄ is associated with the decay of organic matter for the extreme case of rapid extinction. N₂O production drops off with declining O₂ levels as denitrification rates fall. This rapid decay halts the NH₃ flux, with the remaining atmospheric NH₃ being used up by ammonia oxidisers within 6 Myr. Under anoxic conditions, NO₂ production via the fixation of N₂ by lightning could be up to 2 orders of magnitude lower than production in the present day atmosphere. This would be more than balanced by the loss of NO₂ via photolysis, resulting in no net gain of NO₂.

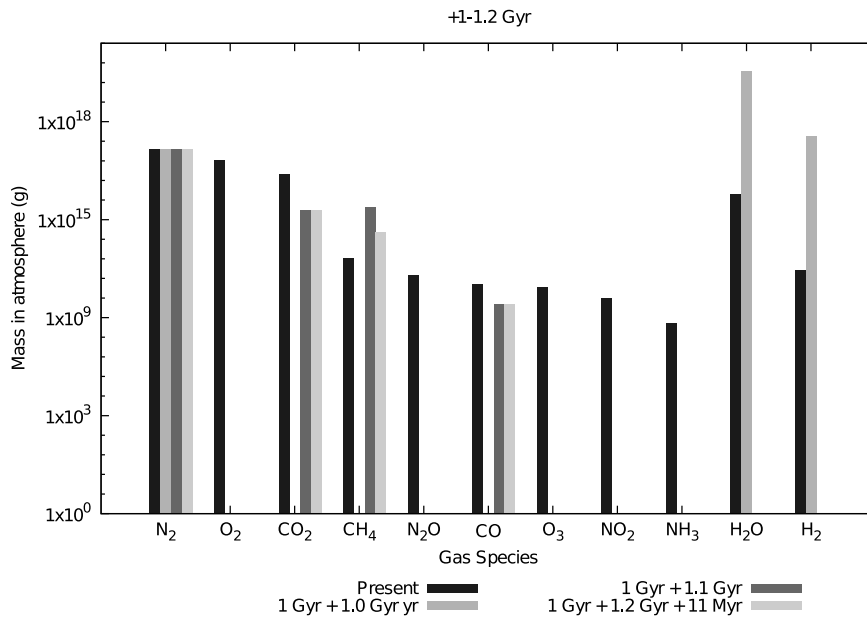


Figure 5.6: (B) Changes in gas species abundances in the atmosphere +2 Gyr from present. Atmospheric H₂O levels fall as the oceans fully evaporate and the remaining water vapour photodissociates, with the liberated hydrogen escaping to space. The loss of atmospheric H₂O slows silicate weathering rates, allowing CO₂ from volcanic sources to build up in the atmosphere once more. Methanogenic microorganisms make use of increased CO₂ availability, producing CH₄ as a by-product, which in turn is used by methanotrophs.

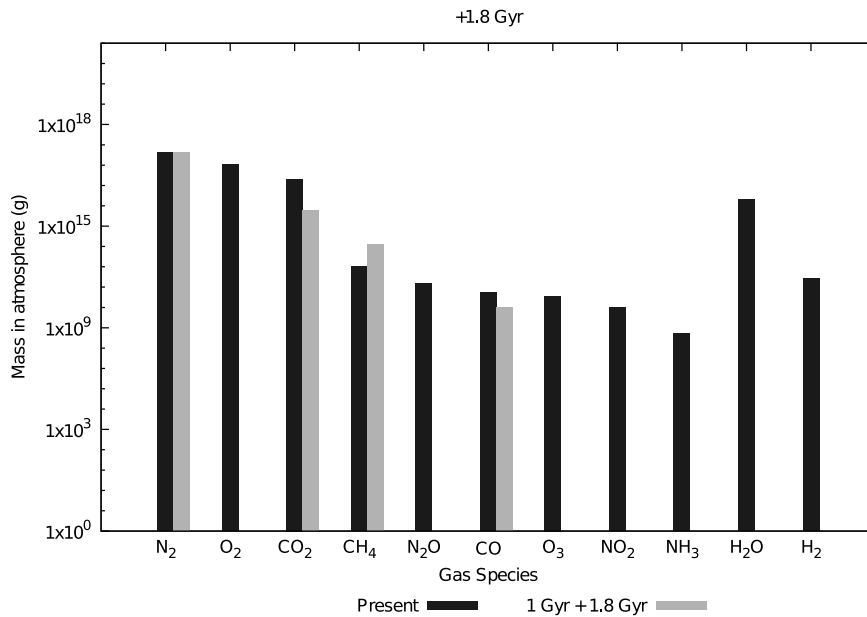


Figure 5.7: (C) Changes in gas species abundances in the atmosphere +2.8 Gyr from present. Only CH₄ produced by methanogenesis remains as a viable biosignature in a largely N₂:CO₂ atmosphere.

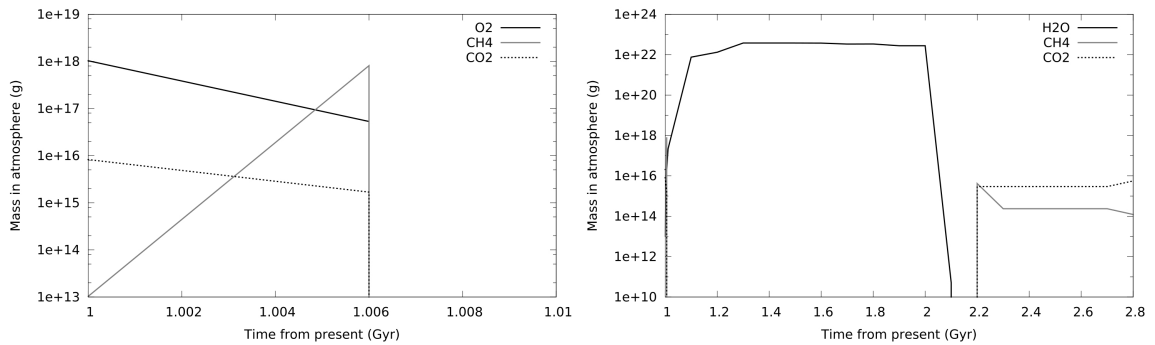


Figure 5.8: The trends followed by biosignature gases over the modelled time period. The left-hand plot shows the behaviour of O₂, CH₄ and CO₂ at the very beginning of the biosignature modelling period. The initial rise in CH₄ is a result of organism decay following the extinction of animals - in this case the extreme case of a rapid extinction of all animals following the extinction of (non-microbial) plants was assumed. CO₂ declines more rapidly as water vapour begins to become a dominant component of the atmosphere, leading to a halt in O₂ production as the final microbial photosynthesisers become extinct. The decline in CO₂ also impacts production of CH₄ by methanogens. High levels of atmospheric water vapour suppress CO₂ levels in the atmosphere (as a result of high silicate weathering rates) until 2.2 Gyr from present when the atmospheric water vapour content has fallen. The geological CO₂ emissions enable CO₂ levels to build up again and increase the production of CH₄ via methanogenesis. Methanotrophs begin metabolising the newly available CH₄, resulting in its gradual decline.

5.3.2 Detectability

For atmospheric abundances similar to present-day levels, CO₂, H₂O and O₂/O₃ would all be remotely detectable with low resolution spectrographs on an extrasolar Earth-like planet (Selsis, 2004; Kaltenegger *et al.*, 2010). The only case where atmospheric O₂ and O₃ would be detectable is in the beginning of the time period covered in (A) (see Figure 5.4). H₂O would be detectable in cases (A) and (B) (Figures 5.5 and 5.6). Estimated CO₂ levels are lower than current atmospheric levels, making the remote detection of this less likely in all three cases. Ethane related to the large-scale decay of plant and animal species, in the extreme case discussed in (A), is theoretically remotely detectable, but water vapour and other atmospheric aerosols could interfere with its detection (Domagal-Goldman *et al.*, 2011). Although not as biologically relevant, H₂ should be detectable at the levels predicted in both cases (A) and (B), producing a particularly strong signal in case (B) (Miller-Ricci & Fortney, 2010). N₂, despite its abundance, is spectrally inactive. It lacks any marked electronic transition (except at extreme UV wavelengths), but its presence can be inferred from collisions between O₂ and N₂ molecules when observing the transmission spectra of planetary atmospheres (Pallé *et al.*, 2009). Oxygen collision complexes and molecular oxygen bands can then be used to derive an average atmospheric N₂ column

density. In low O₂ atmospheres, detecting N₂ may therefore be more challenging. From the minimum abundance limits for detection described in Selsis (2004), only CH₄ would be potentially detectable in cases (A), (B) and (C) - Figures 5.5, 5.6 and 5.7 - with NH₃ being detectable in case (A). All other atmospheric species fall below the minimum abundance thresholds in each case. At current CH₄ levels, the main CH₄ spectral feature is found in the mid-IR wavelength region (at 7.6 μm), but this is largely obscured by adjacent H₂O and N₂O features (Des Marais *et al.*, 2002). The predicted far-future CH₄ levels are approximately an order of magnitude greater than present day levels, which, combined with negligible atmospheric H₂O and N₂O levels would make the 7.6 μm feature clearer and more readily remotely detectable. Other CH₄ features exist at wavelengths between 0.6 and 2.4 μm. Although these features are not significant for levels of CH₄ in the present-day atmosphere, these would be large enough features to be useful for detecting CH₄ at higher abundances similar to those expected on the early Earth between the emergence of life and the Great Oxidation Event (Kaltenegger *et al.*, 2007).

Upcoming space- and ground-based missions such as the James Webb Space Telescope (Gardner *et al.*, 2006) and the European Extremely Large Telescope (Gilmozzi & Spyromilio, 2007) would all be looking in appropriate wavelength ranges to detect such CH₄ features. While space-based telescopes would be suitable for observing all the CH₄ absorption features listed above, dedicated space-based biosignature detection missions are not expected within the next 25 years. Snellen *et al.* (2013) argue that ground-based observations using high-dispersion spectroscopy to filter out interference from gases in Earth's atmosphere represent a strong alternative. This method would be best suited to wavelengths < 5 μm - at greater wavelengths, the sky background is prohibitively bright. Therefore, while the large 7.6 μm CH₄ feature would be best observed from space, those at shorter wavelengths, especially for a planets with high atmospheric CH₄ concentrations, could also be detection from ground-based observations.

However, a positive CH₄ detection may not necessarily indicate the presence of life. CH₄ can be released to the atmosphere abiotically via volcanic activity and serpentinization, for example (Oze *et al.*, 2012; Burton *et al.*, 2013). Building a case for a biological CH₄ source on a late-habitable-stage Earth-like planet may be easier than for younger habitable planets due to the slowing of carbon recycling as a result of the slowing of plate tectonics and a lower abundance of water to drive serpentinization reactions. Recent ex-

perimental work also suggests that a low atmospheric H_2/CH_4 ratio would support the case that CH_4 is being produced by life rather than via serpentinization (Oze *et al.*, 2012). The potentially detectable biosignature gases are summarised in Table 5.2.

Stage of biosphere decline	Biosignature gases
A (1 - 1.011 Gyr)	O_2 , O_3 , H_2O , C_2H_6 , NH_3 , CH_4
B (2 - 2.2 Gyr)	H_2O , CH_4
C (2.8 Gyr)	CH_4

Table 5.2: Summary of the biosignature gases in the atmosphere at different habitability stages in the Earth’s far future, from 1 Gyr from present to 2.8 Gyr from present.

5.3.3 Other biosignatures: Clouds?

A potential refuge for microbial life in the far future would be in the atmosphere where temperatures would be cooler than at maximum land elevation. It has been postulated that if life existed on a more clement early Venus, it could have found its way into the Venusian atmosphere and could be living in the upper cloud decks where temperatures fall within a habitable range (Schulze-Makuch *et al.*, 2004).

If a similar scenario were to occur when Earth’s oceans evaporate, one of the final refuges for life may be in the air. This would depend on the availability of water vapour and nutrients (organic molecules and elements such as nitrogen, phosphorous and iron that are essential for growth - Amato *et al.*, 2007) in the atmosphere. Water vapour and nutrients become concentrated in cloud formations in the troposphere (Amato *et al.*, 2007; Santl-Temkiv *et al.*, 2013), making these particularly suitable potential habitats. Microbial life is known to exist in the atmosphere today, although it is not yet known whether they are just in transit or whether they are actively metabolising and reproducing in the atmosphere. Airborne microorganisms can influence cloud formation (Santl-Temkiv *et al.*, 2013), suggesting that if biological cloud formation can be distinguished from abiotic cloud formation, clouds could be used as bio-indicators of an aerial biosphere.

Biological particles have little to no effect on cirrus clouds (thin, wispy clouds above altitudes of 5 km) (Möhler *et al.*, 2007). Different types of cloud can be distinguished using information on cloud-top pressure (the atmospheric pressure at the cloud top) and optical thickness. Cirrus clouds (the most common type of cloud on Earth, making up 25% of the total global cloud cover and playing a large role in Earth’s radiation budget) have

low cloud-top pressures and low optical thickness, while convective clouds (responsible for most precipitation in the tropics) have a high cloud-top pressure and high optical thickness (Durieux *et al.*, 2003). It is feasible that these properties could be detected in the atmospheric spectra of exoplanets, although if the cloud-top is at a deep layer in the atmosphere and the optical thickness of the cloud layer is high, direct detection is not possible, but a lower limit on cloud-top pressure can be determined (Benneke & Seager, 2012).

In a recent study of the affect of airborne microbial populations on cloud formation, DeLeon-Rodriguez *et al.* (2013) found that 20% of particles sampled in the upper troposphere were bacterial (the remainder being salt, dust etc.). If we assume that generally, 20% of cloud seeding particles are microbial this could make cloud cover itself a biosignature on inhabited, arid planets if the expected abiotic cloud coverage could be estimated. For largely arid, desert planets, high desert dust levels in the atmosphere could influence the predominant cloud type. Saharan desert dust, for example, acts as small cloud condensation nuclei, causing clouds composed of small water droplets ($<14 \mu\text{m}$ radii) to form, reducing coalescence and suppressing precipitation (Rosenfeld *et al.*, 2001). Cloud water droplet size could be determined via remote sensing of exoplanet atmospheres using the rainbow scattering effect (Bailey, 2007); hence, unexpectedly large cloud droplets in the atmospheres of arid planets could provide indirect evidence of microbial cloud seeding.

5.4 The signatures of extinct biospheres?

The fossilised remains of plants and animals would require in-situ sampling to detect, ruling this out as a method of inferring the presence of past life on an extrasolar planet. However, the largest trace of past life on Earth is found in coal, oil and natural gas deposits. In particular, crude oil deposits and the natural gas deposits derived from them, could potentially be remotely detectable. Such deposits have already been suggested as evidence for past life on Mars (McGowen, 2000) and, while detecting them on distant exoplanets would be more difficult due to the limitation on the type of detection tools available and the quality of data obtained, the same could be applied to exoplanets that may once have been suitable for hosting life but no longer exhibit any biosignatures.

When oil is heated above 100-150°C it degrades into natural gas, primarily methane,

which then leaks out into the atmosphere over time. CH_4 would be readily spectrally detectable in a largely water-free atmosphere, as previously discussed (Des Marais *et al.*, 2002). On Earth, the flux of CH_4 to the atmosphere from macro- and micro-seeps of natural gas is 32 Tg yr^{-1} (Kvenvolden & Rogers, 2005), an order of magnitude less than the predicted flux from a microbial biosphere at the end of an Earth-analogue planet's habitable lifetime, suggesting that it may not be distinguishable from biologically produced CH_4 . However, once all life on a planet has become extinct, an atmospheric CH_4 signature of this magnitude could provide evidence that life once existed on that planet.

5.5 Summary

The extinction of all animals and (non-microscopic) plants will happen within 1 Gyr from the present given regional mean temperature predictions for the Earth summarised in Chapter 4. This would alter the biosignatures exhibited by the planet, reducing the vegetation red-edge signal as a result of a decrease in vegetation coverage, combined with a super-continent formation, which could cause the disappearance of this signal within 250 Myr. The oxygen-ozone biosignature would disappear as a result of plant extinctions, happening alongside the extinction of animal species. If oxygen levels decline rapidly, causing rapid animal extinctions, rapid decay of a large mass of biological material could cause a short-lived ethane biosignature.

The world of microbes left behind after the plant and animal extinctions would itself decline over geological time as conditions become increasingly hostile to life. In the early stages of this microbial world (within the first 100 Myr) many familiar atmospheric biosignatures will still be present. However, anoxic conditions combined with declining habitat space eventually favour a chemolithotrophic biosphere, producing methane at detectable levels as its only biosignature. Other biosignatures of life, if present, within the atmosphere could be inferred, although further research in this field is still required before conclusive statements about life in the atmosphere can be made.

6

Applications to other planets within and beyond the solar system

BY predicting the possible course of the evolution of the biosphere on Earth into the far-future, the probable biosphere types on extrasolar Earth analogue planets can be assessed and their likely biosignatures determined.

It is possible that some future discoveries of habitable exoplanets will be planets that are nearing the end of their habitable lifetimes, either due to their position in the habitable zone or the age of their host star. An impression of the stages an inhabited Earth analogue planet orbiting F, G and K type stars would go through is given in Figure 6.1, while the fraction of known terrestrial planets around late-main sequence stars is illustrated in Figure 6.2. Therefore, the biosignatures that such planets would exhibit (assuming a similar evolutionary history to life on Earth) would more likely be similar to those predicted for the far-future Earth in Chapter 5.

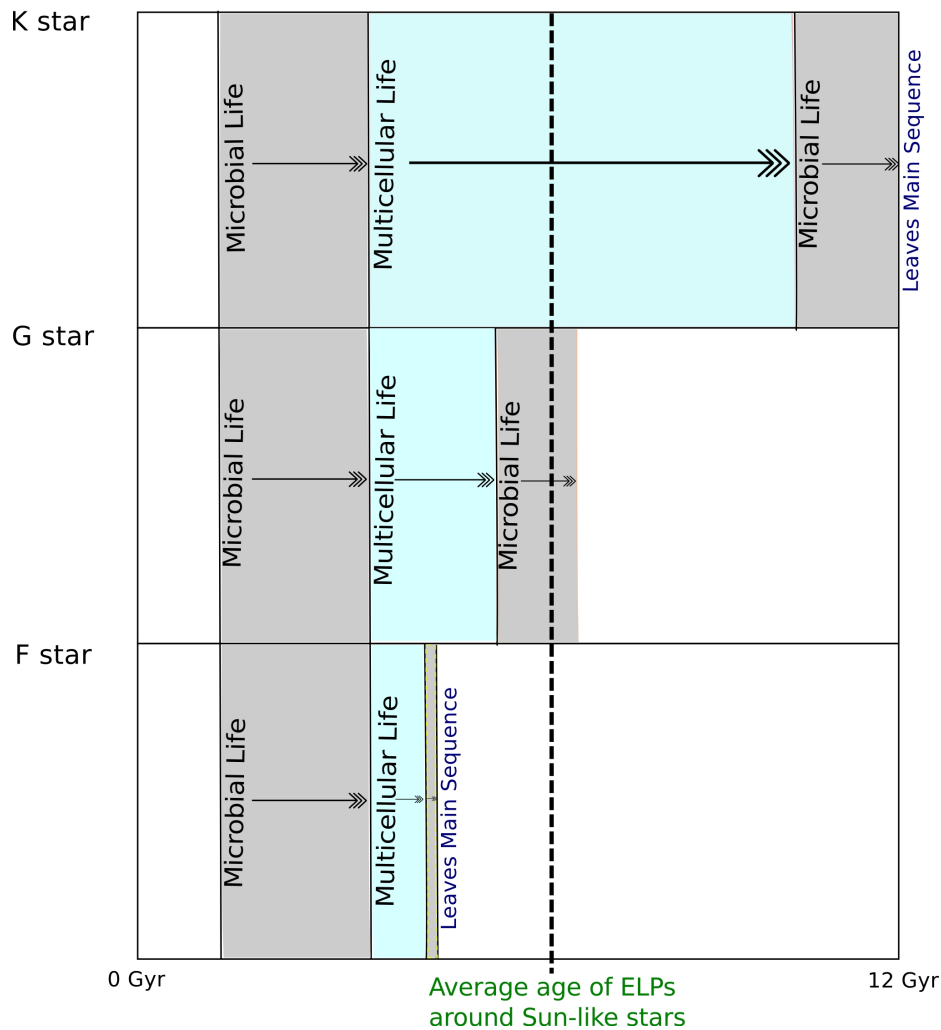


Figure 6.1: Time windows for complex and microbial life on Earth analogue planets orbiting Sun-like stars (F7, G2 and K1 stars) during their main sequence lifetimes. Assuming that the processes leading to multicellular life are the same as on Earth (i.e. approximately 1 Gyr for life to emerge and 3 Gyr for multicellularity to evolve), the potential life spans of a more complex, multicellular biosphere are estimated. Multicellular life was assumed able to persist until surface temperatures reach the moist greenhouse limit for an Earth analogue planet in the continuously habitable zone of the star-type in question. Microbial life is then assumed to dominate until either the maximum temperature for microbial life is exceeded or until the star leaves the main sequence (whichever happens first). The average age of Earth-like planets was found by Lineweaver (2001) to be approximately 6.4 ± 0.9 Gyr based on estimates of the age distribution of terrestrial planets in the universe. This value was obtained by using stellar metallicity as a guide to the suitability of star system for hosting an Earth-like planet. High metallicity stars tend to have close-in giant planets, which would destroy Earth-like planets; low metallicity systems may lack the necessary heavy element availability to form terrestrial planets. By extrapolating stellar formation rates and the rate of build-up of metals an estimate for the average age of Earth-like planets was obtained. This average age falls within microbial and uninhabitable stages for G- and F-type stars, respectively, but falls within the multicellular life stage for K stars.

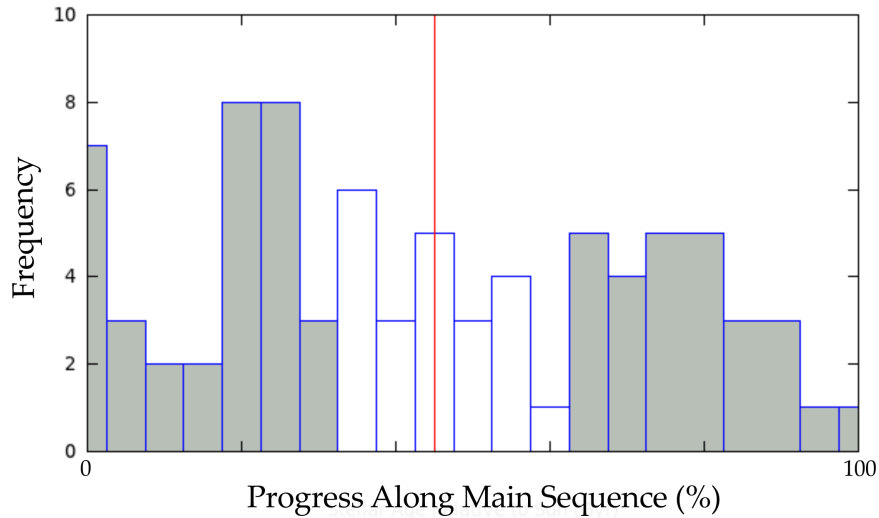


Figure 6.2: Main sequence evolution of currently known terrestrial planet ($10M_{\oplus}$ and less) hosting stars. The left-shaded region represents early microbial biospheres and the right-shaded region represents late microbial biospheres for Earth analogue planets. The central unshaded region represents the stellar age-range within which Earth analogue planets would be more likely to have complex biospheres. The vertical line represents the current age of the Sun. Source: The Extrasolar Planets Encyclopaedia (Schneider, 2010)

6.1 Old stellar systems in the solar neighbourhood

There are 20 G type stars within 10 pc of the Sun, each at varying stages in their main sequence evolutions. Two of these stars (Beta Hydri and Mu Herculis) are nearing the end of their main sequence lives and so are not included in this analysis, because Earth analogues (in a similar position in the HZ to Earth) in these systems are likely to no longer be habitable. Using the past evolution of life on Earth and its expected future course, stages during a G star’s main sequence lifetime can be established as a guide to estimating the likely stage of life on an Earth-like planet in an Earth-like position in its host star’s continuously habitable zone (CHZ). Suitable host stars are identified by using age and mass estimates for known G-type stars within 10 pc of the Sun to determine the stage they are currently at in their main sequence evolution. By scaling this relative to the Sun’s main sequence lifetime, the stage in the habitable evolution of an Earth analogue planet at a position within its host star’s HZ comparable to Earth’s position can be estimated. The results of this comparison are shown in Figure 6.3. A hypothetical Earth analogue planet is placed within the HZ of these systems and its suitability for different forms of life is investigated.

It should be noted that the science of estimating stellar ages is not always a very

precise one (Soderblom, 2010). Determining the age of single stars can be challenging, with different age determination methods resulting in a wide range of possible age values. For stars in the 0.6-1.0 M_{\odot} range, the most precise age determination method has been found to be based on the star's rotation period (Epstein & Pinsonneault, 2014). The rotation rate of low mass stars slows down in a predictable way as they age. The combination of convection and rotation in a star causes complex motions in the star's convective zone, producing and regenerating seed magnetic fields, as a result of the electrically conductive (ionised) gas in the convective zone (Maravell, 2006). Interaction between these fields and the star's ionised wind forces co-rotation of the wind to well beyond the stellar surface, causing angular momentum to be lost and resulting in a slowing of the star's rotation over time (Soderblom, 2010). Other methods, such as asteroseismology (which uses measurements of oscillation modes within a star to determine its density, and hence, age) can produce reasonably constrained age estimates, but these measurements are not always available for the stars in question and, for lower mass stars, the uncertainties associated with this method are greater (Epstein & Pinsonneault, 2014). Rotation periods can generally be accurately measured, making rotation-based age determination a reliable method for Sun-like main sequence stars. Therefore, the stellar ages used in this investigation will be preferentially taken from rotation-based estimates where possible.

Figure 6.3 suggests that for 25% of nearby Sun-like stars, if they hosted an Earth-like planet, those planets would be at the late microbial stage of their habitable lifetimes. The candidate host stars were chosen from those that fall within this "late microbial biospheres" category. Although the lower rotation-based age estimate for Delta Pavonis (δ Pav) places it within this section, a higher estimate exists that places it above this section. Additionally, as δ Pav is speculated to be entering the sub-giant phase of its evolution, this is not a viable candidate star in this case. The best candidate from this sample is Beta Canum Venaticorum (β CVn). Alpha Centauri A (α Cen A) and Tau Ceti (τ Cet) are also investigated. Although the age ranges of the systems are large, α Cen is a good representative of a nearby solar-type star in a multiple stellar system and τ Cet is the only star currently thought to host a HZ planet (τ Cet e). Although more distant, HD 197027 is also investigated. HD 197027 is the closest solar analogue yet found and exhibits a similar elemental abundance pattern to the Sun, suggesting that it may host terrestrial planets. Terrestrial planet formation locks up silicates and metals

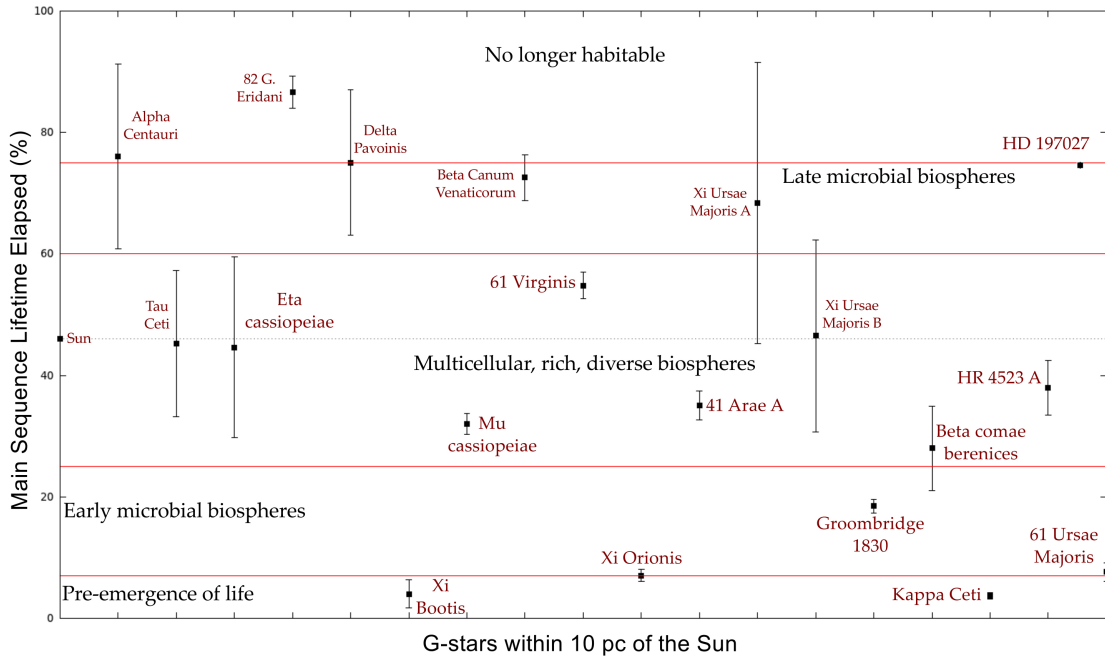


Figure 6.3: Time elapsed on the main sequence for G stars within 10 pc. Habitability stages assume an Earth-like planet in an Earth-like position within the host star’s CHZ. Early habitable stages are based on the history of life on Earth; habitability stages beyond the Sun’s present age are based on predicted biosphere evolution (O’Malley-James *et al.*, 2013). These are used as a guide for classifying the likely stage of life on such a planet. The large ranges for some stars are due to a wide range of quoted age values for these stars. Numerous ages estimates exist for ξ UMa AB, for example, and the age of this system cannot be constrained without more data. The results displayed above suggest that Groombridge 1830 could be a good candidate for the search for a planet at an early stage in its habitable evolution. Source for stellar ages and masses: VizieR catalogue data.

from the proto-planetary disc surrounding a star. These refractory elements are then no longer free to accrete onto the star; hence their absence could be an indication of the presence of terrestrial planets (Monroe *et al.*, 2013). The properties of all these systems are summarised in Table 6.1.

A hypothetical Earth analogue planet (in this case taken to mean a planet identical to the Earth today) is placed within the HZ of these systems such that the same mean surface temperature of the present day Earth is obtained and its suitability for different forms of life is investigated. For the τ Cet system, the HZ super-Earth (τ Cet e) is used instead of an Earth analogue to highlight potential deviations in the process of biosphere decline for habitable super-Earths.

	Spectral Type	Age (Gyr)	Mass (M_{\odot})	Luminosity (L_{\odot})	MS Lifetime (Gyr)**
α Cen A	G2 V	4.4-6.8 ^a	1.08 - 1.20	1.519	7.2
β CVn	G0 V	6.4-7.1 ^b	1.00 - 1.06	1.151	9.3
HD 197027	G3 V	8.2 ^c	0.97	0.9-0.96*	10.8
τ Cet	G8.5 V	5.8-10 ^d	0.787 - 0.814	0.52	17.5

Table 6.1: Summary of the properties of the candidate stellar systems. Unless stated, data obtained from Takeda *et al.* (2007).

a. Lower age limit determined via gyrochronology (Mamajek & Hillenbrand, 2008); upper limit determined via gyrochronology (Epstein & Pinsonneault, 2014).

b. Lower limit determined from gyrochronology (Mamajek & Hillenbrand, 2008); upper limit from revised stellar distance data (Holmberg *et al.*, 2009).

c. Determined from isochrone fitting (Monroe *et al.*, 2013).

d. Upper limit from stellar radius measurements (Di Folco *et al.*, 2004); lower limit from gyrochronology (Mamajek & Hillenbrand, 2008).

*Estimated from effective temperature and mass values.

**Estimated from stellar mass.

6.1.1 Alpha Centauri AB, Beta Canum Venaticorum & HD 197027

α Cen AB

The α Cen system is a three-star system composed of closely orbiting G and K stars (α Cen AB) with a more distant M star companion. The binary pair orbit a common centre of mass on an orbit with an eccentricity of 0.5179 leading to a variation in the separation between them from 11.2 au to 35.6 au over a 79.91 year period. The third more distant companion (α Cen C) orbits the binary pair at 13,000 au and would not impact the stability of orbiting planets or the position of the HZ around the other two stars (Wertheimer & Laughlin, 2006). Studies on the orbital stability of terrestrial planets orbiting either α Cen A or α Cen B have shown that for both stars, stable orbits would be possible within 2 au, with the companion star slightly altering the HZ boundaries (Guedes *et al.*, 2008).

Today, an Earth analogue planet orbiting α Cen A at a distance of 1.25 au would have a comparable mean surface temperature to that of the present-day Earth. Results from the planetary temperature model with increasing stellar luminosity over the star's main sequence evolution suggest that such a planet would remain habitable for approximately 1.9 Gyr from present. Assuming an age for the star of 6 Gyr, this would end the planet's habitable lifetime just before the star is predicted to leave the main sequence (cf. Figure 6.4(a)). If an Earth-like temperature is assumed for an Earth analogue planet at a point

in the host star's main sequence evolution that is equivalent to the Sun's current main sequence stage (approximately 2.36 Gyr ago for α Cen A, assuming a current age of 6 Gyr), the temperature evolution of that planet would render it largely uninhabitable within 1.6 Gyr of that point (cf. Figure 6.5(a)).

The presence of extra stars in a system can influence environmental conditions on a planet - see discussion in Section 6.1.3.

β CVn

A single G-type main sequence star, β CVn is slightly metal-poor in comparison to the Sun, but otherwise is a good, nearby (approximately 8.44 pc away) solar analogue. It has also been listed as one of the astrobiologically interesting stars within 10 pc of the Sun (Porto de Mello *et al.*, 2006). An Earth analogue planet in the β CVn system would be the most likely to host a later-type biosphere as a result of the star's main sequence progress and the small estimated age range compared to other older G stars within 10 pc.

Today an Earth analogue planet at 1.03 au would have a comparable mean surface temperature to the present-day Earth. The surface of such a planet would become uninhabitable within 1.8 Gyr, but a biosphere could remain for up to 2.6 Gyr (cf. Figure 6.4(b)).

If an Earth-like temperature is assumed for an Earth analogue planet at a point in the host star's main sequence evolution that is equivalent to the Sun's current main sequence stage (approximately 2.22 Gyr ago for β CVn) this would place the planet at an orbital distance 0.95 au. Its surface would become uninhabitable within 1 Gyr, but the planet could remain partially habitable for nearly 2.6 Gyr from present (cf. Figure 6.5(b)), suggesting that, if such a planet were to exist, it would be a good present-day candidate for exhibiting the biosignatures of a late-type biosphere.

HD 197027

The HD 197027 system is the most similar solar analogue in terms of mass, luminosity and chemical abundance found to date. It has an age of 8.2 Gyr (determined from isochrone fitting), making it a good test-case for predictions about the future of our own Sun and solar system (Monroe *et al.*, 2013). At approximately 3.6 Gyr older than the Sun, this

encompasses Earth's remaining habitable lifetime. The absence of gas giant planets close to the star (within 2 au) and a similar chemical abundance to the Sun (suggesting elements from the protostellar disc were locked up in planets) supports the case that the system could host terrestrial planets within the HZ (Monroe *et al.*, 2013).

The temperature model suggests that life on a hypothetical Earth analogue with a mean surface temperature equal to that of the present-day Earth (which would place the planet at 0.99 au from the star in this system) could persist for up to 4.3 Gyr from the present. However, the predicted main sequence lifetime for HD 197027 is 10.8 Gyr, which is 2.6 Gyr from its present age. After leaving the main sequence, the luminosity of a $1 M_{\odot}$ star would increase rapidly after a short period of less rapid increase as illustrated in Figure 1.10 (Danchi & Lopez, 2013). Assuming a similar luminosity evolution to that predicted for the Sun, this would result in the planet becoming uninhabitable shortly after this time (cf. Figure 6.4(c)). The rapid change in the pace of the star's luminosity increase would induce rapid planetary temperature increases accelerating climate change and soon sterilising the surface and subsurface (subsurface temperature gradients tend to increase with depth from the surface). However, due to the star having a lower luminosity than the Sun, a more complex biosphere could exist for longer than predicted for the future Earth as a result of a slower rate of planetary temperature increase.

If an Earth-like temperature is assumed for an Earth analogue planet at a point in the host star's main sequence evolution that is equivalent to the Sun's current main sequence stage (approximately 3.23 Gyr ago for HD 197027), the temperature evolution of that planet would render it largely uninhabitable within 3 Gyr (cf. Figure 6.5) of that point (0.23 Gyr before present). Isolated habitable regions could persist for up to a further 0.5 Gyr for high obliquity values ($> 60^{\circ}$), which would allow for the possibility of a very small, fragmented biosphere today.

Biosignatures

For the Earth-analogue examples used for α Cen A, β CVn and HD 197027, the biosignature progression with time would be similar to the progression predicted for the far-future Earth in O'Malley-James *et al.* (2014). The biosignatures associated with a biosphere similar to the present day one on Earth would disappear as organisms analogous to plants and animals on Earth become extinct. On Earth this point occurs approximately 1 Gyr

6.1. Old stellar systems in the solar neighbourhood

Stage of biosphere decline	Biosignature gases	Stage duration					
		α Cen		β CVn		HD 197027	
		(I)	(II)	(I)	(II)	(I)	(II)
Photosynthesis possible*	O ₂ , O ₃ , H ₂ O, C ₂ H ₆ , NH ₃ , CH ₄	0.0-0.6	2.3-1.7	0.0-0.4	2.25-1.45	0.0-1.45	3.2-1.25
Microbial biosphere	H ₂ O**, CH ₄	0.6-1.45	1.7-1.5	0.4-1.8	1.45-1.05	1.45-2.6	1.25-1.0
Extremophile biosphere	CH ₄	1.45-1.9	1.5-0.95	1.8-2.6	1.05-(-0.1)	2.6-2.7	1.0-0.2

Table 6.2: Summary of the modelled atmospheric biosignatures in each stage of the biosphere decline on an Earth analogue planet orbiting α Cen A, β CVn and HD 197027 both for cases when the planet has Earth-like mean temperatures at the host star’s current main sequence evolutionary stage (I) and cases when the planet would have similar mean surface temperatures to Earth at a point in its host star’s past main sequence evolution similar to the Sun’s present stage (II), based on the biosignature progression predicted for the future Earth in O’Malley-James et al. (2014).

*Conditions and biosignatures are Earth-like until towards the end of this period when animal and plant species begin to decline.

**The presence of abundant water vapour as a result of global ocean evaporation would not be a direct biosignature, but would be a notable spectral feature, which, combined with knowledge about the host star’s luminosity and the planet’s orbital semi-major axis, would be an indicator of the probable environmental conditions on the planet. It should be noted that the spectral detection of water vapour in other circumstances would still not provide evidence of life, but would act as an indicator of habitability alongside other evidence of biological activity.

from present. For an Earth analogue in the α Cen A and β CVn systems, this occurs sooner. For such a planet at Earth’s present habitable stage at the current age of each system, the periods during which photosynthesis would be possible (i.e. the time during which atmospheric CO₂ levels are high enough for photosynthesis to take place) would last 0.6 Gyr and 0.2 Gyr for α Cen A and β CVn respectively. For such a planet at a time in each host star’s past equivalent to the present main sequence stage of the Sun, the photosynthetic period would continue for 0.6 Gyr and 0.8 Gyr respectively. For the case of the HD 197027 system the end of photosynthesis comes much later than it would on Earth (due to the star’s slightly lower mass and luminosity than the Sun) - lasting 1.5 Gyr and 2.0 Gyr for present-day and past Earth analogue planets respectively. After this period, oxygen levels are low and rapid ocean evaporation begins. A global microbial biosphere would remain for a time, but this would decline in diversity and biomass as rapid temperature increases caused by increased water vapour in the atmosphere decrease water availability and push all but extremophile species to extinction. Eventually conditions cross all known and theoretical thresholds for life, leading to full extinction of the biosphere. The biosignature progression is summarised in Table 6.2.

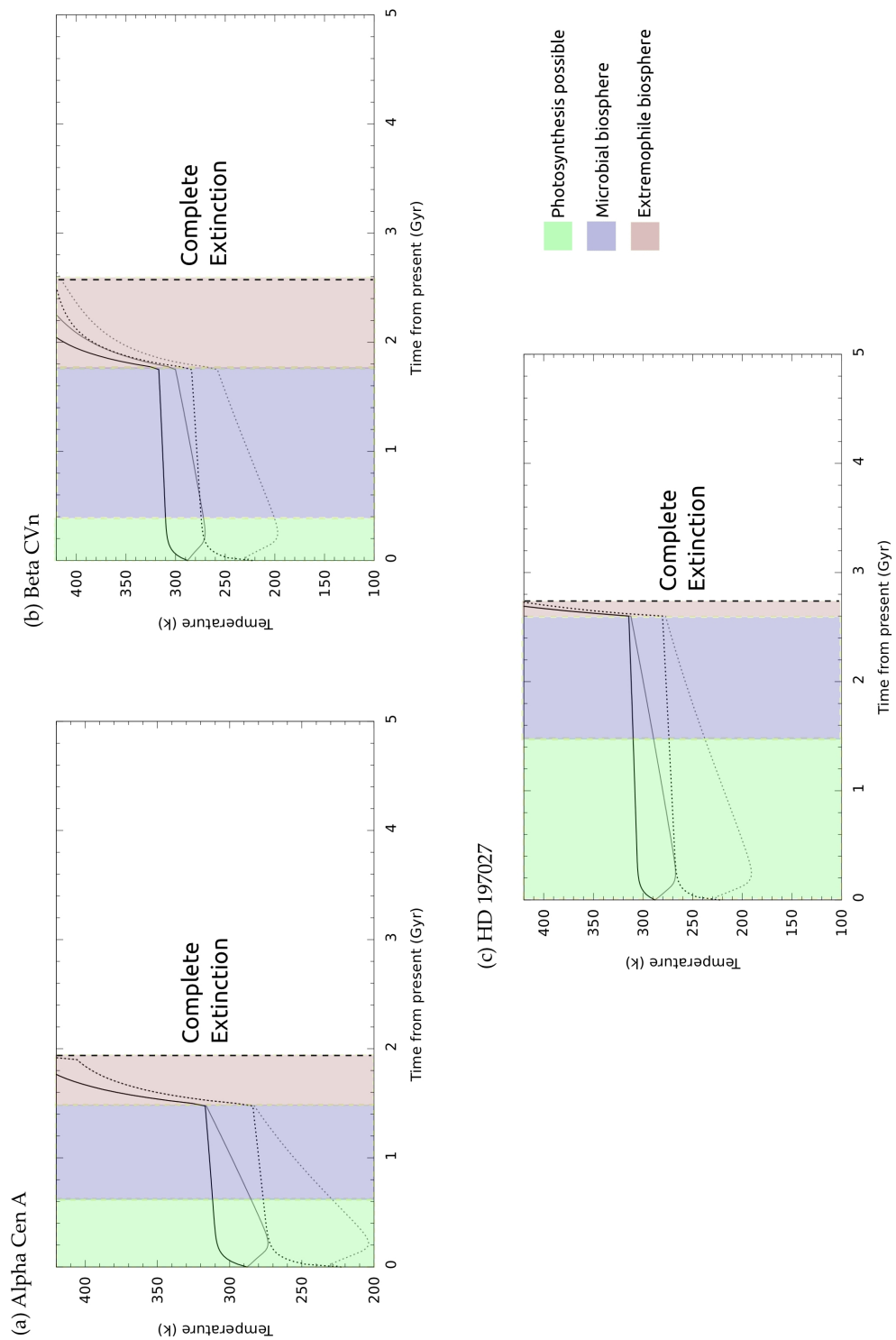


Figure 6.4: Mean temperature evolution at the equator (black) and the poles (grey) with increasing altitude on a present-day Earth analogue planet. Temperatures are derived from the modelled surface temperature and the estimated tropospheric lapse rate from surface level (solid line) to an altitude of 10 km (dashed line). **(a)** α Cen A. Orbiting at 1.25 au the planet's surface becomes uninhabitable within 1 Gyr, but the planet could remain partially habitable for up to 1.9 Gyr from present (shortly before the star is expected to leave the main sequence). **(b)** β CVn. Orbiting at 1.03 au, the surface becomes uninhabitable within 1.8 Gyr, but the planet could remain partially habitable for nearly 2.6 Gyr (shortly before the star is expected to leave the main sequence). **(c)** HD 197027. Orbiting at 0.99 au, the surface becomes uninhabitable within 3.8 Gyr, but the planet could remain partially habitable for up to 4.3 Gyr from present.

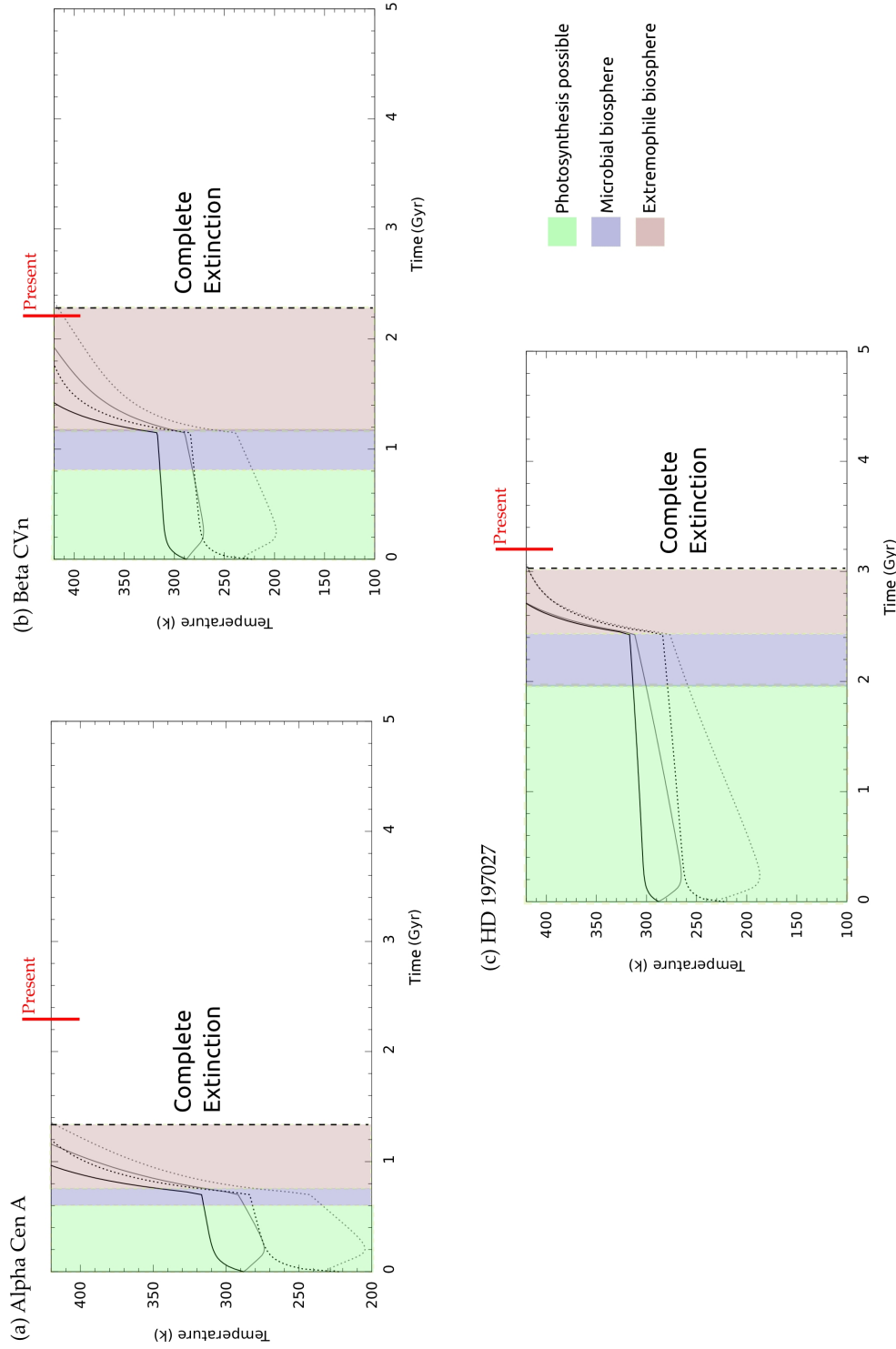


Figure 6.5: Mean temperature evolution at the equator (black) and the poles (grey) with increasing altitude on an Earth analogue planet orbiting (a) α Cen A, (b) β CVn and (c) HD 197027 at a stage equivalent to the Sun's current main sequence stage in these star's lifetimes: 2.36 Gyr before the present for (a), 2.22 Gyr for (b) and 3.23 Gyr for (c). Temperatures are derived from the modelled surface temperature and the estimated tropospheric lapse rate from surface level (solid line) to an altitude of 10 km (dashed line). (a) Orbiting at 0.91 au, the surface becomes uninhabitable within 1 Gyr, but the planet could remain partially habitable for up to 1.6 Gyr from this point (0.76 Gyr before the present time). (b) Orbiting at 0.95 au, the surface becomes uninhabitable within 1 Gyr, but the planet could remain partially habitable for nearly 2.6 Gyr from present (suggesting that if such a planet were to exist, it would be a good present-day candidate for exhibiting the biosignatures of a late-type biosphere). (c) Orbiting at 0.96 au, the surface becomes uninhabitable within 2.7 Gyr, but the planet could remain partially habitable for up to 3 Gyr (0.23 Gyr before present).

6.1.2 Tau Ceti

The τ Cet system could have an age of up to 10 Gyr (Di Folco *et al.*, 2004). While it is not a solar analogue star it is the only late main sequence G star that is currently known to host a terrestrial planet (τ Cet e) in the HZ. While the existence of τ Cet e is still unconfirmed, it serves as a good non-Earth-like test case for this work. τ Cet e is a $4.3 M_{\oplus}$ planet orbiting its star at a distance of 0.552 au with a period of 168 days. If it had an Earth-like atmosphere it would have a mean surface temperature of approximately 70°C . As the planet orbits much closer to its star than 1 au, this system would approach the end of its habitable lifetime earlier in the star's main sequence life than a planet at 1 au would.

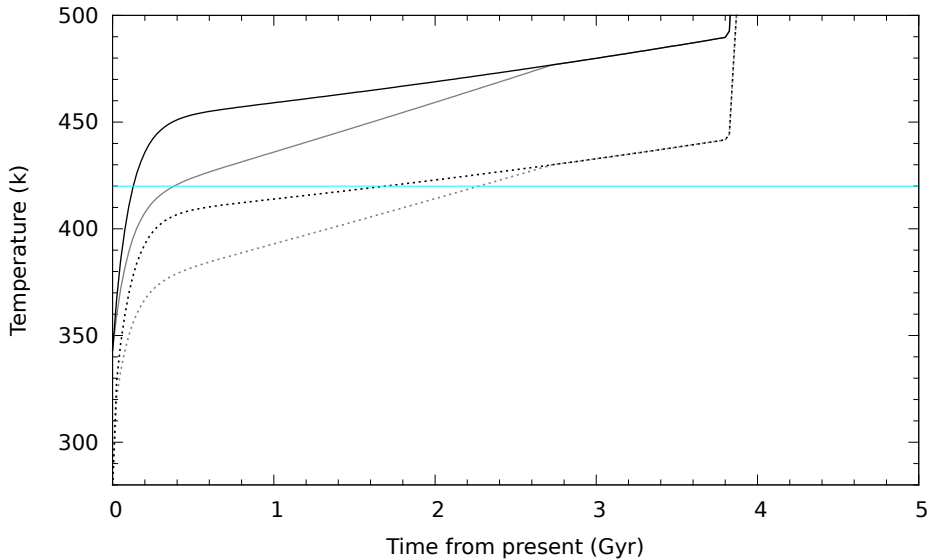


Figure 6.6: Mean temperature evolution at the equator (black) and the poles (grey) with increasing altitude on τ Cet e. Temperatures are derived from the modelled surface temperature and the estimated tropospheric lapse rate from surface level (solid line) to an altitude of 10 km (dashed line). While the surface becomes uninhabitable within 0.2 Gyr, the planet could remain partially habitable for up to 2.2 Gyr from present.

Using an Earth-based climate model suggests that surface temperatures on τ Cet e would cross the upper limits for life (420 K) within 0.2 Gyr (see Figure 6.6). The planet is near the inner edge of the system's HZ, so rapid ocean evaporation begins very shortly after the model begins running. By assuming an Earth-like composition (a rocky planet with a large iron core), a $4.3 M_{\oplus}$ planet would be expected to have a radius of $1.4 R_{\oplus}$, which would give it a surface gravity value of approximately 14 m s^{-2} (Valencia *et al.*, 2007). This allows the lapse rate for the planet's atmosphere to be estimated. High

altitude regions of the planet could remain habitable for up to 2.2 Gyr from present.

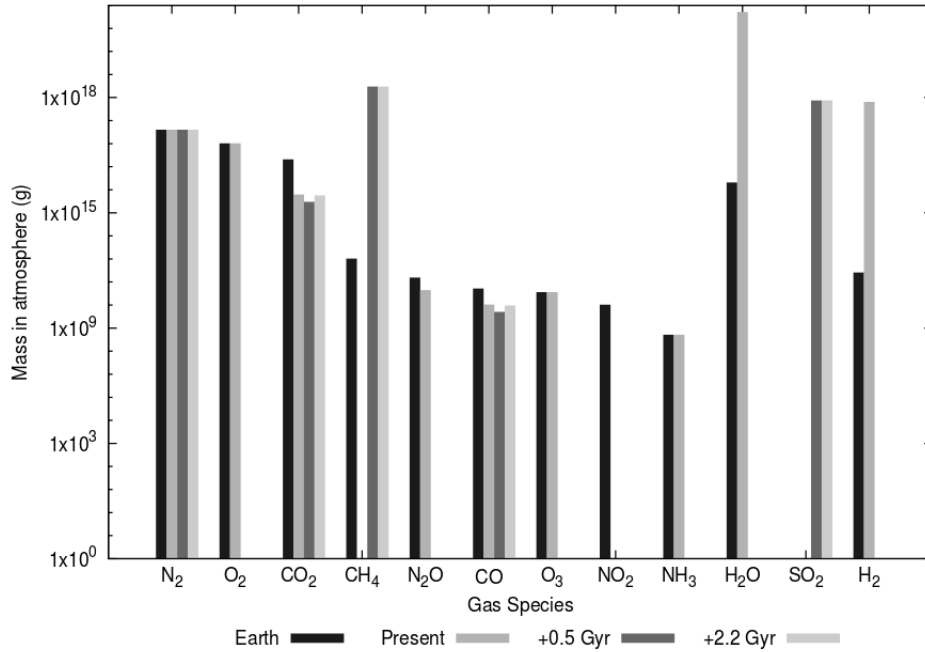


Figure 6.7: Changes in gas species abundances in the atmosphere of Tau Ceti e from the estimated present state to the end of the planet’s habitable lifetime, assuming an Earth-like initial atmospheric composition and an inhabited planet.

For τ Cet e the photosynthesis period has already ended by the beginning of the simulation as a result of the planet’s position near the inner edge of the HZ. Assuming an Earth-like atmosphere, if life were to exist on the planet today it would be microbial, consisting of organisms adapted to extremes of temperature and to anoxic conditions. The planet ends its habitable lifetime with an atmosphere dominated by N₂, CO₂, CH₄ and SO₂, a joint product of methanogenesis and ongoing geological activity.

6.1.3 Earth analogues at the end of their habitable lifetimes

The only star in the chosen star systems that is theoretically capable of hosting an Earth analogue planet, either at the very end stages of its habitable lifetime or at the point where it is about to enter the global microbial biosphere stage of its habitable lifetime, depending on the planet’s position within the HZ, is β CVn. If such a planet was discovered in this system (or a similar star system with a star of a similar type and age), it could provide good experimental evidence, in the form of spectral biosignature detections, for

future predictions about the long-term evolution of Earth's biosphere. From analysis of data collected by the Kepler space telescope, Catanzarite & Shao (2011) estimated that Earth analogue planets are expected to exist in the HZ around 1-3% of Sun-like stars in the galaxy, while Petigura *et al.* (2013) found that up to 22% of Sun-like stars could host HZ Earth-sized planets. Approximately a third of these stars can be expected to be in the later stages of their main sequence evolution (O'Malley-James *et al.*, 2013), making the future detection of such planets in the later stages of their habitable evolutions plausible. Future exoplanet detection and characterisation missions, would be looking within appropriate wavelength ranges to be capable of detecting the predicted end-of-habitable-lifetime biosignatures for super-Earth planets. More advanced observations, involving direct imaging by blocking out the light from the planet's host star, would be needed to analyse the atmospheres of Earth-mass planets. This could be achieved by using a star-shade in conjunction with an existing space telescope such as the JWST (Seager, 2010).

The case of α Cen AB opens the question of how the presence of other stars in a system can influence the end stages of a planet's habitable lifetime. In the α Cen system, neither of the close binary components has a significant influence on the HZ (Forgan, 2012). However, the impact on habitability would have a much greater magnitude when one of the stars in such a system ends its main sequence life. When α Cen A leaves the main sequence and begins evolving through its post-main sequence phases, the enhanced energy outputs of the star would sterilise the HZ of the neighbouring α Cen B system, potentially bringing an abrupt end to the slow process of total biosphere extinction on any life-bearing planets in that system at an earlier point than predicted for a single star system (Beech, 2011).

6.1.4 Super-Earths at the end of their habitable lifetimes - Tau Ceti e

The results for the planet candidate τ Cet e suggest that, assuming it was inhabited with an Earth-like biosphere to begin with, it would be at a transitional stage in its habitable lifetime between the photosynthetic stage and a global anaerobic microbial biosphere. Detecting atmospheric biosignatures in super-Earth atmospheres would be more readily achievable in the near-future, providing an early test-case for predictions made about the far-future evolution of an Earth-like biosphere. However, there are numerous factors that

could effect the rate and form of biosphere decline on a super-Earth planet in addition to those modelled here.

Von Bloh *et al.* (2009) showed that a super-Earth planet could remain habitable for longer than a less massive planet at the same orbital position. A more massive terrestrial planet would experience increased shear stresses and decreased plate thickness, allowing plate tectonics and volcanism (both of which are important for recycling volatiles and stabilising climate) to continue for longer than on a less massive planet (von Bloh *et al.*, 2009; Kaltenegger *et al.*, 2010b). In a similar way to the creation of habitat space by impact hydrothermal systems, volcanic hydrothermal systems could also be used by life. A planet with a higher mass could also end up with a greater water inventory than Earth did during formation (Raymond *et al.*, 2007), although a terrestrial planet with a water mass fraction greater than 0.2% would be more likely to be a water world with no exposed continental rock, leading to less stable climates due to a lack of a stabilising silicate weathering cycle (Cowan & Abbot, 2014). Additionally, the greater surface gravities of such planets would favour hydrogen retention, slowing the water loss rate to space (Miller-Ricci *et al.*, 2009). The higher mass of super-Earth planets compared to Earth-sized planets would result in a higher atmospheric pressure as atmospheric pressure tends to increase with planetary mass (Elkins-Tanton & Seager, 2008). Hence, the boiling point of water would be higher at surface levels than on a less massive planet, suggesting conditions on a super-Earth planet would retain liquid water (at higher temperatures and pressures) for longer, favouring the existence of hyperthermophiles.

The higher surface gravity associated with a higher mass would slow the increase of the atmosphere's lapse rate, enabling a high altitude biosphere to exist for longer than on a less massive planet for the case of τ Cet e. However, a land-based high-altitude biosphere may be rare on super-Earths as a result of the increased tectonic activity of these planets, which leads to a muted surface topography (Cowan & Abbot, 2014), resulting in much less high-altitude land surface than on Earth. If life is able to metabolise and reproduce within an atmosphere, an airborne biosphere may be able to fill this habitable space.

Specifically for the case of the τ Cet system, impact frequency would also have an effect on a planet's habitable evolution. The system has a debris disc around it that is larger than the Kuiper belt in our own solar system, by at least an order of magnitude (Greaves *et al.*,

2004). This would increase the number of comets and asteroids in the system, increasing the frequency of impact events. This could be beneficial for life by creating opportunities for new adaptations to fill empty ecological niches left behind post-impact, but, if the impact frequency is high, this could prevent anything but a microbial biosphere existing on the planet, with microbial life beneath a planet's surface having the best chances of surviving large impact events (Sleep & Zahnle, 1998).

6.2 Binary and multiple star systems

Another source of deviation from Earth-like conditions and Earth-like life on a planet would be found in systems with two, or more, stars. As discussed for the case of α Cen AB in Section 6.1, the presence of another star can influence life on a planet in such a system.

One of the most promising biosignatures for Earth-like life, the presence of O_2 and O_3 in an atmosphere, as a result of oxygenic photosynthesis, could be influenced by the presence of a second star. Crucial for oxygenic photosynthesis is an appropriate atmosphere and sufficient light in the appropriate wavelength range. Life on Earth uses wavelengths from just below 400 nm to about 700 nm (rarely 730 nm) with the energy from two photons used in the transfer of an electron from H_2O to CO_2 . Photon availability for photosynthesis is determined by the emission properties of the Sun and attenuation by the atmosphere and (for aquatic organisms) natural waters (Wolstencroft and Raven, 2002; Kiang *et al.*, 2007a, 2007b; Björn *et al.*, 2009; Milo, 2009; Raven, 2009a). Earth analogue planets around stars for which the maximum photon emission is at different wavelengths to those of the Sun could harbour life using oxygenic photosynthesis that operates by using a different number of photons to transfer an electron from H_2O to CO_2 .

In O'Malley-James *et al.* (2012) the influence of a second star on oxygenic photosynthesis was explored. Specifically, combinations of G and M type stars were investigated; G stars being the only type of star known to host an inhabited planet and M stars being the most abundant stars in the galaxy. The frequency of arrangements of these star types in binary or multiple systems is illustrated in Figure 6.8, which shows that the type of systems of interest make up a major fraction of the binary systems surveyed by Duquennoy & Mayor (1991) in a survey of 164 Sun-like primaries within the solar neighbourhood (within

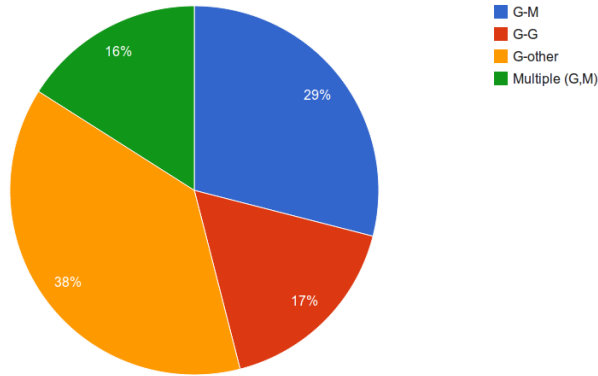


Figure 6.8: Proportion of G-M star and G-G star binaries (and multiple-star systems) in the sample of systems with G star primaries from Duquennoy & Mayor (1991). The type of system of interest in this work appears to be frequent enough to warrant investigation.

250 light-years). Approximately 57% of G stars are found in multiple-star systems, while M stars are less commonly found in multiple systems and have a multiplicity fraction of 25-30% (Lada, 2006; Tarter *et al.*, 2007; RECONS, 2011).

Three scenarios that involve combinations of high-mass ($1 M_{\odot}$) and low-mass ($<0.5 M_{\odot}$) stars are explored: (i) close binary systems (<0.5 au star separation) with planets in p-type planetary orbits (in which the planet orbits both stars as if they were a single star), (ii) wide-binary systems (>3 au star separation) with s-type planetary orbits (in which the planet orbits just one of the stars), and (iii) multiple-star systems that consist of two close stars and one more distant star (a combination of cases (i) and (ii)). In each case an Earth-analogue planet was placed at a stable position within the CHZ and the photon flux density estimated (the greatest flux of photons of a particular wavelength from the star in question) based on assumed stellar parameters for each star type. This is assumed to be the type of photons favoured by the photochemical reactions of photosynthesis, because on Earth, the wavelength range used in the photochemical reactions of photosynthesis is centred on wavelengths (680 nm, 700 nm) just above that of maximum photon flux from the Sun (Wolstencroft & Raven, 2002; Raven, 2011).

The results are presented for each of the possible star combinations in Figure 6.9. It was found that all scenarios permitted stable orbits within the CHZ given reasonable star separations. The calculations of the maximum photon flux wavelength for G and M stars resulted in peaks at 643.9 and 991.9 nm, respectively. This is consistent with results of similar calculations and falls within the range of values quoted in recent liter-

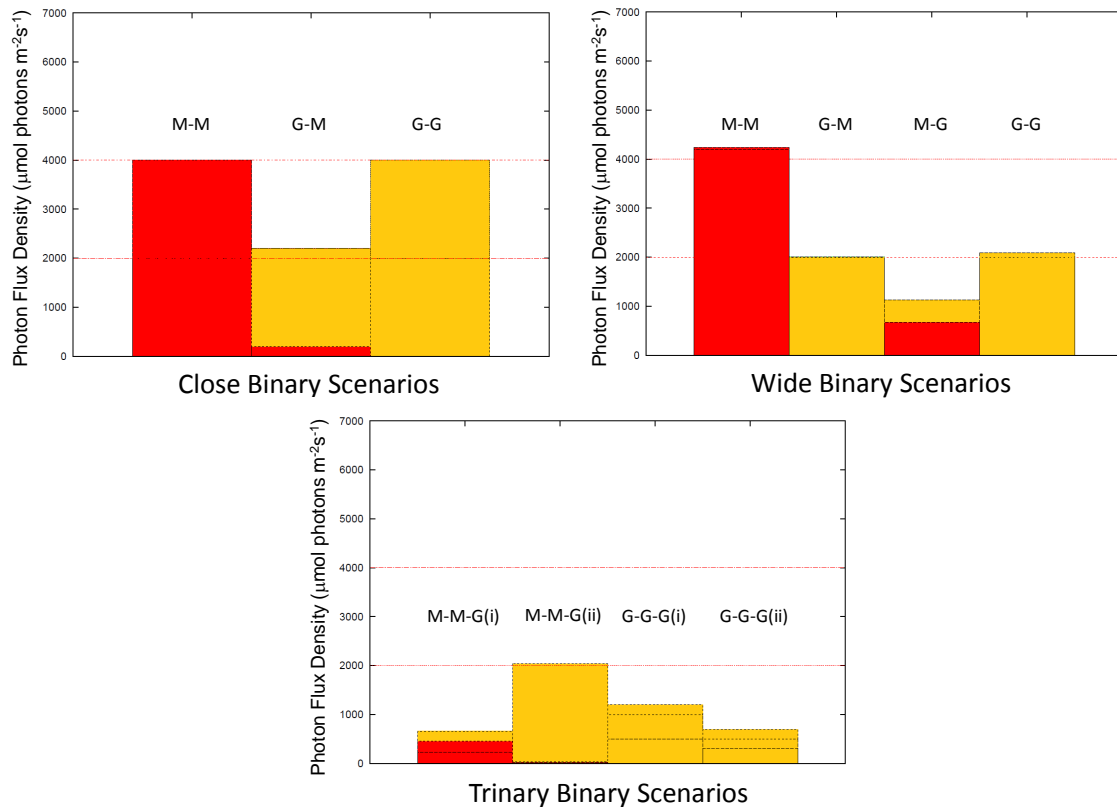


Figure 6.9: Peak (photosynthetic) photon flux density results: Red denotes the PFD from the M stars and yellow the PFD from the G stars in any given configuration. The lower red line indicates the peak PFD on Earth, and the upper red line indicates the theoretical PFD required for IR photosynthesis such that photosynthetic productivity equals that on Earth. (1) Close binaries: The close-binary scenarios all approximate single-star systems in terms of orbital dynamics and light regimes. G star radiation clearly dominates in the G-M star close-binary example. (2) Wide binaries: The M-M, G-M, and G-G cases are all clearly dominated by one particular radiation environment. In the M-G case, although the flux from the second star is low, it could still potentially be exploited for photosynthesis. (3) Triple systems: In case (i) the planet orbits the the first two stars in the description with a distant single-star companion - the third star in the description. In case (ii) the planet orbits the third star with a distant binary companion consisting of the first two stars in the description. All but the M-M-G(ii) case fall below the threshold for an Earth-like level of photosynthesis.

ature (Wolstencroft & Raven, 2002; Nobel, 2005; Kiang *et al.*, 2007b; Milo, 2009); the conclusions drawn here would not be significantly altered by using other values within this range. For close-binary configurations, M-M star, M-G star, and G-G star combinations were considered in orbits close enough that the system dynamics approximated a single star. Similar cases were investigated for wide-binary configurations, only a distinction was drawn between which star hosts the planet. In the trinary star cases, combinations of these wide- and close-binary scenarios were used. In each case, the stars were assumed to be separated by the minimum distance for stable planetary orbits within the CHZ in order to best investigate the influence of the two different radiation regimes. The planet was given a semimajor axis that placed it within the CHZ such that the photon flux from both stars was maximised. An orbital eccentricity of zero was assumed.

There are a number of different arrangements of multiple star systems in which Earth-like planets can be classed as habitable, each providing unique environments and a variety of possibilities for oxygenic photosynthetic life. Changing spectral regimens in such systems would shift the dominantly available radiation between infrared and red radiation at different points in a planet's orbit, which raises the possibility of organisms with two different forms of photosynthetic machinery, or two distinct biospheres, each adapted to use the specific radiation associated with one of its suns. The results presented here are sufficient to demonstrate that binary and multiple star systems are plausible targets in the search for extrasolar oxygenic photosynthesis.

6.3 Martian methane: A cold end to a planet's habitable lifetime?

Mars could provide a local example of a planet in the very end stages of its habitable lifetime, albeit a planet that has become largely uninhabitable as a result of low temperatures and losing an atmosphere, rather than from runaway heating. There is a claim that methane has been detected in plumes emanating from three distinct areas on Mars (Mumma *et al.*, 2003). As the lifetime of methane in Mars' atmosphere is relatively short, the detection of methane implies continual replenishment of the gas. Methane in Earth's atmosphere is largely biological in origin; hence, it has been suggested that this may be an indicator of ongoing biological processes on the planet (Mumma *et al.*, 2003). However,

there are also abiotic mechanisms that could be responsible for the atmospheric methane (McMahon *et al.*, 2013). There are some problems with the Martian methane claims. Methane should have a lifetime of 100s of years in the Martian atmosphere, therefore the short observed lifetime requires a strong methane sink (Zahnle *et al.*, 2011). Also, the detection of methane (both from Earth-based and Mars Express orbital observations) has been called into question (Zahnle *et al.*, 2011) and most recently, NASA's Curiosity rover has not detected methane from the ground (Webster *et al.*, 2013).

Assuming these methane plumes exist and that they have a biological origin, they can be used to infer what known type, or types, of life could be producing them. There has been a long-standing connection between Mars and the search for life beyond Earth (Westall *et al.*, 2000). Numerous potential inhabitants have been suggested and signs of their past or present presence have been searched for, with (to date) no positive detections (Klein, 1979; Westall *et al.*, 2000). It is generally agreed that in its geological past, conditions on Mars were more conducive to the existence of life, whereas today, combinations of sub-zero temperatures, little available liquid water, a thin atmosphere and a weak planetary magnetic field make the planet much more hostile to life (Fairén, 2010). However, there are regions on Mars where conditions overlap with the phase space of the known environmental tolerances of microbial life (Córdoba-Jabonero *et al.*, 2005; Wang *et al.*, 2010). For this reason Mars can be classified as a planet at the end stage of its habitable lifetime.

The best candidate habitable regions on Mars are in deep sediments near the polar ice caps and in permafrost regions, because these both overlap with known inhabited environments on Earth (Morozova *et al.*, 2007). Jones *et al.* (2011) investigated the overlap between habitable conditions on Earth and Mars to determine the extent to which Mars is habitable for terrestrial life and found that approximately 3.2% of the volume of the Martian subsurface could be classed as habitable.

The forms of life best able to survive under Martian conditions are lithoautotrophic organisms. Such life would need to overcome low temperatures, low water availability and high levels of ionising radiation. Mechanisms for surviving and growing under these stress conditions are already known to exist in organisms on Earth, e.g. DNA-repair at sub-zero temperatures (Dieser *et al.*, 2013).

6.3.1 Martian methanogens and methanotrophs?

If the methane plumes are assumed to consist of biologically-produced CH₄, then the best candidate organisms responsible would be methanogens. In environments on Earth where methanogen populations exist, such as in permafrost springs, methanotroph populations are also found, metabolising the CH₄ produced by the methanogens. In this section, the possibilities of methanogen and methanogen-methanotroph populations that could potentially be supported in the methane-plume-producing region of Mars are investigated to determine the expected amount of CH₄ produced in each scenario. By comparing this to the measured amount of CH₄ in the observed plumes, the possibilities of it having either a biological or an abiotic source are evaluated.

What population size is needed?

Previous estimates have been made about the population sizes necessary to produce methane in the quantities and over the timespans observed on Mars. Tung *et al.* (2005) calculated that a population of methanogens living in a 10 m thick layer across the surface of Mars with a concentration of 1 cell ml⁻¹ could be responsible, assuming a habitable temperature of 0°C. Miller *et al.* (2010) deduced that a population of 10²⁰ microbes in 2.5 × 10¹⁵ g of Martian soil could produce methane at the necessary rate to reproduce observations. House *et al.* (2011) ignored the question of whether the methane plumes were biogenic or not and speculated that an annual methane release of this magnitude could support a population of methanotrophs approximately 1.5 × 10²² in size (1 × 10⁴ cells cm⁻²).

What population sizes could the source areas support?

The three sources of the methane plumes during summer in the northern hemisphere were all in near-equatorial regions: east of Arabia Terra, Nili Fossae and the Syrtis Major Quadangle, releasing 19,000 tons with an estimated source strength of ≥ 0.6 kg s⁻¹ (Mumma *et al.*, 2009). To test the hypothesis that the methane release from these areas is biological in origin, two scenarios in which potential population sizes are assessed are explored: (i) a population of subsurface methanogens and (ii) coupled populations of methanogens and methanotrophs.

(i) Subsurface methanogens

Conditions on Mars overlap with the known physical limits for methanogenesis on Earth ($T_{max} = 122^{\circ}\text{C}$, $T_{min} = 0^{\circ}\text{C}$ (Franzmann *et al.*, 1997), but can extend below 0°C if cells have the means to suppress ice formation (Hoehler *et al.*, 2010); pH range: 3-10 (Hoehler *et al.*, 2010); maximum salinity: 5 M Na^+ (Hoehler *et al.*, 2010)). This suggests that methanogenic life on Mars is a possibility. The best terrestrial analogue for Martian methanogens are those found living in permafrost environments on Earth, which are very tolerant to low temperatures and to radiation, desiccation and osmotic stress (Morozova *et al.*, 2007). Methanogens from Siberian permafrost have been shown to have much greater survival rates when exposed to simulated Martian conditions than methanogens from non-permafrost environments (Morozova *et al.*, 2007).

Using the CH_4 flux rates from Morozova *et al.* (2007) of $0.02\text{-}0.09 \text{ nmol CH}_4 \text{ h}^{-1} \text{ g}^{-1}$ and assuming the source population of methanogens to be distributed across the area of the methane plume footprint ($9.7 \times 10^6 \text{ km}^2$ - Mumma *et al.*, 2009) over a depth of 1 cm, the expected methane flux over 1 Martian year (MY) would be $7.5 \times 10^{11} \text{ g}$, which could be reduced to $1.96 - 4.81 \times 10^{11} \text{ g}$ if the methanogens are only active during northern hemisphere summer (178.64 days), which is still a factor of 10-25 times greater than the observed flux ($0.19 \times 10^{11} \text{ g}$), suggesting methanogens alone may not be responsible.

(ii) Methanogens and Methanotrophs

In permafrost springs, methanogens and methanotrophs are often found to be coexisting (Niederberger *et al.*, 2010). On Earth, CH_4 is oxidised with sulphate as a terminal electron acceptor. Sulphates are also common on Mars, therefore the planet could support anaerobic CH_4 oxidation. Sulphate abundance on Mars is similar to levels at permafrost springs on Earth, e.g. the Lost Hammer spring, Canada is sulphate-rich, containing 10% sulphates by weight (Lay *et al.*, 2013), which compares with various measurements (landers, rovers and Near-IR spectroscopy) of Martian soil sulphate content, which has been found to range from 5-9% by weight (Hecht *et al.*, 2009; Gendrin *et al.*, 2005).

Assuming a CH_4 oxidation rate of $10 \text{ nmol g}^{-1} \text{ (sediment) day}^{-1}$ (Liebner & Wagner, 2007), methanotrophs coexisting with methanogens in the same scenario as part (i) would be able to oxidise $4.2 \times 10^{12} \text{ g CH}_4$ during northern hemisphere summer; an order of

magnitude more than the CH_4 produced by methanogens over this time period, suggesting that a coupled population may not produce a CH_4 signature at all. This would imply that (if detections are accurate) the CH_4 plume may not have a biological origin and that Mars is a planet at the end of its habitable lifetime that produces no remotely detectable signatures of life. However, depending on the efficiency with which methanotrophs use the methane produced by methanogens in a coupled population, the observed methane flux could be a product of biological activity. This possible interaction between these two population warrants further investigation.

6.4 Chapter summary

The future of life on Earth is linked to the future main sequence evolution of the Sun, which alters the planetary environment by raising temperatures and driving runaway heating and the gradual extinction of the biosphere. Life on an Earth analogue planet would be similarly affected by the main sequence evolution of its own host star, the properties of which would determine the biosphere's lifespan. Local G stars within 10 pc of the Sun in the late stages of their main sequence evolutions were investigated. By placing an Earth analogue planet within the HZ of suitable systems from this selection, the impact of small variations away from solar stellar properties on the lifetime of a planet's biosphere and the changes in associated biosignatures was determined. This provides a first step towards classifying HZs in terms of the types of biospheres they are likely to support. In particular, the β CVn system was found to be theoretically capable of hosting an Earth analogue planet in the final 100 Myr of its habitable lifetime. This planet could support a sparse extremophile biosphere similar to that predicted for the end of Earth's habitable lifetime, potentially providing a basis for future experimental verification of the predictions about Earth's future biosphere. This will become particularly relevant in the near-future when the first Earth analogue extrasolar planets are confirmed and future missions that are capable of detecting atmospheric biomarkers on such planets, become operational.

Moving away from purely Earth-like scenarios, knowing how a planet's habitability is influenced by its host star, either over time or as a result of having host star types that are different to the Sun, again allows inferences to be made about the types of life that could exist there and the associated biosignatures. Binary and multiple star systems, for example, can cause the types and abundances of plant life, as well as the photosynthetic

reaction that powers them, to differ from those existing under normal Earth-like conditions.

Observations of terrestrial planets within our own solar system can act as test cases for the future, when more information about the compositions of terrestrial exoplanet atmospheres will be known. The example of methane plumes on Mars, for example, demonstrates the process of interpreting potential biosignatures to determine whether or not the presence of life could be responsible. For the case of Mars, assuming the plume detections are accurate, the most likely candidates for producing such a signature, methanogens, may not be responsible for it.

7

Conclusions

EARTH provides us with the only easily accessible laboratory in which to test and explore questions about life in the universe. However, this planet does not only limit us to one example of a biosphere, but provides us with access to information about alien worlds via clues about life on the early Earth and via predictions about the forms of life that could exist in the far-future. In this section, the results about the biospheres at the end of Earth's and other Earth-like planets' habitable lifetimes are summarised and discussed and future work evaluated.

The first step towards predicting these far-future biospheres was to model the changes in mean surface temperature of the planet as the luminosity of the Sun increases over time. As described in Chapter 2, this involved estimating the luminosity of the Sun as it changes over the next few billion years of its main sequence lifetime and allowing this to drive a surface temperature model that also incorporates greenhouse gas changes and orbital parameter changes, such as obliquity and eccentricity. This allowed an estimate for the

general mean temperature trend for different regions of the Earth's surface to be calculated. The model used to estimate future temperature evolution contained some simplifying assumptions. Some factors such as cloud cover and the variability of lunar recession rates were too complicated to incorporate into the model and so were kept constant. Earth-like geophysical and geochemical processes were assumed. Estimates for the magnitude of the heating effects of greenhouse gases were based on simplified relationships between solar insolation and greenhouse gas concentrations in the atmosphere. Similarly, atmospheric absorption of incoming radiation was estimated based on simplified relationships between the incoming radiation and the optical depth of the atmosphere.

By taking surface temperature trends as a guide for the types of life that could live on the planet during a particular future time period, the changes in the biosphere over time into the far-future could be predicted based on the availability of atmospheric gases, modelled using the methods described in Chapter 3 and the likely metabolisms of microbial life best suited to any remaining habitats.

Using the combination of the temperature-luminosity and biosphere models, it was possible to place a time scale on the full extinction of the biosphere. In Chapter 4, the change in temperature over latitude and altitude within the troposphere was presented, along with an expected extinction sequence for all life on Earth, based on these predictions. While plant and animal life was expected to be fully extinguished within the next 1 Gyr, microbial life could survive for up to 2.8 Gyr, given a high obliquity, in a few isolated habitats.

With predictions in place about the nature of the biosphere over the next 3 Gyr, the biosphere model described in Chapter 3 could then be used to predict the biosignatures associated with the extinction of the biosphere over this time period. In Chapter 5, the pace and nature of the extinctions of plants and animals were more fully explored and discussed and estimates on the lifetimes of associated biosignatures made. For the microbial world that follows these extinctions, the biosignature model was used to estimate the type and abundance of biosignature gases that would be associated with this biosphere over time, finding that the strongest and most long-lasting biosignature of such a biosphere could be methane, at an order of magnitude higher level in the atmosphere than on the present-day Earth.

Having established a course for the future evolution of Earth's biosphere, this modelling

7.1. Avoiding total extinction: could life survive an end to habitable conditions (as presently defined on the planet of origin)?

work was then extended in Chapter 6 to investigate the case of biospheres near the end of the habitable lifetime of an Earth analogue planet (here taken to be an exact copy of the Earth) around older main sequence Sun-like stars. The ages of G stars within 10 pc of the Sun, along with their masses, were used to establish each star's progress along the main sequence relative to the Sun. Those that were far enough along the main sequence that conditions on an Earth analogue planet would be similar to those expected during the end stages of the Earth's habitable lifetime were chosen and conditions on a such a planet modelled to determine which system would best be able to host an Earth analogue planet with detectable late-stage microbial biosphere signatures today. The best candidate was found to be β CVn. A similar approach was taken with the super-Earth candidate τ Cet e, to extend the work to less Earth-like conditions. It was found that this planet, if inhabited, could be entering a late microbial biosphere stage, although factors such the enhanced geological activity of super-Earth planets could complicate this assessment. The less Earth-like cases of planets in binary or multiple star systems were also discussed. In these cases the presence of a second star was found to alter the nature of biosignatures caused by photosynthetic life, as a result of the types and availability of stellar radiation in a given system.

In a further deviation from Earth-like scenarios, the case for Mars being a planet reaching the end of its habitable lifetime in a cold state was discussed. The possibility of using methane plumes on Mars as evidence of a surviving martian biosphere was investigated by comparing expected biological methane outputs with observations. The inconclusive results highlight one of the potential drawbacks of searching for evidence of small, fragmented biospheres on dying planets.

7.1 Avoiding total extinction: could life survive an end to habitable conditions (as presently defined on the planet of origin)?

The sequence of events that is described in this work concludes with a definite end to the entire biosphere on a planet once environmental conditions cease to be tolerable to even the most extreme forms of life known to exist on Earth. However, there are some factors that cannot easily be included in models of these events, that are briefly discussed below.

These mechanisms could allow some of the genetic diversity of life on a planet to survive beyond its predicted end-date.

7.1.1 Future evolution

The process of natural selection on Earth over the past 3.8 Gyr has resulted in the continued adaptation of life to a wide variety of environments as conditions changed. Given enough time to adapt, life (albeit, not all forms of life) has proved capable of coping with all environmental changes on Earth to date. Sudden rapid changes result in extinctions of species that are unable to adapt or migrate away in time, but can also create new opportunities. Observations of life on Earth show that any new, or recently vacant environment that can be inhabited, at least by some forms of life, will not remain uninhabited for very long (Cockell, 2014). For example, after the Cretaceous-Paleogene extinction event, many vacant environmental niches were re-inhabited (Pardo & Keller, 2008).

It is possible that life could find a way to adapt to conditions more extreme than it is currently known to tolerate today. Maintaining a similar biosphere to that on Earth today for much longer than predicted.

7.1.2 Passive migration

The transfer of microbial life ejected from a planet as a result of impact events (Wells *et al.*, 2003), and given sufficient protection from the harsh environmental conditions in space, could be one pathway via which some of the genetic diversity of a planet could survive beyond the end of its original host planet's habitable lifetime (Burchell, 2004). Large, globally destructive collisions (involving objects > 1 km in diameter) are expected to occur on Earth every $0.6 \pm 0.1 Myr$ (Stuart & Binzel, 2004).

If the ejected microorganisms were able to survive until they once again happened upon habitable conditions, on another planet or moon, they could act as the seeds for the beginning of a new biosphere. This would, at least initially, be genetically similar to the biosphere in which that life originated.

7.1.3 The role of intelligent life

The extinction sequences presented here all neglect the potential role intelligent life could play in prolonging a biosphere. On Earth, human activities have already been shown to influence climate and environments on local and global scales. It could be argued that, once our understanding of environmental processes improves, as a species, we will soon have the ability to make meaningful and deliberate changes to climate on a global scale. Large-scale geoengineering could maintain clement, habitable conditions for far longer than would naturally be the case. However, the resource and energy cost associated with preventing the extinction of the entire biosphere may eventually become too great to be the best route to maintaining life, especially towards the end of a Sun-like star's main sequence lifetime, when luminosity would rise rapidly and expansion of the star's outer envelope would disrupt planetary orbits. It may be more cost-effective to transport life to other locations that are, or could be made to be, habitable, and would remain that way for geologically long periods of time.

Another option would be to alter life, rather than the environment, essentially accelerating, and possibly out-performing, the relatively slow and random process of natural selection. By altering existing organisms, or creating entirely new ones that are able to survive under future environmental extremes, the continued existence of a rich, diverse biosphere could be prolonged on a planet past the predicted end-points for plant and animal life. However, artificial organisms would presumably still be limited by the tolerances of biochemistry, so the overall lifespan of the biosphere would probably remain unchanged.

This does, however, assume that human-level intelligence would still exist on the far-future Earth. The average species lifetime for mammals (the point at which a species first originates to the point at which it becomes extinct) is about 1 million years. This is an average, so some mammal species will persist for longer than others, but it would be biologically unprecedented for humans to still exist far enough into the future for management of this problem to be an option. However, intelligence as a trait, provided it remained useful to survival, may still persist in the biosphere for long enough to influence the future habitability of the planet.

7.2 Outlook

Knowing how environments and biospheres on a planet respond to the late stages of the evolution of their host star begins to provide a useful set of tools for searching for life on planets that are nearing the ends of their habitable lifetimes. Data from the Kepler space telescope suggest that up to 22% of Sun-like stars could host an Earth-sized planet in the HZ (Petigura *et al.*, 2013). While an Earth-sized planet does not necessarily imply an Earth-mass planet, this figure is still encouraging for the prospect of near-future discoveries of Earth-like planets. Some of these planets will inevitably be at a later stage in their habitable lifetimes than the present day Earth. Therefore, if Earth-like life is present, a different suite of biosignatures to those of the present day Earth would be exhibited, which would provide a platform for testing and refining biosignature predictions, such as those presented here, once appropriate telescopes for analysing such atmospheres are in operation. Expanding the suite of potential biosignatures would not only aid the search for life, but could help to reveal clues about Earth's own future and its eventual fate that models alone could not predict.

The continued study of extreme or unexplored environments on Earth will probably yield more clues about the limits of life, expanding the range of environments that can be classified as habitable. In particular, as touched upon in Chapters 4 and 5, the atmosphere as a potential habitat for life is only just beginning to be explored. It is still not known if organisms can complete their lifecycles within the atmosphere, or whether they are just passively in transit. Recent atmospheric sampling experiments have found that microorganisms are present in the atmosphere at altitudes up to 77 km (Imshenetsky *et al.*, 1978), with the majority being found in the lower troposphere within clouds (Womack *et al.*, 2010). Further exploration of this environment, using a combination of atmospheric samples and atmospheric modelling efforts, would begin to answer these questions. This would further expand the boundaries of the HZ around a star as well as providing further refuges for life at the end of its host planet's habitable lifetime, extending that lifetime past the limits of the surface and subsurface habitats on that planet. Showing that a planetary atmosphere can be a habitat would not only extend the habitable lifetime of an Earth-like planet, but could also enable an atmospheric habitable zone to be defined, increasing the number of habitable and partially habitable environments within, and beyond, the solar

system. The aerial microorganisms that could fill such habitats could have their own unique remotely detectable biosignatures, allowing them to be detected and potentially distinguished from surface life, widening the net in the search for life and increasing our understanding of the nature of life.

Glossary

Archaea: Single-celled organisms with a separate origin to bacteria. Thought to be the first domain of life to appear on Earth.

Archean eon: The second eon in Earth's history, describing the time from 3.8 Gyr ago to 2.5 Gyr ago. The beginning of this eon marked the end of the Late Heavy Bombardment and the first definite evidence of oceans. The oldest fossil evidence of life dates to this time.

Astronomical Unit (au): A measure of distance equal to the mean distance between the Earth and the Sun, approximately 1.5×10^{11} m.

Autotroph: Organisms that obtain organic nutrients from simple inorganic substances.

Bacteria: Single-celled organisms with a separate origin to archaea.

Benthic organisms: In biological terms, benthic organisms are those living in environments below the surface level of a body of water.

Biosignatures: Indicators of the presence of life. These include gases of biological origin in an atmosphere, geochemical traces of life and other features, such as vegetation reflectance.

Biosphere: The entirety of living organisms on a planet, encompassing their relationships to one another and the planet-atmosphere system.

Embryophyte: A sub-kingdom of green plants that includes liverworts, hornworts, mosses and vascular plants, but excludes green algae and related organisms.

Eon: A sub-unit of geological time, marking periods of 0.5 billion years or more. There have been four eons in Earth's history so far.

Eukaryote: A domain of life consisting of organisms composed of one (or more) cells with membranes, nuclei and other features. Includes all plants, animals and fungi.

Genome: This describes the entirety of a particular organism's hereditary information, encoded within its DNA (or RNA for some viruses).

Great Oxygenation Event: This marks the rapid rise in oxygen in Earth's atmosphere 2.4 Gyr ago; a consequence of the evolution of oxygenic photosynthesis.

Gyr: 1×10^9 years.

Hadean eon: The first eon in Earth's history. Covering the time from the formation of the planet 4.54 Gyr ago to 3.8 Gyr ago. Due to the extensive volcanism on the young planet and frequent impacts, the surface was largely molten. No rocks survive from this time, although some zircon crystals, thought to date from this period, have been found deposited in younger rock layers.

Insolation: Solar radiation intercepted by a planet.

Lapse rate: Rate of temperature (or another parameter, if specified) decrease with increasing elevation in an atmosphere.

Late Heavy Bombardment: A period in the early solar system (4.1 - 3.8 Gyr ago) during which there was a high frequency of impact events as a result of the abundance of fragments left over from the formation of the planets.

Latent heat: The energy released during a process that occurs at a constant temperature, e.g. melting, boiling.

Main sequence: The stage of a star's life during which it converts hydrogen to helium in its core, represented by a diagonal strip on the Hertzsprung-Russell diagram (a plot of absolute magnitudes or luminosity, versus effective temperature or spectral type, for stars).

Molecular cloud: A nebula (see *nebula*) with a size and density that results in the formation of molecules. These usually have cold (approximately 20 K) temperatures.

Mycoheterotrophy: A symbiotic relationship between certain plants and fungi that enables the plant to get some (or all) of its energy from the fungi, rather than via photosynthesis.

Nebula: An interstellar cloud of gas, dust and ionised gases.

Organotroph: In microbiology, organisms that obtain hydrogen or electrons from organic substrates.

Phanerozoic eon: Earth's current eon, which began 545 Myr ago. This period saw the emergence of the diverse and complex forms of life that exist on Earth today.

Prokaryotes: Organisms with cells that lack a membrane or nucleus. Includes all archaea and bacteria.

Proterozoic eon: The third eon in Earth's history, covering the time period from 2.5 Gyr ago to 542 Myr ago. Multicellular organisms appeared during this time.

Proto-planetary disc: The disc of gas and dust that remains in orbit around a star after the star has formed. This leftover material eventually coalesces into planets and planetesimals.

Radiolysis: The process by which chemical bonds within molecules are broken as a result of high-energy radiation fluxes.

Serpentinisation: A metamorphic process in which igneous rocks (with low silica contents) are oxidised, then hydrolysed into rocks containing serpentine minerals ($\text{Mg}_3\text{Si}_2\text{O}_5(\text{OH})_4$).

Solar constant (S_0): The flux density of radiation from the Sun at a distance of 1 au (the average Earth-Sun distance).

Supernova: A violent explosion that marks the end of the lifetime of high-mass stars (typically stars with masses greater than $8 M_\odot$). These explosions release complex elements, such as carbon, into the surrounding space, which can then be incorporated into other stars as they form.

Volatiles: Elements or compounds that vaporise at relatively low temperatures (usually used in reference to planetary atmospheres or crusts).

Water activity: A value between 0-1 describing the amount of water available for the hydration of materials. For example, adding salts to water lowers the water activity because there are fewer water molecules available for other hydration interactions.

Online resources

- [1] The VizieR Catalogue Service: <http://vizier.u-strasbg.fr/>
- [2] The Extrasolar Planets Encyclopaedia: <http://exoplanet.eu/>
- [3] The Habitable Exoplanets Catalogue: <http://phl.upr.edu/hec>
- [4] NASA ADS: http://adsabs.harvard.edu/abstract_service.html

Bibliography

- Abe Y., Abe-Ouchi A., Sleep N.H. and Zahnle K.J. (2011) Habitable Zone Limits for Dry Planets. *Astrobiology* 11: 443-460.
- Abramov O. and Mojzsis S.J. (2009) Microbial habitability of the Hadean Earth during the late heavy bombardment. *Nature* 459: 419-422.
- Albert V.A., Jobson R.W., Michael T.P. and Taylor D.J. (2010). The carnivorous bladderwort (*Utricularia*, *Lentibulariaceae*): a system inflates. *J. Exp. Bot.* 61: 5-9.
- Allison S.D. (2006) Brown Ground: A Soil Carbon Analogue for the Green World Hypothesis? *The American Naturalist* 167: 619-627.
- Amato P., Parazols M., Sancelme M., Laj P., Mailhot G. and Delort A.M. (2007) Microorganisms isolated from the water phase of tropospheric clouds at the Puy de Dôme: major groups and growth abilities at low temperatures. *FEMS microbiology ecology* 59: 242-254.
- Angel J.R.P., Cheng A.Y.S., and Wolf N.J. (1986) A space telescope for infrared spectroscopy of Earth-like planets. *Nature* 322: 341-343.
- Anten N.P.R., Schieving F., Medina E., Werger M.J.A. and Schufflen P. (1995) Optimal leaf area indices in C3 and C4 mono- and dicotyledonous species at low and high nitrogen availability. *Physiologia Plantarum* 95: 541-550.
- Arakaki M., Christin P.-A., Nyffeler R., Lendei A., Eggli U., Matthew Ogburn R., Spriggs E., Moore M.J. and Edwards E.J. (2011). Contemporaneous and recent radiations of the world's major succulent plant lineages. *PNAS* 108: 8379-8384.
- Aráujo M.B., Thuiller W. and Pearson R.G. (2006) Climate warming and the decline of amphibians and reptiles in Europe. *J. Biogeogr.* 33: 1712-1728.
- Arnold L., Gillet S., Lardiere O., Riaud P. and Schneider J. (2002) A test for the search for life on extrasolar planets: looking for the terrestrial vegetation signature in the Earthshine spectrum. *Astron. Astrophys.* 392: 231-237.
- Arnould J. and Debus A. (2008) An Ethical Approach to Planetary Protection. *Advances in Space Research* 42: 1089-1095.
- Azua-Bustos A., Urrejola C. and Vicuña R (2012) Life at the dry edge: Microorganisms of the Atacama Desert. *FEBS Letters* 586: 2939-2945.
- Bailey J. (2007) Rainbows, Polarization, and the Search for Habitable Planets. *Astrobiology* 7: 320-332.

- Baker V.R. (2006) Geomorphological Evidence for Water on Mars. *Elements* 2: 139-143.
- Barnes R., Mullins K., Goldblatt C., Meadows V.S., Kasting J.F. and Heller R (2013) Tidal Venuses: Triggering a Climate Catastrophe via Tidal Heating. *Astrobiology* 13: 225-250.
- Barnes R.O. and Goldberg E.D. (1976) Methane production and consumption in anoxic marine sediments. *Geology* 4: 297-300.
- Barrat J.A., Gillet Ph., Lécuyer C., Sheppard S.M.F. and Lesourd M. (1998) Formation of Carbonates in the Tatahouine Meteorite. *Science* 280: 412-414.
- Battista J.R. (1997) Against All Odds: The Survival Strategies of *Deinococcus radiodurans*. *Annu. Rev. Microbiol.* 51: 203-224.
- Beatty D. et al. (2006) Unpublished white paper, 76 p, posted June 2006 by the Mars Exploration Program Analysis Group (MEPAG) at <http://mepag.jpl.nasa.gov/reports/index.html>
- Beech M. (2011) The Far Distant Future of Alpha Centauri. *Journal of the British Interplanetary Society* 64: 387-395.
- Bell E.M. (2012) Life at Extremes: Environments, Organisms and Strategies for Survival. CABI, Oxfordshire, UK.
- Bell F.G. (2004) Engineering Geology and Construction. Spon Press, London, UK, pp. 816.
- Bender M. and Conrad R. (1994) Microbial Oxidation of Methane, Ammonium and Carbon Monoxide, and Turnover of Nitrous Oxide and Nitric Oxide in Soils. *Biogeochemistry* 27: 97-112.
- Benneke B. and Seager S. (2012) Atmospheric Retrieval for Super-Earths: Uniquely Constraining the Atmospheric Composition with Transmission Spectroscopy. *Astrophys. J.* 753: 100-121.
- Benner S. (2013) Planets, Minerals and Life's Origin. *Mineralogical Magazine* 77: 686.
- Benz W., Slattery W.L. and Cameron A.G.W. (1986) The origin of the Moon and the single-impact hypothesis I. *Icarus* 66: 515-535.
- Bernhard A. (2012) The Nitrogen Cycle: Processes, Players, and Human Impact. *Nature Education Knowledge* 3: 25.
- Bills B.G. and Ray R.D. (1999) Lunar orbital evolution: A synthesis of recent results *Geophys. Res. Lett.* 26: 3045-3048.
- Birk J.W., Crutzen P.J. and Roble R.G. (2007) Frequent Ozone Depletion Resulting from Impacts of Asteroids and Comets. In: *Comet/Asteroid Impacts and Human Society*, ed. Bobrowsky, Peter T.; Rickman, Hans. Springer, pp. 225-245.
- Birmingham B.C. and Colman B. (1979) Measurement of carbon dioxide compensation points of freshwater algae. *Plant Physiol.* 64: 892-895.

-
- Björn L.O., Papageorgiou G.C., Blankenship R.E. and Govindjee (2009) A viewpoint: why chlorophyll a? *Photosynth. Res.* 99: 85-98.
- Blackmond D.G. (2004) Asymmetric autocatalysis and its implications for the origin of homochirality. *PNAS* 101: 5732-5736.
- Blair C.C., D'Hondt S., Spivack A.J. and Kingsley R.H. (2007) Radiolytic Hydrogen and Microbial Respiration in Subsurface Sediments. *Astrobiology* 7: 951-970.
- Blank C.E. and Sánchez-Baracaldo (2010) Timing of morphological and ecological innovations in the cyanobacteria - a key to understanding the rise in atmospheric oxygen. *Geobiology* 8: 1-23.
- Blankenship R.E. (2010) Early Evolution of Photosynthesis. *Plant Physiology* 154: 434-438.
- Blum J. and Wurm G. (2008) The Growth Mechanisms of Macroscopic Bodies in Protoplanetary Disks. *Annu. Rev. Astro. Astrophys.* 46: 21-56.
- Blumthaler M., Ambach W. and Ellinger R. (1997) Increase in solar UV radiation with altitude. *Journal of photochemistry and Photobiology B: Biology* 39: 130-134.
- Bohlen S.R. (1987) Pressure-Temperature-Time Paths and a Tectonic Model for the Evolution of Granulites. *J. Geol.* 95: 617-632.
- Bolmont E., Raymond S.N., von Paris P., Selsis F., Hersant F., Quintana E.V. and Barclay T. (2014) Formation, tidal evolution and habitability of the Kepler-186 system. *arXiv preprint* arXiv:1404.4368.
- Bongers L. (1970) Energy Generation and Utilization in Hydrogen Bacteria. *J. Bacteriol.* 104: 145-151.
- Bonner and Liang (1984) β -decay, Bremsstrahlen, and the origin of molecular chirality. *J. Mol. Evol.* 21: 84-89.
- Bonner W.A. (1991) The origin and amplification of biomolecular chirality. *Origins of life and evolution of the biosphere* 21: 59-111.
- Borucki, W.J., Koch, D.G., Basri, G., Batalha, N., Boss, A., Brown, T.M., Caldwell, D., Christensen-Dalsgaard, J., Cochran, W.D., DeVore, E., Dunham, E.W., Dupree, A.K., Gautier, T.N., III, Geary, G.C., Gilliland, R., Gould, A., Howell, S.B., Jenkins, J.M., Kjeldsen, H., Latham, D.W., Lissauer, J.J., Marcy, G.W., Monet, D.G., Sasselov, D., Tarter, J., Charbonneau, D., Doyle, L., Ford, E.B., Fortney, J., Holman, M.J., Seager, S., Steffen, J.H., Welsh, W.F., Allen, C., Bryson, S.T., Buchhave, L., Chandrasekaran, H., Christiansen, J.L., Ciardi, D., Clarke, B.D., Dotson, J.L., Endl, M., Fischer, D., Fressin, F., Haas, M., Horch, E., Howard, A., Isaacson, H., Kolodziejczak, J., Li, J., MacQueen, P., Meibom, S., Prsa, A., Quintana, E.V., Rowe, J., Sherry, W., Tenenbaum, P., Torres, G., Twicken, J.D., Van Cleve, J., Walkowicz, L., and Wu, H. (2011a) Characteristics of Kepler planetary candidates based on the first data set. *Astrophys J* 718: 117-137.
- Borucki, W.J., Koch, D.G., Basri, G., Batalha, N., Brown, T.M., Bryson, S.T., Caldwell,

D., Christensen-Dalsgaard, J., Cochran, W.D., DeVore, E., Dunham, E.W., Gautier, T.N., III, Geary, G.C., Gilliland, R., Gould, A., Howell, S.B., Jenkins, J.M., Latham, D.W., Lissauer, J.J., Marcy, G.W., Rowe, J., Sasselov, D., Boss, A., Charbonneau, D., Ciardi, D., Doyle, L., Dupree, A.K., Ford, E.B., Welsh, J., Allen, C., Buchhave, L.A., Christiansen, J.L., Clarke, B.D., Das, S., Dsert, J., Endl, M., Fabrycky, D., Fressin, F., Haas, M., Horch, E., Howard, A., Isaacson, H., Kjeldsen, H., Kolodziejczak, J., Kulesa, C., Li, J., Lucas, P.W., Machalek, P., McCarthy, D., MacQueen, P., Meibom, S., Miquel, T., Prsa, A., Quinn, S.N., Quintana, E.V., Ragozzine, D., Sherry, W., Shporer, A., Tenenbaum, P., Torres, G., Twicken, J.D., Van, Cleve, J., and Walkowicz, L. (2011b) Characteristics of planetary candidates observed by Kepler II: analysis of the first four months of data. arXiv:1102.0541v2.

Boss A.P. (1996) Evolution of the Solar Nebula. III. Protoplanetary Disks Undergoing Mass Accretion. *Astrophys. J.* 469: 906.

Boston P. J., Frederick R. D., Welch S. M., Werker J., Meyer T. R., Sprungman B., Hildreth-Werker V., Thompson S. L. and Murphy D. L. (2003) Human Utilisation of Subsurface Extraterrestrial Environments. *Gravitational and Space Biology Bulletin* 16: 121-131.

Bowers R.M., Lauber C.L., Wiedinmyer C., Hamady M., Hallar A.G., Fall R., Knight R. and Fierer N. (2009) Characterization of Airborne Microbial Communities at a High-Elevation Site and Their Potential To Act as Atmospheric Ice Nuclei. *App. Env. Microbiol.* 75: 5121-5130.

Boucher, O., D. Randall, P. Artaxo, C. Bretherton, G. Feingold, P. Forster, V.-M. Kerminen, Y. Kondo, H. Liao, U. Lohmann, P. Rasch, S.K. Satheesh, S. Sherwood, B. Stevens and X.Y. Zhang (2013) Clouds and Aerosols. In: *Climate Change 2013: The Physical Science Basis. Contribution of Working Group I to the Fifth Assessment Report of the Intergovernmental Panel on Climate Change* [Stocker, T.F., D. Qin, G.-K. Plattner, M. Tignor, S.K. Allen, J. Boschung, A. Nauels, Y. Xia, V. Bex and P.M. Midgley (eds.)]. Cambridge University Press, Cambridge, United Kingdom and New York, NY, USA.

Boyd E.S., Lange R.K., Mitchell A.C., Havig J.R., Hamilton T.L., Lafrenière M.J., Shock E.L., Peters J.W. and Skidmore M. (2011) Diversity, Abundance, and Potential Activity of Nitrifying and Nitrate-Reducing Microbial Assemblages in a Subglacial Ecosystem. *Appl. Environ. Microbiol.* 77: 4778-4787.

de Boyer Montegut C., Madec G., Fischer A.S., Lazar A. and Iudicone D. (2004). Mixed layer depth over the global ocean: An examination of profile data and a profilebased climatology. *Journal of Geophysical Research: Oceans* 109: C12.

Bradley J.P., Ishii H.A., Gillis-Davis J.J., Cistonc J., Nielsend M.H., Bechtelf H.A., and Martin M.C. (2014) Detection of solar wind-produced water in irradiated rims on silicate minerals. *PNAS* doi: 10.1073/pnas.1320115111

Brasier M., McLoughlin N., Green O. and Wacey D. (2006) A fresh look at the fossil evidence for early Archaean cellular life. *Phil. Trans. R. Soc. Lond. B Biol. Sci.* 361:

887-902.

Briot D. (2010) Earthshine observations and the detection of vegetation on extrasolar planets. In Highlights of Astronomy, Vol. 15, XXVIIIth IAU General Assembly, International Astronomical Union, Paris, pp 699-700.

Broecker W.S., Thurber D.L., Goddard J., Ku T., Matthews R.K. and Mesolella K.J. (1968) Milankovitch hypothesis supported by precise dating of coral reefs and deep sea sediments. *Science* 159: 297300.

Brook E.J., Kurz M.D. and Curtice J. (2009) Flux and size fractionation of ³-He in interplanetary dust from Antarctic ice core samples. *Earth Plan. Sci. Lett.* 286: 565-569.

Buffett B.A. (2000) Clathrate Hydrates. *Annu. Rev. Earth Planet. Sci.* 28: 477-507.

Buick R. (2008) When did oxygenic photosynthesis evolve? *Phil. Trans. R. Soc. B* 363: 2731-2743.

Burchell M.J. (2004) Panspermia today. *Int. J. Astrobiology* 3: 73-80.

Burke B.F. (1986) Detection of planetary systems and the search for evidence of life. *Nature* 322: 340-341.

Burton M.R., Sawyer G.M. and Granieri D. (2013) Deep Carbon Emissions from Volcanoes. *Reviews in Mineralogy & Geochemistry* 75: 951-970.

Buttereld N.J. (2000) *Bangiomorpha pubescens* n. gen., n. sp.: implications for the evolution of sex, multicellularity, and the mesoproterozoic/neoproterozoic radiation of eukaryotes. *Paleobiology* 26: 386-404.

Byrne N., Strous M., Crépeau V., Kartal B., Birrien J.L., Schmid M., Lesongeur F., Schouten S., Jaeschke A., Jetten M., Prieur D., Godfroy A. (2009) Presence and activity of anaerobic ammonium-oxidizing bacteria at deep-sea hydrothermal vents. *ISME J.* 3: 117-123.

Cairns-Smith A.G. (1987) Genetic Takeover and the Mineral Origins of Life. *Cambridge University Press*, pp. 477.

Caldeira K. and Kasting J.F. (1992) The life span of the biosphere revisited. *Nature* 360: 721-723.

Canganella F. and Wiegel J. (2011) Extremophiles: from abyssal to terrestrial ecosystems and possibly beyond. *Naturwissenschaften* 98: 253-279.

Carr J.S. and Najita J.R. (2008) Organic Molecules and Water in the Planet Formation Region of Young Circumstellar Disks. *Science* 319: 1504-1506.

Carr M. H. (1987) Water on Mars. *Nature* 326: 30-35.

Carr M.H., Belton M.J.S., Chapman C.R., Davies M.E., Geissler P., Greenberg R., McEwen A.S., Tufts B.R., Greeley R., Sullivan R., Head J.W., Pappalardo R.T., Klaasen K.P., Johnson T.V., Kaufman J., Senske D., Moore J., Neukum J., Schubert G., Burns J.A.,

Thomas P. and Veverka J. (1998) Evidence for a subsurface ocean on Europa. *Nature* 391: 363-365.

Catanzarite J. and Shao M. (2011) The occurrence rate of Earth analog planets orbiting Sun-like stars. arXiv:1103.1443v1.

Chen Y., Wu L., Boden R., Hillebrand A., Kumaresan D., Moussard H., Baciú M., Lu Y. and Murrell J.C. (2009) Life without light: microbial diversity and evidence of sulfur- and ammonium-based chemolithotrophy in Movile Cave. *The ISME Journal* 3: 1093-1104.

Chivian D, Brodie E.L., Alm E.J., Culley D.E., Dehal P.S., DeSantis T.Z., Gihring T.M., Lapidus A., Lin L-H., Lowry S.R., Moser D.P., Richardson P.M., Southam G., Wanger G., Pratt L.M., Andersen G.L., Hazen T.C., Brockman F.J., Arkin A.P. and Onstott T.C. (2008) Environmental Genomics Reveals a Single-Species Ecosystem Deep Within Earth. *Science* 322: 275-278.

Christensen P.R., Bandfield J.L., Clark R.N., Edget K.S, Hamilton V.E., Hoefen T., Kieffer H.H., Kuzmin R.O., Lane M.D., Malin M.C., Morris R.V., Pearl J.C., Pearson R., Roush T.L., Ruff S.W. and Smith M.D. (2000) Detection of crystalline hematite mineralization on Mars by the Thermal Emission Spectrometer: Evidence for near-surface water. *J. Geophys. Res.* 105: 9623-9642.

Chyba C.F., and Sagan C. (1997) Comets as a source of prebiotic organic molecules for the early Earth. In *Comets and the Origin and Evolution of Life*, Springer New York, pp. 147-173.

Chyba C.F. (2005) Rethinking Earth's Early Atmosphere. *Science* 308: 962-963.

Cisar J.O., Xu D., Thompson J., Swaim W., Hu L. and Kopecko D.J. (2000) An alternative interpretation of nanobacteria-induced biomineralization. *PNAS* 97: 11511-11515.

Clancy P., Brack A., Horneck G. (2005) Looking for Life, Searching the Solar System. Cambridge University Press, Cambridge, UK, pp.352.

Clarke A. and Rothery P. (2008) Scaling of body temperature in mammals and birds. *Funct. Ecol.* 22: 58-67.

Cnossen I., Sanz-Forcada J., Favata F., Witasse O., Zegers T. and Arnold N.F. (2007) Habitat of early life: Solar X-ray and UV radiation at Earth's surface 43.5 billion years ago. *J. Geophys. Res. Planets* 112: E02008.

Cockell C.S. (1999) Life on Venus. *Planet. Space Sci.* 47: 1487-1501.

Cockell C.S. (2003) Impossible Extinction: Natural Catastrophes and the Supremacy of the Microbial World. Cambridge University Press, Cambridge, UK.

Cockell C. S. (2005) Planetary Protection - A microbial ethics approach. *Space Policy* 21: 287-289.

Cockell C.S., Lee P., Broady P., Lim D.S.S., Osinski G.R., Parnell J., Koeberl C., Pesonen L. and Salminen J. (2005) Effects of asteroid and comet impacts on habitats for lithophytic

-
- organisms - A synthesis. *Meteoritics & Planetary Science* 40: 1901-1914.
- Cockell C.S., Schuerger A.C., Billi D., Friedmann E.I. and Panitz C. (2005b) Effects of a simulated martian UV flux on the cyanobacterium, *Chroococcidiopsis* sp. 029. *Astrobiology* 5: 127-140.
- Cockell C.S., Brack A., Wynn-Williams D.D., Baglioni P., Brandstätter F., Demets R., Edwards H.G.M., Gronstal A.L., Kurat G., Lee P., Osinski G.R., Pearce D.A., Pillinger J.M., Roten C-A. and Sancisi-Frey S. (2007) Interplanetary Transfer of Photosynthesis: An Experimental Demonstration of A Selective Dispersal Filter in Planetary Island Biogeography. *Astrobiology* 7: 1-9.
- Cockell C.S. and Raven J.A. (2007) Ozone and life on the Archaean Earth. *Phil. Trans. R. Soc. A* 365: 1889-1901.
- Cockell C.S., Kaltenegger L. and Raven J.A. (2009) Cryptic Photosynthesis - Extrasolar Planetary Oxygen Without a Surface Biological Signature. *Astrobiology* 9: 623-636.
- Cockell C.S. (2014) Trajectories of Martian Habitability. *Astrobiology* 14: 182-203.
- Córdoba-Jabonero C., Zorzano M., Selsis F., Patel M.R., Cockell C.S. (2005) Radiative habitable zones in martian polar environments. *Icarus* 175: 360-371.
- Courtillot V., Davaille A., Besse J. and Stock J. (2003) Three distinct types of hotspots in the Earth's mantle. *Earth Plan. Sci. Lett.* 205: 295-308.
- Coustenis A., Tokano T., Burger M.H., Cassidy T.A., Lopes R.M., Lorenz R.D., Rutherford K.D. and Schubert G. (2010) Atmospheric/Exospheric Characteristics of Icy Satellites. *Space Science Review* 153: 155-184.
- Cowan D.A. (2004) The upper temperature of life - how far can we go? *Trends In Microbiology* 12: 58-60.
- Cowan N.B. and Abbot D.S. (2014) Water Cycling Between Ocean and Mantle: Super-Earths Need Not be Waterworlds. *ArXiv: 1401.0720*.
- Crowe M. (1997) A History of the Extraterrestrial Life Debate. *Zygon* 32: 147-162.
- Curto G. Lo., Mayor M., Benz W., Bouchy F., Hebrard G., Lovis C., Moutou C., et al. (2013) The HARPS search for southern extrasolar planets: XXXIII. New multi-planet systems in the HARPS volume limited sample: a super-Earth and a Neptune in the habitable zone. *arXiv preprint arXiv:1301.2741*.
- Dalsgaard T., Canfield D.E., Petersen J., Thamdrup B. and Acuña-González J. (2003) N₂ production by the anammox reaction in the anoxic water column of Golfo Dulce, Costa Rica. *Nature* 422: 606-608.
- Danchi W.C. and Lopez B. (2013) Effect of metallicity on the evolution of the habitable zone from the pre-main sequence to the asymptotic giant branch and the search for life. *Astrophys. J.* 769: 27.
- Daniel R.M., Van Eckert R., Holden J.F., Truter J. and Crowan D.A. (2004) The stability

of biomolecules and the implications for life at high temperatures. *Geophysical Monograph Series* 144: 25-39.

Darwin C. (1859) *On the Origin of Species*. London: John Murray, Albermarle Street. p. 484

DasSarma S. and DasSarma P. (2012) *Halophiles*. In: eLS. Wiley, Chichester.

Davies P.C.W. and Lineweaver C.H. (2005) Finding a Second Sample of Life on Earth. *Astrobiology* 5: 154-163.

DeLeon-Rodriguez N., Lathem T.L., Rodriguez-R L.M., Barazesh J.M., Anderson B.E., Beyersdorf A.J., Ziemba L.D., Bergin M., Nenes A. and Konstantinidis K.T. (2013) Microbiome of the upper troposphere: Species composition and prevalence, effects of tropical storms, and atmospheric implications. *PNAS* 110: 2575-2580.

Deming D., Seager S., Winn J., Miller-Ricci E., Clampin M., Lindler D., et al. (2009) Discovery and characterization of transiting super Earths using an all-sky transit survey and follow-up by the James Webb Space Telescope. *Publications of the Astronomical Society of the Pacific* 121: 952-967.

Deng F., Chen J.M., Plummer S., Chen M. and Pise J. (2006) Algorithm for Global Leaf Area Index Retrieval Using Satellite Imagery. *IEEE Transactions on Geoscience and Remote Sensing* 44: 2219-2229.

de Vera J.P., Schulze-Makuch D., Khan A., Lorek A., Koncz A., Möhlmann D. and Spohn T. (2013) Adaptation of an Antarctic lichen to Martian niche conditions can occur within 34 days. *Planetary and Space Science*, <http://dx.doi.org/10.1016/j.pss.2013.07.014i>

Des Marais D.J., Harwit M.O., Jucks K.W., Kasting J.F., Lin D.N.C., Lunine J.I., Schneider J., Seager S., Traub W.A., and Woolf N.J. (2002) Remote sensing of planetary properties and biosignatures on extrasolar terrestrial planets. *Astrobiology* 2: 153-181.

Désert J.M., Charbonneau D., Demory B.O., Ballard S., Carter J.A., Fortney J.J., et al. (2011) The hot-Jupiter Kepler-17b: discovery, obliquity from stroboscopic starspots, and atmospheric characterization. *The Astrophysical Journal Supplement Series* 197: 14.

Dieser M., Battista J.R. and Christner B.C. (2013) Double-strand DNA break repair at -15°C . *Appl. Environ. Microbiol.* doi:10.1128/AEM.02845-13.

Di Folco, E., Thévenin F., Kervella P., Domiciano de Souza A., Coudé du Foresto V., Ségransan D. and Morel P. (2004) VLTI near-IR interferometric observations of Vega-like stars - Radius and age of α PsA, β Leo, β Pic, ϵ Eri and τ Cet. *A&A* 426: 601-617.

Dillon M.E., Wang G. and Huey R.B. (2010) Global metabolic impacts of recent climate warming. *Nature* 467: 704-707.

Domagal-Goldman S.D., Meadows V.S., Claire M.W. and Kasting J.F. (2011) Using Biogenic Sulfur Gases as Remotely Detectable Biosignatures on Anoxic Planets. *Astrobiology* 11: 419-441.

-
- Donnadieu Y., Godd ris Y., Ramstein G., N d lec A. and Meert J. (2004) A ‘snowball Earth’ climate triggered by continental break-up through changes in runoff. *Nature* 428: 303-306.
- Doolittle W.F. (2000) The nature of the universal ancestor and the evolution of the pro-
teome. *Current Opinion in Structural Biology* 10: 355-358.
- Duquennoy A. and Mayor M. (1991) Multiplicity among solar-type stars in the solar neigh-
bourhood II: distribution of orbital elements in an unbiased sample. *Astron. Astrophys.*
248: 485-524.
- Durieux L., Machado L.A.T. and Laurent H. (2003) The impact of deforestation on cloud
cover over the Amazon arc of deforestation. *Remote Sens. Environ.* 86: 132-140.
- Edwards K.J., Becker K. and Colwell F. (2012) The Deep, Dark Energy Biosphere: In-
traterrestrial Life on Earth. *Annu. Rev. Earth Planet. Sci.* 40: 551-568.
- Ehhalt D.H. (1974) The Atmospheric Cycle of Methane. *Tellus* 26: 58-70.
- Eldredge N. and Gould S.J (1972) Punctuated equilibria: an alternative to phyletic grad-
ualism. In *Models in paleobiology*, edited by Schopf, T.J.M Freeman, Cooper & Co, San
Francisco, pp 82-115.
- Elkins-Tanton L.T. and Seager S. (2008) Ranges of Atmospheric Mass and Composition
of Super-Earth Exoplanets. *Astrophys. J.* 685: 1237-1246.
- Elmegreen B.G. (1993) Protostars and Planets III. Ed. E.H. Levy and J.I. Lunine. Tucson:
University of Arizona Press, pp 97-124.
- Elvidge C.D. and Lyon R.J.P. (1985) Influence of rock-soil spectral variation on the as-
sessment of green biomass. *Remote Sens. Environ.* 17: 265-269.
- Epstein C.R. and Pinsonneault M.H. (2014) How Good a Clock is Rotation? The Stellar
Rotation-Mass-Age Relationship for Old Field Stars. *Astrophys. J.* 780: 159.
- Fair n A.G., Davila A.F., Gago-Duport L., Amils R. and McKay C.P. (2009) Stability
against freezing of aqueous solutions on early Mars. *Nature* 459: 401-404.
- Fair n A.G., Davila, A.F., Lim D., Bramall N., Bonaccorsi R., Zavaleta J., Uceda E.R.,
Stoker C., Wierzchos J., Dohm J.M., Amilis R., Andersen, D. and McKay C.P. (2010)
Astrobiology through the Ages of Mars: The Study of Terrestrial Analogues to Understand
the Habitability of Mars. *Astrobiology* 10: 821-843.
- Fajardo-Cavazos P., Link L., Jay Melosh H. and Nicholson W.L. (2005) Bacillus subtilis
Spores on Artificial Meteorites Survive Hypervelocity Atmospheric Entry: Implications
for Lithopanspermia. *Astrobiology* 5: 726-736.
- Fajardo-Cavazos P., Langenhorst F., Jay Melosh H. and Nicholson W.L. (2009) Bac-
terial Spores in Granite Survive Hypervelocity Launch by Spallation: Implications for
Lithopanspermia. *Astrobiology* 9: 647-657.
- Falkowski P.G., Katz M.E., Milligan A.J., Fennel K., Cramer B.S., Aubrey M.P., Berner

- R.A., Novacek M.J. and Zapol W.M. (2005) The rise of oxygen over the past 205 million years and the evolution of large placental mammals. *Science* 309: 2202-2204.
- Farrand W.H., Glotch T.D., Rice Jr J.W., Hurowitz J.A. and Swayze G.A. (2009) Discovery of jarosite within the Mawrth Vallis region of Mars: Implications for the geologic history of the region. *Icarus* 204: 478-488.
- Fedo C.M. and Whitehouse M.J. (2002) Metasomatic Origin of Quartz-Pyroxene Rock, Akilia, Greenland, and Implications for Earth's Earliest Life. *Science* 296: 1448-1452.
- Ferry J.G. (2002) Methanogenesis biochemistry. In *Encyclopedia of Life Sciences*, John Wiley & Sons, Ltd.
- Feulner G. (2012) The faint young Sun problem. *Rev. Geophys.* 50: RG2006.
- Field C.B. (1998) Primary Production of the Biosphere: Integrating Terrestrial and Oceanic Components. *Science* 281: 237-240.
- Filella I. and Peñuelas J. (1994) The red edge position and shape as indicators of plant chlorophyll content, biomass and hydric status. *Int. J. Remote Sensing* 15: 1459-1470.
- Fischer T.P. (2008) Fluxes of volatiles (H₂O, CO₂, N₂, Cl, F) from arc volcanoes. *Geochemical Journal* 42: 21-38.
- Flynn K.J., Stoecker D.K., Mitra A., Raven J.A., Glibert P.M., Hansen P.J., Granéli, E. and Burkholder J.M. (2013) A case of mistaken identification: the importance of mixotrophs and the clarification of plankton functional classification. *Journal of Plankton Research* 35: 3-11.
- Forgan D. (2012) Oscillations in the habitable zone around α Centauri B. *MNRAS* 422: 1241-1249.
- Franzmann P.D., Liu Y., Balkwill D.L., Aldrich H.C., De Macario E.C. and Boone D.R. (1997) *Methanogenium frigidum* sp. nov., a psychrophilic, H₂-using methanogen from Ace Lake, Antarctica. *International journal of systematic bacteriology* 47: 1068-1072.
- Frederick J.E. (2011) Principles of Atmospheric Science. Jones & Bartlett Publishers, Ontario, Canada, pp. 211.
- Gaidos E.J., Güdel M. and Blake G.A. (2000) The faint young Sun paradox: an observational test of an alternative solar model. *Geophys. Res. Lett.* 27: 501-503.
- Ganguly S., Nemani R.R., Zhang G., Hashimoto H., Milesi C., Michaelis A., Wang W., Votava P., Samanta A., Melton F., Dungan J.L., Vermote E., Gao F., Knyazikhin Y. and Myneni R.B. (2012) Generating global Leaf Area Index from Landsat: Algorithm formulation and demonstration. *Remote Sensing of Environment* 122: 185-202.
- Gantt B., Meskhidze N. and Kamykowski D. (2009) A new physically-based quantification of marine isoprene and primary organic aerosol emissions. *Atmos. Chem. Phys.* 9: 4915-4927.
- Gardner J.P., Mather J.C., Clampin M., Doyon R., Greenhouse M.A., Hammel H.B.,

-
- Hutchings J.B., Jakobsen P., Lilly S.J., Long K.S., Lunine J.I., McCaughrean M.J., Mountain M., Nella J., Rieke G.H., Rieke M.J., Rix H-W., Smith E.P., Sonneborn G., Stiavelli M., Stockman H.S., Windhorst R.A. and Wright G.S. (2006). The James Webb Space Telescope. *Space Sci. Rev.* 123: 485-606.
- Gaudi B.S. (2012) Microlensing surveys for exoplanets. *Ann. Rev. Astron. Astrophys.* 50: 411-453.
- Geib S.M., Filley T.R., Hatcher P.G., Hoover K., Carlson J.E., Jimenez-Gasco M., Nakagawa-Izumi A., Sleighter R.L. and Tien M. (2008) Lignin degradation in wood-feeding insects. *PNAS* 105: 1293212937.
- Gendrin A., Mangold N., Bibring J.P., Langevin Y., Gondet B., Poulet F., ... and LeMouélic S. (2005) Sulfates in Martian layered terrains: the OMEGA/Mars Express view. *Science* 307: 1587-1591.
- Genthon C., Barnola J.M., Raynaud O., Lorius C., Jouzel J., Barkov N.I., Korotkevitch Y.S. and Kotlyakov V.M. (1987) Vostok ice core: The climate response to CO₂ and orbital forcing changes over the last climatic cycle. *Nature*, 329: 414418.
- Gibson D.G., Glass J.I., Lartigue C., Noskov V.N., Chuang R-Y., Algire M.A., Benders G.A. et al. (2010) Creation of a bacterial cell controlled by a chemically synthesized genome. *Science* 329: 52-56.
- Gillet Ph., Barrat J.A., Heulin Th., Achouak W., Lesourd M., Guyot F. and Benzerara K. (2000) Bacteria in the Tatahouine meteorite: nanometric-scale life in rocks. *Earth Plan. Sci. Lett.* 175: 161-167.
- Gilmour I., Jolley D.W., Watson J.S., Gilmour M.A. and Kelley S.P. (2013) Post-impact heating of a crater lake. *EPSC Abstracts 8*: EPSC2013-177
- Gilmozzi R. and Spyromilio J. (2007) The European extremely large telescope (E-ELT). *The Messenger* 127: 11-19.
- Girguis P.R., Orphan V.J., Hallam S.J. and DeLong E.F. (2003) Growth and Methane Oxidation Rates of Anaerobic Methanotrophic Archaea in a Continuous-Flow Bioreactor. *Appl. Environ. Microbiol.* 69: 5472-5482.
- Givnish T.J., Burkhardt E.L., Happel R.E. and Weintraub J.D. (1984) Carnivory in the bromeliad *Brocchinia reducta*, with a cost/benefit model for the general restriction of carnivorous plants to sunny, moist, nutrient-poor habitats. *American Naturalist* 124: 479-497.
- Gladman B.J., Burns J.A., Duncan M., Lee P.C. and Levison H.F. (1996) The exchange of impact ejecta between terrestrial planets. *Science* 271: 1387-1392.
- Gold T. (1992) The deep, hot biosphere. *PNAS* 89: 6045-6049.
- Goldblatt C. and Watson J.A. (2012) The Runaway Greenhouse: implications for future climate change, geoengineering and planetary atmospheres. *Phil. Trans. R. Soc. A* 370: 4197-4216.

- Gough D.O. (1981) Solar interior structure and luminosity variations. *Solar Phys.* 74: 21-34.
- Grant W.D. (2004) Life at low water activity. *Phil. Trans. R. Soc. Lond. B* 359: 1249-1267.
- Greaves J.S., Wyatt M.C., W. S. Holland W.S. and Dent W.R.F. (2004) The debris disc around Ceti: a massive analogue to the Kuiper Belt. *Mon. Not. R. Astron. Soc.* 351: L54-L58.
- Güdel M. (2007) The Sun in Time: Activity and Environment. *Living Rev. Solar Phys.* 4: 3.
- Guedes J.M., Rivera E.J., Davis E., Laughlin G., Quintana E.V. and Fischer D.A. (2008) Formation and Detectability of Terrestrial Planets around α Centauri B. *Ap. J.* 679: 1582-1587.
- Guillot T. and Hueso R. (2006) The composition of Jupiter: sign of a (relatively) late formation in a chemically evolved protosolar disc. *Mon. Not. R. Astron. Soc.* 367: L47-L51.
- Guinan E.F. and Engle S.G. (2009) The Living with a Red Dwarf Program. *AIP Conf. Proc.* 1135: 221-224.
- Haigh J.D. (2007) The Sun and the Earths Climate. *Living Rev. Solar Phys.*, 4: 2.
- Halmer M.M., Schmincke H.-U. and Graf H.-F. (2002) The annual volcanic gas input into the atmosphere, in particular into the stratosphere: a global data set for the past 100 years. *J. Volcanol. Geoth. Res.* 115: 511-528.
- Hansen C.J., Esposito L., Stewart A.I.F., Colwell J., Hendrix A., Pryor W., et al. (2006) Enceladus' water vapor plume. *Science* 311: 1422-1425.
- Hanslmeier, A. (2010) Life and water. In *Water in the Universe*, Springer Science Series Volume 368: Astrophysics and Space Science Library, Springer, Dordrecht, pp 25-35.
- Hansson A. (1997) *Mars and the Development of Life: Second Edition*. John Wiley & Sons, UK.
- Harvey R.B. (1924) Enzymes of thermal algae. *Science* 60: 481482.
- Hayes J.M. (1967) Organic constituents of meteorites a review. *Geochimica et Cosmochimica Acta* 31: 1395-1440.
- Hecht M.H., Kounaves S.P., Quinn R.C., West S.J., Young S.M.M., Ming D.W., Catling D.C. et al. (2009) Detection of perchlorate and the soluble chemistry of martian soil at the Phoenix lander site. *Science* 325: 64-67.
- Hegde S. and Kaltenegger L. (2013) Colors of Extreme Exo-Earth Environments. *Astrobiology* 13: 47-56.
- Held I.M. and Hou A.Y. (1980) Nonlinear axially symmetric circulations in a nearly in-

-
- viscid atmosphere. *Journal of the Atmospheric Sciences* 37: 515-533.
- Heller R. and Armstrong J. (2014) Superhabitable Worlds. *Astrobiology* 14: 50-66.
- Herwartz D., Pack A., Friedrichs B. and Bischoff A. (2014) Identification of the giant impactor Theia in lunar rocks. *Science* 344: 1146-1150.
- Hester J.J., Desch S.J., Healy K.R. and Leshin L.A. (2004) The Cradle of the Solar System. *Science* 304: 1116-1117.
- Hillenbrand L.A. (1997) On the Stellar Population and Star-Forming History of the Orion Nebula Cluster. *Astron. J.* 113: 1733-1768.
- Hoehler T., Gunsalus R.P. and McInerney M. J. (2010) Environmental constraints that limit methanogenesis. In *Handbook of Hydrocarbon and Lipid Microbiology*, Springer Berlin Heidelberg, pp. 635-654.
- Holden J.F. and Daniel R.M. (2004) The Upper Temperature Limit for Life Based on Hyperthermophile Culture Experiments and Field Observations. *Geophysical Monograph Series* 144: 13-24.
- Holmberg J., Nordström B. and Andersen J. (2009) The Geneva-Copenhagen survey of the solar neighbourhood. III. Improved distances, ages, and kinematics. *A&A* 501: 941-947.
- Horikoshi K. (1999) Alkaliphiles: some applications of their products for biotechnology. *Microbiol. Mol. Biol. Rev.* 63: 735-750.
- Horneck G. and Brack A. (1992) Study of the origin, evolution and distribution of life with emphasis on exobiology experiments in earth orbit. *Advances in Space Biology* 2: 229-262.
- Horneck G., Rettberg P., Reitz G., Wehner J., Eschweiler U., Strauch K., Panitz C., Starke V. and Baumstark-Khan C. (2001) Protection of bacterial spores in space, a contribution to the discussion on panspermia. *Origins of Life and Evolution of the Biosphere* 31: 527-547.
- Horneck G., Stöffler D., Ott S., Hornemann U., Cockell C.S., Moeller R., Meyer C., de Vera J-P., Fritz J., Schade S. and Artemieva N.A. (2008) Microbial Rock Inhabitants Survive Hypervelocity Impacts on Mars-Like Host Planets: First Phase of Lithopanspermia Experimentally Tested. *Astrobiology* 8: 17-44.
- House C.H., Beal E.J. and Orphan V.J. (2011) The Apparent Involvement of ANMEs in Mineral Dependent Methane Oxidation, as an Analog for Possible Martian Methanotrophy. *Life* 1: 19-33.
- Houghton J.T. (2002) *The Physics of Atmospheres*, third ed. Cambridge University Press, Cambridge, UK, pp. 320.
- Howard A.W., Marcy G.W., Bryson S.T., Jenkins J.M., Rowe J.F., Batalha N.M., Borucki W.J., Koch D.G., Dunham E.W., Gautier T.N., III, Van Cleve J., Cochran W.D., Latham D.W., Lissauer J.J., Torres G., Brown T.M., Gilliland R.L., Buchhave L.A., Caldwell D.A., Christensen-Dalsgaard J., Ciardi D., Fressin F., Haas M.R., Howell S.B., Kjeldsen

- H., Seager S., Rogers L., Sasselov D.D., Steffen J.H., Basri G.S., Charbonneau D., Christiansen J., Clarke B., Dupree A., Fabrycky D.C., Fischer D.A., Ford E.B., Fortney J.J., Tarter J., Girouard F.R., Holman M.J., Johnson J.A., Klaus T.C., Machalek P., Moorhead A.V., Morehead R.C., Ragozzine D., Tenenbaum P., Twicken J.D., Quinn S.N., Isaacson H., Shporer A., Lucas P.W., Walkowicz L.M., Welsh W.F., Boss A., Devore E., Gould A., Smith J.C., Morris R.L., Prsa A., and Morton T.D. (2011) Planet occurrence within 0.25 AU of solar-type stars from Kepler. arXiv:1103.2541v1.
- Howarth F.G. (1983) Ecology of Cave Arthropods. *Ann. Rev. Entomol.* 28, 365-289.
- Huete A.R., Jackson R.D. and Post D.F. (1985) Spectral response of a plant canopy with different soil backgrounds. *Remote Sens. Environ.* 17: 37-53.
- Huxley J. (1942) *Evolution: The Modern Synthesis*. John Wiley & Sons, pp. 645.
- Hyde W.T., Crowley T.J., Baum S.K. and Peltier W.R. (2000) Neoproterozoic snowball Earth simulations with a coupled climate/ice-sheet model. *Nature* 405: 425-429.
- Irwin L.N. and Schulze-Makuch D. (2001) Assessing the Plausibility of Life on Other Worlds. *Astrobiology* 1: 143-160.
- Irwin L.N. and Schulze-Makuch D. (2011) *Cosmic Biology: How Life Could Evolve on Other Worlds*. Edited by John Mason. Springer Science+Business Media, New York, NY, USA.
- Johanson C.M. and Fu Q. (2009) Hadley cell widening: Model simulations versus observations. *Journal of Climate* 22: 2713-2725.
- Jolivet E., LHaridon S., Corre E., Forterre P. and Prieur D. (2003) *Thermococcus gammatolerans* sp. nov., a hyperthermophilic archaeon from a deep-sea hydrothermal vent that resists ionizing radiation. *Int. J. Syst. Evol. Microbiol.* 53: 847-851.
- Jones B. (2008) Exoplanets search methods, discoveries, and prospects for astrobiology. *Int. J. Astrobiology* 7: 279-292.
- Jones E.G., Lineweaver C.H. and Clarke J.D. (2011) An Extensive Phase Space for the Potential Martian Biosphere. *Astrobiology* 11: 1017-1033.
- Jones H.G. (2013) *Plants and Microclimate. A Quantitative Approach to Environmental Plant Physiology*. 3rd Edition. Cambridge University Press, Cambridge. ISBN 978-0-521-27959-8.
- Jönsson K.I., Rabbow E., Schill R.O., Harms-Ringdahl M. and Rettberg P. (2008) Tardigrades survive exposure to space in low Earth orbit. *Current biology* 18: R729-R731.
- Kallistova A.Y., Kevbrina M.V., Nekrasova V.K., Glagolev M.V., Serebryanaya M.I. and Nozhevnikova A.N. (2005) Methane Oxidation in Landfill Cover Soil. *Microbiology* 74: 608-614.
- Kaltenegger L. and Selsis F. (2007) Biomarkers set in context. In *Extrasolar Planets: Formation, Detection and Dynamics*, edited by R. Dvorak, Wiley, Weinheim, pp 79-98.

-
- Kaltenegger L., Traub W.A., and Jucks K. (2007) Spectral evolution of an Earth-like planet. *Astrophys. J.* 658: 598-616.
- Kaltenegger L. (2010) Characterizing habitable exomoons. *Astrophys. J. Lett.* 712: L125.
- Kaltenegger L., Selsis F., Fridlund M., Lammer H., Beichman C., Danchi W., Eiroa C., Henning T., Herbst T., Léger A., Liseau R., Lunine J., Paresce F., Penny A., Quirrenbach A., Röttgering H., Schneider J., Stam D., Tinetti G. and White G.J. (2010) Deciphering spectral fingerprints of habitable exoplanets. *Astrobiology* 10: 89-102.
- Kaltenegger L., Henning W.G. and Sasselov D.D. (2010b) Detecting Volcanism on Extrasolar Planets. *Astron. J.* 140: 1370-1380.
- Kara A.B., Rochford P.A. and Hurlbur H.E. (2003) Mixed layer depth variability over the global ocean. *Journal of Geophysical Research: Oceans* 108: C3.
- Kashefi K. and Loveley D.R. (2003) Extending the Upper Temperature Limit for Life. *Science* 301: 934.
- Kasting J.F. (1988) Runaway and moist greenhouse atmospheres and the evolution of Earth and Venus. *Icarus* 74: 472-494.
- Kasting J. F. and Brown L. L. (1998) The early atmosphere as a source of biogenic compounds. In: *The Molecular Origins of Life*, Ed. Andri Brack, Cambridge University Press, pp.35-56.
- Kasting J.F. and Catling D. (2003) Evolution of a Habitable Planet. *Annu. Rev. Astron. Astrophys.* 41: 429-463.
- Kasting J.F. and Ono S. (2006) Palaeoclimates: the first two billion years. *Phil. Trans. R. Soc. B* 361: 917-929.
- Kasting J.F. (2008) Chapter 8: The Primitive Earth, Prebiotic Evolution and Astrobiology, edited by J. T-F. Wong and A. Lazcano.
- Kasting J.F. (2011) Atmospheric Composition on the Hadean/Early Archaean Earth: The Importance of CO. GSA Annual Meeting, Minneapolis.
- Kawahara H., Matsuo T., Takami M., Fujii Y., Kotani T., Murakami N., Tamura M. and Guyon O. (2012) Can Ground-based Telescopes Detect the Oxygen 1.27 μm Absorption Feature as a Biomarker in Exoplanets? *Ap. J.* 758: 13.
- Kemp T.S. (2006) The origin of mammalian endothermy: a paradigm for the evolution of complex biological structure. *Zool. J. Linnean Soc.* 147: 473-488.
- Kiang N., Siefert J., Govindjee and Blankenship R.E. (2007a) Spectral signatures of photosynthesis I: review of Earth organisms. *Astrobiology* 7: 222-251.
- Kiang N., Segura A., Tinetti G., Govindjee, Blankenship R.E., Cohen M., Siefert J., Crisp D. and Meadows V.S. (2007b) Spectral signatures of photosynthesis II: coevolution with other stars and the atmosphere on extrasolar worlds. *Astrobiology* 7: 252-274.

- Kieft T.L., McCuddy S.M., Onstott T.C., Davidson M., Lin L-H., Mislowack B., Pratt L., Boice E., Lollar B.S., Lippmann-Pipke J., Pfiffner S.M., Phelps T.J., Gihring T, Moser D. and van Heerden A. (2005) Geochemically Generated, Energy-Rich Substrates and Indigenous Microorganisms in Deep, Ancient Groundwater. *Geomicrobiol. J.* 22: 325-335.
- King A.J., Cragg S.M., Li Y., Dymond J., Guille M.J., Bowles D.J., Bruce N.C., Graham I.A. and McQueen-Mason S.J. (2010) Molecular insight into lignocellulose digestion by a marine isopod in the absence of gut microbes. *PNAS* 107: 5345-5350.
- Kite E.S., Williams J-P., Lucas A. and Aharonson O. (2014) Low palaeopressure of the martian atmosphere estimated from the size distribution of ancient craters. *Nature Geoscience* 7: 335-339.
- Klein H.P. (1979) The Viking mission and the search for life on Mars. *Reviews of Geophysics* 17: 1655-1662.
- Koeberl C. (2006) The record of impact processes on the early Earth: A review of the first 2.5 billion years. *Processes on the Early Earth: Geological Society of America Special Paper* 405: 1-22.
- Kolb V.M. (2007) On the applicability of the Aristotelian principles to the definition of life. *Int. J. Astrobiology* 6: 51-57.
- Kopparapu R.K., Ramirez R., Kasting J.F., Eymet V., Robinson T.D., Mahadevan S., Terrien R.C., Domagal-Goldman S., Meadows V. and Deshpande R. (2013) Habitable zones around main sequence stars: new estimates. *Astrophys. J.* 765: 131.
- Kopparapu R.K. (2013) A revised estimate of the occurrence rate of terrestrial planets in the habitable zones around Kepler M-dwarfs. *Astrophys. J. Lett.* 767: L8.
- Koshland D.E. Jr. (2002) The seven pillars of life. *Science* 295: 2215-2216.
- Kvenvolden K.A. and Rogers B.W. (2005) Gaia's breath - global methane exhalations. *Marine and Petroleum Geology* 22: 579-590.
- Landis G. A. (2003), Colonization of Venus, Conference on Human Space Exploration, Space Technology & Applications International Forum, Albuquerque NM, Feb. 2-6 2003, Accessed via: http://itwas.gg/space/VenusColony_STAIF03.pdf.
- Larson R.B. (2003) The physics of star formation. *Rep. Prog. Phys.* 66: 1651-1697.
- Laskar J., Joutel F. and Robutel P. (1993b) Stabilization of the Earths obliquity by the Moon. *Nature* 361: 615-617.
- Laskar, J., Correia, A.C.M., Gastineau, M., Joutel, F., Levrard, B. and Robutel, P. (2004) Long term evolution and chaotic diffusion of the insolation quantities of Mars. *Icarus* 170: 343-364.
- Laskar J. and Gastineau M. (2009) Existence of collisional trajectories of Mercury, Mars and Venus with the Earth. *Nature* 459: 817-819.

-
- Lay C-Y., Mykytczuk N.C.S., Yergeau É., Lamarche-Gagnon G., Greer C.W. and Lyle G. (2013) Defining the functional potential and active community members of a sediment microbial community in a high Arctic hypersaline subzero spring. *Appl. Environ. Microbiol.* 79: 3637-3648.
- Leake J.R and Cameron D.D. (2010) Physiological ecology of mycoheterotrophy. *New Phytol.* 185: 601-605.
- Léger A., Pirre M., and Marceau F.J. (1993) Search for primitive life on a distant planet: relevance of O₂ and O₃ detection. *Astron. Astrophys.* 277: 309-313.
- Léger A., Mariotti J.M., Mennesson B., Ollivier M., Puget J.L., Rouan D. and Schneider J. (1996) Could we search for primitive life on extrasolar planets in the near future? *Icarus* 123: 249-255.
- Leutscher M., Jeannin P-Y and Haerberli W. (2005) Ice Caves as an indicator of winter climate evolution: a case study from the Jura Mountains. *The Holocene* 15, 982-993.
- Levenson B.P. (2011) Planet temperatures with surface cooling parameterized. *Adv. Space Res.* 47: 2044-2048.
- Liebner S. and Wagner D. (2007) Abundance, distribution and potential activity of methane oxidizing bacteria in permafrost soils from the Lena Delta, Siberia. *Env. Microbiol.* 9:107-117.
- Lin L-H., Slater G.F., Lollar B.S., Lacrampe-Couloume G. and Onstott T.C. (2005) The yield and isotopic composition of radiolytic H₂, a potential energy source for the deep subsurface biosphere. *Geochimica et Cosmochimica Acta* 69: 893-903.
- Lin L-H., Wang P-L., Rumble D., Lippmann-Pipke J., Boice E., Pratt L.M., Lollar B.S., Brodie E.L., Hazen T.C., Andersen G.L., DeSantis T.Z., Moser D.P., Kershaw D. and Onstot T.C. (2006) Long-Term Sustainability of a High-Energy, Low-Diversity Crustal Biome. *Science* 314: 479-482.
- Lineweaver C.H. (2001) An estimate of the age distribution of terrestrial planets in the universe: quantifying metallicity as a selection effect. *Icarus* 151: 307-313.
- Liou K.N. (2002) An Introduction to Atmospheric Radiation. *Volume 84 of International Geophysics*, Academic Press, 583 pages.
- Lissauer J.J., Barnes J.W. and Chambers J.E. (2012) Obliquity variations of a moonless Earth. *Icarus* 217: 77-87.
- Liu D.Y., Ding W.X., Jia Z.J. and Ca Z.C. (2011) Relation between methanogenic archaea and methane production potential in selected natural wetland ecosystems across China. *Biogeosciences* 8: 329-338.
- Longbottom R. and Kolbeinsen L. (2008) Proceedings of the 4th Ulcos seminar. Available on: http://www.ulcos.org/en/docs/seminars/Ref30%20-%20SP12_Longtbottom_FRAME_LKv2.pdf.

- Lorenz R.D. and McKay C.P. (2003) A simple expression for vertical convective fluxes in planetary atmospheres. *Icarus* 165: 407-413.
- Lovelock J.E. and Kaplan I.R. (1975) Thermodynamics and the recognition of alien biospheres. *Proc R Soc Lond B Biol Sci* 189: 167-181.
- Lovelock J.E. and Whitfield M. (1982) Life span of the biosphere. *Nature* 296: 561-563.
- Lu J., Vecchi G.A. and Reichler T. (2007) Expansion of the Hadley cell under global warming. *Geophys. Res. Lett.* 34: L06805.
- Luo W. and Stoddard P.R. (2002) Comparative Hypsometric Analysis of Earth, Venus and Mars: Evidence for Extraterrestrial Plate Tectonics? *33rd Annual Lunar and Planetary Science Conference*, March 11-15, 2002, Houston, Texas, abstract no.1512.
- Lundin R., Lammer H. and Ribas I. (2007) Planetary magnetic fields and solar forcing: implications for atmospheric evolution. *Space Science Reviews* 129: 245-278.
- Lunine J.I. (1999) *Earth: Evolution of a Habitable World*. Cambridge University Press, Cambridge, UK, pp. 319.
- Lutz S., Anesio A.M., Jorge Villar S.E. and Benning L.G. (2014) Variations of algal communities cause darkening of a Greenland glacier. *FEMS microbiology ecology* DOI: 10.1111/1574-6941.12351.
- Lynch R.C., King A.J., Farías M.E., Sowell P., Vitry C. and Schmidt S.K. (2012). The potential for microbial life in the highest elevation (> 6000 m.a.s.l.) mineral soils of the Atacama region. *J. Geophys. Res.* 117: G02028.
- Maberly S.C. (1996) Diel, episodic and seasonal changes in pH and concentrations of inorganic carbon in a productive lake. *Freshw. Biol.* 35: 579-598.
- Madden M.E., Bodnar R.J. and Rimstidt J.D. (2004) Jarosite as an indicator of water-limited chemical weathering on Mars. *Nature* 431: 821-823.
- Mahli Y. (2002) Carbon in the atmosphere and terrestrial biosphere in the 21st century. *Phil. Trans. R. Soc. Lond. A* 360: 2925-2945.
- Maimaiti J., Zhang Y., Yang J., Cen Y-P., Layzell D.B., Peoples M. and Dong Z. (2007) Isolation and characterization of hydrogen-oxidizing bacteria induced following exposure of soil to hydrogen gas and their impact on plant growth. *Env. Microbiol.* 9: 435-444.
- Makarov V.V., Beichman C.A., Catanzarite J.H., Fischer D.A., Lebreton J., Malbet F. and Shao M. (2009) Starspot jitter in photometry, astrometry, and radial velocity measurements. *Astrophys. J. Lett.* 707: L73.
- Malady J.L., Vestling M.M., Baumler D., Boekelheide N., Kaspar C.W. and Banel J.F. (2004) Tetraether-linked membrane monolayers in *Ferroplasma* spp a key to survival in acid. *Extremophiles* 8: 411-419.
- Mamajek E.E. and Hillenbrand L.A. (2008) Improved Age Estimation for Solar-Type Dwarfs Using Activity-Rotation Diagnostics. *Astrophys. J.* 687: 1264.

-
- Mancinelli R.L. (1995) The Regulation of Methane Oxidation in Soil. *Appl. Environ. Microbiol.* 49: 581-605.
- Maravell N.S. (2006) Space Science: New Research. Nova Science Publishers, NY, USA, pp. 363.
- Margot J.L., Campbell D.B., Jurgens R.F. and Slade M.A. (1999) Topography of the Lunar Poles from Radar Interferometry: A Survey of Cold Trap Locations. *Science* 284: 1658-1660.
- Marion G.M., Fritsen C.H., Eicken H. and Payne M.C. (2003) The Search for Life on Europa: Limiting Environmental Factors, Potential Habitats, and Earth Analogues. *Astrobiology* 3: 785-811.
- Mason S.F. (1984) Origins of biomolecular handedness. *Nature* 311: 19-23.
- Martin W. and Russell M.J. (2007) On the origin of biochemistry at an alkaline hydrothermal vent. *Phil. Trans. R. Soc. B* 362: 1887-1925.
- Mayor M., Marmier M., Lovis Ch., Udry S., Ségransan D., Pepe F., Benz W., et al. (2011) The HARPS search for southern extra-solar planets XXXIV. Occurrence, mass distribution and orbital properties of super-Earths and Neptune-mass planets. arXiv:1109.2497.
- McCaughrean M.J. and O'dell, R.C. (1996) Direct Imaging of Circumstellar Disks in the Orion Nebula. *Astron. J.* 111: 1977.
- McGowen III J.F. (2000) Oil and Natural Gas on Mars. In *Instruments, Methods and Missions for Astrobiology III* Ed. Richard B. Hoover. *Proceedings of SPIE* 4137: 63-74.
- McGuffie K. and Henderson-Sellers A. (2005) A Climate Modelling Primer, 3rd Edition. John Wiley & Sons Ltd., West Sussex, England.
- McKay C.P. and Marinova M.M. (2001) The physics, biology, and environmental ethics of making Mars habitable. *Astrobiology* 1: 89-109.
- McKay C.P., Porco C.C., Altheide T., Davis W.L. and Kral T.A. (2008) The Possible Origin and Persistence of Life on Enceladus and Detection of Biomarkers in the Plume. *Astrobiology* 8: 909-919.
- McLean D.M. (1991) A climate change mammalian population collapse mechanism. In *Energy and Environment*, eds. Kainlauri, E., Johansson, A., Kurki-Suonio, I. & Geshwiler, M., p. 93100. ASHRAE, Atlanta, Georgia.
- McMahon S., Parnell J. and Blamey N.J.F. (2013) Sampling methane in basalt on Earth and Mars. *Int. J. Astrobiol.* 12: 113-122.
- McMahon S., O'Malley-James J.T. and Parnell J. (2013) Circumstellar habitable zones for deep terrestrial biospheres. *Planet. Space Sci.* 85: 312318.
- McMillan M. and Rushforth S.R. (1985) The Diatom Flora of a Steam Vent of Kilauea Crater, Island of Hawaii. *Pacific Science* 39: 294-301.

- Meadows A.J. (2007) *The Future of the Universe*. Springer-Verlag London Limited 2007.
- Menesson B. and Mariotti J.M. (1997) Array configurations for a space infrared nulling interferometer dedicated to the search for earthlike extrasolar planets. *Icarus* 128: 202-212.
- de Meijer R.J., Anisichkinc V.F. and van Westrenen W. (2013) Forming the Moon from terrestrial silicate-rich material. *Chemical Geology* 345: 40-49.
- Milankovitch M. (1941) Kanon der Erdbestrahlung, *R. Serbian Acad. Spec. Publ.*, 132 *Sect. Math. Nat. Sci.*, 33 (Canon of insolation and the ice-age problem, English translation by Israel Program for Scientific Translations, Jerusalem, 1969).
- Mileikowsky C., Cucinotta F., Wilson J.W., Gladman B., Horneck G., Lindegren L., Melosh J., Rickman H., Valtonen M. and Zheng J.Q. (2000) Natural transfer of viable microbes in space. Part 1. From Mars to Earth and Earth to Mars. *Icarus* 145: 391-427.
- Miller S.L and Urey H.C. (1959) Organic Compound Synthesis on the Primitive Earth. *Science* 130: 245-251.
- Miller S.L. and Lazcano A. (1995) The origin of life did it occur at high temperatures? *Journal of molecular evolution* 41: 689-692.
- Miller J.D., Case M.J. Straat P.A. and Levin G.V. (2010) Mars microbes may make methane: the Viking view. *SPIE*, doi: 10.1117/2.1201007.003176.
- Miller-Ricci E. and Fortney J.J. (2010) The Nature of the Atmosphere of the Transiting Super-Earth GJ 1214b. *Astrophys. J. Lett.* 716: L74-L79.
- Miller-Ricci E., Seager S. and Sasselov D. (2009) The atmospheric signatures of super-Earths: how to distinguish between hydrogen-rich and hydrogen-poor atmospheres. *Astrophys. J.* 690: 1056-1057.
- Milo R. (2009) What governs the reaction center excitation wavelength of photosystems I and II? *Photosynth. Res.* 101: 59-67.
- Mitchell J.F.B. (1989) The “greenhouse” effect and climate change. *Reviews of Geophysics* 27: 115-139.
- Mitrofanov I., Anfimov D. and Kozyrev A. (2002) Maps of surface hydrogen from the High Energy Neutron Detector, Mars Odyssey. *Science* 297: 78-81.
- Möhler O., Demott P.J., Vali G. and Levin Z. (2007) Microbiology and atmospheric processes: the role of biological particles in cloud physics. *Biosciences Discussions* 4: 2559-2591.
- Mojzsis S.J., Arrhenius G., McKeegan K.D., Harrison T.M., Nutman A.P. and Friend C.R.L. (1996) Evidence for life on earth before 3800 million years ago. *Nature* 384: 55-59.
- Monroe T.R., Melédez J., Ramirez I., Yong D., Bergemann M., Asplund M., Bedell M., Mai M.T., Bean J., Lind K., Alves-Brito A., Casagrande L., Castro M., Do Nascimento J-D., Bazot M and Freitas F.C. (2013) High Precision Abundances of the Old Solar Twin

-
- HIP 102152: Insights in Li depletion from the oldest sun. *Astrophys. J. Lett.* 744: L32.
- Mooney H.A. (1972) The Carbon Balance of Plants. *Annual Review of Ecology and Systematics* 3: 315-346.
- Moorbath S. (2005) Dating earliest life. *Nature* 434: 155.
- Moreira D. and Purificación López-García P. (2009) Ten reasons to exclude viruses from the tree of life. *Nature Reviews Microbiology* 7: 306-311.
- Morozova D., Möhlmann D. and Wagner D. (2007) Survival of Methanogenic Archaea from Siberian Permafrost under Simulated Martian Thermal Conditions. *Orig. Life Evol. Biosph.* 37: 189-200.
- Mojzsis S.J., Harrison T.M. and Pidgeon R.T. (2001) Oxygen-isotope evidence from ancient zircons for liquid water at the Earth's surface 4,300 Myr ago. *Nature* 409: 178-181.
- Mumma M.J., Villanueva G.L., Novak R.E., Hewagama T., Bonev B.P., DiSanti M.A., Avi M. Mandell A.M. and Smith M.D. (2009) Strong Release of Methane on Mars in Northern Summer 2003. *Science* 323: 1041-1045.
- Néron de Surgy O. and Laskar J. (1997) On the long term evolution of the spin of the Earth. *Astron. & Astrophys.* 318: 975-989.
- Nicholas Hewitt C. and Davison B. (1997) Field measurements of dimethyl sulphide and its oxidation products in the atmosphere. *Phil. Trans. R. Soc. Lond. B* 352: 183-189.
- Niederberger T.D., Perreault N.N., Tille S., Lollar B.S. Lacrampe-Couloume G., Andersen D., Greer C.W., Pollard W. and Whyte L.G. (2010) Microbial characterization of a subzero, hypersaline methane seep in the Canadian High Arctic. *ISME* 4: 1326-1339.
- Nisbet E.G., Cann J.R. and Van Dover C.L. (1995) Origin of Photosynthesis. *Nature* 373: 479.
- Nisbet E.G. and Sleep N.H. (2001) The Habitat and Nature of Early Life. *Nature* 409:1083-1091.
- Nuth J.A., Brearley A.J. and Scott E.R.D. (2005) Microcrystals and Amorphous Material in Comets and Primitive Meteorites: Keys to Understanding Processes in the Early Solar System. *Chondrites and the Protoplanetary Disk ASP Conference Series* 341: 675-700.
- Ohata T., Furukawa T. and Osada K. (1994) Glacioclimatological Study of Perennial Ice in the Fuji Ice Cave, Japan. Part 2. Interannual Variation and Relation to Climate. *Arctic Alpine Res.* 26, 238-244.
- Olsson-Francis K., de la Torre R., Cockell C.S. (2010) Isolation of Novel Extreme-Tolerant Cyanobacteria from a Rock-Dwelling Microbial Community by Using Exposure to Low Earth Orbit. *App. Env. Microbiol.* 76: 2115-2121.
- O'Malley-James J.T., Raven J.A., Cockell C.S., Greaves J.S. (2012) Life and Light: Exotic Photosynthesis in Binary and Multiple Star Systems. *Astrobiology* 12: 115-124.

- O'Malley-James J.T., Cockell C.S., Greaves J.S. and Raven J.A. (2014) Swansong Biospheres II: The final signs of life on terrestrial planets near the end of their habitable lifetimes. *Int. J. Astrobiology*, doi:10.1017/S1473550413000426
- O'Malley-James J.T., Greaves J.S., Raven J.A. and Cockell C.S. (2013) Swansong Biospheres: Refuges for life and novel microbial environments on terrestrial planets near the end of their habitable lifetimes. *Int. J. Astrobiology* 12: 99-112.
- O'Malley-James J.T. and Lutz S. (2013) From Life to Exolife: The interdependence of astrobiology and evolutionary biology. In: *Evolutionary Biology: Exobiology and Evolutionary Mechanisms*, ed. Pierre Pontarotti. Springer, pp. 95-108.
- Oparin A. I. (1924) *The Origin of Life*. Moscow: Moscow Worker publisher.
- Orcutt B.N., Sylvan J.B., Knab N.J. and Edwards K.J. (2011) Microbial Ecology of the Dark Ocean above, at and below the Seafloor. *Microbiol. Mol. Biol. Rev.* 75: 361-422.
- Orphan V. J., Hinrichs K.-U., Ussler III W., Paull C.K., Taylor L.T., Sylva S.P., Hayes J.M. and Delong E.F. (2001). Comparative Analysis of Methane-Oxidizing Archaea and Sulfate-Reducing Bacteria in Anoxic Marine Sediments. *Appl. Environ. Microbiol.* 67: 1922-1934.
- Owen, T. (1980) The search for early forms of life in other planetary systems: future possibilities afforded by spectroscopic techniques. In *Strategies for the Search for Life in the Universe*, edited by M.D. Papagiannis, Reidel, Dordrecht, the Netherlands, pp 177-188.
- Ozawa H. and Ohmura A. (1997) Thermodynamics of a global-mean state of the atmosphere: a state of maximum entropy increase. *J. Climate* 10: 441-445.
- Oze C., Jones L.C., Goldsmith J.I. and Rosenbauer R.J. (2012) Differentiating biotic from abiotic methane genesis in hydrothermally active planetary surfaces. *PNAS* 109: 9750-9754.
- Pace N.R. (2001) The universal nature of biochemistry *PNAS* 98: 805-808.
- Paillard A.A. (2010) Climate and the orbital parameters of the Earth. *C. R. Geosc.* 342: 273-285.
- Pallé E., Osorio M.R.Z., Barrena R., Montañés-Rodríguez P. and Martín E.L. (2009) Earth's transmission spectrum from lunar eclipse observations. *Nature* 459: 814-816.
- Pallé, E. (2010) Earthshine observations of an inhabited planet. *EAS Publication Series* 41: 505-516.
- Palmer P.I., Jacob D.J., Fiore A.M. and Martin R.V. (2003) Mapping isoprene emissions over North America using formaldehyde column observations from space. *J. Geophys. Res.* 108: 4180.
- Papaloizou J.C.B. and Terquem C. (2006) Planet formation and migration. *Rep. Prog. Phys.* 69: 119-180.
- Papanastassiou D.A. and Wasserburg G. (1969) Initial strontium isotopic abundances and

-
- the resolution of small time differences in the formation of planetary objects. *Earth Planet. Sci. Lett.* 5: 361-376.
- Pardo A. and Keller G. (2008) Biotic effects of environmental catastrophes at the end of the Cretaceous and early Tertiary: *Guembelitria* and *Heterohelix* blooms. *Cretaceous Research* 29: 1058-1073.
- Parker E.T., Cleaves H.J., Dworkin J.P., Glavin D.P., Callahan M., Aubrey A., Lazcano A. and Bada J.L. (2011) Primordial synthesis of amines and amino acids in a 1958 Miller H₂S-rich spark discharge experiment. *PNAS* 108: 5526-5531.
- Parnell J., Boyce A.J. and Blamey N.J.F. (2010) Follow the methane: the search for a deep biosphere, and the case for sampling serpentinites, on Mars. *Int. J. Astrobiol.* 9: 193-200.
- Pavlov A.K., Shelegedin V.N., Vdovina M.A. and Pavlov A.A. (2010) Growth of microorganisms in Martian-like shallow subsurface conditions: laboratory modelling. *Int. J. Astrobiology* 9: 51-58.
- Pedersen K. (2000) Exploration of deep intraterrestrial microbial life: current perspectives. *FEMS Microbiol. Lett.* 185: 9-16.
- Penny D. and Poole A. (1999) The nature of the last universal common ancestor. *Current opinion in genetics & development* 9: 672-677.
- Pierazzo E. and Chyba C.F. (1999) Amino acid survival in large cometary impacts. *Meteoritics and Planetary Science* 34: 909-918.
- Pigliucci M. (2009) An Extended Synthesis for Evolutionary Biology. *Ann. N.Y. Acad. Sci.* 1168: 218-228.
- Pilcher C.B. (2003) Biosignatures of Early Earths. *Astrobiology* 3: 471-486.
- Pinto J.P., Randall Gladstone G. and Yung Y.L. (1980) Photochemical production of formaldehyde in Earth's primitive atmosphere. *Science* 210: 183-185.
- Piso A-M. A. and Youdin A.N. (2014) On the Minimum Core Mass for Giant Planet Formation at Wide Separations. *Astrophys. J.* 786: 21.
- Porembski S., Theisen I. and Barthlott W. (2006) Biomass allocation patterns in terrestrial, epiphytic and aquatic species of *Utricularia* (Lentibulariaceae). *Flora Morphology, Distribution, Functional Ecology of Plants* 201: 477-482.
- Porto de Mello G., Fernandez del Peloso E. Luan Ghezzi L. (2006) Astrobiologically Interesting Stars Within 10 Parsecs of the Sun. *Astrobiology* 6: 308-331.
- Prinn R.G., and B. Fegley B.R.U.C.E. (1987) The atmospheres of Venus, earth, and Mars-A critical comparison. *Ann. Rev. Earth Planet. Sci.* 15: 171-212.
- Rapp D. (2008) Assessing Climate Change: Temperatures, Solar Radiation and Heat Balance. Springer-Praxis, Chichester, UK, pp.420.

- Raven J.A. and Cockell C.S. (2006) Influence on photosynthesis of starlight, moonlight, planetlight and light pollution (reflections on photosynthetically active radiation in the Universe). *Astrobiology* 6: 668-675.
- Raven J.A. (2007) Photosynthesis in watercolours. *Nature* 448: 418.
- Raven J.A. (2009a) Functional evolution of photochemical energy transformations in oxygen-producing organisms. *Funct. Plant Biol.* 36: 505-515.
- Raven J.A. (2009b) Contributions of anoxygenic and oxygenic phototrophy and chemolithotrophy to carbon and oxygen fluxes in marine environments. *Aquat Microb Ecol* 56:177192.
- Raven J.A., Giordano M., Beardall J. and Maberly S.C. (2012) Algal evolution in relation to atmospheric CO₂: carboxylases, carbon-concentrating mechanisms and carbon oxidation cycles. *Phil. Trans. R. Soc. B* 367: 493-507.
- Raymond S.N., Quinn T. and Lunine J.I. (2007) High-Resolution Simulations of The Final Assembly of Earth-Like Planets. 2. Water Delivery And Planetary Habitability. *Astrobiology* 8: 66-84.
- van Regenmortel M. H. V. (2000) 7th Report of the International Committee on Taxonomy of Viruses. Eds. van Regenmortel, M. H. V. et al., *Academic Press, San Diego, 2000*, pp. 3-16.
- Reith F. (2012) Life in the deep subsurface. *Geology* 39: 287-288.
- Rettberg P., Rabbow E., Panitz C. and Horneck G. (2004) Biological space experiments for the simulation of Martian conditions: UV radiation and Martian soil analogues. *Adv. Space Res.* 33: 1294-1301.
- Ribas I., Guinan E.F., Gúdel M. and Audard M. (2005) Evolution of Solar Activity Over Time and Effects on Planetary Atmospheres. I. High-Energy Irradiances (1-1700 A). *Astrophys. J.* 622: 680-694.
- Rice B. (2002) Carnivorous plants: classic perspectives and new research. *Biologist* 49: 245-249.
- Righter K. and OBrien D.P. (2011) Terrestrial planet formation. *PNAS* 108: 9165-19170.
- del Rio R.A. (1999) The influence of global warming in Earth rotation speed. *Annales Geophysicae* 17: 806-811.
- Robertson E.C. (1988) Thermal properties of rocks. *USGS Open-File Report R290*: 88-441.
- Rosenfeld D., Rudich Y. and Lahav R. (2001) Desert dust suppressing precipitation: A possible desertification feedback loop. *PNAS* 98: 5975-5980.
- Rosing M.T. (1999) C-13-depleted carbon microparticles in >3700-Ma seaor sedimentary rocks from west Greenland. *Science* 283: 674-676.
- Roth L., Saur J., Retherford K.D., Strobel D.F., Feldman P.D., McGrath M.A. and Nimmo

-
- F. (2014) Transient Water Vapor at Europas South Pole. *Science* 343: 171-174.
- Rothschild L.J. and Mancinelli R.L. (2001) Life in extreme environments. *Nature* 409: 1092-1101.
- Rowe J.F., Bryson S.T., Marcy G.W., Lissauer J.J., Jontof-Hutter D., Mullally F., Gilliland R.L., et al. (2014) Validation of Kepler's Multiple Planet Candidates. III. Light Curve Analysis and Announcement of Hundreds of New Multi-planet Systems. *Astrophys. J.* 784: 45.
- Running S.W., Peterson D.L., Spanner M.A. and Teuber K.B. (1986) Remote Sensing of Coniferous Forest Leaf Area. *Ecology* 67: 273-276.
- Russel M.J., Nitschke W. and Branscomb E. (2013) The inevitable journey to being. *Phil. Trans. R. Soc. B* 368: 20120254.
- Sagan C. and Morowitz H. (1967) Life in the Clouds of Venus. *Nature* 215: 1259-1260.
- Sagan C. and Mullen G. (1972) Earth and Mars: Evolution of Atmospheres and Surface Temperatures. *Science* 177: 52-56.
- Sagan C. and Saltpeter E.E. (1976) Particles, environments, and possible ecologies in the Jovian atmosphere. *Astrophys. J.* 32: 737-755.
- Sage R.F. and Zhu X-G. (2011) Exploiting the engine of C₄ photosynthesis. *J. Exp. Bot.* 62: 2989-3000.
- Santl-Temkiv T., Finster K., Dittmar T., Hansen B.M., Thyrhaug R., Nielsen N.W. and Karlson U.G. (2013) Hailstones: a window into the microbial and chemical inventory of a storm cloud. *PloS one* 8: e53550.
- Santosh M. (2010) A synopsis of recent conceptual models on supercontinent tectonics in relation to mantle dynamics, life evolution and surface environment. *J.Geodyn.* 50: 116-133.
- Sawyer C.N. and McCarty P.L. (1967) Chemistry for Sanitary Engineers. McGraw-Hill Book Company Inc., pp.446-447.
- Scalo J., Kaltenegger L., Segura A., Fridlund M., Ribas I., Kulikov Y., Grenfell J., Rauer H., Odert P., Leitzinger M., Selsis F., Khodachenko M., Eiroa C., Kasting K., and Lammer H. (2007) M stars as targets for terrestrial exoplanet searches and biosignature detection. *Astrobiology* 7: 85-166.
- Schidlowski M. (1988). A 3800-million-year isotopic record of life from carbon in sedimentary rocks. *Nature* 333: 313-318.
- Schirmack J., Böhm M., Brauer C., Löhmannsröben H.G., de Vera J.P., Möhlmann D. and Wagner D. (2013) Laser spectroscopic real time measurements of methanogenic activity under simulated Martian subsurface analog conditions. *Planetary and Space Science*, <http://dx.doi.org/10.1016/j.pss.2013.08.019i>
- Schmidt S., Raven J.A and Paungfoo-Lonhienne C. (2013) The mixotrophic nature of

photosynthetic plants. *Functional Plant Biology* 40: 425-438.

Schneider J. (2014) The Extrasolar Planets Encyclopaedia. Available online at <http://exoplanet.eu>.

Schokraie E., Warnken U., Hotz-Wagenblatt A., Grohme M.A, Hengherr S., Förster F., Schill R.O., Frohme M., Dandekar T., Schnölzer M. (2012) Comparative proteome analysis of *Milnesium tardigradum* in early embryonic state versus adults in active and anhydrobiotic state. *PLoS ONE* 7: e45682.

Schrenk M.O., Edwards K.J., Goodman R.M., Hamers R.J. and Banfield J.F. (1998) *Science* 279: 1519-1522.

Schulze-Makuch D. and Irwin L.N. (2002) Reassessing the Possibility of Life on Venus: Proposal for an Astrobiology Mission. *Astrobiology* 2: 197-202.

Schulze-Makuch D. and Irwin L.N. (2008) Life in the universe: expectations and constraints (Vol. 3). Springer, Chicago USA.

Schulze-Makuch D., Grinspoon D.H., Abbas O., Irwin L.N. and Bullock M.A. (2004) A Sulfur-Based Survival Strategy for Putative Phototrophic Life in the Venusian Atmosphere. *Astrobiology* 4: 1-8.

Schulze-Makuch D., Grinspoon D.H. (2005) Biologically Enhanced Energy and Carbon Cycling on Titan. *Astrobiology* 5: 560-567.

Seager S., Turner E.L., Schafer J. and Ford E.B. (2005) Vegetation's red edge: a possible spectroscopic biosignature of extraterrestrial plants. *Astrobiology* 5: 372-390.

Seager S. (2010) Exoplanet Atmospheres: Physical Processes. Ed. Spergel D.N., Princeton University Press.

Seager S., Schrenk M. and Bains W. (2012) An Astrophysical View of Earth-based Metabolic Biosignature Gases. *Astrobiology* 12: 61-82.

Seckbach J. and Oren A. (2000) Extremophilic microorganisms as candidates for extraterrestrial life. In *International Symposium on Optical Science and Technology* pp. 89-95.

Sekercioglu C.H., Schneider S.H., Fay J.P. and Loarie S.R. (2007) Climate change, elevational range shifts, and bird extinction. *Conserv. Biol.* 22: 140-150.

Selsis F. (2004) The Atmosphere of Terrestrial Exoplanets: Detection and Characterization. *Extrasolar Planets: Today and Tomorrow, ASP Conference Series* 321: 170-182.

Sephton M.A. (2002) Organic compounds in carbonaceous meteorites. *Nat. Prod. Rep.* 19: 292311.

Shain D.H., Mason T.A., Farrell A.H. and Michalewicz L.A. (2001) Distribution and behavior of ice worms (*Mesenchytraeus solifugus*) in south-central Alaska. *Can. J. Zool.* 79: 1813-1821.

Shapiro R. (1987) *Origins: A Skeptic's Guide to the Creation of Life on Earth*. Bantam Books, pp. 332.

-
- Shapiro R. and Schulze-Makuch D. (2009) The Search for Alien Life in Our Solar System: Strategies and Priorities. *Astrobiology* 9: 335-343.
- Sharma A., Scott J.H., Cody G.D., Fogel M.L., Hazen R.M., Hemley R.J. and Huntress W.T. (2002) Microbial activity at gigapascal pressures. *Science* 295: 1514-1516.
- Shaviv N.J. (2003) Toward a solution to the early faint Sun paradox: A lower cosmic ray flux from a stronger solar wind. *Journal of Geophysical Research: Space Physics* (19782012) 108: A12.
- Shaw A.H. (2006) Astrochemistry: from Astronomy to Astrobiology. John Wiley & Sons, UK.
- Shen Y., Buick R. and Canfield D.E. (2001) Isotopic evidence for microbial sulphate reduction in the early Archaean era. *Nature* 410: 77-81.
- Shirley J. H., Fairbridge R. W. (1997), Encyclopedia of planetary sciences, Springer ISBN:978-0-412-06951-2.
- Showman A.P., Cho J.Y-K. and Menou K. (2010) Atmospheric Circulation of Extrasolar Planets. In *Exoplanets* (S. Seager, Ed.), University of Arizona Press, pp. 471-516.
- Showstack R. (2012) Evidence suggests water once flowed vigorously on Mars. *Eos, Transactions American Geophysical Union* 93: 402-403.
- Shporer A., O'Rourke J.G., Knutson H.A., Szabó G.M., Zhao M., Burrows A. et al. (2014) Atmospheric Characterization of the Hot Jupiter Kepler-13Ab. *Astrophys. J.* 788: 92.
- Shuster D.L. and Weiss B.P. (2005) Martian Surface Paleotemperatures from Thermochronology of Meteorites. *Science* 309: 594-600.
- Siebert L., Simkin T. and Kimberly P. (2010) Volcanoes of the World, third edition. University of California Press, Berkley and Los Angeles, CA.
- Silburt A., Gaidos E. and Wu Y. (2014) A Statistical Reconstruction of the Planet Population Around Kepler Solar-Type Stars. *arXiv preprint* arXiv:1406.6048.
- Sleep N.H. and Zahnle K. (1998) Refugia from asteroid impacts on early Mars and the early Earth. *J. Geophys. Res.* 103: 28529-28544.
- Smith L.A., Jim Hendry M., Wassenaar L.I. and Lawrence J. (2012) Rates of microbial elemental sulfur oxidation and ^{18}O and ^{34}S isotopic fractionation under varied nutrient and temperature regimes. *Appl. Geochem.* 27: 186-196.
- Snellen I.A.G., de Kok R.J., le Poole R., Brogi M. and Birkby J. (2013) Finding extraterrestrial life using ground-based high-dispersion spectroscopy. *Astrophys. J.* 764: 182.
- Soderblom D.R. (2010) The Ages of Stars. *Annu. Rev. Astron. Astrophys.* 48: 581-629.
- Sørensen J. (1982) Reduction of Ferric Iron in Anaerobic, Marine Sediment and Interaction with Reduction of Nitrate and Sulfate. *Appl. Environ. Microbiol.* 43: 319-323.
- Spiegel D.S., Menou K. and Scharf C.A. (2008) Habitable Climates. *Astrophys. J.* 681:

1609-1623.

Spiegel D.S., Raymond S.N., Dressing C.D., Scharf C.A. and Mitchell J.L. (2010) Generalized Milankovitch Cycles and Long-Term Climatic Habitability. *Astrophys. J.* 721: 1308-1318.

Squyres S.W., Kasting J.F. (1994) Early Mars: How Warm and How Wet? *Science* 265: 744-749.

Stan-Lotter H. (2008) Extremophiles, the Physicochemical Limits of Life (Growth and Survival). In *Complete Course in Astrobiology* ed. Gerda Horneck, Petra Rettberg. John Wiley & Sons Ltd.

Steele A., Goddard D.T., Stapleton D., Smith J., Tapper R., Grady M., McKay D.S., Gibson E.K., Thomas-Keprta K.L. and Beech I.B. (1997) Atomic Force Microscopy imaging of ALH84001 fragments. In *28th Lunar and Planetary Science Conference*, Houston, March, 1997.

Stephenson R.F. (1997) Historical Eclipses and Earth's Rotation. Cambridge University Press. Cambridge, UK.

Stetter K.O. (1994) The lesson of archaeobacteria. In: Bengtson S. (ed) Early life on earth: Nobel symposium No. 84. Columbia University Press, New York, pp. 114-122.

Stevens T.O. (1997) Subsurface lithoautotrophic microbial ecosystems (SLMEs) in igneous rocks: prospects for detection. *Proc. SPIE 3111, Instruments, Methods, and Missions for the Investigation of Extraterrestrial Microorganisms*, 358-365.

Stofan E.R., Elachi C., Lunine J.I., Lorenz R.D., Stiles B., Mitchell K.L., et al. (2007) The lakes of Titan. *Nature* 445: 61-64.

Stöffler D., Horneck G., Ott S., Hornemann U., Cockell C.S., Moeller R., Meyer C., de Vera J-P., Fritz J. and Artemieva N.A. (2007) Experimental evidence for the potential impact ejection of viable microorganisms from Mars and Mars-like planets. *Icarus* 186: 585-588.

Straub K.L., Benz M., Schink B. and Widdel F. (1996) Anaerobic, nitrate-dependent microbial oxidation of ferrous iron. *Appl. Environ. Microbiol.* 62: 1458-1460.

Strom R.G., Schaber G.G. and Dawson, D.D. (1994) The global resurfacing of Venus. *J. Geophys. Res.* 99: 10899-10926.

Strother P.K., Battison L., Brasier M.D. and Wellman C.H. (2011) Earth's earliest non-marine eukaryotes. *Nature* 473: 505-509.

Strous M., Pelletier E., Mangenot S., Rattei T., Lehner A., Taylor M.W., Horn M., Daims H., Bartol-Mavel D., Wincker P., Barbe V., Fonknechten N., Vallenet D., Segurens B., Schenowitz-Truong C., Médigue C., Collingro A., Snel B., Dutilh B.E., Op den Camp H.J., van der Drift C., Cirpus I., van de Pas-Schoonen K.T., Harhangi H.R., van Niftrik L., Schmid M., Keltjens J., van de Vossenberg J., Kartal B., Meier H., Frishman D., Huynen M.A., Mewes H.W., Weissenbach J., Jetten M.S., Wagner M. and Le Paslier

-
- D. (2006). Deciphering the evolution and metabolism of an anammox bacterium from a community genome. *Nature* 440: 790-794.
- Stuart J.S. and Binzel R.P. (2004) Bias-corrected population, size distribution, and impact hazard for the near-Earth objects. *Icarus* 170: 295-311.
- Summons R.E., Jahnke L.L., Hope J.M. and Logan G.A. (1999) 2-Methylhopanoids as biomarkers for cyanobacterial oxygenic photosynthesis. *Nature* 400: 554-557.
- Suzuki I., Takeuchi T.L., Yuthasastrakosol T.D. and Oh J.K. (1990) Ferrous Iron and Sulfur Oxidation and Ferric Iron Reduction Activities of *Thiobacillus ferrooxidans* Are Affected by Growth on Ferrous Iron, Sulfur, or a Sulfide Ore. *Appl. Environ. Microbiol.* 56: 1620-1626.
- Suzuki I., Chan C.W. and Takeuchi T.L. (1992) Oxidation of Elemental Sulfur to Sulfite by *Thiobacillus thiooxidans* Cells. *Appl. Environ. Microbiol.* 58: 3767-3769.
- Svedhem H., Titov D.V., Taylor F.W. and Witasse O. (2007) Venus as a more Earth-like planet. *Nature* 450: 629-632.
- Tajika E. (2008) Theoretical Constraints on Early Earths Environment. *Viva Origino* 36: 55-60.
- Takai T., Nakamura K., Toki T., Tsunogai U., Miyazaki M., Miyazaki J., Hirayama H., Nakagawa S., Nunoura T. and Horikoshi K. (2008) Cell proliferation at 122°C and isotopically heavy CH₄ production by a hyperthermophilic methanogen under high-pressure cultivation. *PNAS* 105: 10949-10951.
- Takeda G., Ford E.B., Sills A., Rasio F.A., Fischer D.A. and Valenti J.A. (2007) Structure and Evolution of Nearby Stars with Planets. II. Physical Properties of 1000 Cool Stars from the SPOCS Catalog. *ApJS* 168: 297-318.
- Tartakovsky B., Manuel M.-F. and Guiot S.R. (2005) Degradation of trichloroethylene in a coupled anaerobicaerobic bioreactor: Modeling and experiment. *Biochem. Eng. J.* 26: 72-81.
- Tera F., Papanastassiou D.A., and Wasserburg G.J. (1974) Isotopic evidence for a terminal lunar cataclysm. *Earth Planet. Sci. Lett.* 14: 281-304.
- Teske A.P. (2005) The deep subsurface biosphere is alive and well. *TRENDS in microbiol.* 13: 402-404.
- Thomas D.N. and Dieckmann G.S. (2009) Sea Ice - 2nd Edition. John Wiley & Sons, Chichester, UK.
- Thomas-Keprta K.L., Clemett S.J., McKay D.S., Gibson E.K. and Wentworth S.J. (2009) Origins of magnetite nanocrystals in Martian meteorite ALH8400. *Geochimica et Cosmochimica Acta* 73: 6631-6677.
- Thompson P.J., Hicks R.D., Chyba C.F., McKay C.P. (2006) Comets and the Origin and Evolution of Life. *Advances in Astrobiology and Biogeophysics*. Springer, pp.363.

- Tice M.M. and Lowe D.R. (2004) Photosynthetic microbial mats in the 3,416-Myr-old ocean. *Nature* 431: 549-552.
- Tie X., Zhang R., Brasseur G. and Lie W. (2002) Global NO_x production by lightning. *J. Atmos. Chem.* 43: 61-74.
- Tinetti G., Meadows V.S., Crisp D., Kiang N.Y., Kahn B.H., Fishbein E., Velusamy T., and Turnbull M. (2006) Detectability of planetary characteristics in disk-averaged spectra II: synthetic spectra and light-curves of Earth. *Astrobiology* 6: 881-900.
- Tinetti G., Deroo P., Swain M.R., Griffith C.A., Vasisht G., Brown L.R., et al. (2010) Probing the terminator region atmosphere of the hot-Jupiter XO-1b with transmission spectroscopy. *Astrophys. J. Lett.* 712: L139.
- Tinetti G. and EChO Team (2012) EChO - Exoplanet Characterisation Observatory. *Exp. Astron.* 34: 311-353.
- Tolli J.D., Sievert S.M. and Taylor C.D. (2006) Unexpected Diversity of Bacteria Capable of Carbon Monoxide Oxidation in a Coastal Marine Environment, and Contribution of the Roseobacter-Associated Clade to Total CO Oxidation. *Appl. Environ. Microbiol.* 72: 1966-1973.
- Tomasella L., Marzari F. and Vanzani V. (1996) Evolution of the Earth obliquity after the tidal expansion of the Moon orbit. *Planet. Space Sci.* 44: 427-430.
- de la Torre R., Sancho L.G., Horneck G., de los Ríos A., Wierzchos J., Olsson-Francis K., Cockell C.S., Rettberg P., Berger T., de Vera J.P., Ott S., Frías J.M., Melendi P.G., Lucas M.M., Reina M., Pintado A. and Demets R. (2010) Survival of lichens and bacteria exposed to outer space conditions Results of the Lithopanspermia experiments. *Icarus* 208: 735-748.
- Trail D., Bruce Watson E. and Tailby N.D. (2011) The oxidation state of Hadean magmas and implications for early Earths atmosphere. *Nature* 480: 79-82.
- Trainer M.G., Pavlov A.A., DeWitt H.L., Jimenez J.L., McKay C.P., Toon O.B. and Tolbert M.A. (2006) Organic haze on Titan and the early Earth. *PNAS* 103: 18035-18042.
- Trenberth K.E. and Stepaniak D.P. (2004) The flow of energy through the Earth's climate system. *Quarterly Journal of the Royal Meteorological Society* 130: 2677-2701.
- Trenberth K.E., Fasullo J.T. and Kiehl J. (2009) Earth's Global Energy Budget. *Bull. Amer. Meteorol. Soc.* 90: 311-323.
- Tung H.C., Bramall N.E. and Price P.B. (2005) Microbial origin of excess methane in glacial ice and implications for life on Mars. *PNAS* 102: 18292-18296.
- Tuttle M.D. and Stevenson D.E. (1977) Variation in the Cave Environment and its Biological Implications. National Cave Management Symposium Proceedings, 1977, Adobe Press, Albuquerque, NM, pp.108-121.

-
- Tyrrell T. (2013) *On Gaia. A Critical Investigation of the Relationship between Life and Earth.* pp. + 311. Princeton University Press, Princeton and Oxford.
- Ulloa O., Canfield D.E., DeLong E.F., Letelier R.M. and Stewart F.J. (2012) Microbial oceanography of anoxic oxygen minimum zones. *PNAS* 109: 15996-16003.
- Valencia D., Sasselov D.D. and O'Connell R.J. (2007) Detailed Models of Super-Earths: How Well Can We Infer Bulk Properties? *Astrophys. J.* 665: 1413-1420.
- Vásquez M., Pallé E. and Montañés Rodríguez P. (2010) *The Earth as a Distant Planet,* Springer Science+Business Media, New York, NY, 10013.
- De Vera J-P. (2012) Lichens as survivors in space and on Mars. *Fungal Ecology* 5: 472-479.
- Von Bloh W., Cuntz M., Schröder K.-P., Bounama C. and Franck S. (2009) Habitability of Super-Earth Planets Around Other Suns: Models Including Red Giant Branch Evolution. *Astrobiology* 9: 593-602.
- Wakefield A.E., Gotelli N.J., Wittman S.E. and Ellison A.M. (2005) Prey Addition Alters Nutrient Stoichiometry of the Carnivorous Plant *Sarracenia purpurea*. *Ecology* 86: 1737-1743.
- Walker J.C.G. (1991) Feedback Processes in the Biogeochemical Cycles of Carbon. In *Scientists on Gaia*, edited by S.H. Schneider and P.J. Boston, The MIT Press, Cambridge, Massachusetts, pp.183-190.
- Wang A., Freeman J.J., Bell III J.F. and Jolliff J.L. (2010), Potential Habitable Zone Within the Subsurface of Equatorial Region on Mars", *Astrobiology Science Conference 2010*, Accessed via: <http://www.lpi.usra.edu/meetings/abscicon2010/pdf/5400.pdf>.
- Ward P.D. and Brownlee D. (2002) *The Life and Death of Planet Earth.* Times Books, New York.
- Wardell L.J., Kyle P.R. and Chaffin C. (2004) Carbon dioxide and carbon monoxide emission rates from an alkaline intra-plate volcano: Mt. Erebus, Antarctica. *J. Volcanol. Geoth. Res.* 131: 109-121.
- Warren S.G. and Schneider S.T. (1979) Seasonal simulation as a test for uncertainties in the parameterizations of a Budyko-Sellers zonal climate model. *J. Atmos. Sci.* 36: 1377-1391.
- Webster C.R., Mahaffy P.R., Atreya S.K., Flesch G.J., Christensen L.E. et al. (2013) Measurements of Mars Methane at Gale Crater by the SAM Tunable Laser Spectrometer on the Curiosity Rover. *Lunar and Planetary Science XLIV*, abstract 1366.
- Wells L.E., Armstrong J.C. and Gonzalez G. (2003) Reseeding of early Earth by impacts of returning ejecta during the late heavy bombardment. *Icarus* 162: 38-46.
- Wertheimer J.G. and Laughlin G. (2006) Are Proxima and Alpha Centauri Gravitationally Bound? *Astron. J.* 132: 1995-1997.
- Westall F., Brack A., Hofmann B., Horneck G., Kurat G., Maxwell J., et al. (2000) An

- ESA study for the search for life on Mars. *Planetary and Space Science* 48: 181-202.
- Wiechert U., Halliday A.N., Lee D-C., Snyder G.A., Taylor L.A. and Rumble D. (2001) Oxygen isotopes and the Moon-forming giant impact. *Science* 294: 345-348.
- Wilde S.A., Valley J.W., Peck W.H. and Graham C.M. (2001) Evidence from detrital zircons for the existence of continental crust and oceans on the Earth 4.4 Gyr ago. *Nature* 409: 175-178.
- Williams D. and Kasting, J.F. (1997) Habitable Planets with High Obliquities. *Icarus* 129: 254-267.
- Williams D.R. (1999), Venus Fact Sheet, NASA Goddard Space Flight Center.
- Williams D.M. and Gaidos E. (2008) Detecting the glint of starlight on the oceans of distant planets. *Icarus* 195: 927-937.
- Williams E., Mushtak V., Rosenfeld D., Goodman S. and Boccippio D. (2005) Thermodynamic conditions favorable to superlative thunderstorm updraft, mixed phase microphysics and lightning flash rate. *Atmos. Res.* 76: 288-306.
- Williams J.P. and Cieza L.A. (2011) Protoplanetary Disks and Their Evolution. *Annu. Rev. Astro. Astrophys.* 49: 67-117.
- Williams K.E., McKay C.P., Toon O.B. and Head J.W. (2010) Do ice caves exist on Mars? *Icarus* 209: 358-368.
- Williams R.M.E., Grotzinger J.P., Dietrich W.E., Gupta S., Sumner D.Y., Wiens R.C., et al. (2013) Martian fluvial conglomerates at Gale crater. *Science* 340: 1068-1072.
- Wittenmyer R.A., Tinney C.G, Butler R.P., O'Toole S.J., Jones H.R.A., Carter B.D., Bailey J., and Horner J. (2011) The frequency of low-mass exoplanets. III. Toward eta-Earth at short periods. arXiv:1103.4186v1.
- Woese C. (1998) The universal ancestor. *Proc. Natl. Acad. Sci. USA* 95: 6854-6859.
- Wolf E.T. and Toon O.B. (2014) Controls on the Archean Climate System Investigated with a Global Climate Model. *Astrobiology* 14: 241-253.
- Wolstencroft, R.D. and Raven, J.A. (2002) Photosynthesis: likelihood of occurrence and possibility of detection on Earth-like planets. *Icarus* 157: 535-548.
- Womack A.M., Bohannon B.J.M. and Green J.L. (2010) Biodiversity and biogeography of the atmosphere. *Phil. Trans. R. Soc. B* 365, 3645-3653.
- Wood C.A. (1984) Calderas: A Planetary Perspective. *J. Geophys. Res.* 89: 8391-8406.
- Wordsworth R. and Pierrehumbert R. (2014) Abiotic oxygen-dominated atmospheres on terrestrial habitable zone planets. *ArXiv Preprint*: arXiv:1403.2713.
- Worth R.J., Sigurdsson S. and House C.H. (2013) Seeding Life on the Moons of the Outer Planets via Lithopanspermia. *Astrobiology* 13: 1155-1165.

-
- Wright J.T. and Gaudi B.S. (2013) Exoplanet Detection Methods. In: *Planets, Stars and Stellar Systems. Volume 3: Solar and Stellar Planetary Systems*, ed. T.D. Oswalt, L. French, P. Kalas, Springer Science+Business Media Dordrecht.
- Yayanos A.A. (1995) Microbiology to 10,500 meters in the deep sea. *Annu. Rev. Microbiol.* 49: 777-805.
- Yoder J.A., Chambers M.J., Tank J.L. and Keeney G.D. (2009) High temperature effects on water loss and survival examining the hardiness of female adults of the spider beetles, *Mezium affine* and *Gibbium aequinoctiale*. *Journal of Insect Science* 9: Article 68.
- Yoshida M. and Santosh M. (2011) Future supercontinent assembled in the northern hemisphere. *Terra Nova* 23: 333-338.
- Zahnle K., Schaefer L. and Fegley B. (2010) Earth's Earliest Atmospheres. *Cold Spring Harbor perspectives in biology* 2: a004895.
- Zahnle K., Freedman R.S. and Catling D.C. (2011) Is there methane on Mars? *Icarus* 212: 493-503.
- Zenoff V.F., Sineriz F. and Farías M.E. (2006) Diverse responses to UV-B radiation and repair mechanisms of bacteria isolated from high-altitude aquatic environments. *Applied and environmental microbiology* 72: 7857-7863.
- Zhou Z., Takaya N., Nakamura A., Yamaguchi M., Takeo K. and Shoun H. (2002) Ammonia fermentation, a novel anoxic metabolism of nitrate by fungi. *J. Biol. Chem.* 277: 1892-1896.
- Zuo Y. and Jones R.D. (1996) Photochemical production of carbon monoxide in authentic rainwater. *Geophys. Res. Lett.* 23: 2769-2772.